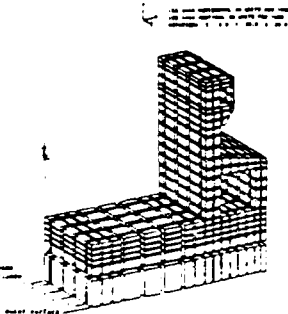
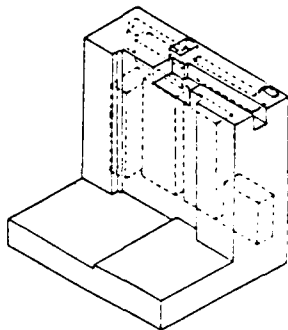
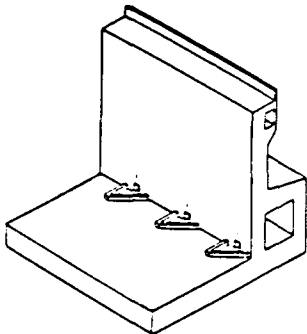




US Army Corps
of Engineers



DTIC FILE COPY TECHNICAL REPORT SL-87-21

12

THERMAL STRESS ANALYSES OF MISSISSIPPI RIVER LOCK AND DAM 26(R)

by

Anthony A. Bombich, C. Dean Norman
Structures Laboratory

and

H. Wayne Jones

Information Technology Laboratory

DEPARTMENT OF THE ARMY
Waterways Experiment Station, Corps of Engineers
PO Box 631, Vicksburg, Mississippi 39180-0631

DTIC
ELECTE
AUG 18 1987
S **D**
02-D



July 1987

Final Report

Approved For Public Release, Distribution Unlimited

AD-A183 664

Prepared for US Army Engineer District, St. Louis
St. Louis, Missouri 63101-1986

87 8 14 068

Unclassified
 SECURITY CLASSIFICATION OF THIS PAGE

AD A183 664

REPORT DOCUMENTATION PAGE				
1a. REPORT SECURITY CLASSIFICATION Unclassified		1b. RESTRICTIVE MARKINGS		
2a. SECURITY CLASSIFICATION AUTHORITY		3. DISTRIBUTION / AVAILABILITY OF REPORT Approved for public release; distribution unlimited.		
2b. DECLASSIFICATION / DOWNGRADING SCHEDULE				
4. PERFORMING ORGANIZATION REPORT NUMBER(S) Technical Report SL-87-21		5. MONITORING ORGANIZATION REPORT NUMBER(S)		
6a. NAME OF PERFORMING ORGANIZATION See reverse.	6b. OFFICE SYMBOL (If applicable)	7a. NAME OF MONITORING ORGANIZATION		
6c. ADDRESS (City, State, and ZIP Code) See reverse.		7b. ADDRESS (City, State, and ZIP Code)		
8a. NAME OF FUNDING / SPONSORING ORGANIZATION See reverse.	8b. OFFICE SYMBOL (If applicable)	9. PROCUREMENT INSTRUMENT IDENTIFICATION NUMBER		
8c. ADDRESS (City, State, and ZIP Code) See reverse.		10. SOURCE OF FUNDING NUMBERS		
		PROGRAM ELEMENT NO.	PROJECT NO.	TASK NO.
				WORK UNIT ACCESSION NO.
11. TITLE (Include Security Classification) Thermal Stress Analyses of Mississippi River Lock and Dam 26(R)				
12. PERSONAL AUTHOR(S) See reverse.				
13a. TYPE OF REPORT Final report	13b. TIME COVERED FROM TO	14. DATE OF REPORT (Year, Month, Day) July 1987	15. PAGE COUNT 329	
16. SUPPLEMENTARY NOTATION Available from National Technical Information Service, 5285 Port Royal Road, Springfield, VA 22161.				
17. COSATI CODES			18. SUBJECT TERMS (Continue on reverse if necessary and identify by block number)	
FIELD	GROUP	SUB-GROUP	Aging-creep model Incremental Pile loads	
			Concrete properties construction Temperature	
			Finite element method Mass concrete Thermal stress	
19. ABSTRACT (Continue on reverse if necessary and identify by block number) <p>This report describes an investigation to analyze selected monoliths of Mississippi River Lock and Dam 26 (Replacement) (L&D 26(R)) for thermal and construction induced stresses using three-dimensional (3-D) finite element methods (FEM). The St. Louis District recommended that one of several commercially available general purpose FEM codes be used to perform the analysis. The guidelines to accomplish the goals of the study were developed into evolutionary four-phase plan. The first phase was to evaluate and select a code from the recommended candidates best capable of modeling the problem. Evaluation criteria included the capability to simulate incremental construction, materials aging, time-stopping, inclusion of a comprehensive element library with capability to easily implement user-defined material models, the ability to model large numbers of reinforcing bars, and have efficient numerical solutions with flexible means for selecting time steps. The program was also required to be user-oriented, be well documented by the developer, and</p>				
20. DISTRIBUTION / AVAILABILITY OF ABSTRACT <input checked="" type="checkbox"/> UNCLASSIFIED / UNLIMITED <input type="checkbox"/> SAME AS RPT <input type="checkbox"/> DTIC USERS		21. ABSTRACT SECURITY CLASSIFICATION		
22a. NAME OF RESPONSIBLE INDIVIDUAL		22b. TELEPHONE (Include Area Code)		22c. OFFICE SYMBOL

Unclassified

SECURITY CLASSIFICATION OF THIS PAGE

6a + c. NAME OF PERFORMING ORGANIZATION/ADDRESS (Continued).

USAEWES, Structures Laboratory and Information Technology Laboratory, PO Box 631, Vicksburg, MS 39180-0631.

8a + c. NAME/ADDRESS OF FUNDING/SPONSORING ORGANIZATION (Continued).

US Army Engineer District, St. Louis, St. Louis, MO 63101-1986.

12. PERSONAL AUTHOR(S) (Continued).

Bombich, Anthony A.; Norman, C. Dean (Structures Laboratory); and Jones, H. Wayne (Information Technology Laboratory).

19. ABSTRACT (Continued).

have a high potential for remaining at the state-of-the-art level. After evaluation, a review committee selected the ABAQUS program as the code best suited to solution of the problem.

During the second phase, a solution/method verification was performed based on test case problems. Simple problems with known solutions were tested to verify that the ABAQUS program would give exact or reasonable results as appropriate.

In phase three a series of two-dimensional (2-D) solutions of L&D 26(R) monoliths L-13 and L-17 were conducted using both ABAQUS and the WES2DT programs. The WES2DT program had been verified during previous projects where 2-D approximations were appropriate. The 2-D solutions ranged from single-step, gravity-only loading through staged, incremental construction thermal stress analyses that included some or all of the effects of temperature, gravity, pile elasticity and creep. The WES2DT program employed a simple creep model. An aging-creep model developed for a related project was used with ABAQUS.

Phase four provided for 3-D FEM solutions of the two monoliths. All work was completed for the 3-D FEM analyses except for actually conducting the computer runs. Computer costs and limitations on computer resources prohibited execution of planned computer runs except for one gravity turn-on analysis of L-13. Although the computer runs were not made, complete documentation of the 3-D problem solution up to the actual execution of the computer runs are included in this report.

Even though the 3-D analyses, as planned, could not be completed, it was felt that the objectives relating to the conduct of incremental construction thermal analyses of mass concrete utilizing a modern, general purpose FEM code were realized. These included successful 2-D incremental thermal analyses in which all construction, environmental, and thermal properties aspects were adequately handled by ABAQUS. Most of the important aspects of 2-D incremental thermal analyses were also acceptable except for modeling early-age materials properties. Reliable early-age materials properties data did not exist for L&D 26(R) concrete at the time of the study; consequently, aging modulus, creep, and shrinkage data were taken from other test results. This led to calculation of excessive thermal stresses and creep relaxation at early time.

Results indicated that concrete stresses and the distribution of pile loads beneath the monoliths are significantly affected by the assumptions made in the analysis such as single-stage gravity turn-on versus staged, incremental construction with temperature effects, and also aging, creep, and shrinkage. Analyses such as described in this report are an effective means for establishing the basis for mass concrete construction temperature control plans. More research is required to fully develop incremental construction FEM analyses in this construction support role as well as to delineate the extent to which incremental construction analyses should be incorporated into structural design.

Unclassified

SECURITY CLASSIFICATION OF THIS PAGE

PREFACE

The work described in this report was conducted for the US Army Engineer District, St. Louis, by the Concrete Technology Division (CTD) of the Structures Laboratory (SL) and the Information Research Division (IRD) of the Information Technology Laboratory (ITL), US Army Engineer Waterways Experiment Station (WES). The investigation was authorized by DA Form 2544, Intra-Army Order for Reimbursible Services, No. ED84-12, dated December 1983.

The investigation was accomplished under the general supervision of Messrs. Bryant Mather, Chief, SL; James T. Ballard, Assistant Chief, SL; John M. Scanlon, Chief, CTD; and Dr. N. Radhakrishnan, Chief, ITL, and under the direct supervision of Mr. C. Dean Norman, Program Manager. This report was written by Messrs. Anthony A. Bombich and C. Dean Norman, CTD, and H. Wayne Jones, ITL.

COL Dwayne G. Lee, CE, is Commander and Director of WES. Dr. Robert W. Whalin is Technical Director.

Accession For	
NTIS CRA&I	<input checked="" type="checkbox"/>
DTIC TAB	<input type="checkbox"/>
Unannounced	<input type="checkbox"/>
Justification	
by	
Distribution/	
Availability Codes	
Dist	Avail and/or Special
A-1	



CONTENTS

	<u>Page</u>
PREFACE	1
CONVERSION FACTORS, NON-SI TO METRIC (SI) UNITS OF MEASUREMENT	5
PART I: INTRODUCTION	6
Background	6
Objective	7
Scope	7
PART II: SELECTION OF FINITE ELEMENT PROGRAM	9
General	9
ABAQUS - General Description	9
PART III: ABAQUS PROGRAM - CODE VERIFICATION AND MODIFICATIONS	11
General	11
Code Verification	11
Group A: Problems with Known Solutions	11
Group B: Problems Simulating Incremental Construction	12
Program Modification	16
PART IV: WES2DT PROGRAMS	17
General	17
Temperature Calculation Program	17
Stress and Strain Calculation Program	18
PART V: INPUT DATA AND MODELED PARAMETERS	19
General	19
Concrete and Other Properties	19
Age-dependent Concrete Properties	19
Other Properties	25
Pile Stiffnesses	26
Monolith L-13	28
Monolith L-17	29
Construction Parameters and Boundary Conditions	30
Lift Heights	30
Placement Rates	31
Ambient Air Temperature and Foundation Temperature	31
Construction Start Dates, Placement Temperature	33
Thermal Boundary Conditions	33
Mechanical Boundary Conditions	34
PART VI: FINITE ELEMENT MODELS	35
General	35
Two-Dimensional Models, L-13	36
ABAQUS model selection	36
WES2DT model selection	38
Two-Dimensional Models, L-17	38
ABAQUS model selection	38
WES2DT model selection	42
Three-Dimensional Model, L-13	42
Three-Dimensional Model, L-17	45

PART VII: THERMAL ANALYSES OF MONOLITH L-13	49
Presentation of Results	49
Two-dimensional temperature analysis	49
Three-dimensional temperature analysis	49
Discussion of Results	49
Two-dimensional temperature analysis	49
Three-dimensional temperature analysis	50
 PART VIII: STRESS ANALYSES OF MONOLITH L-13	 87
Presentation of Results	87
Two-dimensional gravity loading	87
Two-dimensional gravity and thermal loading	87
Two-dimensional gravity and thermal loading including creep	88
Two-dimensional gravity and thermal loading including creep and shrinkage	88
Three-dimensional gravity loading	88
Discussion of Results	89
Gravity turn-on analyses	89
Incremental construction with gravity loading ABAQUS versus WES2DT	89
Gravity turn-on versus incremental construction	90
Two-dimensional gravity and thermal loading	91
Two-dimensional gravity and thermal loading including creep	93
Two-dimensional gravity and thermal loading including creep and shrinkage	94
Pile loads	95
Cracking potential	98
 PART IX: THERMAL ANALYSES OF MONOLITH 17	 190
Presentation of Results	190
Two-dimensional temperature analysis	190
Three-dimensional temperature analysis	190
Discussion of Results	191
Two-dimensional temperature analysis	191
 PART X: STRESS ANALYSES OF MONOLITH 17	 201
Presentation of Results	201
Two-dimensional gravity loading	201
Two-dimensional gravity and thermal loading	201
Two dimensional gravity and thermal loading including creep	202
Two-dimensional gravity and thermal loading including creep and shrinkage	202
Discussion of Results	202
Gravity turn-on analysis	202
Incremental construction with gravity loading ABAQUS versus WES2DT	203
Gravity turn-on versus incremental construction	203
Two-dimensional gravity and thermal loading	204
Two-dimensional gravity and thermal loading including creep	206
Two-dimensional gravity and thermal loading including creep and shrinkage	207
Pile loads	208
Cracking potential	211
 PART XI: CONCLUSIONS AND RECOMMENDATIONS	 259
 REFERENCES	 262

APPENDIX A:	ABAQUS TWO-DIMENSIONAL NODE FILE USED FOR MONOLITH L-17 . . .	A1
APPENDIX B:	ABAQUS TWO-DIMENSIONAL ELEMENT FILE USED FOR MONOLITH L-17	B1
APPENDIX C:	ABAQUS TWO-DIMENSIONAL THERMAL ANALYSIS INPUT COMMAND FILE FOR MONOLITH L-17	C1
APPENDIX D:	ABAQUS TWO-DIMENSIONAL STRESS ANALYSIS INPUT COMMAND FILE FOR MONOLITH L-17	D1
APPENDIX E:	ABAQUS JOB CONTROL LANGUAGE FILES USED WITH CYBERNET SYSTEM FOR STRESS AND THERMAL ANALYSES OF MONOLITH L-17)	E1
APPENDIX F:	ABAQUS HEAT GENERATION SUBROUTINE DFLUX, FILE "LDFLUX" USED IN 2-D, L-17 ANALYSIS	F1
APPENDIX G:	ABAQUS USER SUBROUTINE MPC, MULTIPLE POINT CONSTRAINT VERSION USED WITH MONOLITH L-17	G1
APPENDIX H:	MATERIAL USER SUBROUTINE UMAT, VERSION: "UMAT1" 2-D MODULUS ROUTINE WITHOUT CREEP USED WITH MONOLITH L-17 . . .	H1
APPENDIX I:	ABAQUS USER SUBROUTINE UMAT, VERSION: "UMAT2", AGING CREEP WITH SHRINKAGE USED WITH MONOLITH L-17	I1

CONVERSION FACTORS, NON-SI TO SI (METRIC) UNITS OF MEASUREMENT

Non-SI units of measurement used in this report can be converted to SI (metric) units as follows:

<u>Multiply</u>	<u>By</u>	<u>To Obtain</u>
Btu (International Table) per pound (mass) . degree Fahrenheit	4,186.8	joules per kilogram Kelvin
Btu (International Table) . inch per hour . square inch . degree Fahrenheit	20.7688176	watts per metre Kelvin
Fahrenheit degrees	5/9	Celsius degrees or Kelvins*
feet	0.3048	metres
inches	0.0254	metres
kips (force) per inch	1.213659	kilonewtons per metre
miles per hour (U. S. statute)	1.609347	kilometres per hour
pounds (force) per square inch	6.894757	kilopascals
pounds (mass) per cubic inch	27,679.899	kilograms per cubic metre
pounds (mass) per cubic foot	16.01846	kilograms per cubic metre

* To obtain Celsius (C) temperature reading from Fahrenheit (F) readings, use the following formula: $C = (5/9)(F-32)$. To obtain Kelvin (K) readings, use $K = (5/9)(F-32) + 273.15$.

THERMAL STRESS ANALYSES OF MISSISSIPPI

MISSISSIPPI RIVER LOCK AND DAM 26(R)

PART I: INTRODUCTION

Background

1. In November of 1983, the Waterways Experiment Station (WES) was asked by St. Louis District, Corps of Engineers, to analyze the lower gate monolith and one intermediate monolith of Mississippi River Lock and Dam 26(R) for thermal and construction induced stresses and also normal operating conditions using three-dimensional (3-D) finite element methods (FEM). It was also requested that WES use one of the computer programs ADINA, ANSYS, or ABAQUS to perform the analysis. The general objective of this analysis effort was to adapt a general-purpose finite element program with state-of-the-art numerical formulations, large element libraries, and easily implemented user-defined material model to the problem of thermal stress analysis of mass concrete structures. In a cooperative effort the Concrete Technology Division (CTD) of the Structures Laboratory (SL) and the Information Technology Laboratory (ITL) prepared and submitted a cost estimate and scope of work to conduct the analysis. Personnel of the St. Louis District (LMSD), CTD, and ITL, met at WES in December 1983 to review and discuss the cost estimate and proposal. All present at this meeting agreed to the general analysis approach to be used, but it was pointed out that the effective solution of a stress analysis problem such as this might require significant modifications of currently available general-purpose finite element programs. However, it was anticipated that an acceptable solution could be obtained with only minor modifications of existing finite element programs.

2. Monoliths L-13 and L-17 were selected for the analysis so that two-dimensional (2-D) and three-dimensional (3-D) effects could be studied both in

terms of thermal gradients and stress distributions. Symmetric half-section isometric projections of monoliths L-13 and L-17 are shown in Figure 1.

Objective

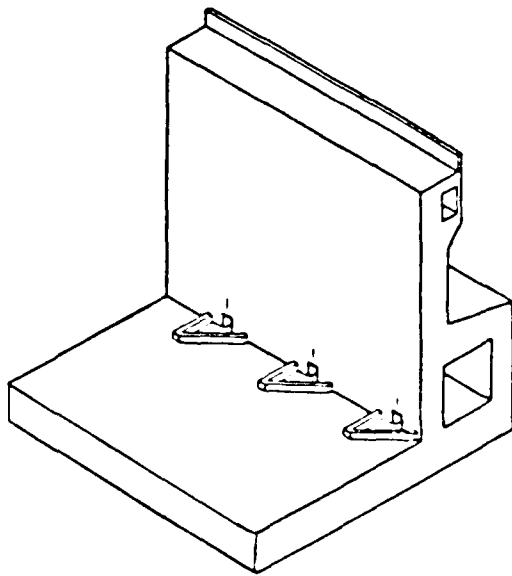
3. The objective of this investigation was to conduct 2- and 3-D thermal stress analyses of selected monoliths of Lock and Dam 26(R) using a modern general-purpose finite element program.

Scope

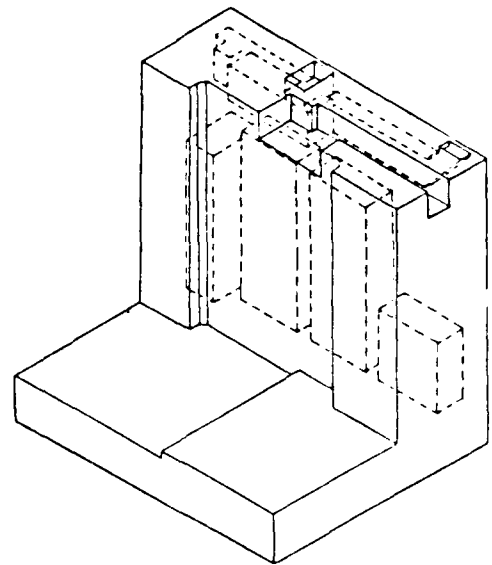
4. To accomplish the objectives of this study within the guidelines set by the St. Louis District, a four-phase investigation plan was developed. The originally developed plan is presented below.

<u>Phase</u>	<u>Finite Element Investigation Plan</u>
I	Selection of most effective finite element program(s) to accomplish the goals of the investigation. This involves evaluating the capabilities of the available three-dimensional programs to model the problem.
II	Solution-method verification based on test case problems. This involves solving simple problems for which solutions are available and verifying that the program gives exact or reasonable results as appropriate.
III	Solution of two-dimensional problems. Two-dimensional solutions will be obtained for monolith L-13 using the WES2DT program which has been verified based on previous projects where 2-D approximations were appropriate. The WES2DT program also has a simple creep model. Two-dimensional solutions will also be obtained for monolith L-13 using the new code and compared with results from the WES2DT program. A decision was made later to include 2-D analyses of monolith L-17 with both the new program and WES2DT. Results from these 2-D analyses form a basis for interpreting and evaluating results from 3-D analyses.
IV	Solution of three-dimensional problems. A 3-D analysis will be conducted on monolith L-13. This analysis is primarily designed to demonstrate the effects of 3-D thermal gradients on essentially a 2-D structural geometry. A fully 3-D analysis will be conducted on monolith L-17 which is truly a 3-D structure. Although at the beginning of the study it was intended that complete 3-D thermal stress analyses would be conducted, the computer costs and limitations on computer resources prohibited

this work. In this report any discussions concerning 3-D thermal stress analyses of L-13 and L-17 are directed toward work performed up to conducting the actual computer runs. Also, due to lack of reliable early-time materials properties data for L&D 26(R) at the time of this study, aging modulus, creep, and shrinkage were taken from other concrete test results. The point to be made here is that the objective of the study was to conduct rational, consistent incremental construction analyses of mass concrete structures. It is quite simple to go back and rerun any of the analyses presented in this report with different early-time material properties.



(a) Monolith L-13



(b) Monolith L-17 with internal voids indicated

Figure 1. Symmetric half-section isometric projections of Lock and Dam 26(R) monoliths used in thermal stress investigation.

PART II: SELECTION OF THE FINITE ELEMENT PROGRAM

General

5. The approach taken in selecting the finite element program to be used in the Lock and Dam 26(R) analysis was to review the capabilities and flexibility of each recommended program in light of the requirements of the problem to be analyzed. Specific requirements included capability to simulate incremental construction, a large element library with capability to implement user-defined material models with relative ease, capability to model significant numbers of reinforcing bars with relative ease, efficient numerical solution procedures with flexible means for selecting solution time steps, etc. In addition, it was desired that the program be user-oriented, receive a high caliber of technical and scientific support from the developer, and have a high potential for staying at the state-of-the-art level.

6. The review of the FEM programs was conducted by personnel of the ITL and the CTD. The review consisted of discussing actual experiences with the different programs, reviewing technical journal articles which compare FEM programs (1)*, meeting with representatives of Cybernet Division - Control Data Corporation, and discussions with personnel of other governmental laboratories directly involved with FEM applications.

7. Based on the criteria and review method discussed above, the review committee unanimously agreed to select ABAQUS for the Lock and Dam 26(R) project.

ABAQUS - General Description

8. ABAQUS, developed by Hibbitt, Karlsson, and Sorensen, Inc., is a general-purpose structural and heat transfer analysis program. The theoretical

* Numbers in parentheses refer to references at the end of this report.

formulation is based on the finite element stiffness method with some hybrid formulations included as necessary. The program includes both user and automatic control of solution step size. Input is in free format, key worded, and makes use of set definitions for easy cross reference. A broad element library is included in ABAQUS, and any combination of elements can be used in the same model. A wide variety of constitutive models is also provided in ABAQUS, and these model can essentially be used with any element type. User-defined material models are incorporated with relative ease through the UMAT subroutine. Reinforcement (rebar) can be added to any element. Static and dynamic response in stress analysis can be conducted as well as steady-state and transient heat transfer problems. The incremental construction problem can be effectively simulated through the model change option where previously defined elements can be included or removed from the analysis in a specified solution step. Specific details of element type and boundary conditions used will be presented in the various analysis phases of this report.

PART III: ABAQUS PROGRAM - CODE VERIFICATION AND MODIFICATION

General

9. The code verification phase was to serve two purposes: (a) to verify the operation of the program on problems with known solutions and its extension to problems where results were not known but could be analyzed by the investigators to determine that solutions followed rational and expected behavior patterns, and (b) to verify the investigators' ability to direct the program operation to solve desired problems by using the many different program features.

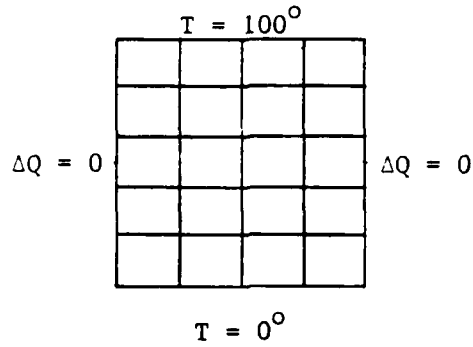
Code Verification

10. To verify the code, several simple example problems were used and are discussed in terms of two groups. Group A consists of problems with known solutions. The finite element (FE) grids for these example problems are shown in Figure 2. Group B consists of the example problem shown in Figure 3 which was used to exercise and test most of the procedures needed to solve the mass concrete incremental construction problem under consideration.

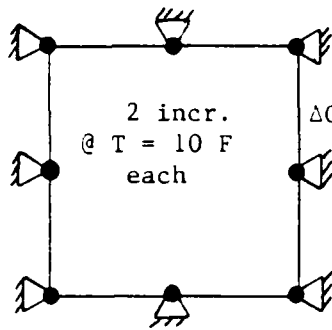
Group A: problems with known solutions

11. Figure 2a shows a square plate with constant temperature specified on each boundary. The steady-state temperature distribution was determined with ABAQUS and checked against the closed form solution. Very good agreement was found between these results.

12. Figures 2b and 2c show two single-element models using the eight-node plane strain element. These models were subjected to two temperature steps of 10 degrees F each while E changed with age. All nodes were restrained during the temperature change in model 2b, whereas, only two nodes

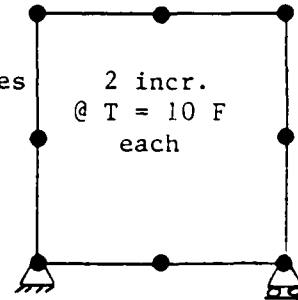


(a) Grid used to test steady-state temperature calculations



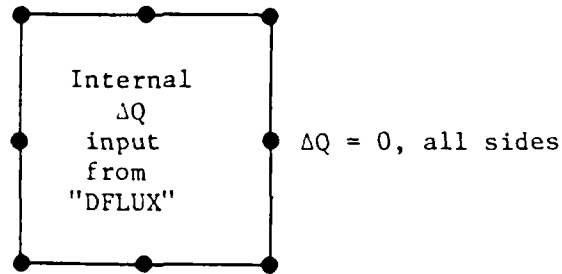
(b) Fully restrained

$\Delta Q = 0$, all sides



(c) Unrestrained

Single-element models to test thermal stress calculations with variable "E" versus age



(d) Single-element heat transfer model used to test user subroutine "DFLUX"

Figure 2. Finite element grids used in ABAQUS code verification for Group A problems with known solutions.

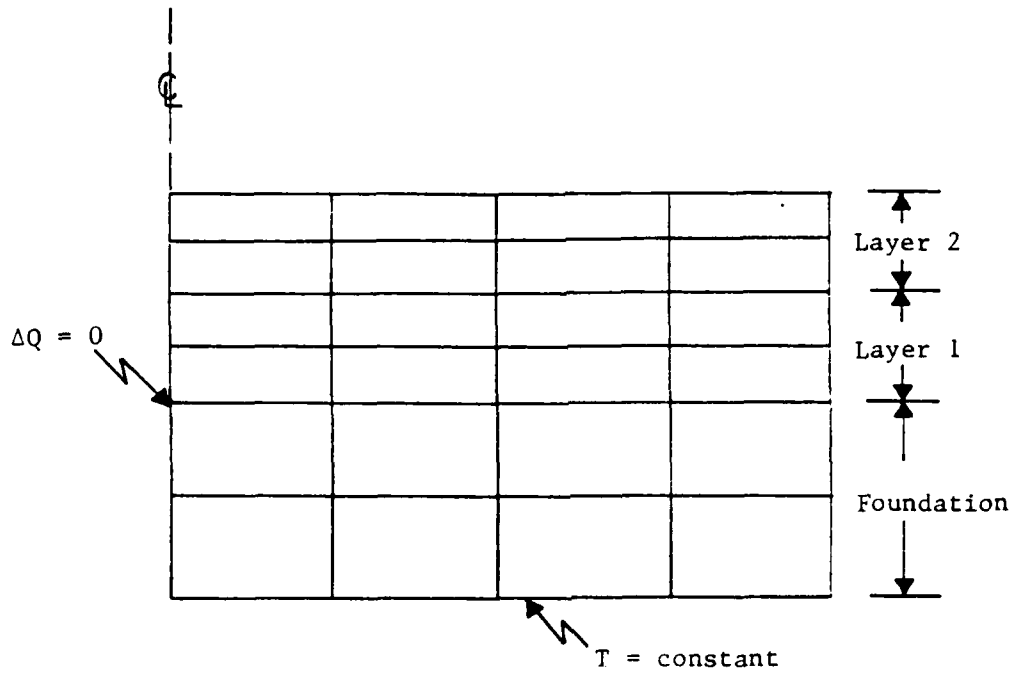
were partially restrained in model 2c. Results showed correct, equal stresses in the x , y , and z normal directions at each calculation step proportional to the temperature change and E values. All nodes except the two shown were free to translate in model 2c. The results showed that the restraint provided in the z normal direction by the plane strain conditions produced correct, equal stresses in the x and y directions due to the Poisson effect at each calculation step.

13. Figure 2d shows a single-element model using the eight-node, 2-D heat transfer element. In this example problem, the user subroutine DFLUX was tested. DFLUX was written to provide concrete heat of hydration input to ABAQUS thermal simulations. The adiabatic boundaries of the model prevented heat exchange. The results showed that the sequences of temperature changes in the model exactly reproduced the heat generation data provided to DFLUX.

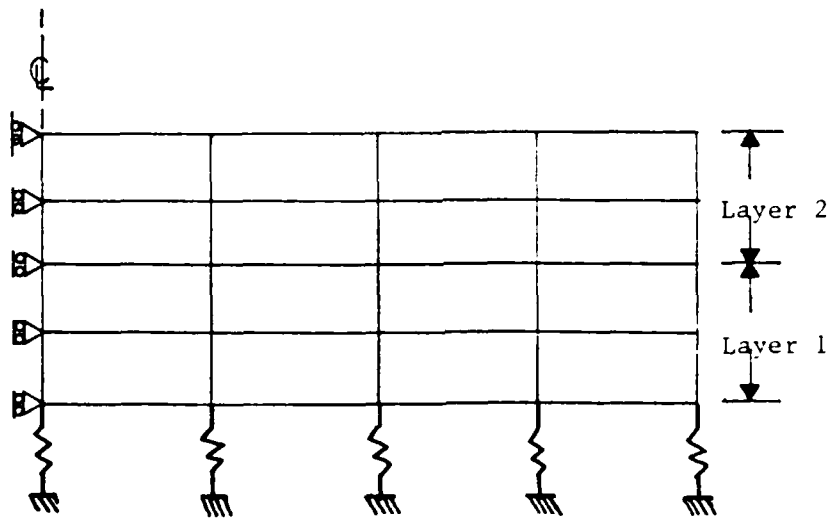
Group B: problems simulating
incremental construction

14. Figure 3a shows a problem consisting of 24 eight-node elements which was used to simulate most of the procedures needed in the actual thermal stress analyses of monoliths L-13 and L-17. This example has a soil foundation and two lifts of concrete which were placed at 5-day intervals. The temperature distribution is determined in the FE system throughout the incremental construction process. Next, the grid in Figure 3b was used to perform the stress analysis. The soil foundation was not included in the stress analysis, but linear springs to simulate piles were added to support the structure just as in the actual problem. The structure was then constructed in two lifts to simulate the incremental construction process. The temperatures which were calculated in the earlier temperature analysis were included as loads to the stress analysis. The following procedures were examined.

- a. Eight-node, 2-D element behavior for temperature analysis and stress analysis.



(a) Grid used for temperature analysis during incremental construction with heat generation



(b) Grid used for stress analysis during incremental construction with temperature loadings

Figure 3. Finite element grids used in ABAQUS code verification for Group B problems simulating incremental concrete construction.

- b. Linear spring element behavior.
- c. Gravity loading.
- d. Thermal stresses.
- e. Incremental Construction behavior.
- f. Combination of temperature analysis and stress analysis.
- g. Time-dependent modulus of elasticity.
- h. Gap element behavior.
- i. Applied pressures and concentrated loads.
- j. Plotting of displaced grid and stress contours.

15. During the analysis of the results of this example it was determined that the incremental construction process was not simulated properly. The program developers were asked to supply a version of ABAQUS which could perform this task as required. To obtain this capability the new ABAQUS Version 4.5 was developed.

16. To model the initial temperature equilibrium behavior at the interface of an intact element and a newly placed element, the use of gap elements was examined. After making runs without elements, with gap elements, and with modified temperatures at those interfaces, it was determined that adequate results were obtainable by using modified temperatures along only the interface between the soil foundation and the first lift of concrete during the temperature analysis. This was very desirable since the use of gap elements would have greatly complicated that grid generation for the actual models to be analyzed.

Program modification

17. As a result of the verification examples, four modifications were made to the program. The first modification was to enable the program to use time-dependent material properties (E and ν). The second modification was to enable the program to perform the incremental construction analysis in a more consistent manner. Although the program was already able to remove and include elements of the structure as desired, this procedure had to be modified to be consistent with the E and ν time variations for newly added materials. This was implemented in ABAQUS. The third required modification to ABAQUS was to develop and implement a time-dependent, aging creep model for material behavior. This was performed by adding a new material subroutine to the program. This subroutine has been developed and implemented in ABAQUS for 2-D problems, and a version for 3-D problems is being developed. The fourth modification was to produce the user subroutine DFLUX to permit incremental concrete heat of hydration data to be generated by ABAQUS for the incremental thermal calculations.

PART IV: WES2DT PROGRAMS

General

18. This section describes the two-dimensional WES2DT FE programs that have been used at WES for more than 10 years for conducting thermal studies of Corps projects. WES2DT is based on two FE thermal analyses programs prepared for the Corps during the late 1960's. The first program, developed by Dr. Edward Wilson of the University of California at Berkeley (2) and modified for use at the WES, calculates the temperatures within a mass concrete structure. A second program, written by R. S. Sandhu et. al. also at Berkeley (3) and modified at WES, calculates the thermal stresses and strains within the structure resulting from gravity and the thermal loads. In the WES2DT program construction layer (lift) and material interfaces must correspond to an element boundary. The element type used in WES2DT is a four-node quadrilateral with linear temperature and displacement fields.

Temperature Calculation Program

19. The temperature program calculates temperatures at each node in the FEM model. These calculations are based upon concrete placement temperature, heat generated, and the thermal properties of the concrete which govern heat flow within an element and loss or gain across boundaries due to ambient conditions which are controlled by a surface heat transfer coefficient simulating wind or surface insulation or both. Calculated temperatures are output at prescribed intervals for all nodes in the model at a particular stage of construction. A value of temperature is determined for each new concrete element at 6 hr after placement which is assumed to be the final temperature at which an element is stress free. Element stress-free temperatures and calculated nodal temperatures are then used for stress/strain calculation by WES2DT.

Stress and Strain Calculation Program

20. This program calculates the displacements at each node and the strains and stresses developed in each element in the FEM model due to thermal and gravity loads. It was discovered that the program was designed with a plane strain formulation in which both z-direction stresses and strains are zero. In thermal stress problems this eliminates z-direction Poisson effects on x- and y-direction stresses. When creep is considered, stresses at each time step in the analysis are modified for stress relaxation at constant strain. Creep parameters are stored and the change in stress stored as residual stress to be included in the next time step analysis. When these stored values are applied during the next time step analysis, strains are then modified for creep.

21. A modification to account for pile restraint was incorporated into the thermal stress program as a direct result of requirements for previous thermal studies. The pile element used is a simple two-node element modeled mathematically as a linear spring. Actual pile stiffness data are used to determine stiffness of the pile elements. The individual stiffnesses in a pile group are totaled so that the stiffnesses can be applied on average horizontal area bases rather than a discrete pile basis to facilitate 2-D analysis with piles included. The pile groups in this study were rows of piles parallel to the flow axis of each monolith.

22. A one-dimensional bar (truss) element is used to simulate reinforcement steel. Since the program is 2-D, the reinforcement parallel to the model is input as the equivalent cross-sectional area per unit depth. Reinforcement and pile elements are superimposed on the finite element model sharing nodes with quadrilateral, plain strain elements.

PART V: INPUT DATA AND MODELED PARAMETERS

General

23. This section describes the input data and modeled parameters used in all FEM analyses conducted for this investigation. The first section describes the materials properties for concrete and foundation as well as pile stiffnesses used. The second section describes the construction parameters and boundary conditions assumed in the analyses.

Concrete and Other Properties

24. The input data used for the thermal and mechanical properties of concrete were either the same values used in earlier thermal studies for Lock and Dam 26(R) or were based upon tests conducted in the interim period since these studies were completed. The concrete is assumed to have a nominal compressive strength of 3000 psi* using Type II cement with a heat of hydration limit and 25 percent replacement by solid volume of pozzolan (fly ash).

25. Concrete properties data carried over from previous studies included adiabatic temperature rise and creep. New data based upon tests of Lock and Dam 26(R), Phase I, project mixture 4A includes modulus of elasticity, Poisson's ratio, specific heat, thermal conductivity, and coefficient of linear thermal expansion.

Age-dependent concrete properties

26. Adiabatic temperature rise data assumed in the study are shown in Figure 4a. Modulus of elasticity as a function of age used by the WES FEM program WES2DT and the ABAQUS UMAT1 subroutine (without creep) is shown in Figure 4b.

* A table of factors converting non-SI units of measurement to SI (metric) units is presented on page 5.

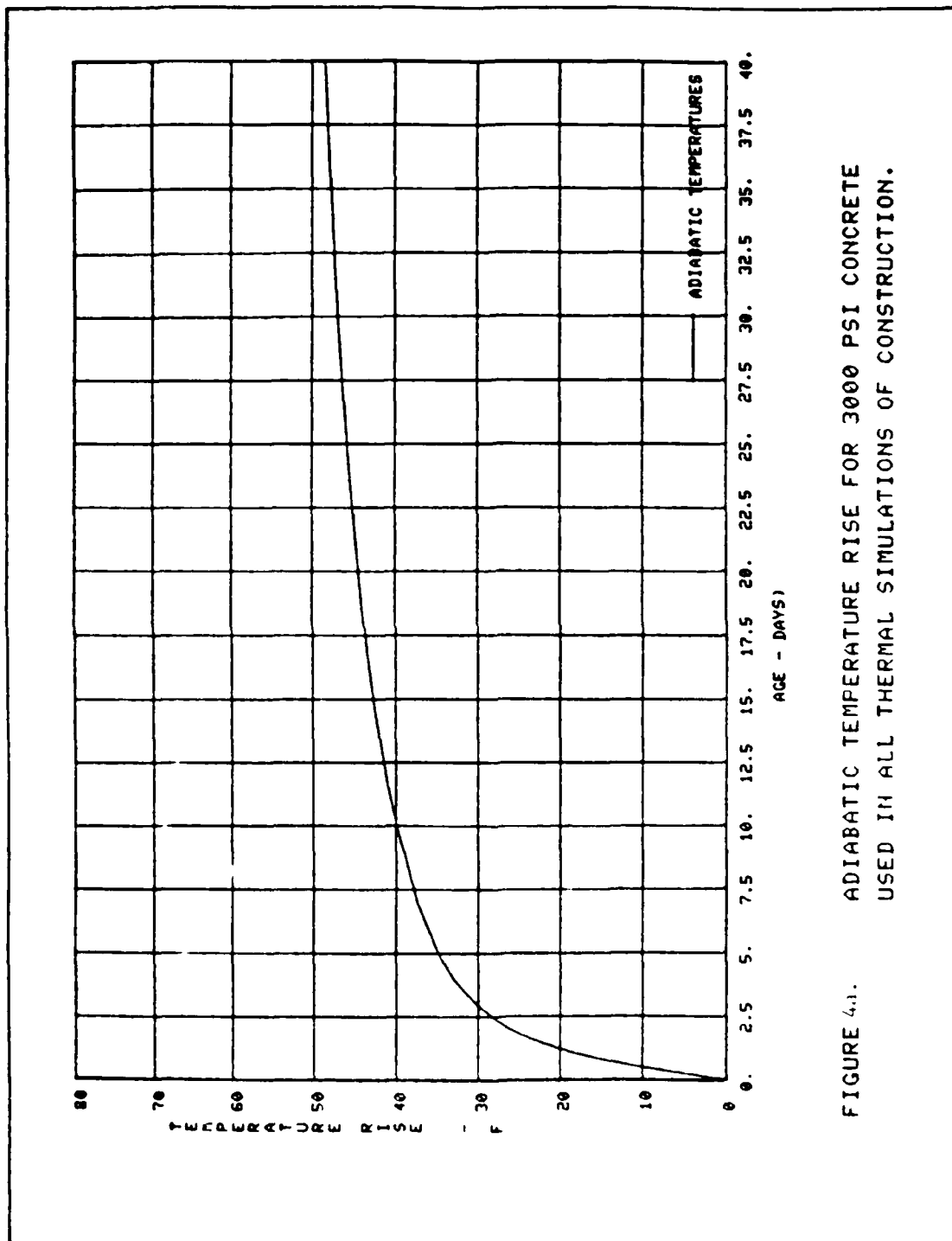


FIGURE 4.1. ADIABATIC TEMPERATURE RISE FOR 3000 PSI CONCRETE USED IN ALL THERMAL SIMULATIONS OF CONSTRUCTION.

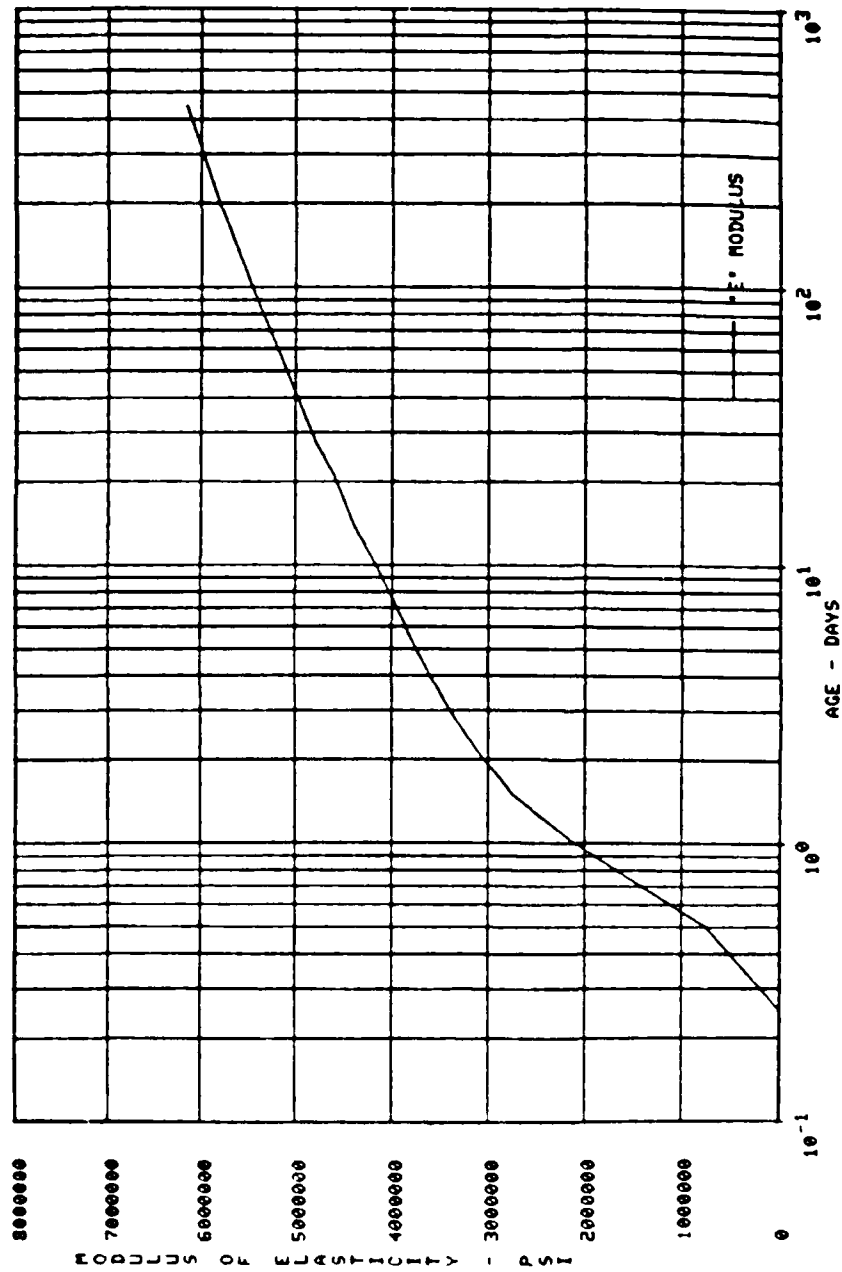


FIGURE 4b. MODULUS OF ELASTICITY VS AGE FOR 3000 PSI CONCRETE USED IN ALL STRESS CALCULATIONS.

27. Creep properties used in the WES2DT code were taken from tests conducted at WES on concrete from Port Allen Lock (4). Generally, creep strains for this concrete are low, thus conservative, for mixtures in the current investigation. The creep data were fit to McHenry's equation (5,6),

$$e_c(\sigma, t, T) = \sigma \sum_{i=1}^N A_k(T) (1 - e^{-m_i(t-T)})$$

where

σ - applied stress

e_c - creep strain

t - time after placement

T - age at loading.

$N = 2$ was found to give a satisfactory fit of experimental data. Values of creep relaxation coefficients A_1 and A_2 versus time are given in Figure 4c. Values of constants $m_1 = 0.45$ and $m_2 = 0.0285$ were used. Figure 4d shows the creep data at several loading ages produced by the creep coefficients shown in Figure 4c using McHenry's equation.

28. Creep modeling in ABAQUS was accomplished with an aging creep model that was developed in a related research program at WES (7). The 2-D aging creep model with cracking was developed in the ABAQUS-UMAT subroutine format. The model, designated UMAT2 for this investigation, includes the effects of aging on the elastic modulus and cracking strength and the effects of changing temperatures on the creep compliance, the elastic modulus, and the ultimate/cracking strength. Creep properties are given in the form

$$e^c/\sigma = [A(1 - e^{-rt}) + Bt] e^{-Q/RT}$$

where

e^c - creep strain due to stress σ

σ - applied stress

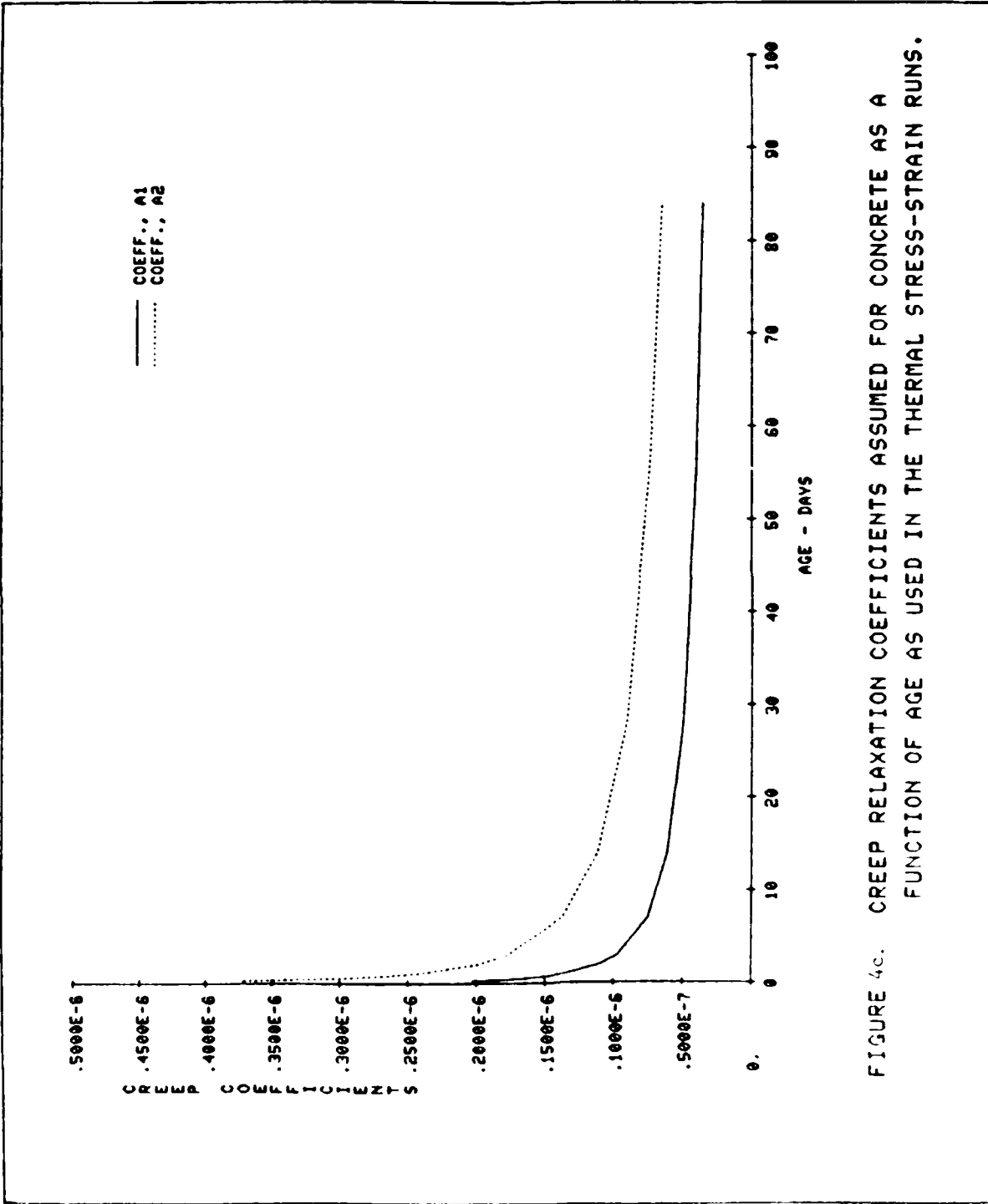


FIGURE 4c. CREEP RELAXATION COEFFICIENTS ASSUMED FOR CONCRETE AS A FUNCTION OF AGE AS USED IN THE THERMAL STRESS-STRAIN RUNS.

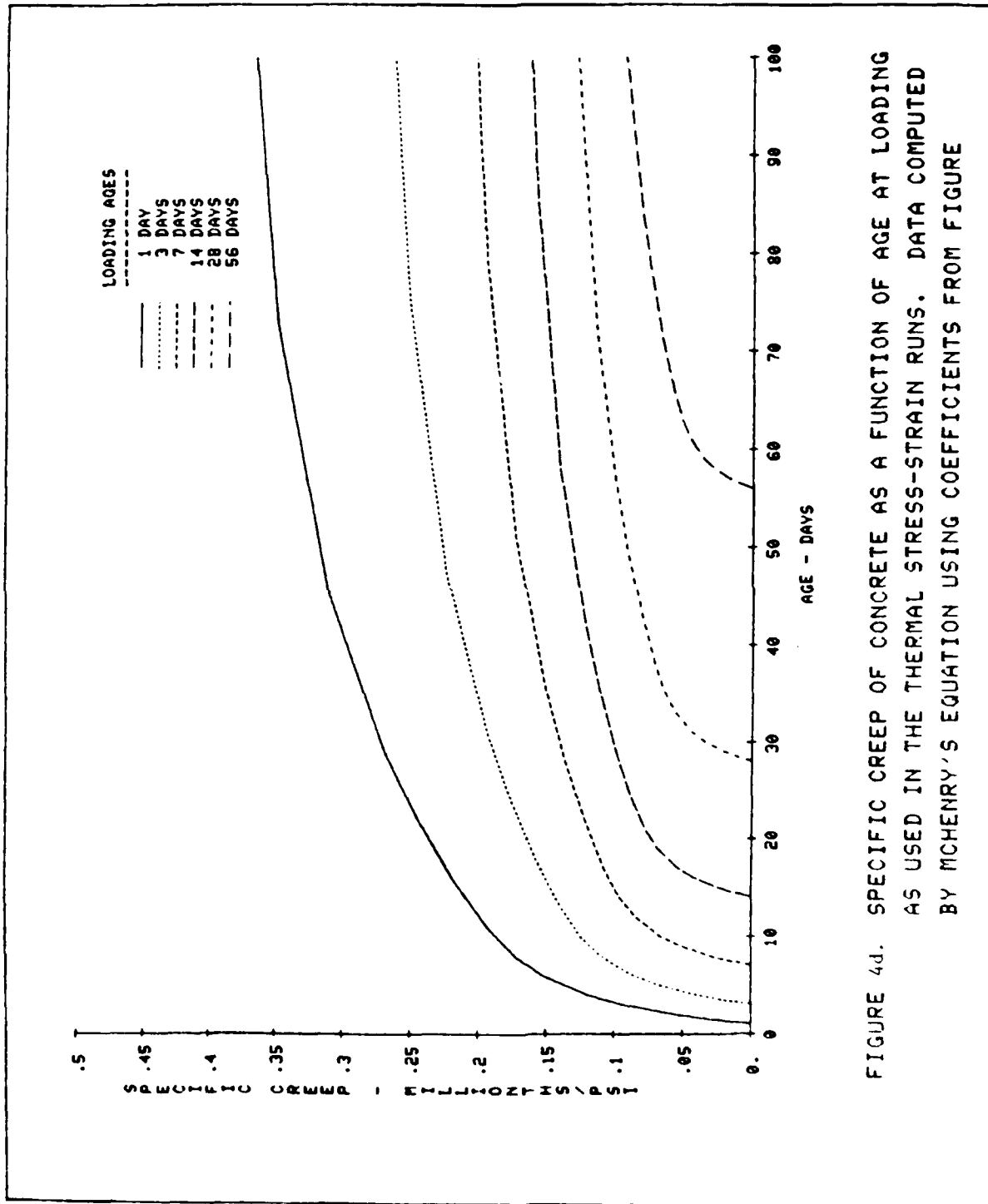


FIGURE 4d. SPECIFIC CREEP OF CONCRETE AS A FUNCTION OF AGE AT LOADING AS USED IN THE THERMAL STRESS-STRAIN RUNS. DATA COMPUTED BY MCHENRY'S EQUATION USING COEFFICIENTS FROM FIGURE

t - time

T - temperature

R - gas constant

r,A,B,Q - material constants.

The elastic modulus and ultimate strength can be expressed as functions of age (t) and temperature (T) as $E(t,T)$ and $\sigma_u(t,T)$, respectively. The cracking strain (ϵ^c) is assumed to be 10 percent of the absolute value of the compressive strain at ultimate strength. Poisson's ratio (ν) is assumed to be constant. The creep properties and the properties $E(t,T)$, $\sigma_u(t)$, ϵ_f , and ν are included in a separate subroutine in a form that can be modified by the user. The E versus time data used in UMAT2 was based upon the data shown in Figure 4b except that the numerical fit provided by the model developer produced higher values of E for the first two days of age. The creep data used came from tests of silica fume concrete and produced specific creep values slightly higher than the creep data shown in Figure 4d. Shrinkage data was linear until 1 day at a rate of 100 millionths per day and non-linear thereafter with typical values of approximately 300, 350, and 400 millionths at 10, 25, and 50 days, respectively.

Other properties

29. Additional properties data used as input to the computer programs are shown in Table 1. Included are data for concrete, the soil foundation, and air when modeling the internal voids of monolith L-17. The values for some of the properties are modified to accomplish a modeling technique. For example, the density and modulus, E, of the soil in the WES2DT stress analyses were assigned very low values to effectively eliminate the soil because the actual elements could not be removed. An abnormally high value of thermal conductivity was assigned to air to simulate the combined heat transfer effects of convection and conduction when air elements are actually included in the model.

Table 1.

Materials Data Used in FE Investigation.Concrete

Thermal conductivity	0.09789 Btu-in./hr-in. ² -°F
Specific heat	0.21 Btu/lb-°F
Density	0.08714 lb/in. ³ (151 lb/ft ³)
Coefficient of thermal expansion	4.5 x 10 ⁻⁶ in./°F
Poisson's ratio	0.17

Foundation

Thermal conductivity	0.066 Btu-in./hr-in. ² -°F
Specific heat	0.45 Btu/lb-°F
Density (temperature calculation)	0.0758 lb/in. ³ (131 lb/ft ³)
Density (stress calculation)	0.0000006 lb/in. ³ (or ~ 0)*
Coefficient of thermal expansion	4.5 x 10 ⁻⁶ in./°F*
Poisson's ratio	0.35
Modulus of elasticity	1.0 psi*

Air (for voids in L-17 with ABAQUS temperature calculations only)

Thermal conductivity	1000. Btu-in./hr-in. ² -°F**
Specific heat	0.24 Btu/lb-°F
Density	0.000046 lb/in. ³

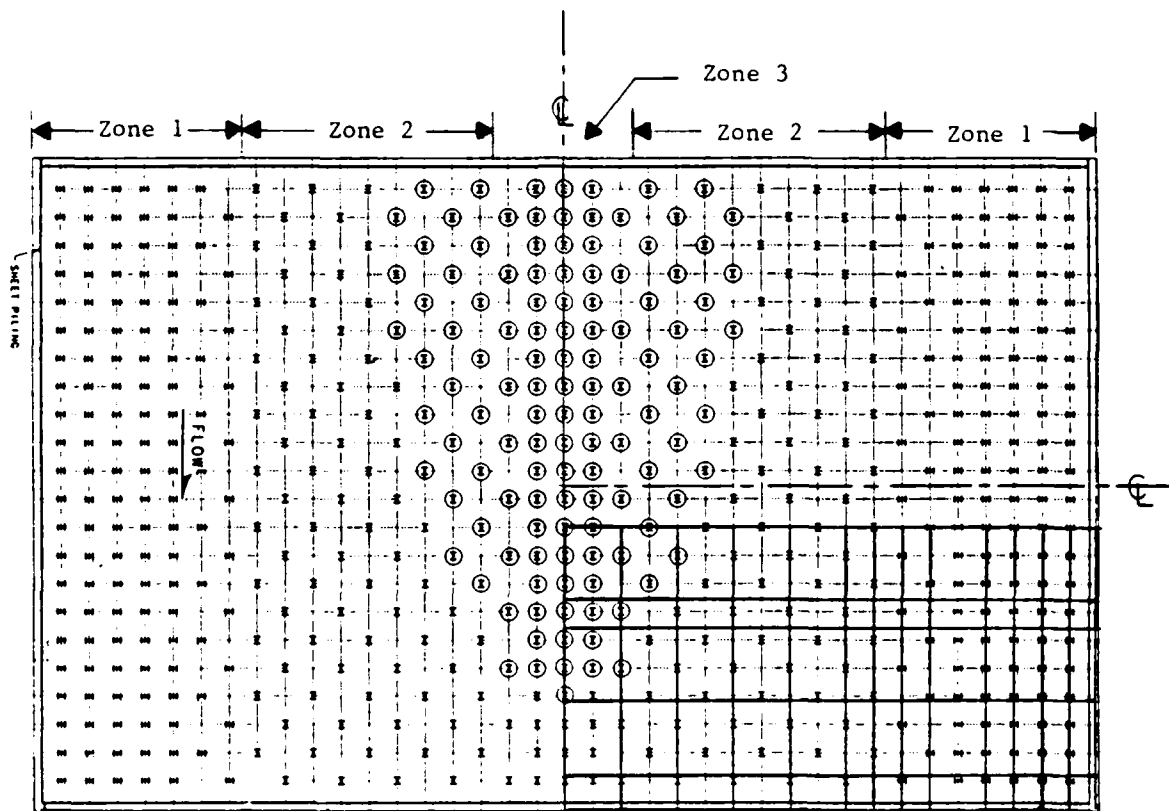
* Values used in runs with WES2DT program only to eliminate soil effects. Foundation not included in stress runs with ABAQUS.

** Modeled value for air used combines the effects of convection and conduction in an enclosed void with ABAQUS.

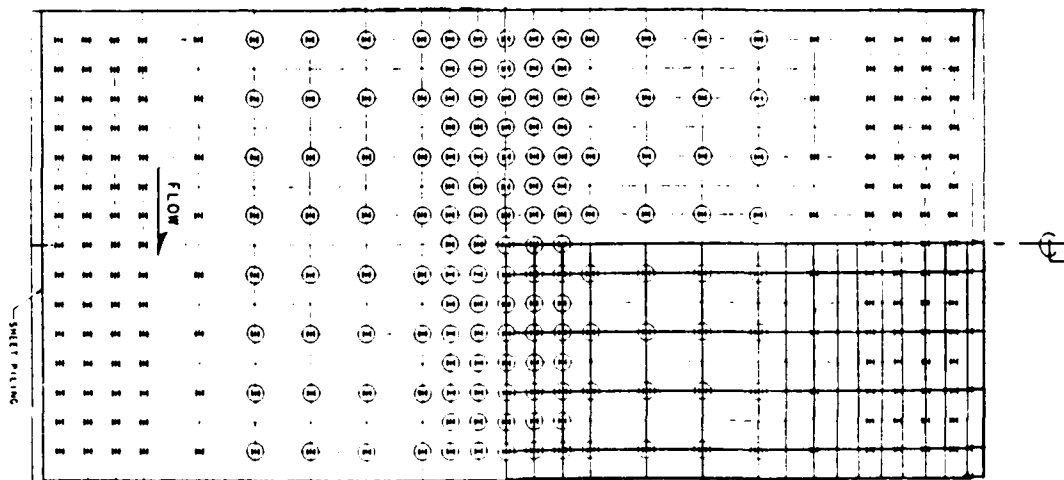
Pile Stiffnesses

30. Individual pile stiffnesses for H-piles were supplied by St. Louis District. Pile stiffnesses for strong soil pile support were used because earlier thermal studies on several projects conducted at WES indicated that the strong pile constant assumptions produced the highest thermal stresses.

31. Each two-dimensional FE model of monoliths L-13 and L-17 represents a plane transverse to the flow axis of the structure. The pile stiffnesses actually used represent the average stiffness of each row of piles parallel to the flow axis per inch thickness into the model. Figures 5a and 5b show the plan pile layouts for monoliths L-13 and L-17.



(b) Monolith 17



(a) Monolith 13

SCALE: 1" = 10'

⊙ ENCLOSED PILE INDICATES TENS. ON ANCHORS ATTACHED TO PILE

Figure 5. Location of piles in monoliths 1-13 and 1-17 including plan overlay of three-dimensional finite element grids.

32. Monolith L-13 In monolith L-13 there are either 8 or 15 piles in the flow dimension of the monolith at increasing horizontal distances from the axis. All individual piles were specified to have the same pile stiffnesses and all are oriented with the strong axis in the horizontal direction of the model (transverse to the flow). Therefore, the stiffnesses used in the 2-D analyses differ by the two pile densities only. These stiffnesses and bases for calculation for monolith L-13 are shown in Tables 2 and 3.

Table 2.

Individual Pile Stiffnesses, Monolith L-13
(Strong Pile Constants)

	Stiffness/Pile (kips/in.)
F _x (horizontal, strong axis)	54.6
F _y (horizontal, weak axis)	44.2
F _z (axial)	896.4

Table 3.

Pile Stiffnesses Used in Two-Dimensional
Stress Analyses, Monolith L-13
(Flow-direction distance = 84 ft)
(Stiffnesses are per 1.0-in. thickness)

	Distance of Flow-Direction Row of Piles from Flow Axis (ft)		
	0, 5, 10	15, 25, 35, 45, 55	65, 70, 75, 80
No. of Piles in Row	15	8	15
Stiffness (k) (kips/in.)			
Vertical	13.349*	7.1143	13.339
Horizontal	0.8125*	0.4333	0.8125

* Values at 0 ft reduced by (0.5 x k) due to location at symmetric boundary.

33. Monolith L-17 In monolith L-17 there are either 11 or 22 piles in the flow direction. The transverse distance from the flow axis outward was divided by St. Louis District into three pile stiffness zones as shown in Figure 5b. Piles in zones one and two have the same individual pile stiffnesses, however, the strong axis of the piles in zone one are transverse to the flow axis while the strong axis of piles in zone two are in the flow direction. Zone-three piles are also oriented with the strong axis in the flow direction. The stiffnesses used and bases for calculation for monolith L-17 are shown in tables 4 and 5. The stiffnesses were determined for each flow-direction row of piles individually and not for an area average of all piles in a pile zone.

34. In 3-D models of monoliths L-13 and L-17, individual piles are discretely modeled. Therefore, the stiffness values used are those provided in the first table above for each monolith. Piles were oriented in the directions described earlier and shown in Figure 5.

Table 4.

Individual Pile Stiffnesses, Monolith L-17
(Strong Pile Constants)

	Stiffness/Pile (kips/in.)	
	Zones 1 and 2 (HP 14 x 73)	Zone 3 (HP 14 x 117)
F_x^* (horizontal, strong axis)	66.88	66.88
F_y^* (horizontal, weak axis)	44.61	36.10
F_z^* (axial)	2375.	1478.

* As per axis direction convention provided with data from St. Louis District.

Table 5.

File Stiffnesses Used in Two-Dimensional
Stress Analyses, Monolith L-17
(Flow-Direction distance = 116 ft)
(Stiffnesses are per 1.0-in. thickness)

	Distance of Flow-Direction Row of Piles from Flow Axis (ft)					
	0	5	10	15, 20, 25, 30, 35, 40, 45, 50, 55	60, 65	70, 75, 80, 85, 90
Pile Zone	3	3	3	2	1	1
No. of Piles/Row	22	22	11	11	11	22
Strong Axis Direction	with flow	with flow	with flow	with flow	with flow	transverse to flow
Stiffness (k) (kips/in.)						
Vertical	11.680*	23.359	11.680	18.768	18.768	37.536**
Horizontal	0.285*	0.570	0.285	0.352	0.528	1.057**

* Values at 0 ft reduced by (0.5 x k) due to location at symmetry boundary.

** Values at 90 ft reduced by (0.663 x k) due to larger area of influence associated with this row of piles.

Construction Parameters and Boundary Conditions

Lift heights

35. Lift heights used in the FE models for both monoliths L-13 and L-17 were based upon those provided in the plans supplied by the District. Five-ft lifts were used in the base and 8- to 10-ft lifts were used in the wall of monolith L-13. Lift heights ranged from 3 ft to 5 ft in the base, 6 ft in the lower wall, and 5 to 5.5 ft in the upper wall of monolith L-17. The actual locations of lifts are shown on the FE models in Figures 2a-2e in Part VI of this report.

Placement rates

36. A concrete placement interval of 5 days between lifts was used throughout the study. Although actual placement may progress more slowly, a rate of 5 days per lift was used as the most possible case. This rate also allows less time for lift surfaces to cool between placements of lifts than at slower rates of placement. The higher internal temperatures and thermal stresses that result become the maximum values attainable at the most rapid allowable placement rate.

Ambient air temperature and foundation temperature

37. Air temperatures used were provided by the District and are representative of the project site. Figure 6 contains the mean ambient temperature versus time of the year data used in the study. The data are characterized by a sinusoidal curve peaking in August and having minimum temperatures in January. Including daily variation in temperature was felt to be beyond the scope of this study.

38. Foundation temperature was assumed to be a constant 55° F at a depth of 20 ft below the lowest elevation of each monolith. In this manner the constant temperature was specified at el. 344 ft in monolith L-13 and el. 338 ft in monolith L-17. The value of 55° F represents mean annual temperature for the project site. The initial temperature distributions within the soil were determined in a preliminary finite element calculation in which the upper surface of the soil was exposed to the ambient temperature data shown in Figure 6 and the constant value of 55° F along the lower model boundary. This heat flow simulation was run over a scaled time period exceeding one year so that final values accounted for the thermal momentum of the soil mass in responding to ambient temperature changes.

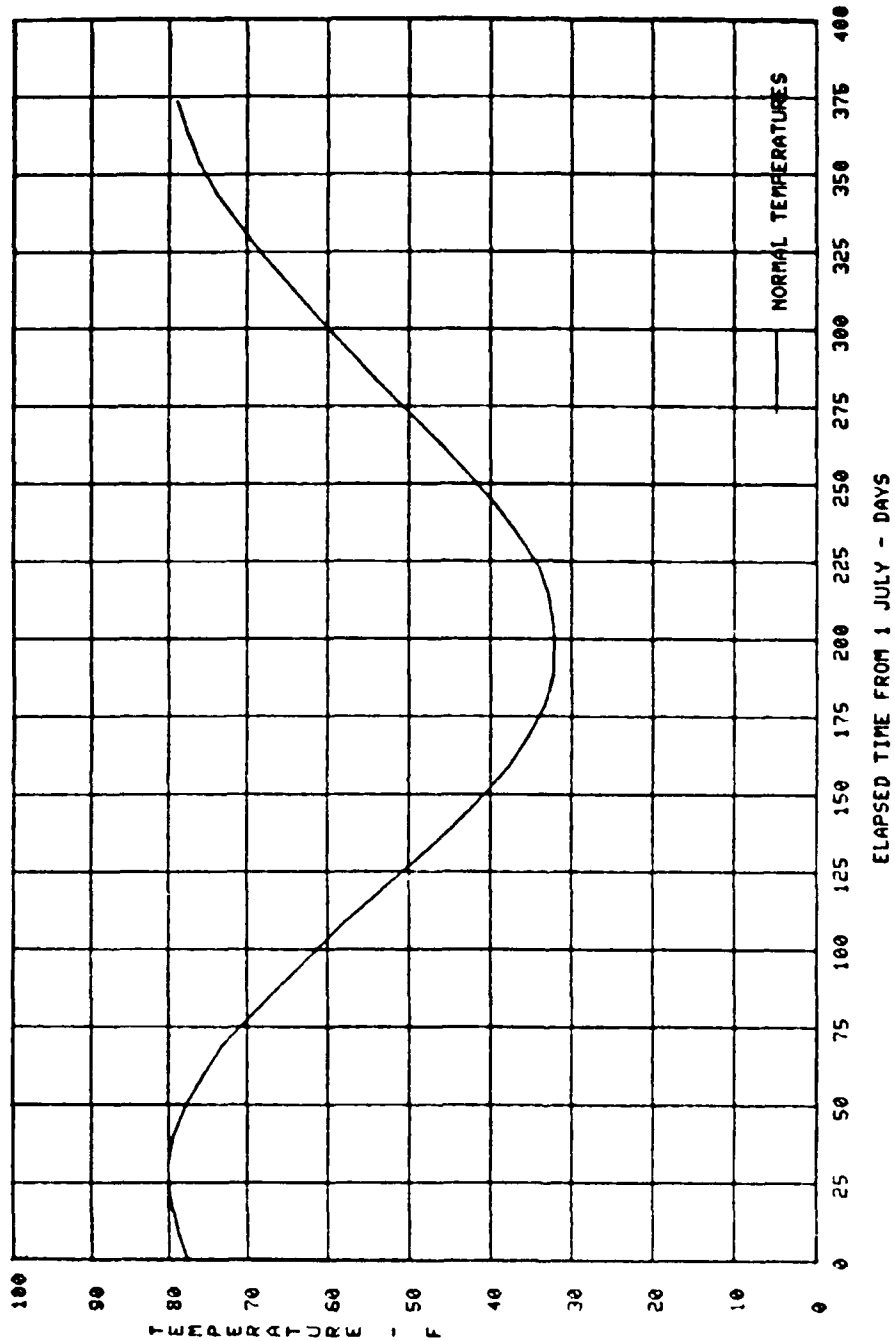


FIGURE 6 - MEAN DAILY AMBIENT TEMPERATURES FOR ALTON, IL. USED IN TEMPERATURE RUNS. DATA REPRESENTS EXPECTED NORMAL TEMPERATURES.

Construction start dates,
placement temperature

39. All computer runs in this investigation were based upon a construction start date of 1 July. Previous investigations indicated that an early summer construction start generally produces highest thermal stresses when compared to other start times during the year.

40. A maximum placement temperature of 65° F was used in all areas of the structure. During summer construction this will probably require that some of the mixing water be added as crushed ice.

Thermal boundary conditions

41. The lower boundary of the soil was fixed at 55 F as described earlier. No horizontal heat flow was permitted through the vertical soil boundaries. Heat flow was also not permitted horizontally through the vertical centerline of the monoliths represented by the extreme left side of the models.

42. The thermal boundary condition that controls heat exchange between the structure and the ambient air is a surface heat transfer coefficient. It is composed of a convection coefficient that defines heat exchange with surrounding air as well as a conduction heat transfer coefficient which defines the heat flow through the formwork.

43. The convection heat transfer coefficient is based upon surface air velocity. An air velocity of 10 mph was used for external surfaces and a velocity of 1 mph was used for the surfaces of unenclosed voids such as galleries, culverts, and recesses. It was assumed that unenclosed voids would be exposed to and ventilated by ambient air, but with reduced air flow. The enclosed voids (internal rooms) in monolith L-17 were treated similarly until the enclosing concrete of lift 8 was placed. At void closure, the FE grid in the void area was activated as air elements. This permitted the temperature of the void to vary as a function of surrounding concrete temperatures as in

reality. This modeling scheme was considered adequate even though convection heat exchange between the void and concrete surfaces and the vertical stratification of the air could not be included.

44. On external, vertical surfaces and non-enclosed recesses the insulating effect equivalent to 3/4-in. plywood forms was included in the heat transfer coefficient for the first 2 days after placement of a lift. After the second day in order to simulate form removal, the heat transfer coefficient included only convection effects of the wind. On internal, vertical formed surfaces and the horizontal upper void surfaces of monolith L-13, the effect of forms was left in place until seven days after placement of the enclosing cover lift to simulate the forming practices in such areas. In monolith L-17 all formwork heat transfer effects were removed at the time that the void cover lift was placed as described in Paragraph 43 above. All exposed horizontal surfaces were given heat transfer coefficients equivalent to convection wind effects only. No supplemental insulation was included. In 3-D runs, the flow-direction end of the monoliths were assumed free. That is, adjoining monoliths were not assumed to exist in these simulations.

Mechanical boundary conditions

45. Because it was assumed that the piles elements would carry the concrete loads, the soil was ignored in all stress runs. The symmetric boundaries were fixed in the horizontal directions. All other surfaces were assumed free including the ends of the monolith in 3-D runs.

PART VI: FINITE ELEMENT MODELS

General

46. The primary goal of this investigation has been to analyze selected monoliths of Lock and Dam 26(R) for thermal and construction induced stresses based upon calculations using state-of-the-art FE technology. While efforts were directed toward this goal, a substantial amount of developmental work and investigative analyses were conducted to implement the mechanics of using ABAQUS for incremental construction thermal stress analysis, to assess the requirements for acceptable modeling accuracy, and to evaluate the results of these analyses. These factors required development of many FE models, both two- and three-dimensional, in order to complete this investigation. The following sections describe these models, including the analytical bases, and the other considerations taken in their development.

47. Monoliths L-13 and L-17 were requested for FE analyses in this investigation. L-13 represents a typical lock chamber monolith, which due to its common transverse-section geometry, was considered ideal for comparative two- (2-D) and three-dimensional (3-D) analyses. L-17 is the lower gate monolith which is more massive, and has geometric features which include large, non-symmetrically located internal voids or rooms, non-symmetrical external recesses, and different chamber floor thicknesses. These features point strongly toward a requirement for 3-D analysis. Symmetric, half-section isometric projections of monoliths L-13 and L-17 are shown in Figure 1. Internal voids in L-17 are indicated.

48. All 2-D models developed for this investigation represent sectional planes transverse to the flow axis. The monoliths were assumed symmetric relative to the flow axis, therefore, each 2-D model consists of one-half of the transverse cross section. In all cases the axis of symmetry lies at the

left side of the model. The 3-D models consist of quarter sections of the monoliths with symmetric axes located at the flow axis and halfway between the upstream and downstream faces. Actually, the 3-D model of L-17 is not exact geometrically because the monolith is not symmetric in the flow direction. This subject is further explained below.

49. In all FE models the soil was included for the temperature analysis. With ABAQUS, the soil was removed from the stress analysis with spring (pile) elements added to support the structure. The WES2DT program did not permit removing the soil elements. As an alternative, the mechanical properties of the soil were changed to appropriate values (see Table 1) which effectively removed the soil. Pile elements were added to support the structure in a manner identical to that when using ABAQUS.

Two-Dimensional Models, L-13

ABAQUS model selection

50. Based primarily on past experience with the WES2DT program, a grid was selected for use with ABAQUS that was expected to have an adequate number of degrees of freedom to capture the essential features of the temperature and stress response expected for the problem especially considering the higher order elements available in ABAQUS. This FE grid referred to as the coarse grid is shown in Figure 7a and is characterized by two elements per lift, vertically, and two elements wide across individual sections of the culvert and wall stem. To insure that this grid was adequate, a more refined grid, Figure 7b, was also developed to be used for the 2-D analyses. The refined grid is characterized by three elements per lift, vertically, and three elements wide across individual sections of the culvert and wall stem. The assumption made was as follows: if the results of analyses using the two grids are in close agreement, the amount of refinement in the first grid would be sufficient since

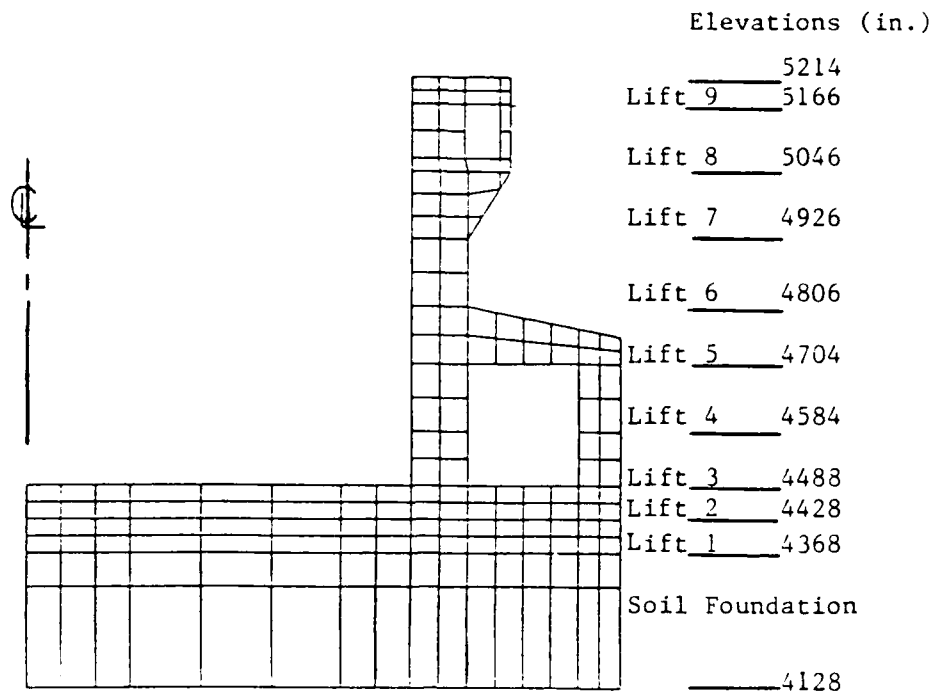


Figure 7a. Monolith 13, two-dimensional finite element grid 1 (160 Element Model) for ABAQUS

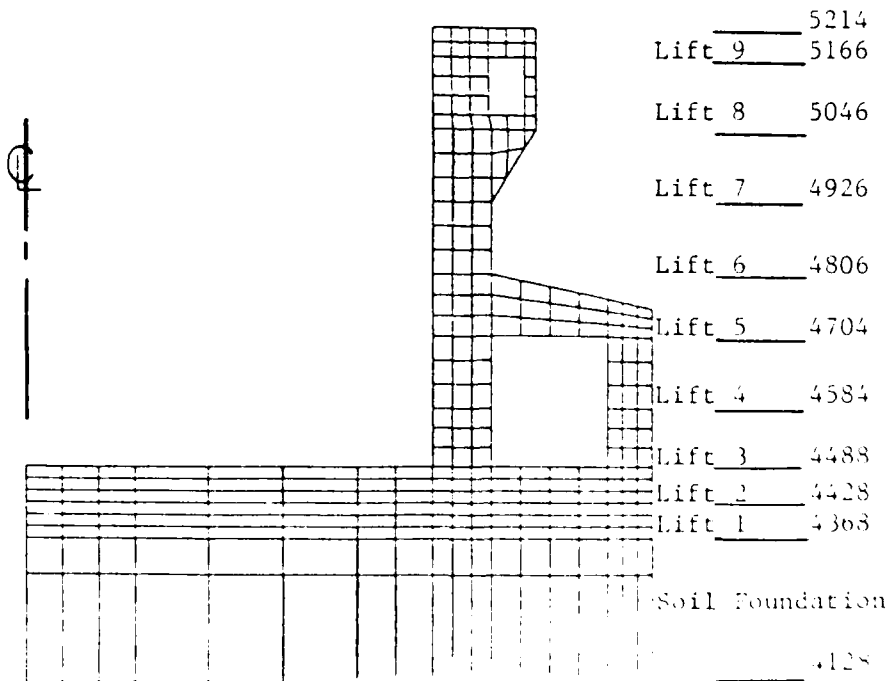


Figure 7b. Monolith 13, two-dimensional finite element grid 2 (264 Element Model) for ABAQUS

similar grids have been used in the past with WES2DT. This being the case, preparation of only one grid each would be required for 2-D analyses of L-17 and for all 3-D analyses.

WES2DT model selection

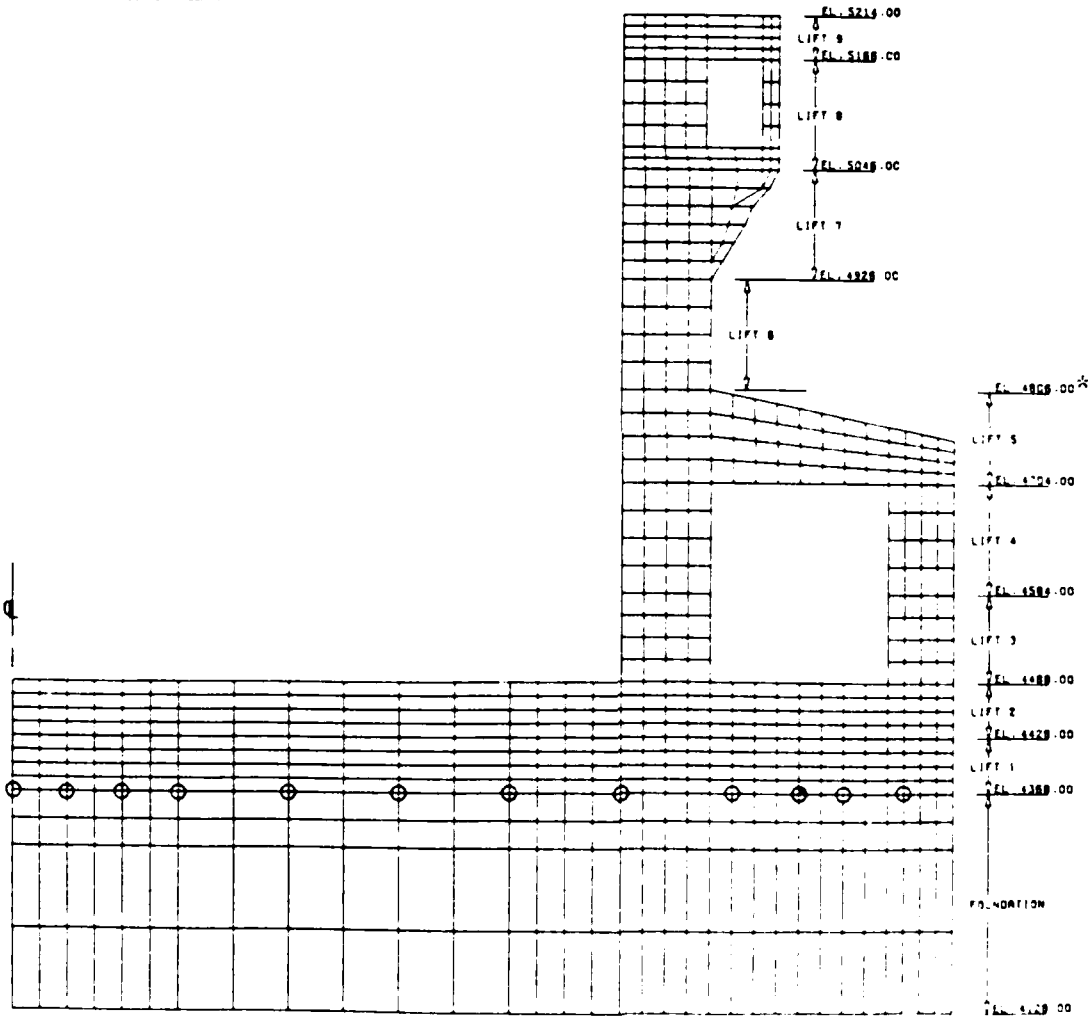
51. The FE grid of L-13 developed for use with the WES2DT program was based upon the coarse-grid model used with ABAQUS, but with an exception. The WES2DT program uses four-node elements with linear temperature distribution and linear displacement functions while ABAQUS was run with eight-node elements using quadratic temperature and displacement functions. In order to make reasonable comparisons between the two programs the grid developed for WES2DT was designed to coincide with the nodal locations in the ABAQUS model. This process yielded four elements in the WES2DT grid for every one in the ABAQUS equivalent grid. The FE grid used to model L-13 for the WES2DT program is shown in Figure 7c.

Two-Dimensional Models, L-17

ABAQUS model selection

52. The element density criteria used to establish the 2-D grid for L-17 was similar to that used for the coarse-grid FE model of L-13, namely, using two elements vertically per lift. The element density horizontally generally conforms to the locations of rows of piles which are oriented parallel to the flow axis and also to the location of internal voids. The 2-D section of L-17 chosen was that located at Station 26 + 13 near the downstream end which contained the smallest amount of voids. This section was expected to experience the largest temperature rise and was the same one used for an earlier temperature study using the WES2DT program. This section passes through the smaller of the internal voids in L-17 and through a machinery recess at the top of the monolith.

MONOLITH L-13. MES FOR PROGRAM



0 - indicates pile element locations
 * - elevations are in inches

Figure 7c. Monolith 13, two-dimensional finite element grid used with WES-2DT programs.

53. Voids and recesses were not gridded in all previous FE models. With ABAQUS, elements can be activated or deactivated dynamically as the incremental construction process is simulated. This feature provided an opportunity for a new approach in FE grid preparation for L-17. A sectional grid which represents the maximum floor and wall thicknesses was fashioned. By locating the grid to coincide with recesses and voids as well as construction joints between lifts, virtually any cross section of L-17 could be modeled by merely deactivating the appropriate elements which represented voids or recesses. This was particularly useful when dealing with the internal voids.

54. In L-13 the culvert and upper access gallery pass through the entire length of the monolith. It was assumed when modeling the thermal boundary conditions that these voids would be ventilated by ambient temperature air, but with a lower velocity than that on exposed external surfaces. In L-17 the internal voids are exposed to ambient temperature air only until the enclosing concrete is placed. Except for doorways to the adjacent voids, these voids are enclosed. After closure, the air temperatures in the voids must become a functions of the concrete surface temperatures surrounding each of the voids.

55. The ABAQUS 2-D model of L-17 shown in Figure 7d contains the full sectional grid as described above with two shaded areas included. The elements in the upper shaded area represent the machinery recess and were deactivated permanently. The elements in the lower shaded area, which represents the internal, closed void, were deactivated only until the covering lift (No. 8) was placed. The void elements were then activated with the properties of air. Thereafter, these air elements were an integral part of the model. This procedure was an effective means of modeling the thermal boundary of the void. The only limitation to this modeling technique is that convection heat transfer will in reality cause air in the void to stratify with the warmer air rising to

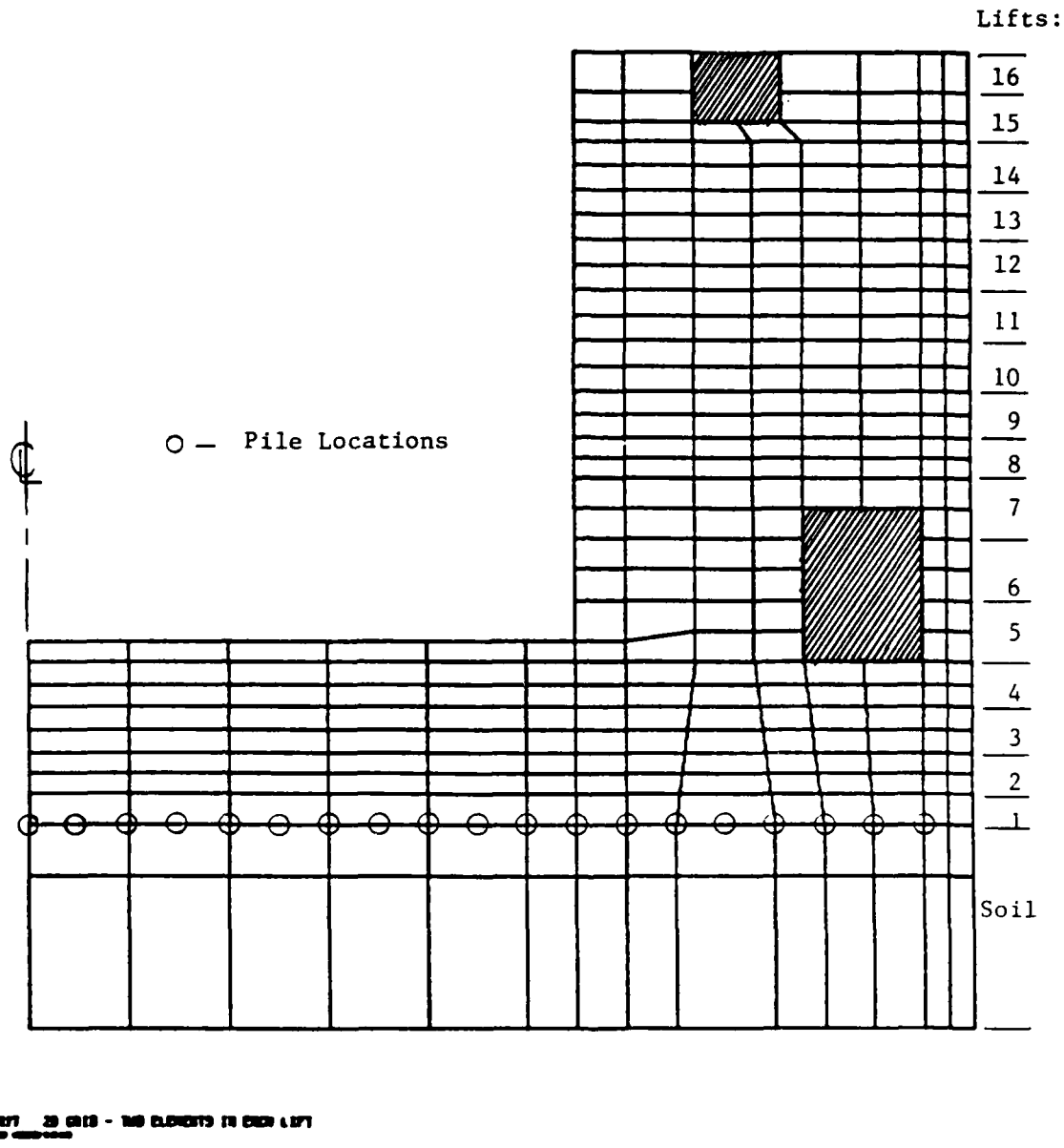


Figure 7d. Monolith 17, two-dimensional finite element model, ABAQUS, program (316 elements)

the ceiling. This minor error is acceptable in light of the benefits derived from implementing this modeling technique.

WES2DT model selection

56. The 2-D FE grid of L-17 designed for use with WES2DT program for an earlier thermal study of L & D 26(R) is shown in Figure 7e. This grid, therefore, does not compare exactly with the one prepared for use with ABAQUS as was the case for L-13. However, if the four-element-for-one technique for designing a comparable WES2DT FE grid from an ABAQUS grid was followed for L-17 as was employed for L-13, the WES2DT grid generally compares. One major difference is that the WES2DT grid only extends vertically through lift 13 (el. 420.5 ft.) whereas the ABAQUS grid extends the full 16-lift height of the monolith (el. 434.5 ft.). Through the first 13 lifts, the WES2DT grid consisted of over 900 elements which was considered a practical upper limit. Because the primary areas of interest were the chamber floor and lower wall, the top lifts were not gridded. Instead, the top surface of lift 13 was insulated appropriately at the scheduled time of placing lift 14 to simulate the correct temperature conditions in the monolith. Equivalent gravity loads for lifts 14-16 were simulated by applying surface pressure to the top of lift 13 at the appropriate times of placement of the subsequent lifts.

Three-Dimensional Model, L-13

57. As described earlier, the 3-D FE model prepared for L-13 is a quarter section of the monolith. This model shown in Figure 8a is made up of five element planes in the flow direction each with a sectional grid identical to the coarse-grid 2-D model. The four interfaces planes between these five element planes coincide with the location of those complete rows of piles oriented transverse to the flow direction. Figure 5a shows a plan view of the quarter-section L-13 3-D model superimposed on the pile layout with vertical

DEMOLITION GATE MONOLITH OF STATION 13 + 00.00

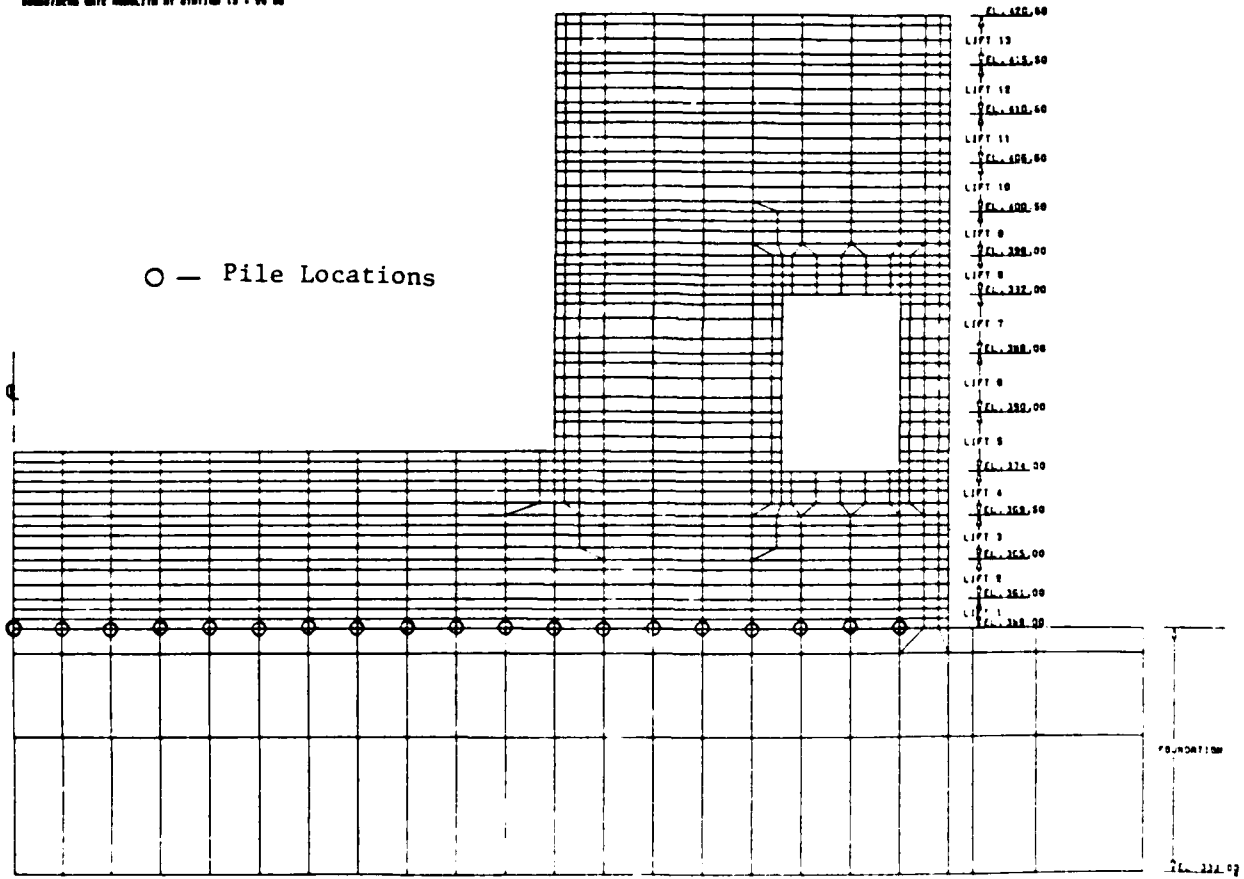


Figure 7e. Monolith 17, two-dimensional finite element model, WESZDT program (908 elements)

y
x
z
153.4444 HORIZONTAL IN UNITS PER INCH
153.4444 VERTICAL IN UNITS PER INCH
ROTATION: Z 0.0 Y 30.0 X 20.0

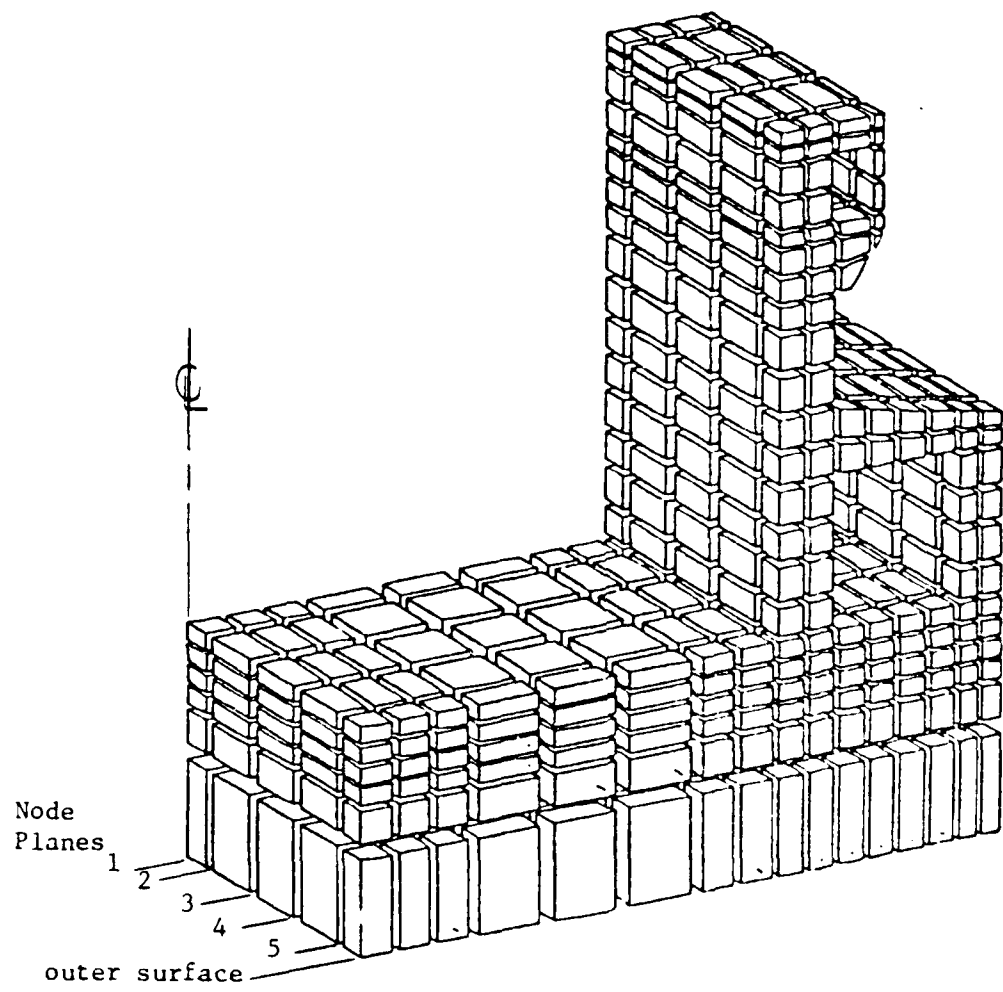


Figure 8a. Three-Dimensional Grid of Monolith L 13

element boundary projections shown. The grid was designed to model the geometry of the monolith with a minimum number of elements in the flow direction which were adequate to provide acceptable results and have element boundaries coinciding with pile locations. The 20-node 3-D elements that were used have nodes located at the element corners and midway between corners. As seen in Figure 5a, most of the piles coincided with these nodal locations in the model. For those that did not, a capability within ABAQUS was used that permitted creation of extra nodes at these unassigned pile locations.

Three-Dimensional Model, L-17

58. It was recognized very early in the investigation that proper 3-D modeling of L-17 would require a half-section symmetric representation of the monolith. This was due to the non-symmetric geometry in the flow direction. However, constraints identified by the developers of ABAQUS and those recognized by the investigators indicated that a half-section model was not feasible. In fact it was recognized that even a minimally discretized quarter-section model would severely tax available computer and project resources due to the massiveness of the monolith. The primary constraint was a practical upper limit of approximately 1000 elements.

59. It was evident that several trade-offs would be necessary for the L-17 3-D model. The construction plan for L-17 indicated concrete placement in 16 lifts. It had been determined from the ABAQUS incremental construction evaluations and L-13 2-D grid comparisons that at least two elements vertically per lift were preferred for adequate calculation accuracy. It was also evident after examination of the geometric features that a minimum of six elements were required in the flow direction in order to model the geometric features, which included voids and recesses, and to include the actual flow direction axis of symmetry. Based upon the 5-ft by 5-ft spacing of the basic pile location grid,

it was evident that the maximum size of a 3-D element in the floor slab was 10-ft square in plan. Smaller elements were necessary in the wall. These criteria were used to lay out a preliminary grid. The resulting grid size was close to 2000 elements or nearly double the practical limit.

60. To keep within the 1000-element practical limit several changes had to be made. First, except for lift 5, each lift was gridded with only one element vertically rather than two. The number of element planes in the flow direction had to be reduced from six to five. In order to properly model the monolith and discrete piles, it was necessary for element boundaries in the flow direction to correspond to every other transverse row of piles. Therefore, the resulting quarter-section boundary transverse to the flow is not located at the monolith midpoint in the flow direction. The 3-D nodes is slightly less than one-half the monolith dimension in the flow direction.

61. The basic 3-D grid resembled an reversed "L" shape for the floor and wall similar to that used for the 2-D L-17 model. All voids and recesses were similarly obtained by deactivating the appropriate elements. Figures 8b and 8c are isometric projections of the L-17 3-D grid. Figure 8b shows the basic grid with external, deactivated elements shaded while Figure 8c shows the grid with the deactivated elements removed. Figure 8d shows the basic sectional element plane and the five elements planes with the internal and external deactivated elements shaded.

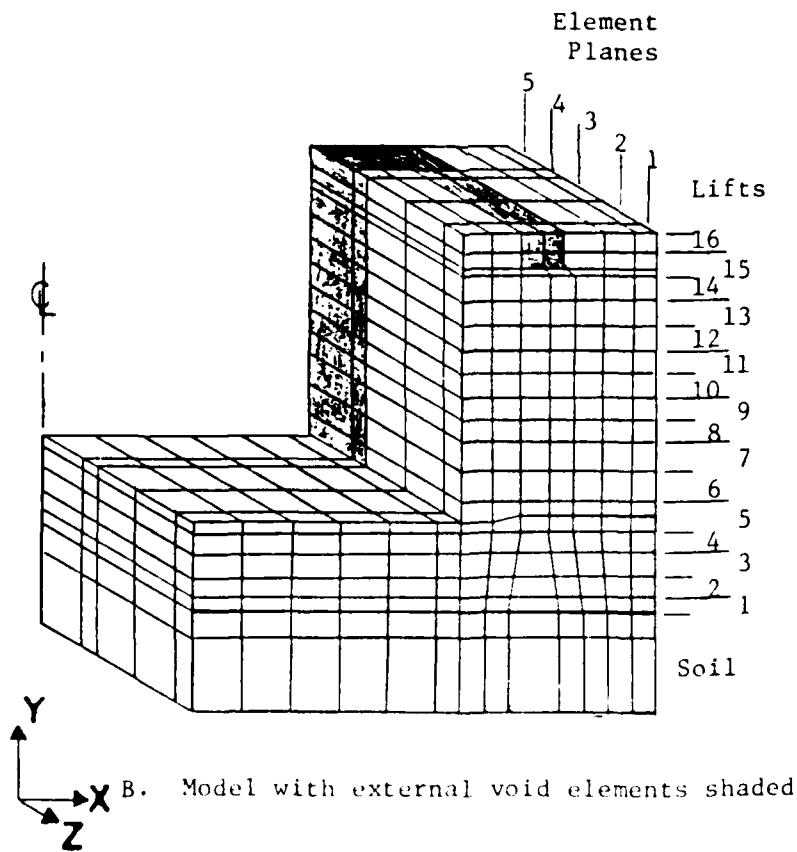
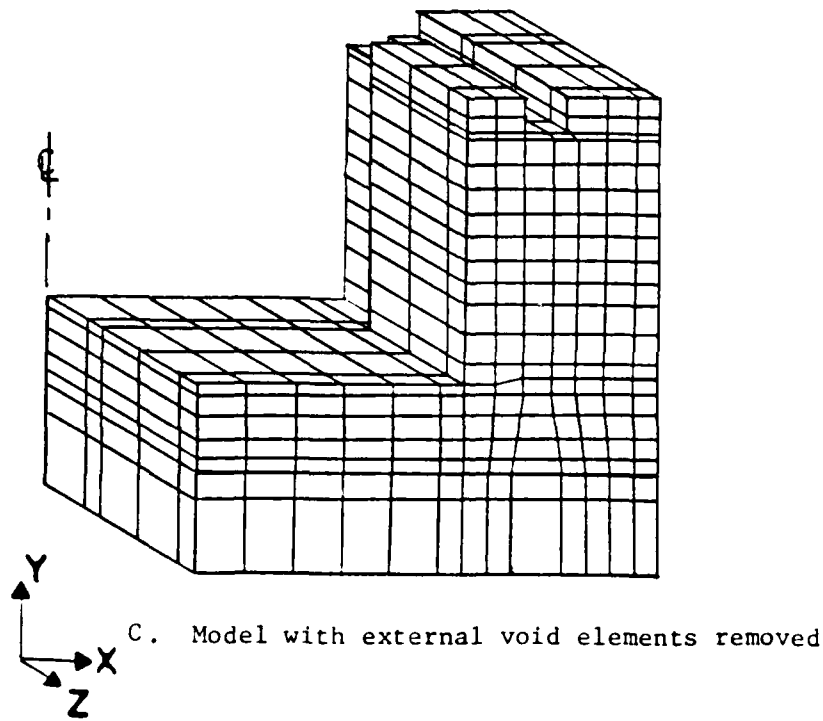
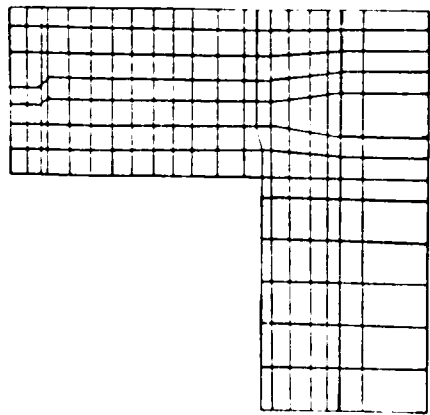
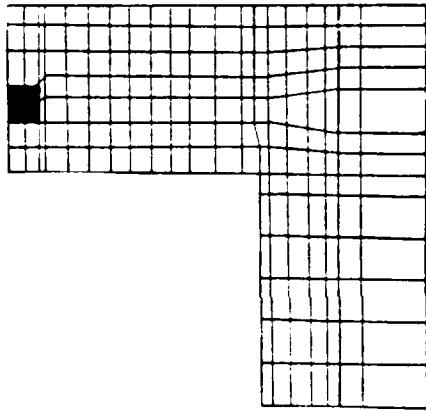


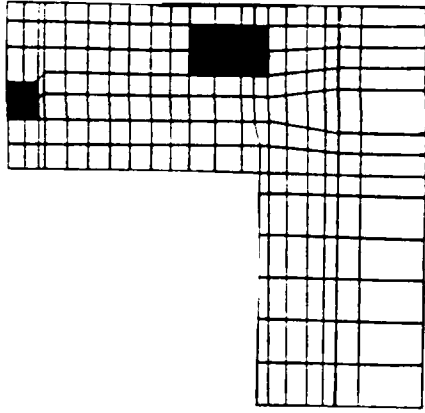
Figure 8. Monolith 17, three-dimensional finite element model, ABAQUS program (910 elements)



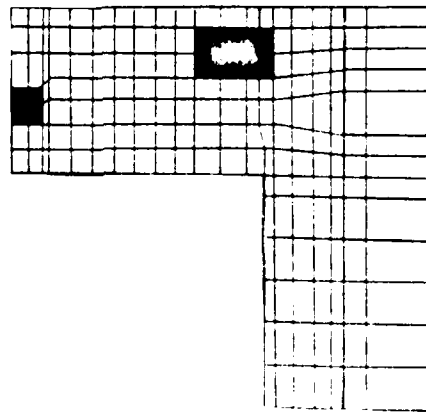
Basic Element Plane



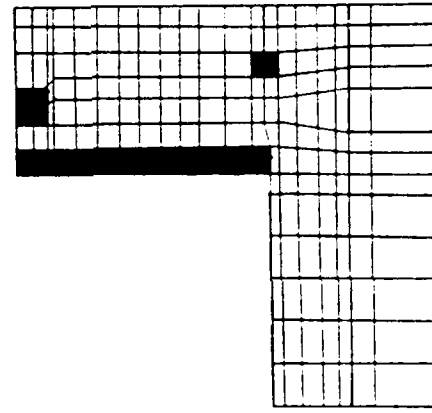
Element Plane 1
(outer surface)



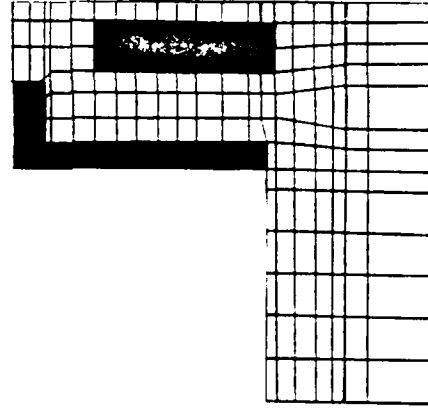
Element Plane 2



Element Plane 3



Element Plane 4



Element Plane 5

■ - Void Elements

Figure 8d. Element Planes for Monolith 17, three-dimensional model showing internal and external voids.

PART VII: THERMAL ANALYSES OF MONOLITH L-13

Presentation of Results

Two-dimensional temperature analysis

62. Temperature analyses of monolith L-13 were performed using both the ABAQUS and WES2DT programs. Figures 9a thru 9d show results from the ABAQUS program using FE grid 1 (Figure 7a) at four stages of construction. Figures 10a thru 10d show the results of the ABAQUS program using FE grid 2 (Figure 7b) at four stages of construction. Results from the WES2DT program using a FE grid (Figure 7c) functionally equivalent to that of ABAQUS FE grid 1 are shown in Figures 11a thru 11d for the same four stages of construction used for presenting ABAQUS data.

Three dimensional temperature analysis

63. The ABAQUS program was used to make a 3-D analysis of monolith L-13 using the FE grid shown in Figure 4. These results are shown using contour plots (Figures 12a - 12d thru 15a - 15d) which show temperatures on faces of elements in the five element planes (Figure 8) of the structure at four stages of construction. Four of the element planes are internal, one is an outer surface.

Discussion of Results

Two-dimensional temperature analysis

64. The ABAQUS results for FE grids 1 and 2 were virtually identical. It was evident from these runs that the refinement in grid 1 was adequate for the temperature analysis. The comparison of ABAQUS results to WES2DT results was also excellent. The only minor discrepancy came in the contours 5 days

after lift 5 was placed (Figures 9c, 10c, and 11c) in the lift 5 concrete. Here the ABAQUS results show a larger area with temperatures above 95° F in lift 5. This seems more realistic since the base slab exhibited a similar contour pattern at the the same time after placement (Figures 9a, 10a, and 11a). Only localized differences were seen between these different analyses, with maximum values and the general temperature distribution in very good agreement at all stages of the construction sequence.

Three-dimensional temperature analysis

65. Upon examining the temperature contour plots of the base slab, Figures 12b thru 12c, it is evident that the temperature distribution was constant along the monolith in the direction of flow (z-direction). This was expected since the problem closely approximates 2-D assumptions for constant boundary conditions on the outer surface and centerline. Only in the vicinity of five feet of the outer surface did any variation take place. This is shown in Figure 12a. Similar response is shown by the contours for all other stages of construction (Figures 13 thru 15). The contours within the monolith (away from the exposed outer surface) also match, almost identically, the ABAQUS 2-D plots from Figures 9 thru 10. These contours show that monolith L-13, for these boundary conditions, is a 2-D problem.

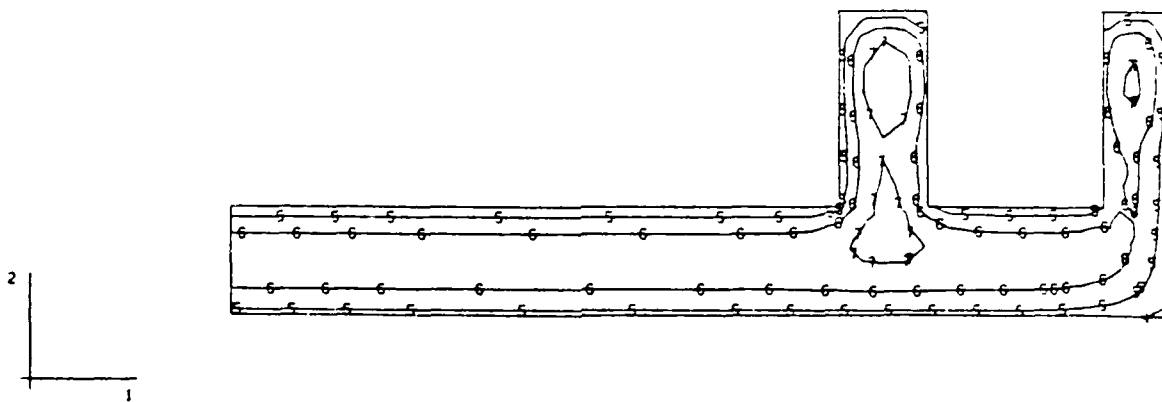
TEMP.
 I. D. VALUE
 1 +6.50E+01
 2 +7.00E+01
 3 +7.50E+01
 4 +8.00E+01
 5 +8.50E+01
 6 +9.00E+01
 7 +9.50E+01
 8 +1.00E+02
 9 +1.05E+02
 10 +1.10E+02
 11 +1.15E+02



LIFT2 - M13 - COARSE MODEL
 STEP 4 INCREMENT 6 ABAQUS VERSION 4.5-147

Figure 9a. Temperature distribution in structure 5 days after lift 2 is placed (from analysis using first grid)

TEMP.
 I.D. VALUE
 1 +6.50E-01
 2 +7.00E-01
 3 +7.50E-01
 4 +8.00E-01
 5 +8.50E-01
 6 +9.00E-01
 7 +9.50E-01
 8 +1.00E-02
 9 +1.05E-02
 10 +1.10E-02
 11 +1.15E-02



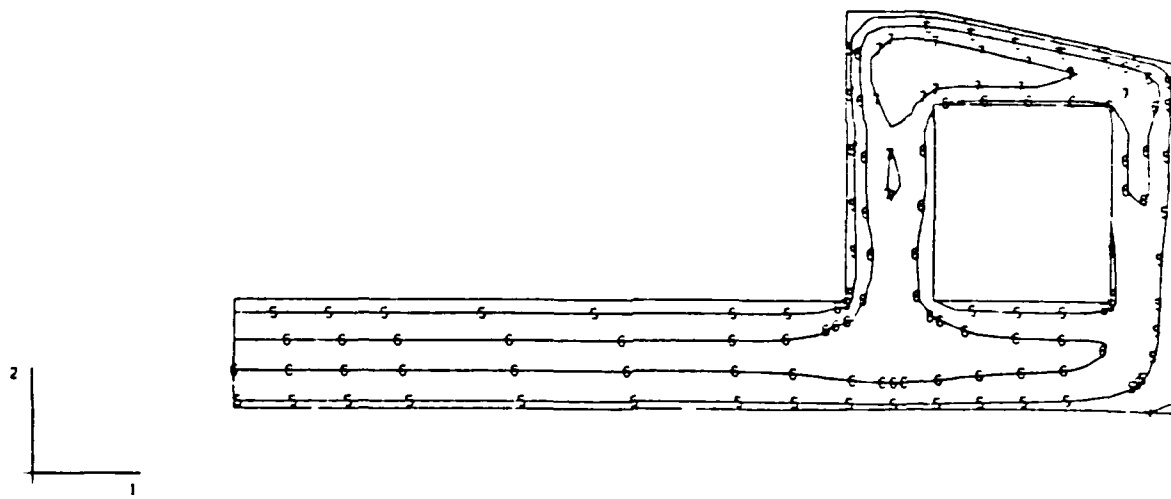
LIFT4 - M13 - COARSE MODEL

STEP 8 INCREMENT 6

- ABAQUS VERSION 4.5-147

Figure 9b. Temperature distribution in structure 5 days after lift 4 is placed (from analysis using first grid)

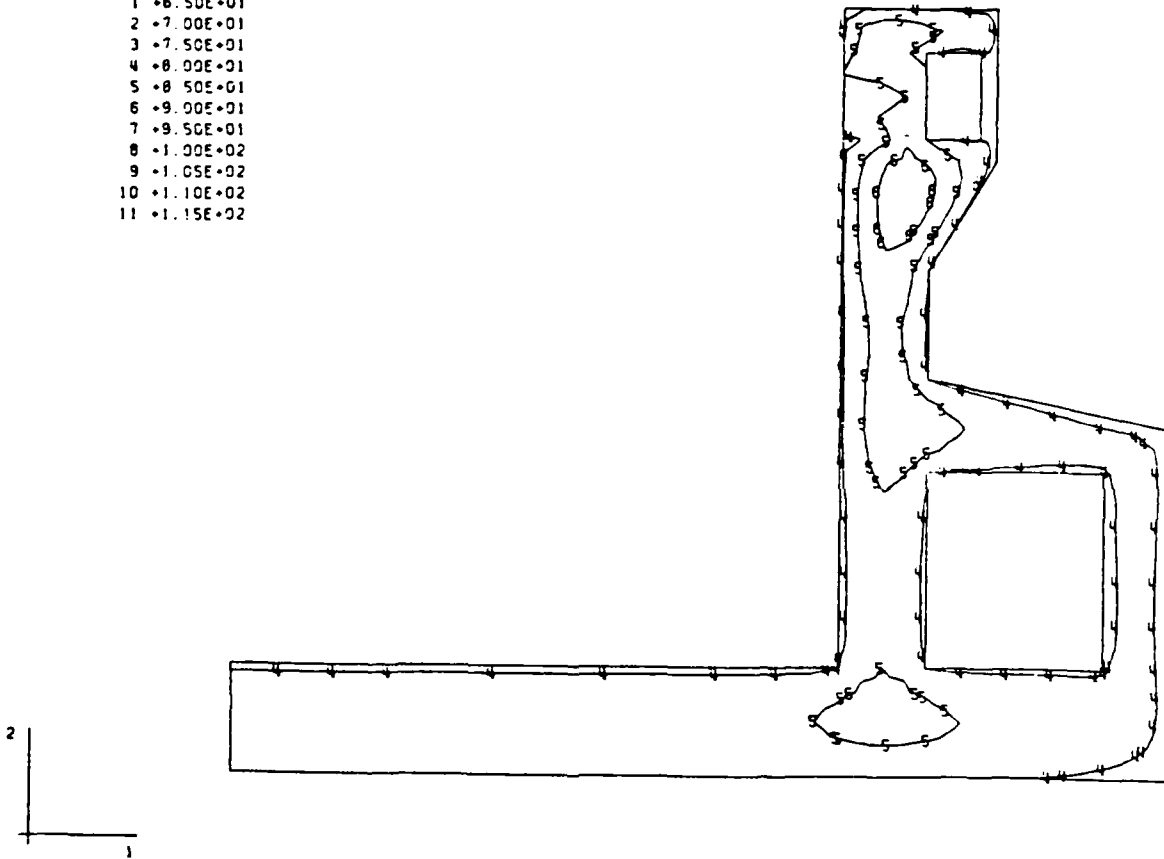
TEMP.
 I. D. VALUE
 1 +6.50E-01
 2 +7.00E-01
 3 +7.50E-01
 4 +8.00E-01
 5 +8.50E-01
 6 +9.00E-01
 7 +9.50E-01
 8 +1.00E-02
 9 +1.05E-02
 10 +1.10E-02
 11 +1.15E-02



LIFTS - M13 - COARSE MODEL
 STEP 10 INCREMENT 6 ABAQUS VERSION 4.5.147

Figure 9c. Temperature distribution in structure 5 days after lift 5 is placed (from analysis using first grid)

TEMP.
 I. D. VALUE
 1 +6.50E+01
 2 +7.00E+01
 3 +7.50E+01
 4 +8.00E+01
 5 +8.50E+01
 6 +9.00E+01
 7 +9.50E+01
 8 +1.00E+02
 9 +1.05E+02
 10 +1.10E+02
 11 +1.15E+02



LIFT9 - M13 - COARSE MODEL

STEP 18 INCREMENT 10

ABAQUS VERSION 4-5-147

Figure 9d. Temperature distribution in structure 7 days after lift 9 is placed (from analysis using first grid)

TEMP.
 I. D. VALUE
 1 +6.50E+01
 2 +7.00E+01
 3 +7.50E+01
 4 +8.00E+01
 5 +8.50E+01
 6 +9.00E+01
 7 +9.50E+01
 8 +1.00E+02
 9 +1.05E+02
 10 +1.10E+02
 11 +1.15E+02



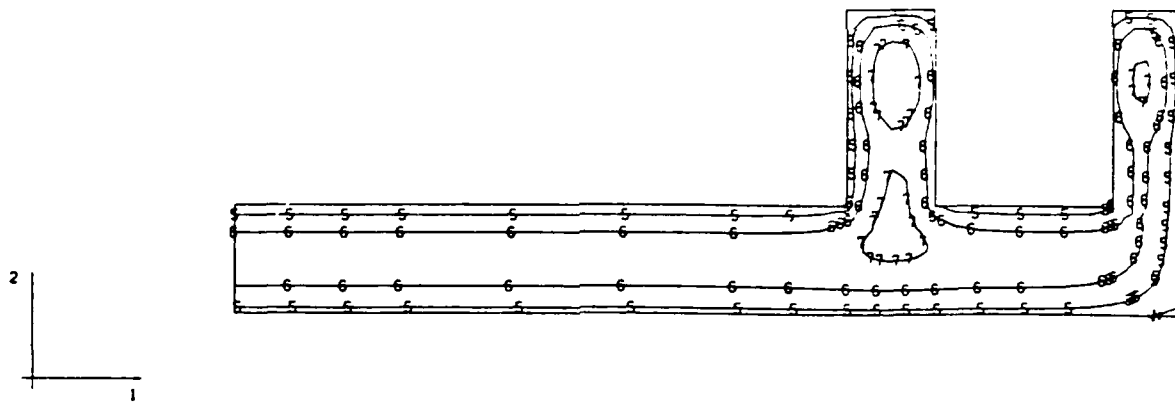
LIFT2 - M13 - FINE MODEL

STEP 4 INCREMENT 6

ABAQUS VERSION 4.5-147

Figure 10a Temperature distribution in structure 5 days after lift 2 is placed (from analysis using second grid)

TEMP.
 I. D. VALUE
 1 +6.50E+01
 2 +7.00E+01
 3 +7.50E+01
 4 +8.00E+01
 5 +8.50E+01
 6 +9.00E+01
 7 +9.50E+01
 8 +1.00E+02
 9 +1.05E+02
 10 +1.10E+02
 11 +1.15E+02



LIFT4 - M13 - FINE MODEL

STEP 8 INCREMENT 6

ABAQUS VERSION 4.5-147

Figure 10b. Temperature distribution in structure 5 days after lift 4 is placed (from analysis using second grid)

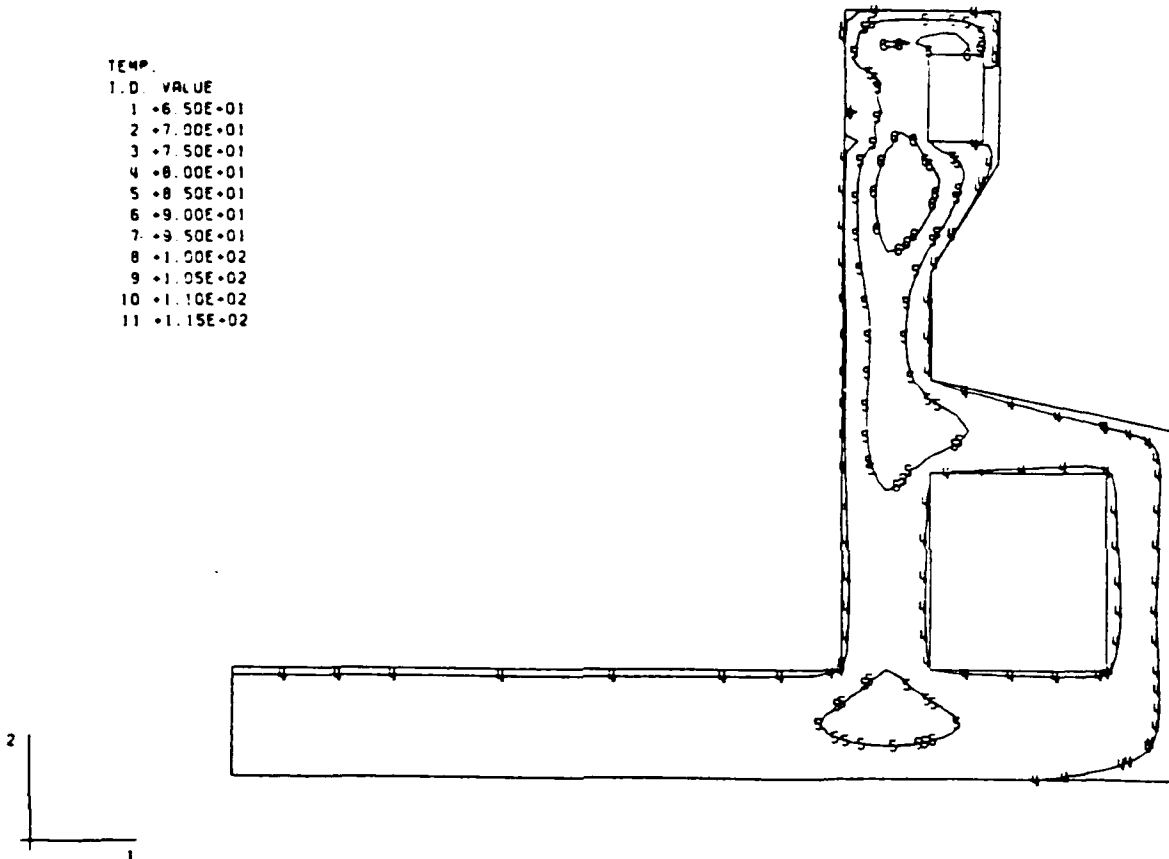
TEMP.
 I.D. VALUE
 1 +6.50E+01
 2 +7.00E+01
 3 +7.50E+01
 4 +8.00E+01
 5 +8.50E+01
 6 +9.00E+01
 7 +9.50E+01
 8 +1.00E+02
 9 +1.05E+02
 10 +1.10E+02
 11 +1.15E+02



LIFTS - M13 - FINE MODEL
 STEP 10 INCREMENT 6 ABAQUS VERSION 4-5-147

Figure 10c. Temperature distribution in structure 5 days after lift 5 is placed (from analysis using second grid)

TEMP.
 I.D. VALUE
 1 +6.50E-01
 2 +7.00E-01
 3 +7.50E-01
 4 +8.00E-01
 5 +8.50E-01
 6 +9.00E-01
 7 +9.50E-01
 8 +1.00E-02
 9 +1.05E-02
 10 +1.10E-02
 11 +1.15E-02



LIFT9 - M13 - FINE MODEL

STEP 10 INCREMENT 10

ABAQUS VERSION 4-5-147

Figure 10d. Temperature distribution in structure 7 days after lift 9 is placed (from analysis using second grid)

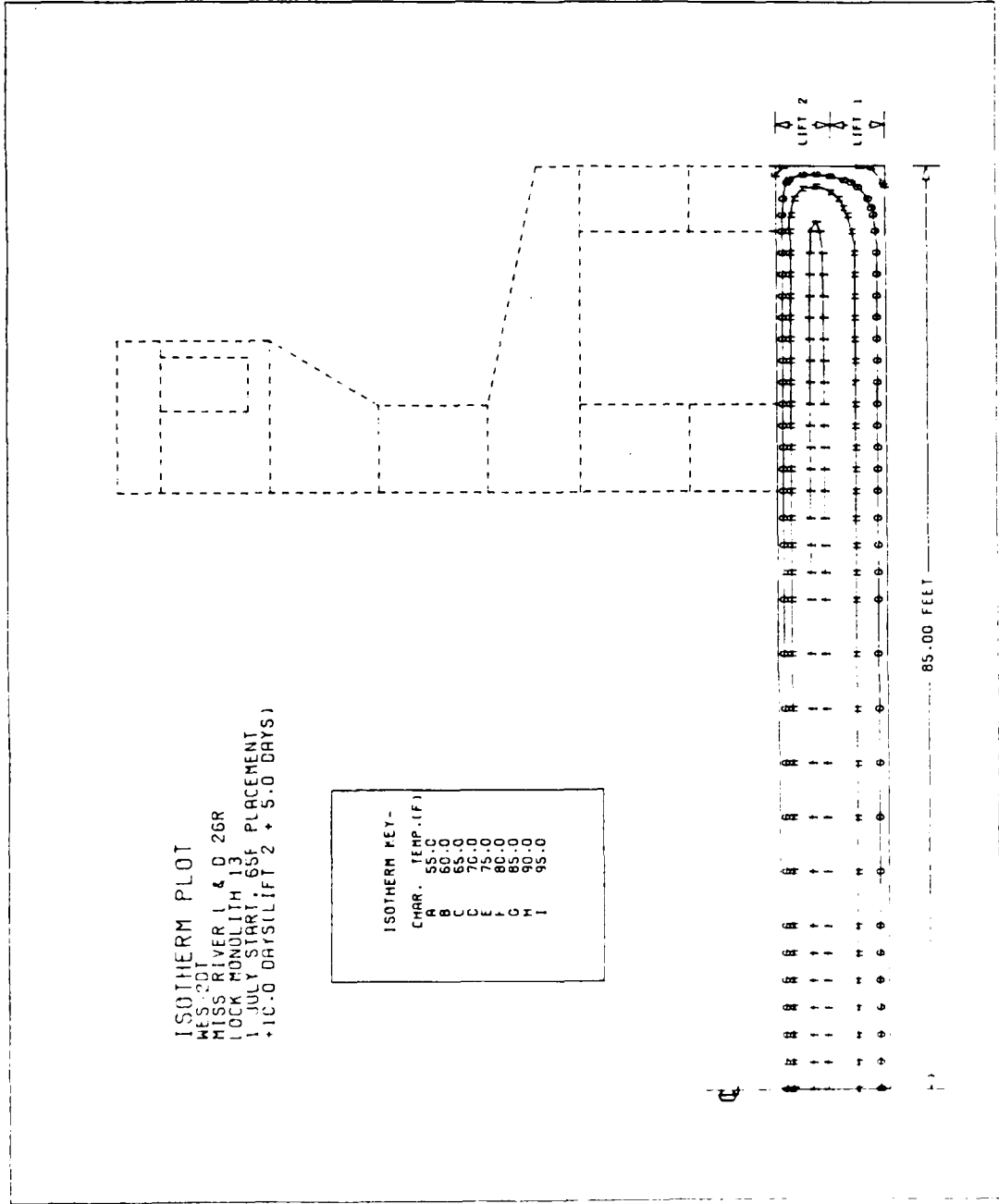


Figure 11a. Temperature distribution in structure 5 days after lift 2 is placed from WES-2DT program.

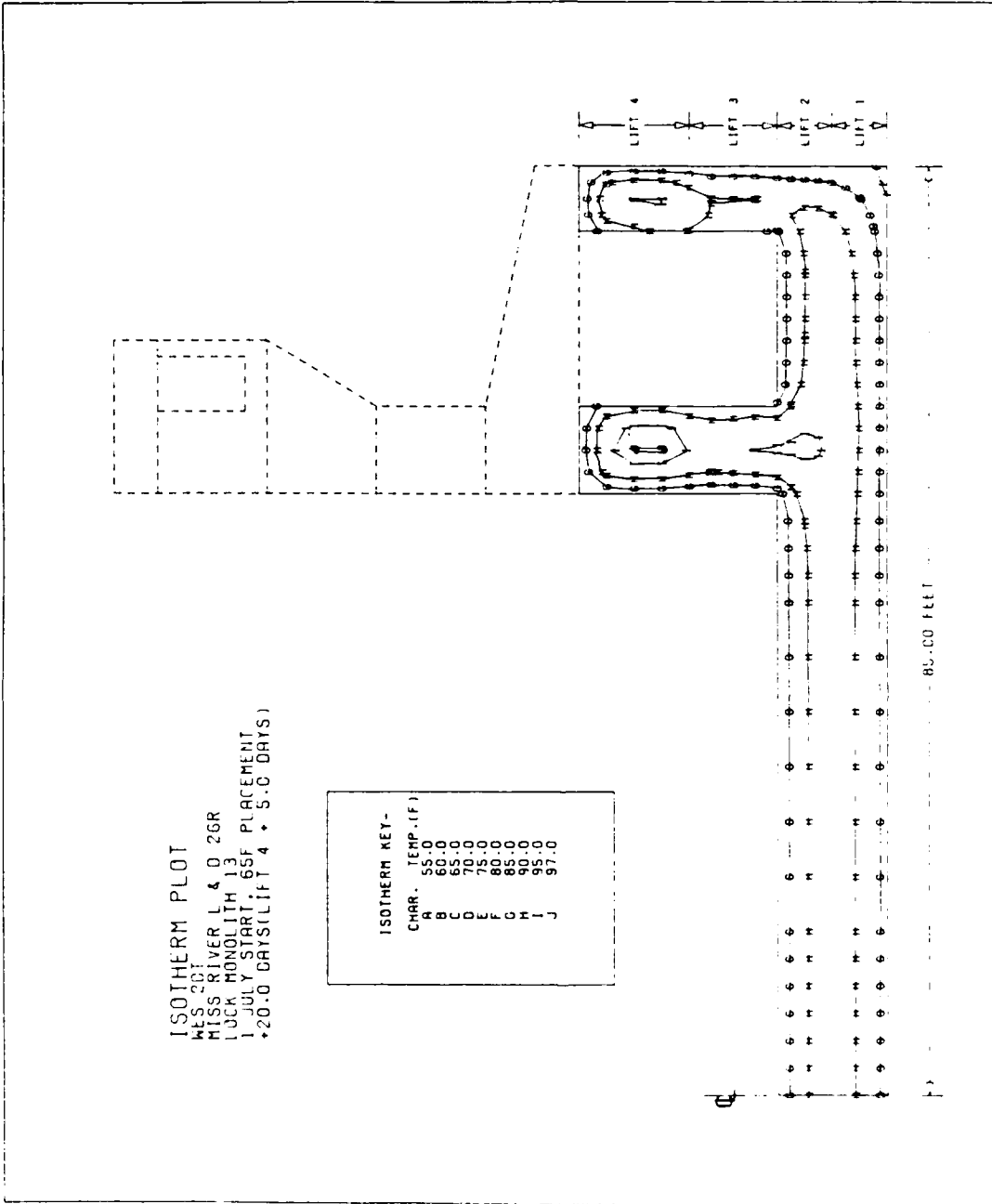


Figure 11b. Temperature distribution in structure 5 days after lift 4 is placed from WES-2DT program.

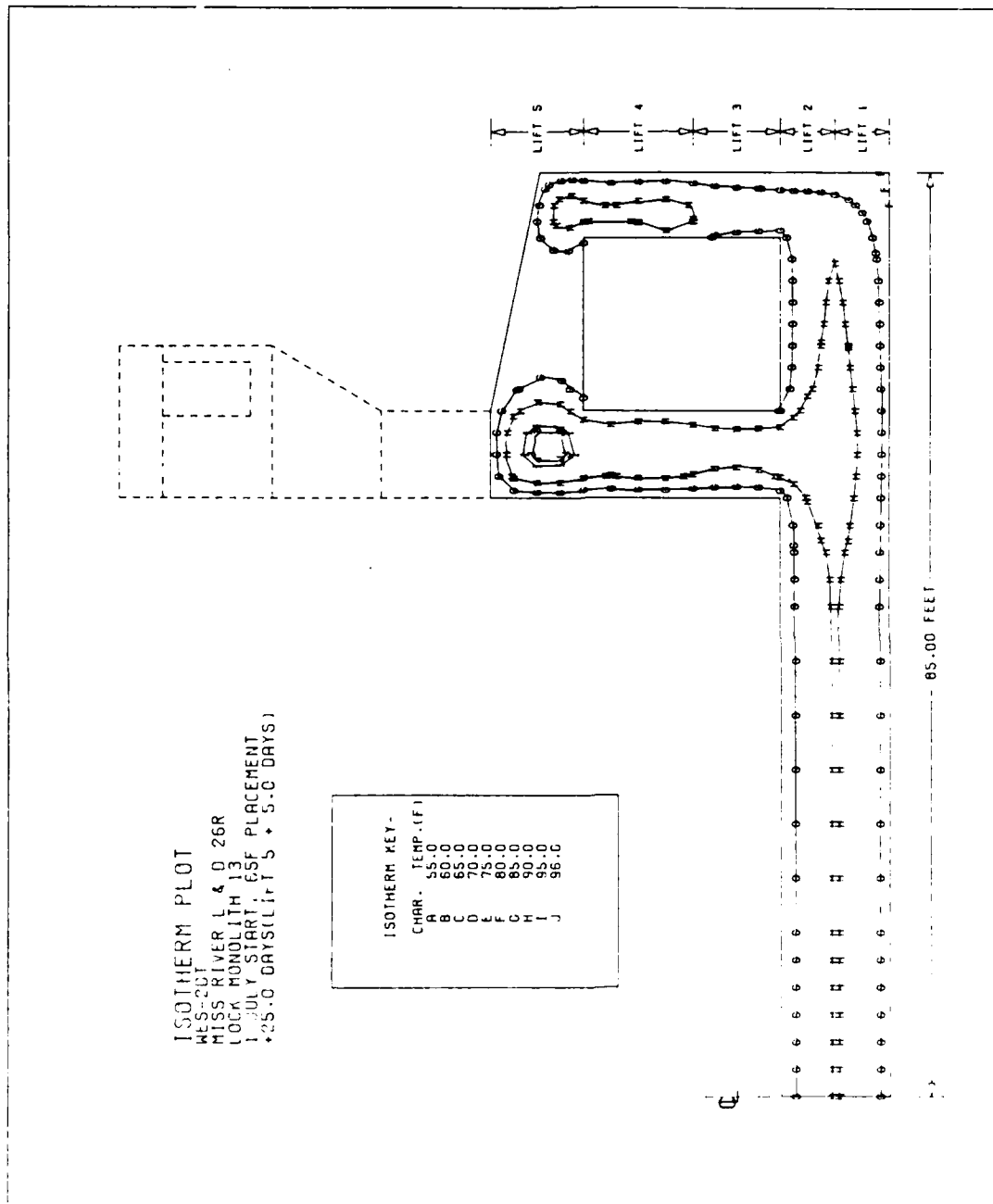


Figure 11c. Temperature distribution in structure 5 days after lift 5 is placed from WES-2DT program.

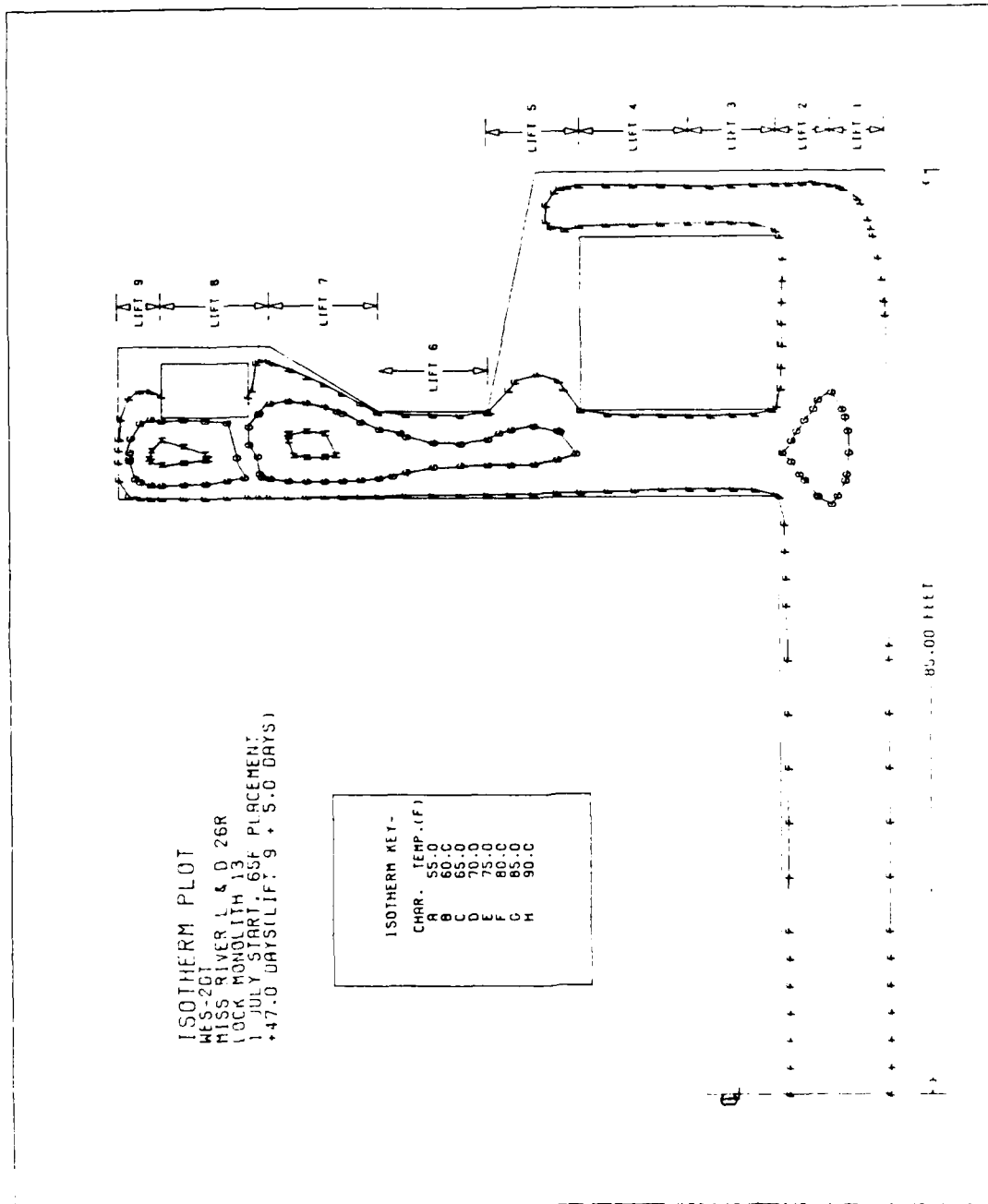
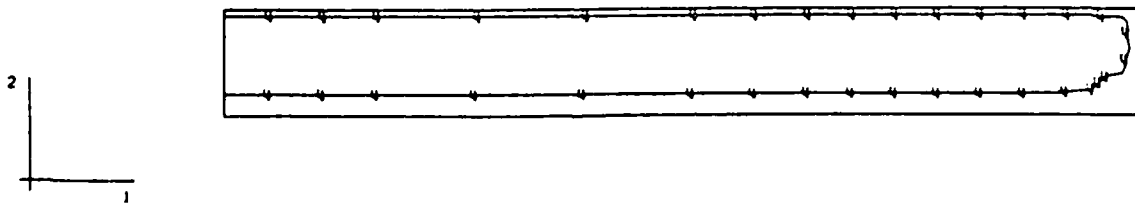


Figure 11d. Temperature distribution in structure 7 days after lift 9 is placed using WES- 2DT program.

TEMP.
 I.D. VALUE
 1 +6.50E+01
 2 +7.00E+01
 3 +7.50E+01
 4 +8.00E+01
 5 +8.50E+01
 6 +9.00E+01
 7 +9.50E+01
 8 +1.00E+02
 9 +1.05E+02
 10 +1.10E+02
 11 +1.15E+02



LIFT2 - M13 - 3D GRID MODEL - OUTER SURFACE
 STEP 4 INCREMENT 8

Figure 12a. Temperature distribution in outer surface of structure 5 days after lift 2 is placed.

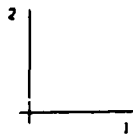
TEMP.
 I.D. VALUE
 1 +6.50E+01
 2 +7.00E+01
 3 +7.50E+01
 4 +8.00E+01
 5 +8.50E+01
 6 +9.00E+01
 7 +9.50E+01
 8 +1.00E+02
 9 +1.05E+02
 10 +1.10E+02
 11 +1.15E+02



LIFT2 - M13 - 3D GRID MODEL - NODE PLANE 5
 STEP 4 INCREMENT 6 ABAQUS VERSION 4.5-147

Figure 12b. Temperature distribution in node plane 5 of structure 5 days after lift 2 is placed.

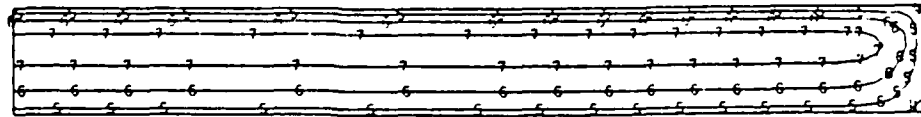
TEMP.
 1.0. VALUE
 1 +6.50E+01
 2 +7.00E+01
 3 +7.50E+01
 4 +8.00E+01
 5 +8.50E+01
 6 +9.00E+01
 7 +9.50E+01
 8 +1.00E+02
 9 +1.05E+02
 10 +1.10E+02
 11 +1.15E+02



LIFT2 - M13 - 3D GRID MODEL - NODE PLANE 4
 STEP 4 INCREMENT 6 ABAQUS VERSION 4-5-147

Figure 12c. Temperature distribution in node plane 4 of structure 5 days after lift 2 is placed.

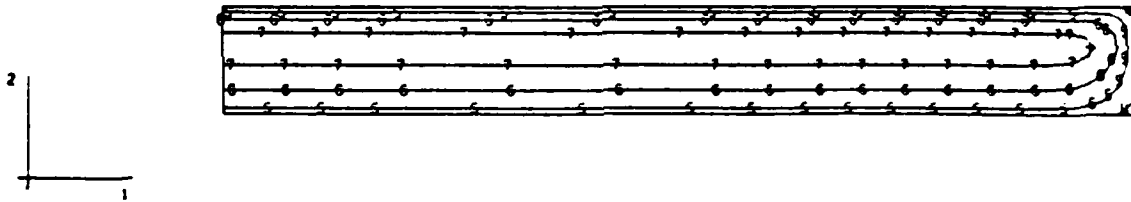
TEMP.
 I.D. VALUE
 1 +6.50E+01
 2 +7.00E+01
 3 +7.50E+01
 4 +8.00E+01
 5 +8.50E+01
 6 +9.00E+01
 7 +9.50E+01
 8 +1.00E+02
 9 +1.05E+02
 10 +1.10E+02
 11 +1.15E+02



LIFT2 - M13 - 3D GRID MODEL - NODE PLANE 3
 STEP 4 INCREMENT 6 ABAQUS VERSION 4-5-147

Figure 12d. Temperature distribution in node plane 3 of structure 5 days after lift 2 is placed.

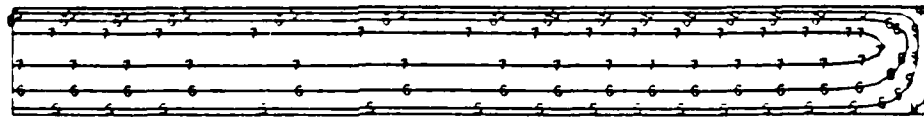
TEMP.
 I.D. VALUE
 1 +6.50E+01
 2 +7.00E+01
 3 +7.50E+01
 4 +8.00E+01
 5 +8.50E+01
 6 +9.00E+01
 7 +9.50E+01
 8 +1.00E+02
 9 +1.05E+02
 10 +1.10E+02
 11 +1.15E+02



LIFT2 - M13 - 3D GRID MODEL - NODE PLANE 2
 STEP 4 INCREMENT 6 ABAQUS VERSION 4-5-147

Figure 12e. Temperature distribution in node plane 2 of structure 5 days after lift 2 is placed.

TEMP.
 I.D. VALUE
 1 -6.50E-01
 2 +7.00E-01
 3 +7.50E-01
 4 +8.00E-01
 5 +8.50E-01
 6 +9.00E-01
 7 +9.50E-01
 8 +1.00E-02
 9 +1.05E-02
 10 +1.10E-02
 11 +1.15E-02



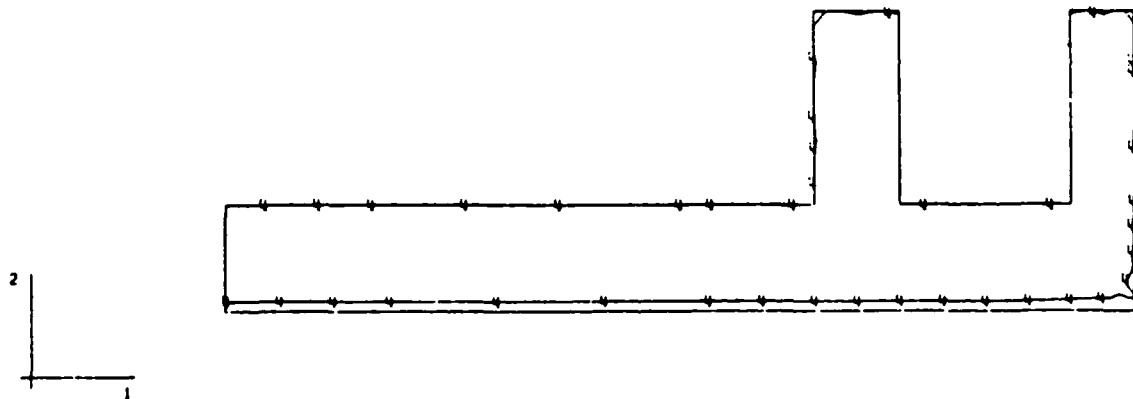
LIFT2 - M13 - 3D GRID MODEL - CENTERLINE

STEP 4 INCREMENT 8

ADROUS VERSION 4-5-147

Figure 12f. Temperature distribution in the centerline of structure 5 days after lift 2 is placed.

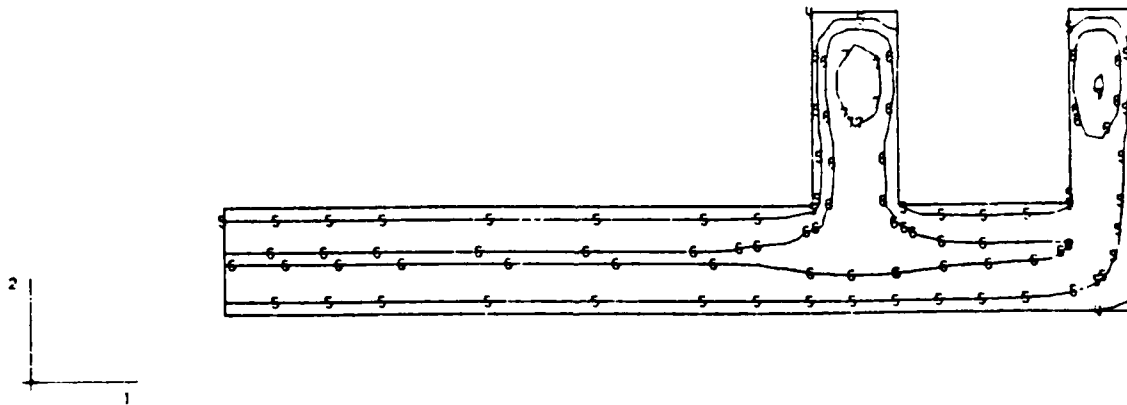
TEMP.
 I. D. VALUE
 1 +6.50E+01
 2 +7.00E+01
 3 +7.50E+01
 4 +8.00E+01
 5 +8.50E+01
 6 +9.00E+01
 7 +9.50E+01
 8 +1.00E+02
 9 +1.05E+02
 10 +1.10E+02
 11 +1.15E+02



LIFT4 - M13 - 3D GRID MODEL - OUTER SURFACE
 STEP 8 INCREMENT 4 ABAQUS VERSION 4.5-147

Figure 13a. Temperature distribution in outer surface of structure 5 days after lift 4 is placed.

TEMP.
 I. D. VALUE
 1 +6.50E+01
 2 +7.00E+01
 3 +7.50E+01
 4 +8.00E+01
 5 +8.50E+01
 6 +9.00E+01
 7 +9.50E+01
 8 +1.00E+02
 9 +1.05E+02
 10 +1.10E+02
 11 +1.15E+02



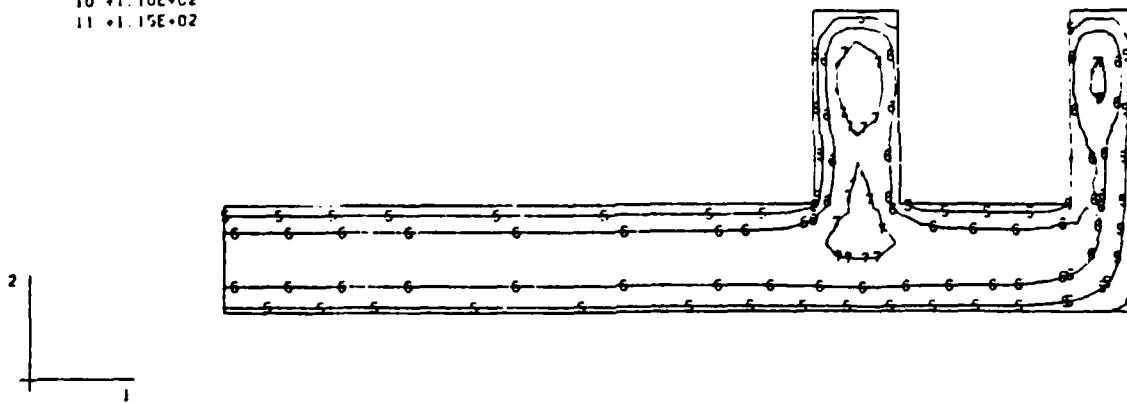
LIFT4 - M13 - 3D GRID MODEL - NODE PLANE 5

STEP 9 INCREMENT 6

ABAQUS VERSION 4.5-147

Figure 13b. Temperature distribution in node plane 5 of structure 5 days after lift 4 is placed.

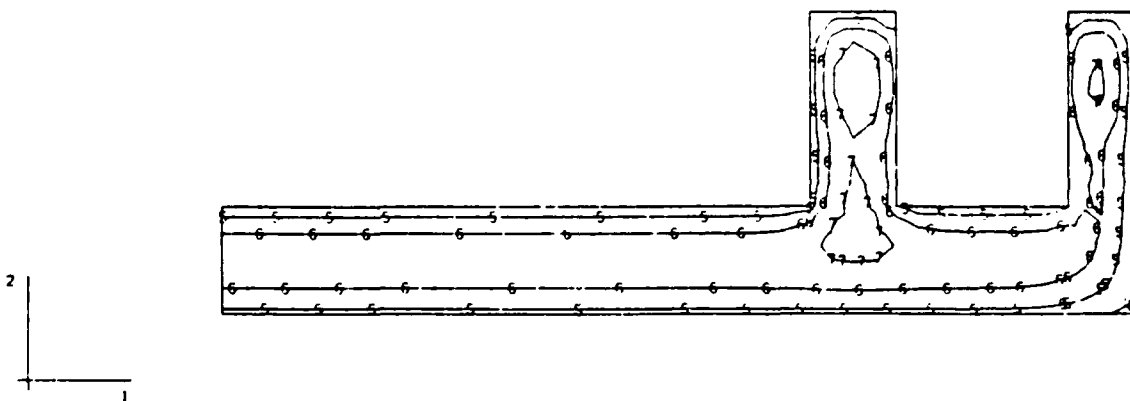
TEMP.
 I. D. VALUE
 1 +6.50E+01
 2 +7.00E+01
 3 +7.50E+01
 4 +8.00E+01
 5 +8.50E+01
 6 +9.00E+01
 7 +9.50E+01
 8 +1.00E+02
 9 +1.05E+02
 10 +1.10E+02
 11 +1.15E+02



LIFT4 - M13 - 3D GRID MODEL - NODE PLANE 4
 STEP 9 INCREMENT 6 ABAQUS VERSION 4-5-147

Figure 13c. Temperature distribution in node plane 4 of structure 5 days after lift 4 is placed.

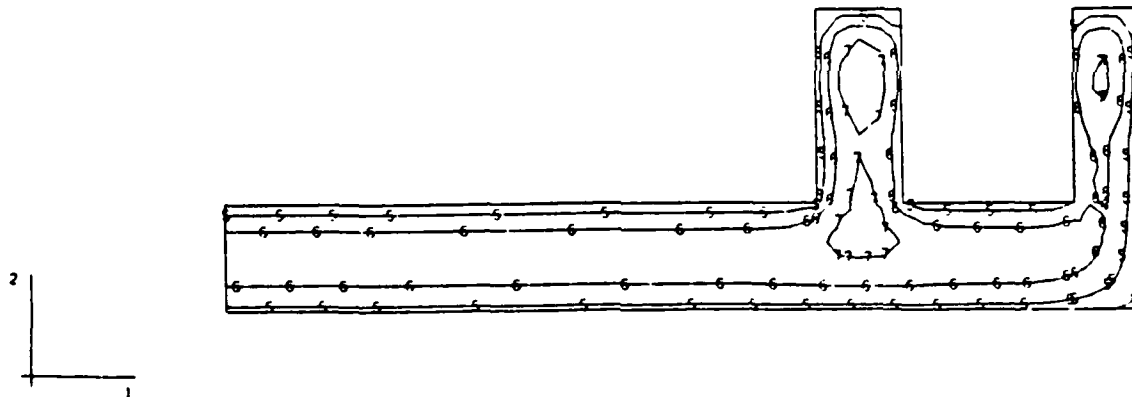
TEMP.
 I. O. VALUE
 1 +6.00E+01
 2 +7.00E+01
 3 +7.50E+01
 4 +8.00E+01
 5 +8.50E+01
 6 +9.00E+01
 7 +9.50E+01
 8 +1.00E+02
 9 +1.05E+02
 10 +1.10E+02
 11 +1.15E+02



LIFT4 - M13 - 3D GRID MODEL - NODE PLANE 3
 STEP 9 INCREMENT 6 ABAQUS VERSION 4.5-147

Figure 13d. Temperature distribution in node plane 3 of structure 5 days after lift 4 is placed.

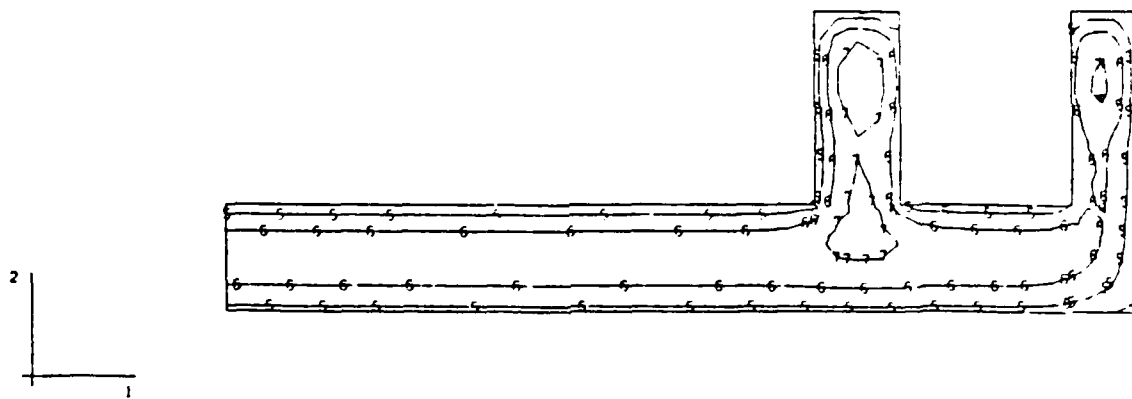
TEMP.
 1.0. VALUE
 1 +6.50E+01
 2 +7.00E+01
 3 +7.50E+01
 4 +8.00E+01
 5 +8.50E+01
 6 +9.00E+01
 7 +9.50E+01
 8 +1.00E+02
 9 +1.05E+02
 10 +1.10E+02
 11 +1.15E+02



LIFT4 - M13 - 3D GRID MODEL - NODE PLANE 2
 STEP 9 INCREMENT 8 ARAQUS VERSION 4-5-147

Figure 13e. Temperature distribution in node plane 2 of structure 5 days after lift 4 is placed.

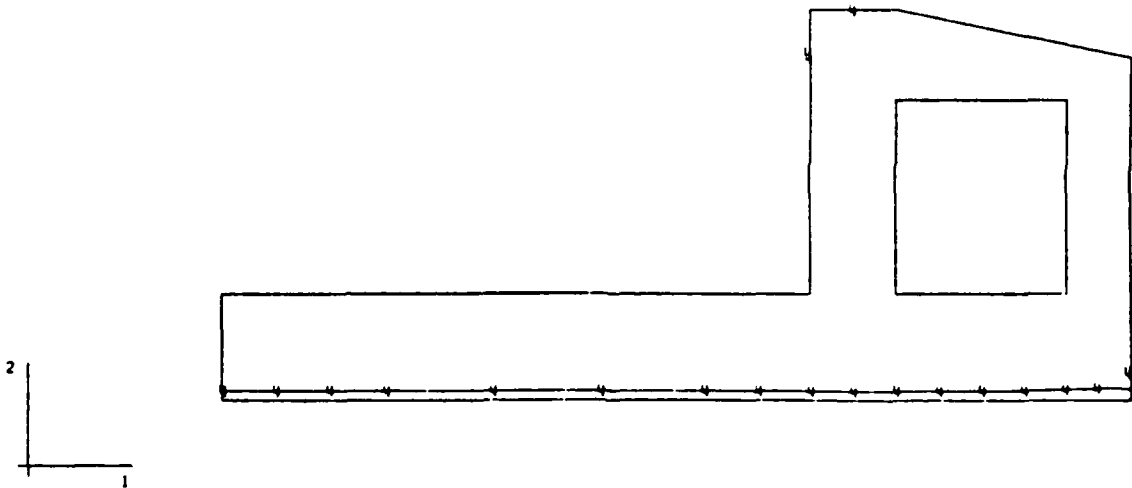
TEMP.
 I.D. VALUE
 1 +6.50E+01
 2 +7.00E+01
 3 +7.50E+01
 4 +8.00E+01
 5 +8.50E+01
 6 +9.00E+01
 7 +9.50E+01
 8 +1.00E+02
 9 +1.05E+02
 10 +1.10E+02
 11 +1.15E+02



LIFT4 - M13 - 3D GRID MODEL - CENTERLINE
 STEP 9 INCREMENT 6 AARQUS VERSION 4-5-147

Figure 13f. Temperature distribution in the centerline of structure 5 days after lift 4 is placed.

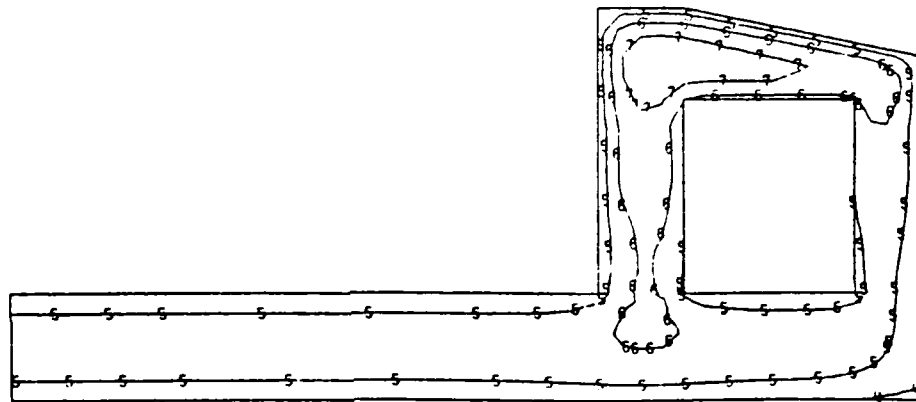
TEMP.
 I. O. VALUE
 1 +6.50E+01
 2 +7.00E+01
 3 +7.50E+01
 4 +8.00E+01
 5 +8.50E+01
 6 +9.00E+01
 7 +9.50E+01
 8 +1.00E+02
 9 +1.05E+02
 10 +1.10E+02
 11 +1.15E+02



LIFTS - M13 - 3D GRID MODEL - OUTER SURFACE
 STEP 10 INCREMENT 6 ABAQUS VERSION 4.5-147

Figure 14a. Temperature distribution in outer surface of structure 5 days after lift 5 is placed.

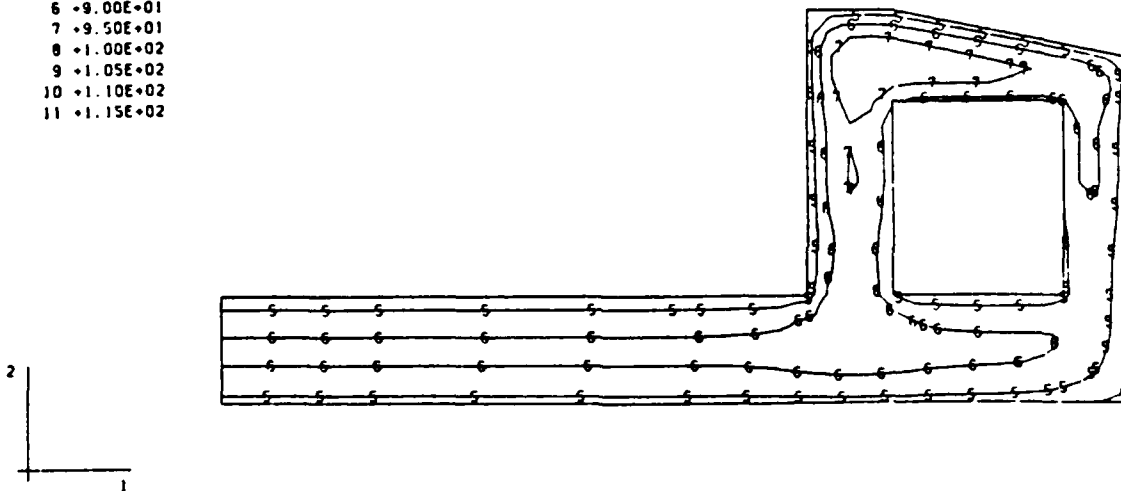
TEMP.
 1. D. VALUE
 1 +6.50E+01
 2 +7.00E+01
 3 +7.50E+01
 4 +8.00E+01
 5 +8.50E+01
 6 +9.00E+01
 7 +9.50E+01
 8 +1.00E+02
 9 +1.05E+02
 10 +1.10E+02
 11 +1.15E+02



LIFTS - M13 - 3D GRID MODEL - NODE PLANE 5
 STEP 10 INCREMENT 6 ABAQUS VERSION 4.5-147

Figure 14b. Temperature distribution in node plane 5 of structure 5 days after lift 5 is placed.

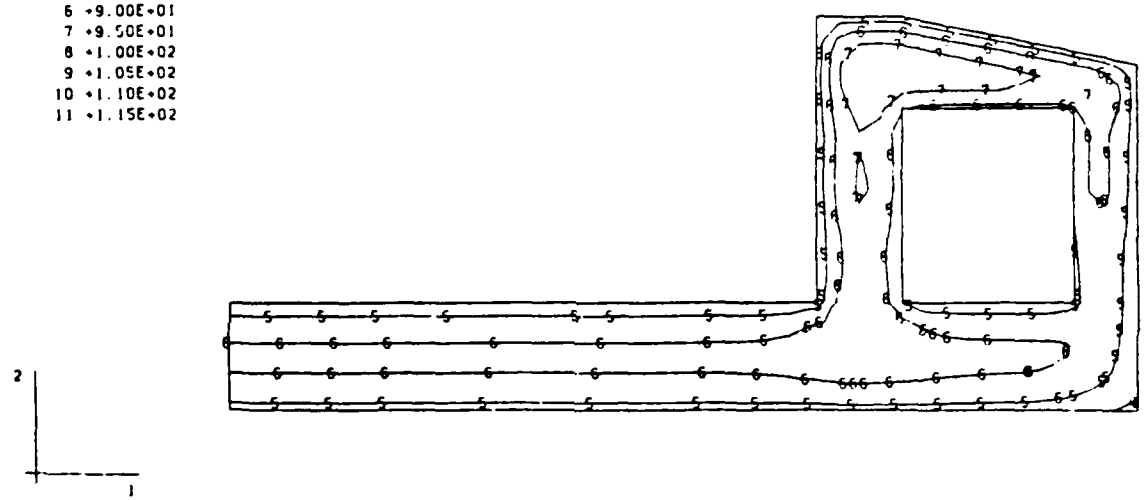
TEMP.
 I. D. VALUE
 1 +6.50E+01
 2 +7.00E+01
 3 +7.50E+01
 4 +8.00E+01
 5 +8.50E+01
 6 +9.00E+01
 7 +9.50E+01
 8 +1.00E+02
 9 +1.05E+02
 10 +1.10E+02
 11 +1.15E+02



LIFTS - M13 - 3D GRID MODEL - NODE PLANE 4
 STEP 10 INCREMENT 6 ABAQUS VERSION 4-5-147

Figure 14c. Temperature distribution in node plane 4 of structure 5 days after lift 5 is placed.

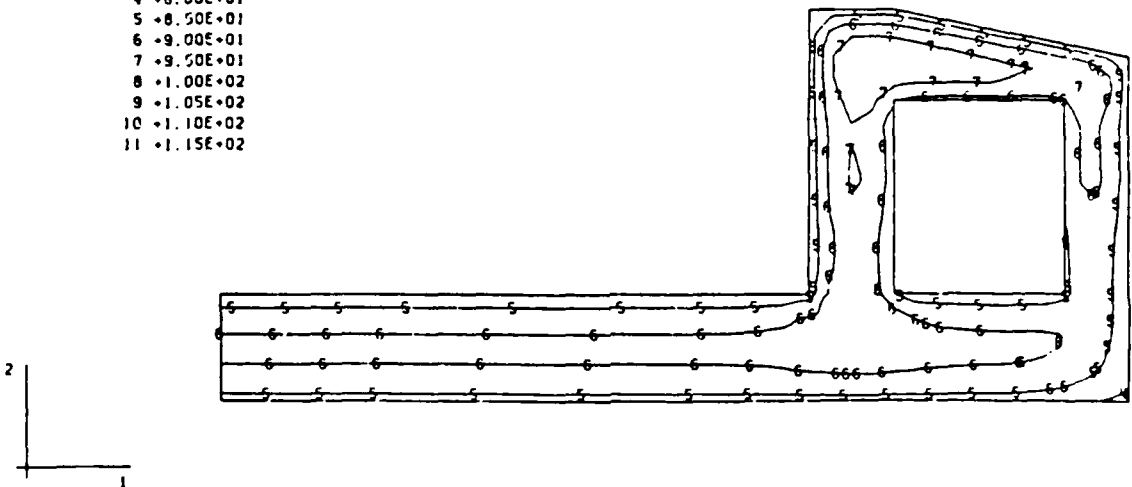
TEMP.
 I. D. VALUE
 1 +6.50E+01
 2 +7.00E+01
 3 +7.50E+01
 4 +8.00E+01
 5 +8.50E+01
 6 +9.00E+01
 7 +9.50E+01
 8 +1.00E+02
 9 +1.05E+02
 10 +1.10E+02
 11 +1.15E+02



LIFTS - M13 - 3D GRID MODEL - NODE PLANE 3
 STEP 10 INCREMENT 6 ABAQUS VERSION 4-5-147

Figure 14d. Temperature distribution in node plane 3 of structure 5 days after lift 5 is placed.

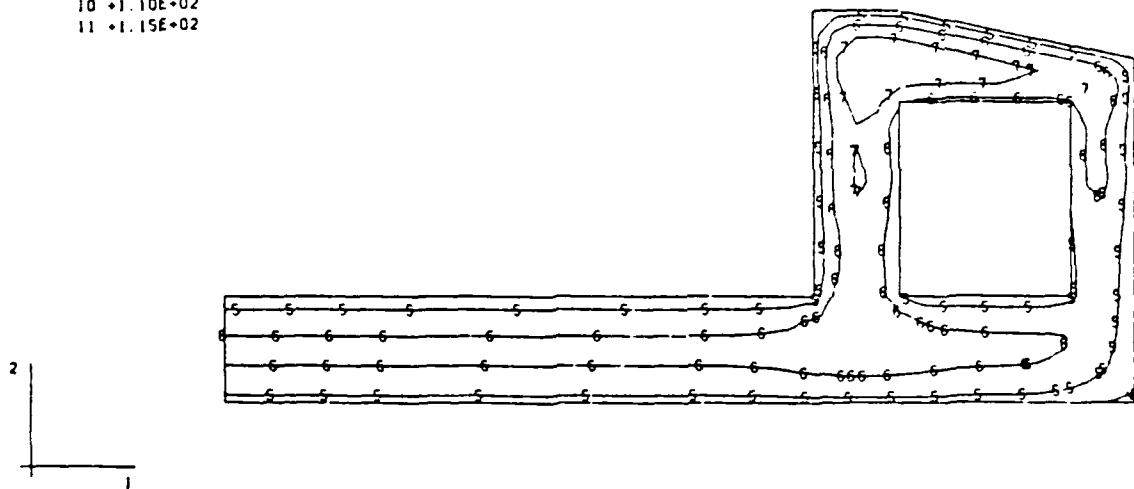
TEMP.
 I.D. VALUE
 1 +6.50E+01
 2 +7.00E+01
 3 +7.50E+01
 4 +8.00E+01
 5 +8.50E+01
 6 +9.00E+01
 7 +9.50E+01
 8 +1.00E+02
 9 +1.05E+02
 10 +1.10E+02
 11 +1.15E+02



LIFTS - M13 - 3D GRID MODEL - NODE PLANE 2
 STEP 10 INCREMENT 6 ABAQUS VERSION 4.5-147

Figure 14e. Temperature distribution in node plane 2 of structure 5 days after lift 5 is placed.

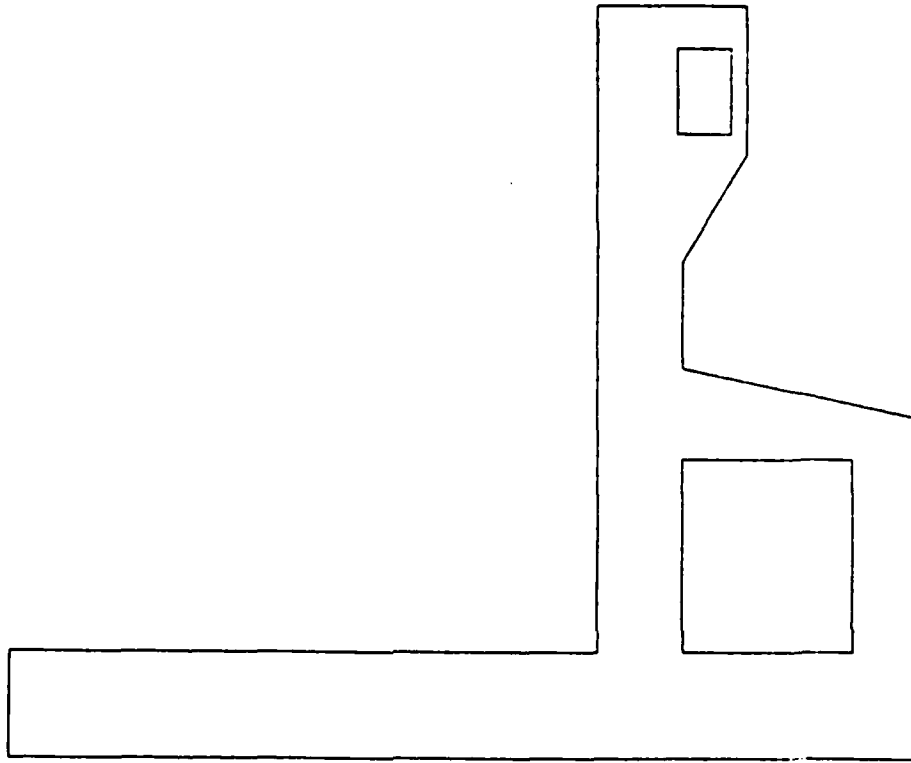
TEMP.
 I.D. VALUE
 1 +6.50E+01
 2 +7.00E+01
 3 +7.50E+01
 4 +8.00E+01
 5 +8.50E+01
 6 +9.00E+01
 7 +9.50E+01
 8 +1.00E+02
 9 +1.05E+02
 10 +1.10E+02
 11 +1.15E+02



LIFTS - M13 - 3D GRID MODEL - CENTERLINE
 STEP 10 INCREMENT 6 ABAQUS VERSION 4-5-147

Figure 14f. Temperature distribution in the centerline of structure 5 days after lift 5 is placed.

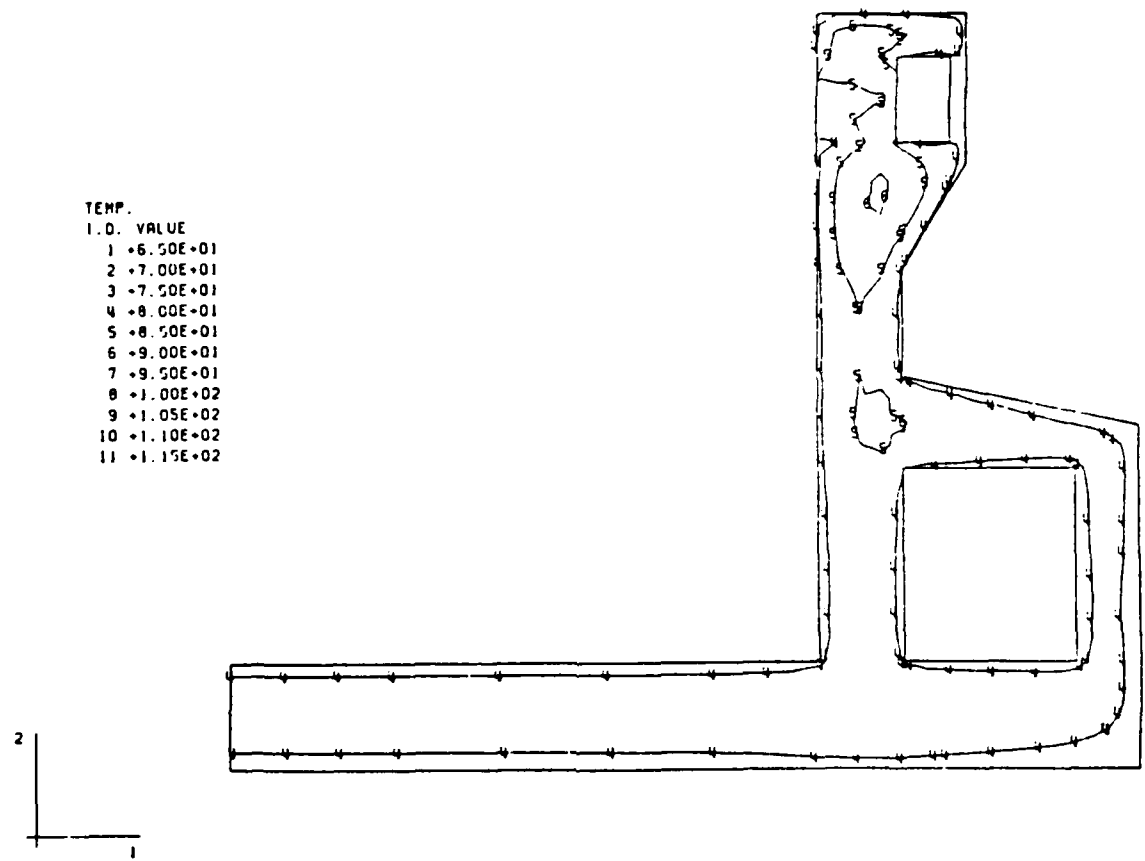
TEMP.
 I.D. VALUE
 1 +6.50E+01
 2 +7.00E+01
 3 +7.50E+01
 4 +8.00E+01
 5 +8.50E+01
 6 +9.00E+01
 7 +9.50E+01
 8 +1.00E+02
 9 +1.05E+02
 10 +1.10E+02
 11 +1.15E+02



LIFT9 - M13 - 3D GRID MODEL - OUTER SURFACE
 STEP 10 INCREMENT 10 ABAQUS VERSION 4-5-147

Figure 15a. Temperature distribution in outer surface of structure 7 days after lift 9 is placed.

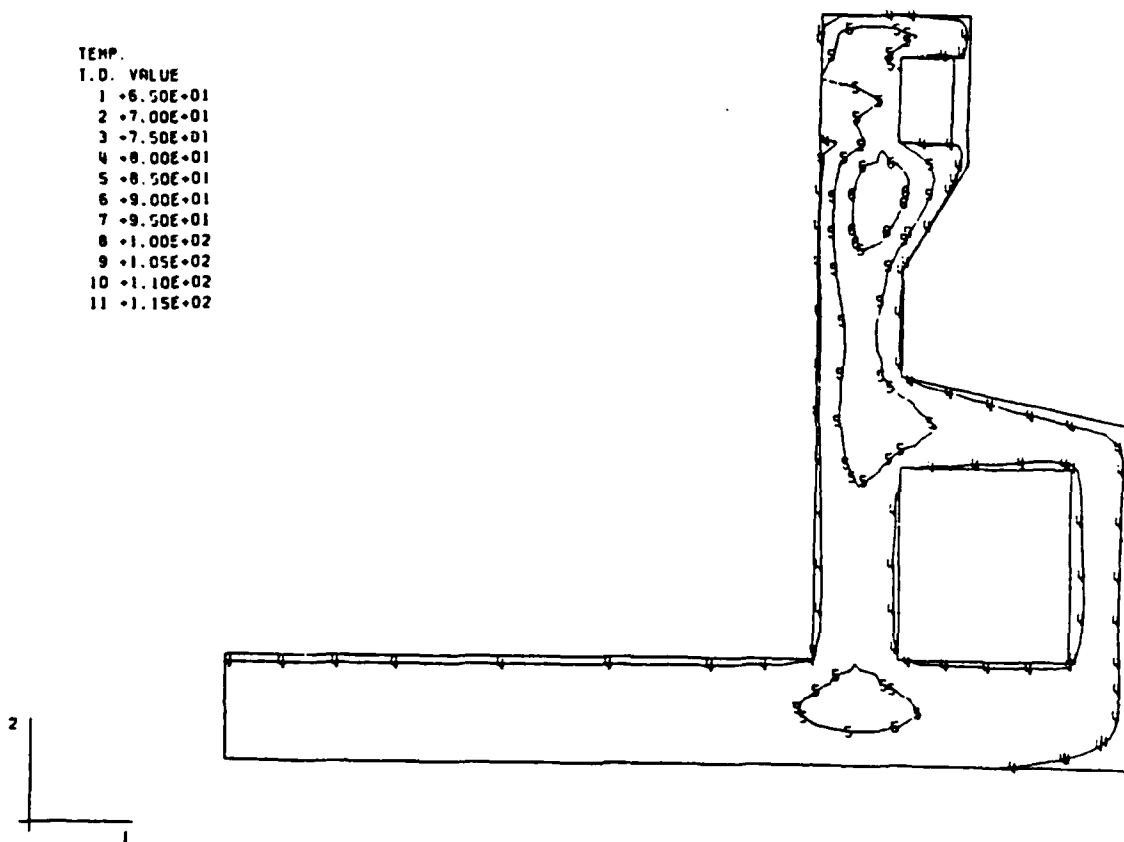
TEMP.
 I.D. VALUE
 1 +6.50E+01
 2 +7.00E+01
 3 +7.50E+01
 4 +8.00E+01
 5 +8.50E+01
 6 +9.00E+01
 7 +9.50E+01
 8 +1.00E+02
 9 +1.05E+02
 10 +1.10E+02
 11 +1.15E+02



LIFT9 - M13 - 3D GRID MODEL - NODE PLANE 5
 STEP 10 INCREMENT 10 ABAQUS VERSION 4-5-147

Figure 15b. Temperature distribution in node plane 5 of structure 7 days after lift 9 is placed.

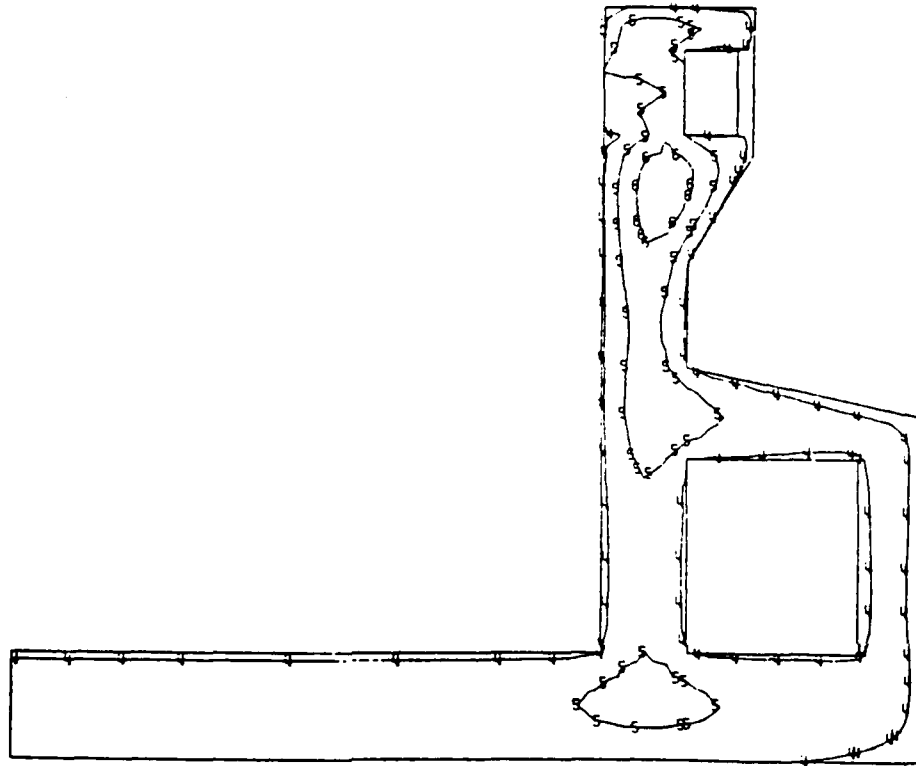
TEMP.
 T. D. VALUE
 1 +6.50E+01
 2 +7.00E+01
 3 +7.50E+01
 4 +8.00E+01
 5 +8.50E+01
 6 +9.00E+01
 7 +9.50E+01
 8 +1.00E+02
 9 +1.05E+02
 10 +1.10E+02
 11 +1.15E+02



LIFT9 - M13 - 3D GRID MODEL - NODE PLANE 4
 STEP 10 INCREMENT 10 ABAQUS VERSION 4-5-147

Figure 15c. Temperature distribution in node plane 4 of structure 7 days after lift 9 is placed.

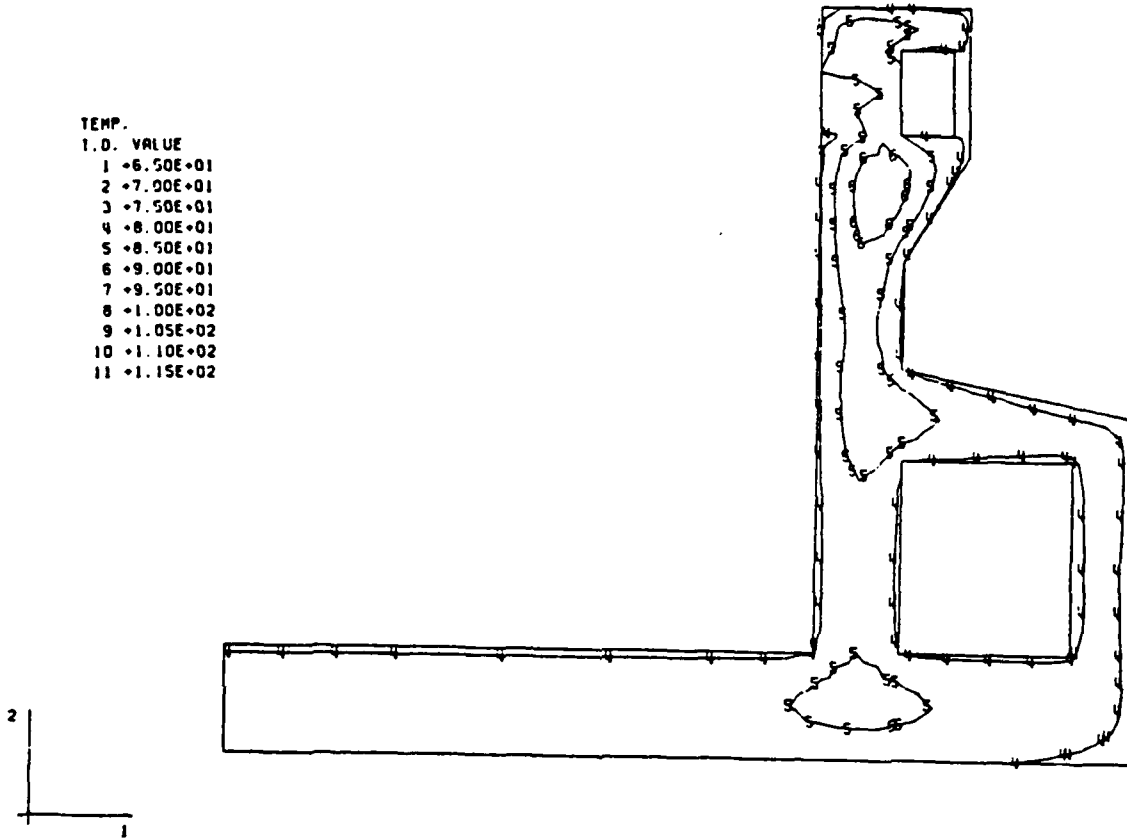
TEMP.
 I.D. VALUE
 1 +6.50E+01
 2 +7.00E+01
 3 +7.50E+01
 4 +8.00E+01
 5 +8.50E+01
 6 +9.00E+01
 7 +9.50E+01
 8 +1.00E+02
 9 +1.05E+02
 10 +1.10E+02
 11 +1.15E+02



LIFT9 - M13 - 3D GRID MODEL - NODE PLANE 3
 STEP 10 INCREMENT 10 ABAQUS VERSION 4-5-147

Figure 15d. Temperature distribution in node plane 3 of structure 7 days after lift 9 is placed.

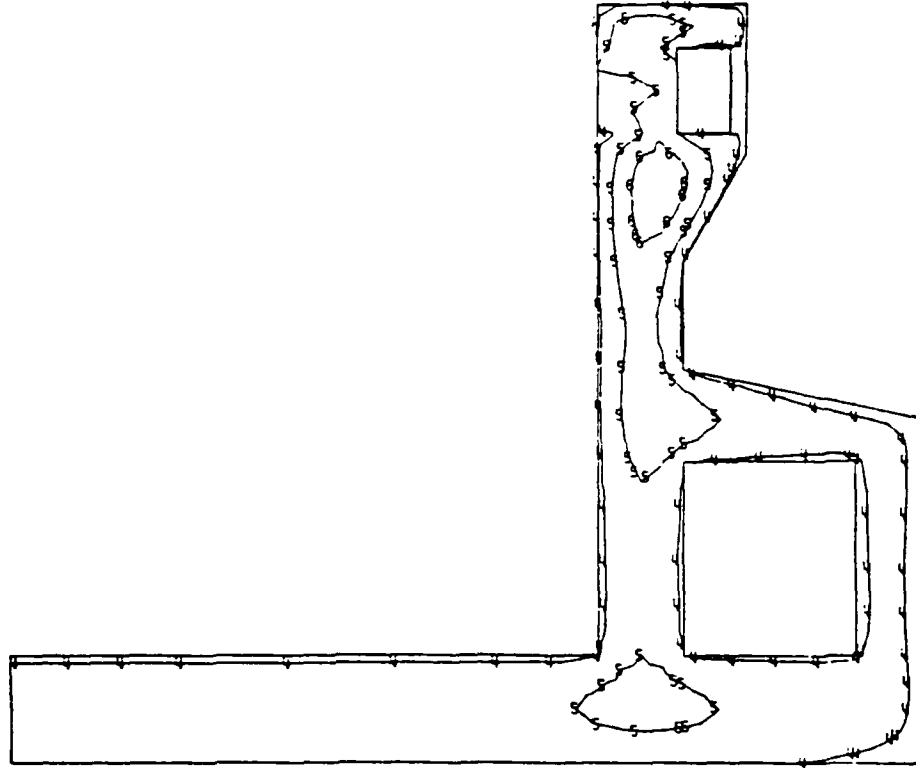
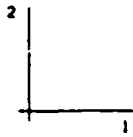
TEMP.
 I. D. VALUE
 1 +6.50E+01
 2 +7.00E+01
 3 +7.50E+01
 4 +8.00E+01
 5 +8.50E+01
 6 +9.00E+01
 7 +9.50E+01
 8 +1.00E+02
 9 +1.05E+02
 10 +1.10E+02
 11 +1.15E+02



LIFT9 - M13 - 3D GRID MODEL - NODE PLANE 2
 STEP 18 INCREMENT 10 ABAQUS VERSION 4.5-147

Figure 15e. Temperature distribution in node plane 2 of structure 7 days after lift 9 is placed.

TEMP.
 I.D. VALUE
 1 +6.50E+01
 2 +7.00E+01
 3 +7.50E+01
 4 +8.00E+01
 5 +8.50E+01
 6 +9.00E+01
 7 +9.50E+01
 8 +1.00E+02
 9 +1.05E+02
 10 +1.10E+02
 11 +1.15E+02



LIFT9 - M13 - 3D GRID MODEL - CENTERLINE

STEP 10 INCREMENT 10

ABAQUS VERSION 4-5-147

Figure 15f. Temperature distribution in the centerline of structure 7 days after lift 9 is placed.

PART VIII: STRESS ANALYSES OF MONOLITH L-13

Presentation of Results

Two-dimensional gravity loading

66. The ABAQUS program was used to perform the 2-D stress analysis of monolith L-13 for both instantaneous gravity turn-on of the entire structure and an incremental construction build-up sequence of the structure. Figures 16a and 16b show the displaced structure and maximum principal (tensile) stress contours, respectively, for the gravity turn-on analysis for a Young's Modulus (E) of 3.12×10^6 psi. Figures 17a and 17b give the same results for $E = 4.80 \times 10^6$ psi. These modulus values correspond to the ACI modified and normal compressive strength of the concrete at 28 days, respectively. Figures 18a thru 18d and 19a thru 19b show the displaced structure and maximum principal stress contours, respectively, for four stages of construction using incremental construction sequencing. This incremental construction analysis uses the material modulus calculation routine UMAT1. WES2DT was used to make the same incremental construction analysis. Figures 20a thru 20d and 21a thru 21d show the resultant displacement vector plots and principal stress vector plots, respectively, from this analysis.

Two-dimensional gravity and thermal loading

67. The ABAQUS program was used to perform the 2-D stress analysis including gravity and temperature loading for FE grids 1 and 2 using the modulus routine UMAT1. The displaced structure plots from grids 1 and 2 are given in Figures 22a thru 22d and 24a thru 24d, respectively. The maximum principal stress contours for both grids are given in Figures 23a thru 23d and 25a thru 25d, respectively. The new modulus subroutine UMAT2 (concrete aging creep model) was used with ABAQUS with grid 1 to make the analysis when E

did not depend on temperature and E did depend on temperature. The displaced structure and maximum principal stress contours are given in Figures 26a thru 26d and 27a thru 27d for E not a function of temperature. Figures 28a thru 28d and 29a thru 29d show the displacement and maximum principal stress contours for E as a function of temperature. A WES2DT analysis was made of this same gravity and temperature loading. The resultant displacement vector plots are shown in Figures 30a thru 30d. The principal stress vector plots are shown in Figures 31a thru 31d.

Two-dimensional gravity and thermal loading including creep

68. ABAQUS was used in incremental construction analyses of the structure using FE grid 1 with the modulus subroutine UMAT2. Displaced-structure plots are shown in Figures 32a thru 32d. Maximum principal stress contours are shown in Figures 33a thru 33d. WES2DT was also used to make the same analysis. Figures 34a thru 34d show resultant displacement vectors and Figures 35a thru 35d show principal stress vectors from the WES2DT analysis.

Two-dimensional gravity and thermal loading including creep and shrinkage

69. ABAQUS was used to make this analysis using FE grid 1 and modulus subroutine UMAT2. Displaced-structure plots for this analysis are shown in Figures 36a thru 36d. Maximum principal stress contours are shown in Figures 37a thru 37b.

Three-dimensional gravity loading

70. ABAQUS was used to perform a 3-D gravity turn-on analysis of monolith L-13 using the FE grid in Figure 8a. The displaced structure at the element faces in the 5 element planes in Figure 8d are shown in Figures 38a thru 38e.

Discussion of Results

Gravity turn-on analyses

71. Comparisons of gravity turn-on analyses of monolith L-13 made with $E = 3.12 \times 10^6$ psi and $E = 4.8 \times 10^6$ psi seen in Figures 16 and 17, respectively, showed both the displacements and stresses to be in close agreement. Maximum principal stresses are slightly higher for $E = 4.8 \times 10^6$ psi as expected. Also, comparisons of displacements between these 2-D runs and the 3-D gravity turn-on run seen in Figure 38 closely agree.

Incremental construction with gravity loading only ABAQUS versus WES2DT

72. Incremental construction analyses of monolith L-13 with gravity loading only were conducted with ABAQUS and WES2DT. Comparison of displacement results in Figures 18 and 20 show the results to be very similar. The largest deflection of the base slab occurs midway between the centerline and the outer edge of the monolith after placement of two lifts (Figures 18a and 20a). This is because the loading is uniform and the pile support is weaker in this area. As concrete in the wall was placed and the loading was no longer uniform, displacements of the slab under the wall increased and maximum displacements in the slab shifted outward toward the edge of the slab (Figures 18b-c and 20b-c).

73. Stress comparisons between the ABAQUS and WES2DT programs required comparing principal stress in contour and vector plots (Figures 19 and 21), respectively, because these were the available modes of displaying principal stress from the two programs. Although comparing data from contour and vector plots was not an easy task, it did appear that maximum tensile stresses occurred in the same locations with both programs. In addition, the location of these maximum tensile stresses coincided with locations of maximum slab curvature, namely on the top of the slab at the centerline and at the bottom of

the slab directly under the vertical cantilever section of the wall. The two programs use different methods for starting the stress calculations in a new lift. The slight differences in stress distributions calculated by the two programs in some areas can be attributed to the different lift start-up methods and are amplified by rapidly increasing values of E at early ages.

Gravity turn-on versus
incremental construction

74. Comparisons between whole-structure gravity turn-on and incremental construction simulation with gravity loading only with ABAQUS showed predictable results. In gravity turn-on analyses, the maximum displacements in the slab were nearly equal under the wall and lower at the centerline of the monolith. In incremental construction analyses, maximum displacements in the slab occurred directly under the vertical cantilever section of the wall with lower displacements near the outer edge of the slab and at the centerline. The displacements in the wall were characteristically different between gravity turn-on and incremental construction analyses. During incremental construction, each successive lift is placed up to its planned elevation. Therefore, the displacement of the top of each lift decreases at higher elevations in the structure. Conversely, in the gravity turn-on analysis, the maximum displacement occurs at the top of the wall because all displacements accumulate at the highest elevation. These results have thus exhibited known modes of displacement for gravity turn-on and incremental construction analyses.

75. Stress contours resulting from ABAQUS calculations of gravity turn-on and incremental construction were very similar as expected. Stress values within the base slab were slightly higher due to use of a constant, mature E (28-day value) whereas the incremental construction analysis used aging E values which are lower at early age.

Two-dimensional
gravity and thermal loading

76. When thermal effects due to heat of hydration of cement were added to the loading, the predominant changes in the response of the structure were an elongation of the base slab and a downward curvature of the outer end of the base slab. These effects were observed from the both the ABAQUS and WES2DT results. This response is illustrated by comparing Figures 22,24,26,28, and 30. Elongation of the slab is due to thermal expansion. The curvature of the base slab occurs as a result of differential thermal expansion between a new lift and previous lifts. The concrete temperature rise data shown in Figure 4a shows that a new lift can undergo thermal expansion equivalent to a potential temperature rise of 35° F during the first five days after placement. The previous lift during the same time period (its second 5 days) can only experience thermal expansion equivalent to a 5° F temperature rise. The differential longitudinal expansion due to the temperature rise in each lift causes the downward curvature of the outer portion of the slab. The curvature is not actually as pronounced as the temperature differential between the two lifts would indicate because the E, hence stiffness, of the newer lift is lower than that of the previous lift. Effectively, only a part of the temperature differential thus causes curvature of the slab.

77. The addition of thermal loading caused an increase in tensile stresses on the top surface of the base slab near the outer edge after placement of lift 2. Tensile stresses also increased along the vertical wall surfaces and compressive stresses developed in the center of wall masses. These stresses in the wall develop due to the differential expansion from the thermal gradients between the cooler outer surfaces and the warm interiors. In ABAQUS maximum principal stress contour plots include z-direction stresses which result from the absolute restraint to thermal expansion in its plane

strain formulation in two ways. First, z-direction compressive stresses increase x- and y- direction tensile stresses due to Poisson effect in ABAQUS. And z-direction out-of-plane stresses may be included in 2-D maximum principal stress plots. Therefore, z-direction stresses may be mixed in with x - y plane stresses in the ABAQUS principal stress plots. It is understood that subsequent ABAQUS versions will include only in-plane stresses in these plots.

78. Comparison of principal stress contours (Figures 23 and 25) using ABAQUS grids 1 and 2 (Figures 7a and 7b) showed virtually identical results. Comparisons of displacements (Figures 22 and 24) also showed very close agreement. It was concluded, based upon these results, that the coarse mesh of FE grid 1 was adequate for all subsequent analyses of monolith L-13.

79. Comparisons were also made between analyses results from ABAQUS and from WES2DT that included thermal loading. Comparisons between results from the two programs must be tempered by the realization that ABAQUS plane strain calculations effectively fully restrain z-direction expansion and WES2DT does not. Consequently, z-direction stresses develop in ABAQUS which through Poisson effect modify x- and y-direction stresses. In WES2DT, z-direction stresses are not calculated so that they are effectively zero with no resulting Poisson effect. In addition, stress plots in ABAQUS may include z-direction stresses. With these points in mind, examination of displacement plots from the two programs (Figures 22 and 30) showed very similar deflection patterns at all locations. Comparison of maximum principal stress plots (Figures 23 and 31) showed tensile stress results that compared very well in location and magnitude. When maximum principal stresses were compressive, stresses were generally lower from ABAQUS. This may be the result of the different considerations for plain strain calculations by ABAQUS and WES2DT.

80. All previously described analyses with ABAQUS employed the modulus

subroutine UMAT1 in which the E versus age function was entered as tabular input. ABAQUS modulus subroutine UMAT2 (aging creep model) enters E versus age data by a mathematical function representation. When UMAT2 was first used, several initial comparative FE analyses were run to identify any differences between UMAT1 and UMAT2 without employing creep or shrinkage to establish bases of comparisons between the two subroutines. UMAT2 incorporates E as a function of temperature as well as age. Comparative runs were made to identify the differences introduced for the temperature dependence of E for the range of temperatures encountered in these analyses. The displaced grid (Figures 26 and 28) and principal stress contour (Figures 27 and 29) plots show that temperature dependence of E does not appreciably affect the results. Comparisons of the E versus age representations used in UMAT1 and UMAT2 were made by comparing displaced grid (Figures 22 and 28) and principal stress contour (Figures 23 and 29) plots. These results show that elongation and downward curvature of the base slab (lifts 1 and 2) are slightly greater for the UMAT2. In locations of maximum tensile stresses, UMAT2 produced stresses up to 100 percent higher than those by UMAT1 after five days after placement of lift 2. These higher stresses from UMAT2 were determined to be the direct result of much higher values of E during the first day in the functional representation used in UMAT2. The method for expressing E versus time in the aging creep model will require modification in the future to better express E values for the first day or so of age. This could not be done in time to be used in this study. The remainder of the analyses were made using ABAQUS modulus subroutine UMAT2 with the realization that early-age stresses would be higher than normal.

Two-dimensional gravity and thermal loading including creep

81. Analyses of L-13 which included gravity and thermal loading with creep were conducted using both ABAQUS-UMAT2 with FE grid 1 and WESDOT

AD-A103 664

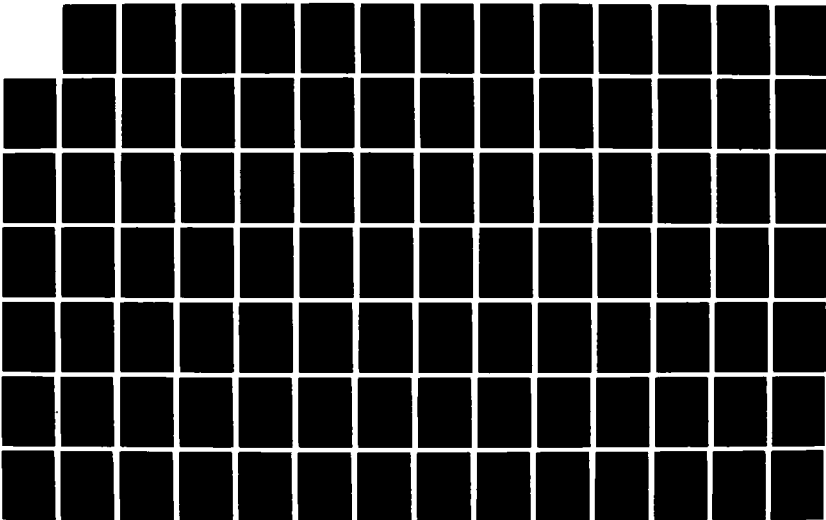
THERMAL STRESS ANALYSES OF MISSISSIPPI RIVER LOCK AND
DAM 26(R)(U) ARMY ENGINEER WATERWAYS EXPERIMENT STATION
VICKSBURG MS STRUCTURES LAB A A BOMBICH ET AL. JUL 87
NES/TR/SL-87-21

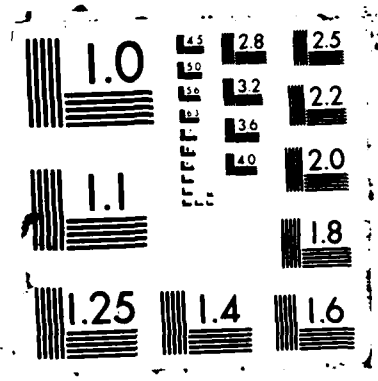
2/4

UNCLASSIFIED

F/G 13/13

NL





effects of creep changed the deflected response of the monolith. Although the displacement trends (Figures 32 and 34) produced by ABAQUS and WES2DT compared remarkably well, magnitudes of deflection were higher with ABAQUS.

82. When comparing the principal stress plots without creep for ABAQUS and WES2DT (Figures 23 and 31) to principal stress plots for the two programs with creep (Figures 33 and 35), the following observations were made. The relaxation of stresses due to creep with ABAQUS-UMAT2 reduced peak principal stresses in the base slab from 300 psi (Figure 29a) to 150 psi (Figure 33a) at five days after placement of lift 2. At 5 days after placement of lift 4, peak principal stresses in the base slab were reduced from 250 psi (Figure 23b) to 50 psi (Figure 33b). With WES2DT the similar comparison showed reduction of peak principal stresses due to creep in the base slab from 150 psi (Figure 31a) to 115 psi (Figure 35a) at 5 days after placement of lift 2 and from 90 psi (Figure 31b) to 50 psi (Figure 35b) at 5 days after placement of lift 4. These comparisons show that initial stresses are much higher and relaxation due to creep is much greater with ABAQUS-UMAT2 than with WES2DT. The higher initial stresses are consistent with the fact that the early-age E values are greater with UMAT2. As discussed in paragraph 28, it was known that the creep data incorporated into UMAT2 would produce slightly greater creep relief than the data used by WES2DT. Also, since the highest rate of creep occurs when these stresses are high, a proportionately larger amount of stress relief resulted with ABAQUS. At later times as the initial, high thermal gradients and the resulting thermal stresses are reduced, the excessively relaxed stresses are further reduced. This process accounts for the large decrease in stresses seen in the base slab in Figure 35b.

Two-dimensional gravity and thermal loading including creep and shrinkage

83. An ABAQUS analysis was conducted on L-13 using UMAT2 with gravity

and thermal loading including creep and shrinkage. The addition of this autogenous shrinkage caused noticeably different results. Comparison of ABAQUS analyses with creep, but with and without shrinkage showed both different displacement and principal stress response. Comparison of displaced grids (Figures 32 and 36) for analyses with and without shrinkage, respectively, shows that the addition of shrinkage cancels some of the thermal elongation of lift 2 and reduces the differential thermal expansion between lifts 1 and 2 that had produced downward curvature of the outer end of the base slab. Subsequently, further shrinkage caused deflections of the slab directly under the vertical cantilever section of the wall to increase substantially (Figures 36a - 36d). Comparison of maximum principal stresses showed that at 5 days after placement of lift 2, stresses in the base slab were greater and nearly symmetrical about the lift 1-lift 2 interface when shrinkage was applied. In fact, stresses increased in several areas of the wall. Although the creep and shrinkage data used in these ABAQUS FE analyses are not based upon the results of tests of Lock and Dam 26R concrete which may cause the results to deviate slightly, it is evident from these analyses that inclusion of creep and shrinkage are necessary for proper thermal stress evaluation.

Pile loads

84. The load in a pile is directly proportional to the deflection of the pile head, therefore, the distribution of pile loads underneath the base slab is dependent principally upon the base slab deflections. Table 6 gives the vertical pile loads from analyses using ABAQUS and WES2DT. Also included are pile loads supplied by St. Louis District. The ABAQUS results using a Young's modulus modified by ACI agree very closely with the St. Louis District values in a gravity turn-on analysis. Since the ABAQUS and WES2DT modulus values were not to be modified for the remaining analyses, an ABAQUS analysis

Table 6. Vertical Pile Loads for Monolith 13
(7 Days after placement of last lift)

Pile No.	St. Louis District	GRAVITY TURN-ON			GRAVITY ONLY		GRAVITY & THERMAL LOADS				GRAVITY & THERMAL LOADS		
		ABAQUS		ABAQUS (UMAT1)	WES2DT	ABAQUS (UMAT1)		ABAQUS (Grid #1)		WES-2DT	(W/CREEP)		(W/CREEP & SHRINK.)
		E1	E2			Grid #1	Grid #2	(UMAT2*)	(UMAT2)		ABAQUS	WES2DT	
1	86.2	89.6	96.1	75.0	71.0	71.9	71.4	72.4	72.4	68.9	45.3	65.6	45.0
2	88.3	91.5	97.5	78.9	75.5	75.5	75.2	74.9	74.9	73.4	50.5	70.4	50.2
3	94.2	96.9	101.7	90.2	89.0	86.2	86.1	81.8	82.2	86.6	65.8	84.7	65.3
4	103.4	105.6	108.6	107.6	111.4	102.7	102.8	92.6	93.4	108.2	92.9	108.5	92.2
5	128.1	128.1	126.6	146.5	157.0	139.2	139.7	118.3	120.1	152.2	151.8	156.5	152.0
6	155.0	153.2	147.3	181.1	191.8	171.1	171.3	144.1	146.4	185.2	208.5	192.7	211.2
7	177.8	175.5	166.6	203.7	211.9	192.0	193.0	165.8	168.2	204.1	250.4	213.2	257.5
8	190.2	189.6	180.8	208.3	211.9	197.1	197.9	179.9	181.7	204.0	257.8	212.1	270.8
9	191.1	191.1	186.6	194.2	188.8	189.5	189.9	189.3	189.3	185.2	210.9	187.4	222.3
10	189.6	189.6	188.0	185.7	177.7	187.8	187.8	197.4	196.5	179.8	184.0	177.9	189.1
11	188.8	188.8	189.8	179.4	175.6	190.8	190.8	210.3	208.5	182.6	169.5	179.0	164.3
12	189.2	190.3	193.2	176.6	179.2	200.9	199.7	230.6	228.1	195.5	178.3	189.8	155.9

NOTE - All pile loads are in KIPS/PILE

GRAVITY TURN-ON

GRAVITY ONLY

GRAVITY AND THERMAL LOADS

St. Louis District

E1

E2

UMAT1

UMAT2

UMAT2*

- Instantaneous placement of entire structure in one step

- Incremental construction of structure in lifts with only gravity applied

- Incremental construction of structure in lifts with gravity and temperature loading

- Pile loads supplied by St. Louis District (E = 3,120,000 psi)

- ABAQUS results using E = 3,120,000 psi (28-day strength modified by ACI code)

- ABAQUS results using E = 4,800,000 psi (28-day strength)

- Original modulus calculation routine used with ABAQUS, only considers aging of the concrete

- Revised modulus routine which may include aging, creep, shrinkage and E is a function of temperature

- New modulus routine which can include aging, creep, shrinkage and E as a function of temperature

was also made with the unmodified 28-day Young's modulus. The stiffer concrete slightly redistributed the pile loads with the higher loads still being located under the wall at the outer edge of the base slab. The maximum pile loads from these analyses were all less than 200 kips/pile.

85. When the wall was constructed incrementally with only gravity loads applied, the ABAQUS and WES2DT programs predicted more significant redistribution of the pile loads with maximum values of 200-210 kips/pile occurring underneath the wall.

86. As thermal loading was added, the ABAQUS-UMAT1 results for grid 1 and grid 2 were almost identical. The results of ABAQUS using the new modulus subroutine UMAT2, for both modulus as a function of temperature and constant with temperature, gave very similar results. No further analyses were made with the modulus held constant with temperature since it caused no significant change in pile loads. However the predicted pile loads using UMAT2 were redistributed from the ones using UMAT1. The larger pile loads were reduced under the wall and moved farther toward the outer edge of the base slab. Maximum pile loads were approximately 230 kips/pile for the ABAQUS-UMAT2 analysis. WES2DT results showed close agreement in magnitude and trend with the ABAQUS results using UMAT1.

87. When creep was included in the analysis, both ABAQUS and WES2DT redistributed the pile loads. Both gave lower pile loads at the centerline, lower loads at the outer edge, and higher loads under the wall. The ABAQUS results showed more extreme changes in each instant. WES2DT results ranged from 66 kips/pile at the centerline to 213 kips/pile under the wall. ABAQUS results showed 45 kips/pile at the centerline and 258 kips/pile under the wall. These ABAQUS values are 10 - 15 percent higher than WES2DT values. The higher pile loads can be attributed to higher creep occurring in ABAQUS at early times

after placement of a lift when the modulus is excessively high. The WES2DT pile loads are very similar in magnitude and distribution to those obtained earlier when only gravity loading was included in an incremental construction analysis.

88. When shrinkage was added to the ABAQUS analysis, the pile loads were slightly redistributed from those where only creep was included. Higher values were predicted under the vertical cantilever section of the wall and lower values at the outer edge of the base slab.

89. While the gravity turn-on analysis method gives adequate pile load input for use in design, the incremental construction method should give loads closer to the actual values since it more closely models the actual construction sequence. However, the incremental method will be slightly more expensive and difficult to perform since data to define the modulus as a function of time is needed and a series of solutions is performed.

Cracking potential

90. Comparisons of results were made to evaluate the potential for cracking of the concrete in the analyses that were made in this investigation. Modulus of rupture test results from Lock and Dam 26R, Phase I mixture 4c concrete yielded values of 124 psi, 280 psi, 300 psi, and 464 psi at 1-, 3-, 7-, and 28-days age, respectively. If these values are used as a simple cracking initiation limit for tensile stresses, the following conclusions can be made regarding crack potential in monolith L-13.

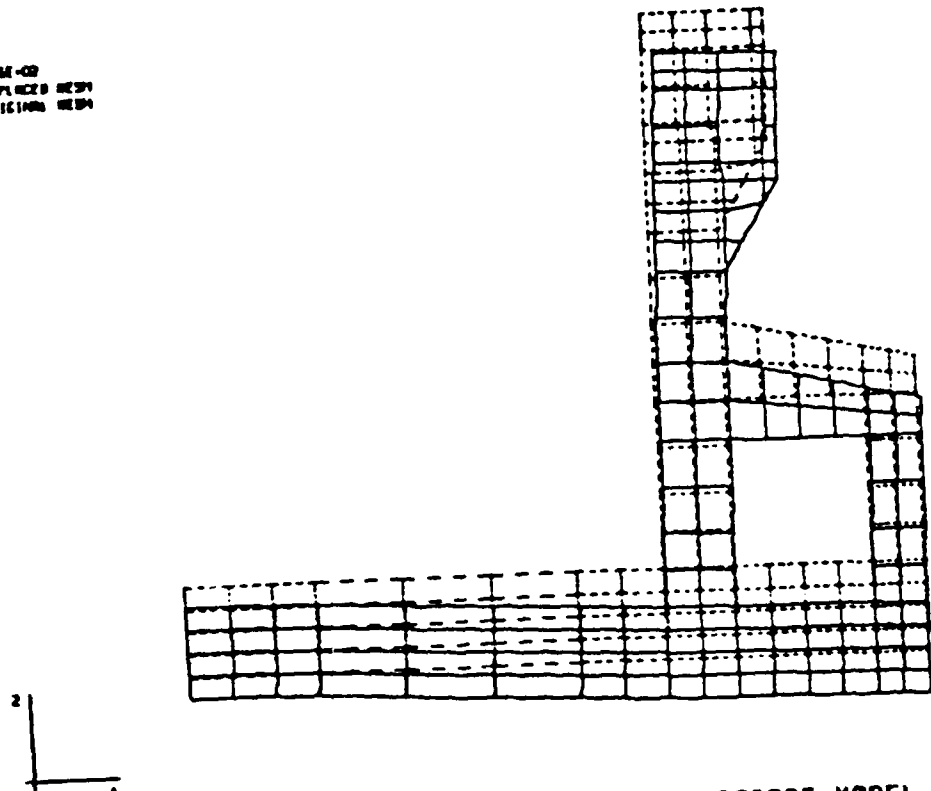
91. First, maximum principal stresses computed in WES2DT analyses did not exceed 150 psi in tension under any state of loading and this level was reached after 3-days age without any stress relief due to creep. With creep peak tensile stresses were 20-40 percent less. Consequently, maximum tensile stresses were less than 50 percent of modulus of rupture at any age even

without benefit of creep.

92. Secondly, maximum principal tensile stresses computed in ABAQUS analyses using UMAT1, which employed the identical modulus versus time relationship as WES2DT analyses, did not exceed 200 psi and only after 3-days age. Even without the benefit of stress relief through creep, which should relax stresses by 20-40 percent, these peak tensile stresses are only around 70 percent of modulus of rupture at 3-day.

93. Finally, maximum principal tensile stresses computed in ABAQUS analyses using UMAT2, which contained an excessively high modulus function for the first day or so of age, exceeded 300 psi at 3- to 5-days age without creep and 150 psi with creep. Considering that the computed early-age stresses were high due to the abnormally high initial modulus used in UMAT2, it is probable that values of 100 psi or less with creep at 3-days age can be expected. This reinforces the conclusion reached with the WES2DT analyses that peak tensile stresses are less than 50 percent of modulus of rupture in this structure.

STEP 1
MPC. FUNCTION - +2.0E+02
DISPLACED LINES - DISPLACED MESH
ORIGINAL LINES - ORIGINAL MESH

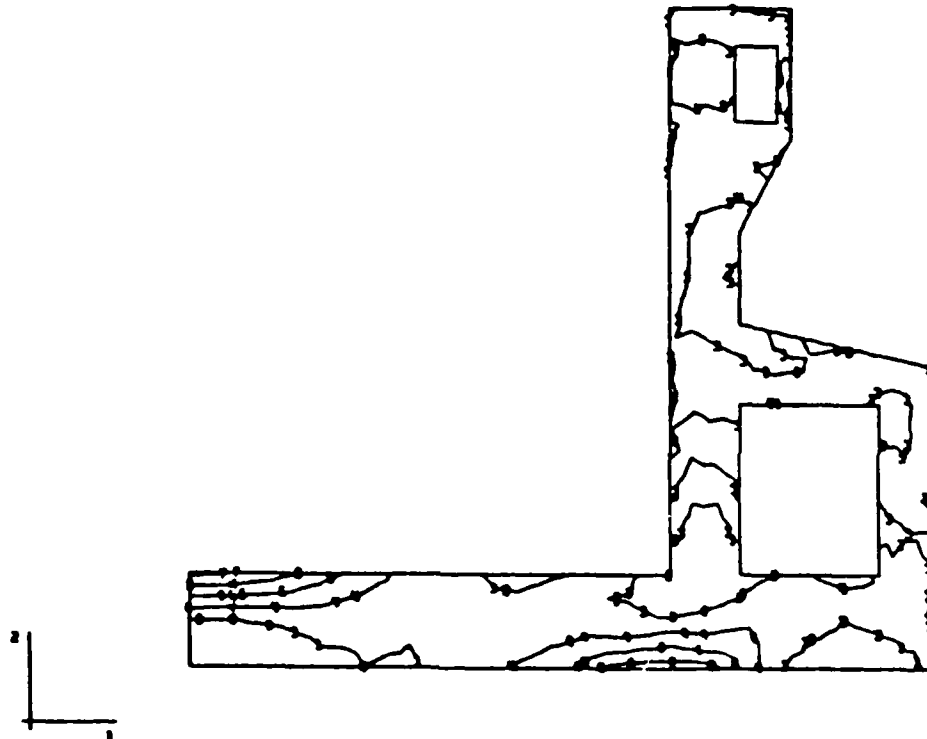


ENTIRE STRUCTURE - MPC - M 13 - COARSE MODEL
STEP 1 ELEMENT 1 REVISED VERSION 6-8-1977

Figure 16a. Displaced structure from gravity turn-on analysis,
 $E = 3.12 \times 10^6$ psi

MAX. PRINCIPAL STRESS

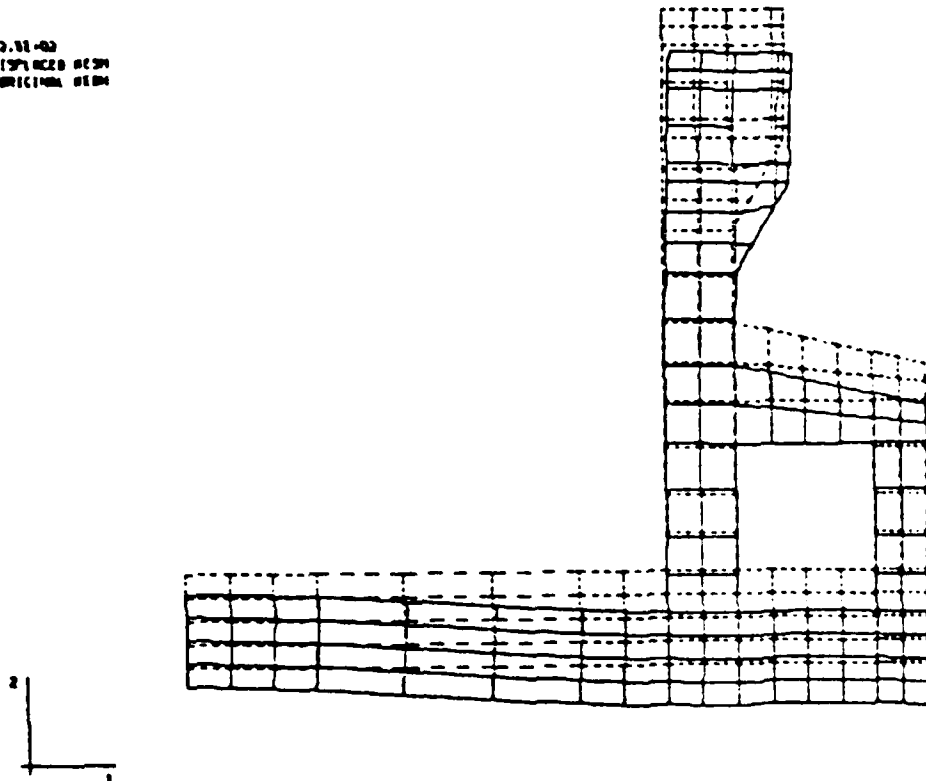
- S.O. VALUE
- 1 -1.00E+02
 - 2 -5.00E+01
 - 7 -2.77E+13
 - 4 -3.00E+01
 - 5 -1.00E+02
 - 8 -1.00E+02
 - 7 -2.00E+02
 - 6 -2.00E+02
 - 9 -3.00E+02



ENTIRE STRUCTURE - MPC - M 13 - COARSE MODEL
STEP 1 INCREMENT 1 REVISED VERSION 9-8-1977

Figure 16b. Maximum principal stress contours for gravity turn-on analysis.
 $E = 3.12 \times 10^6$ psi

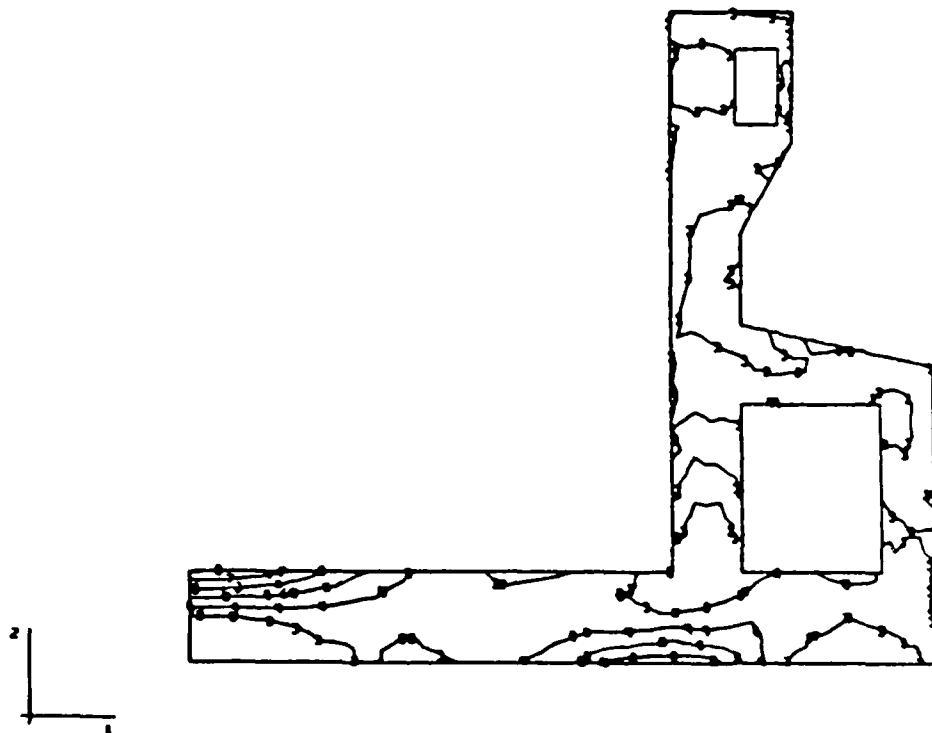
DISPL.
SCALE FACTOR = +2.0E+02
SOLID LINES - DISPLACED BEAM
DASHED LINES - ORIGINAL BEAM



ENTIRE STRUCTURE - MPC - M 13 - COARSE MODEL
STEP 1 INCREMENT 1 MESSAGE NUMBER 6-6-147

Figure 17a. Displaced structure from gravity turn-on analysis.
 $E = 4.8 \times 10^6$ psi

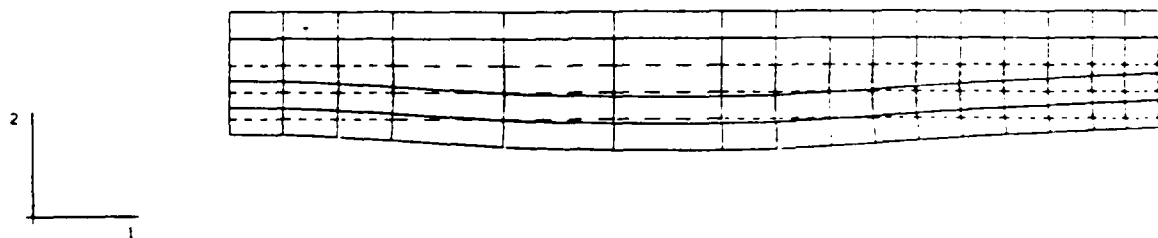
MAX. PRINCIPAL STRESS	
1. NO.	2. VALUE
1	-1.00E+02
2	5.00E+01
3	-2.77E+13
4	5.00E+01
5	-1.00E+02
6	-1.00E+02
7	2.00E+02
8	-2.50E+02
9	3.00E+02



ENTIRE STRUCTURE - MPC - M 13 - COARSE MODEL
 STEP 1 FREQUENCY 1 REVISION NUMBER 0-0-107

Figure 17b. Maximum principal stress contours for gravity turn-on analysis,
 $E = 4.8 \times 10^6$ psi

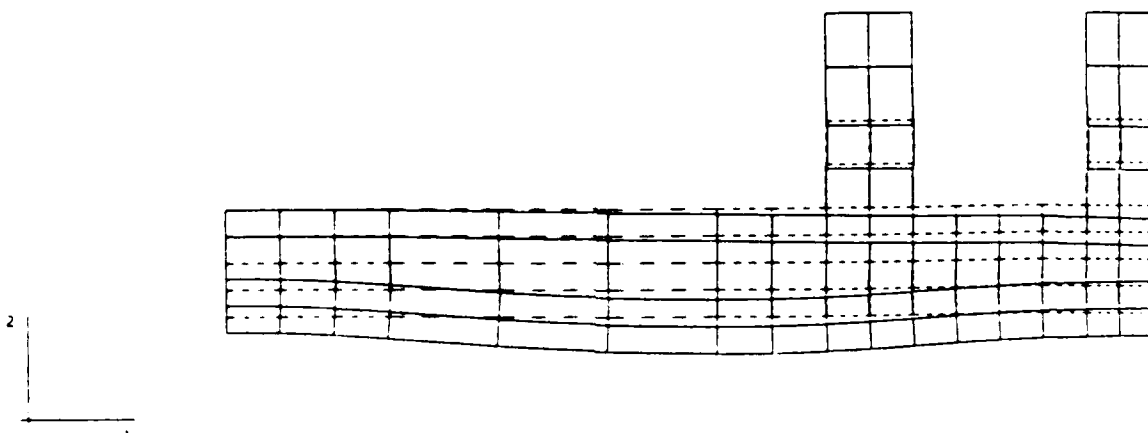
DISPL.
MAG. FACTOR = +2.5E-02
SOLID LINES - DISPLACED MESH
DASHED LINES - ORIGINAL MESH



LIFT2 - M13 - COARSE MODEL
STEP 8 INCREMENT 1 ABAQUS VERSION 4-5-147

Figure 18a. Displaced structure 5 days after lift 2 is placed,
gravity loading only, no creep, using program ABAQUS
with first grid

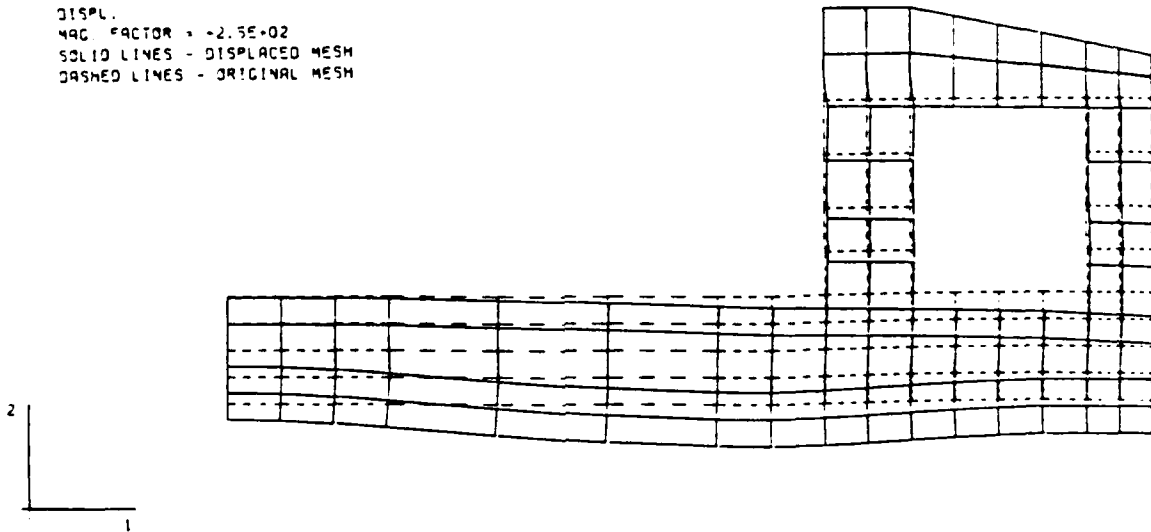
DISPL
MAG FACTOR = 2.5E-02
SOLID LINES = DISPLACED MESH
DASHED LINES = ORIGINAL MESH



LIFT4 - M13 - COARSE MODEL
STEP 15 INCREMENT 1 ABAQUS VERSION 4.5-147

Figure 18b. Displaced structure 5 days after lift 4 is placed,
gravity loading only, no creep, using program ABAQUS
with first grid

DISPL.
MAG FACTOR = +2.5E-02
SOLID LINES - DISPLACED MESH
DASHED LINES - ORIGINAL MESH



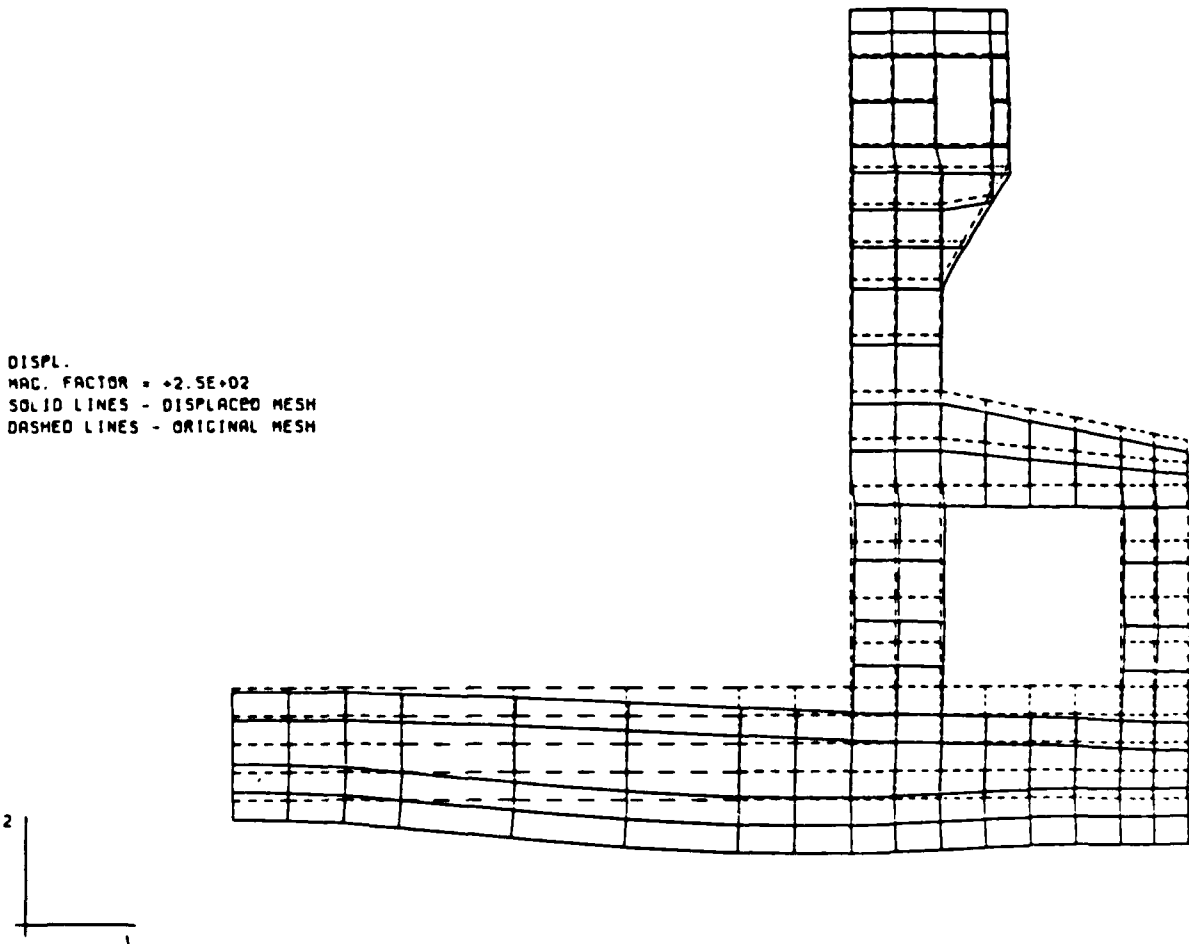
LIFTS - M13 - COARSE MODEL

STEP 20 INCREMENT 1

ABAQUS VERSION 4.5-147

Figure 18c. Displaced structure 5 days after lift 5 is placed,
gravity loading only, no creep, using program ABAQUS
with first grid

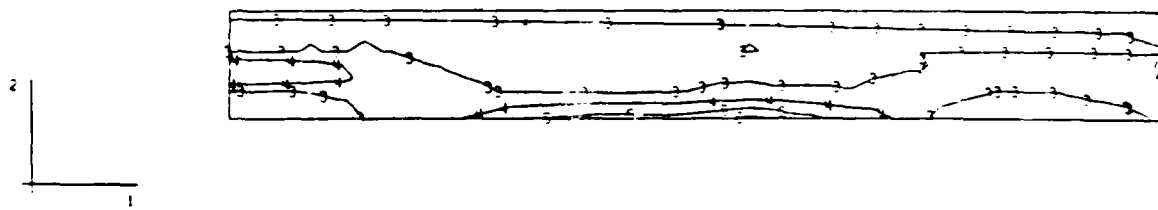
DISPL.
MAC. FACTOR = +2.5E+02
SOLID LINES - DISPLACED MESH
DASHED LINES - ORIGINAL MESH



LIFT9 - M13 - COARSE MODEL
STEP 36 INCREMENT 2 ABAQUS VERSION 4.5-147

Figure 18d. Maximum principal stress (tensile) contours in structure 7 days after placement of lift 9, gravity loading only, no creep, using program ABAQUS (UMAT 1) first grid

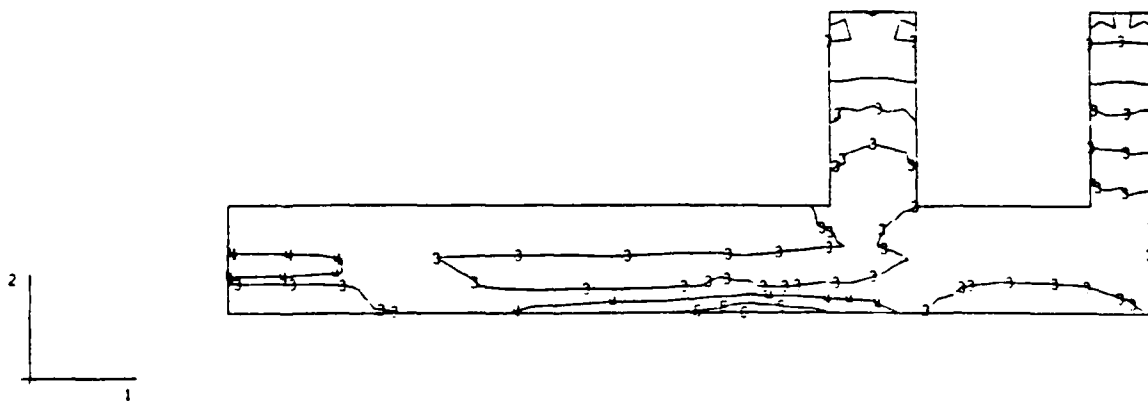
MAX. PRINCIPAL STRESS
 I. D. VALUE
 1 -1.00E-02
 2 -5.00E-01
 3 -2.27E-13
 4 +5.00E-01
 5 +1.00E-02
 6 +1.50E-02
 7 +2.00E-02
 8 +2.50E-02
 9 +3.00E-02



LIFT2 - M13 - COARSE MODEL
 STEP 8 INCREMENT 1 ABAQUS VERSION 4-5-147

Figure 19a. Maximum principal stress (tensile) contours in structure 5 days after placement of lift 2, gravity loading only, no creep, using program ABAQUS with first grid

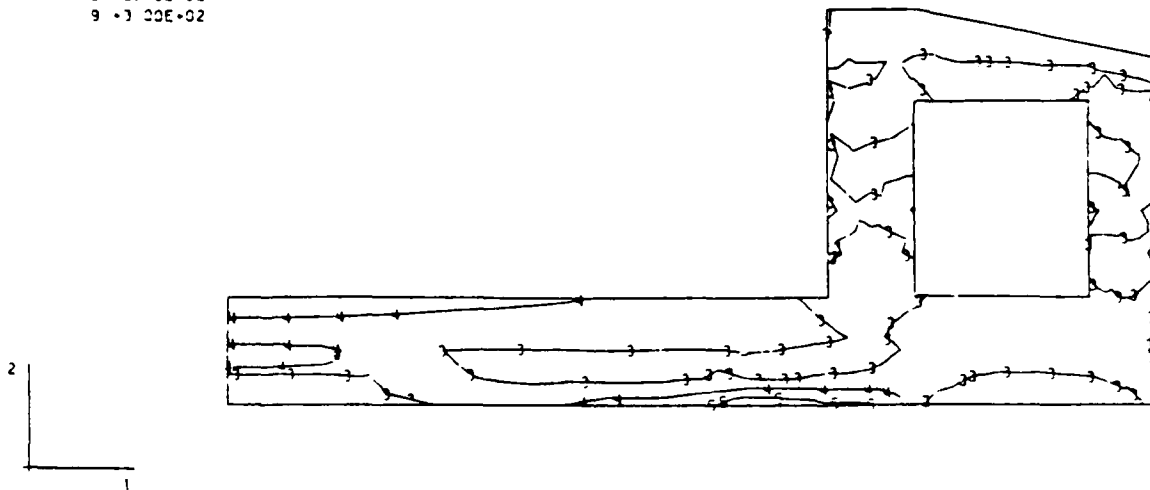
MAX. PRINCIPAL STRESS
 I.D. VALUE
 1 -1.00E+02
 2 -5.00E+01
 3 -2.27E+13
 4 +5.00E+01
 5 +1.00E+02
 6 +1.50E+02
 7 +2.00E+02
 8 +2.50E+02
 9 +3.00E+02



LIFT4 - M13 - COARSE MODEL
 STEP 16 INCREMENT 1 ABAQUS VERSION 4-5-147

Figure 19b. Maximum principal stress (tensile) contours in structure 5 days after placement of lift 4, gravity loading only, no creep, using program ABAQUS with first grid

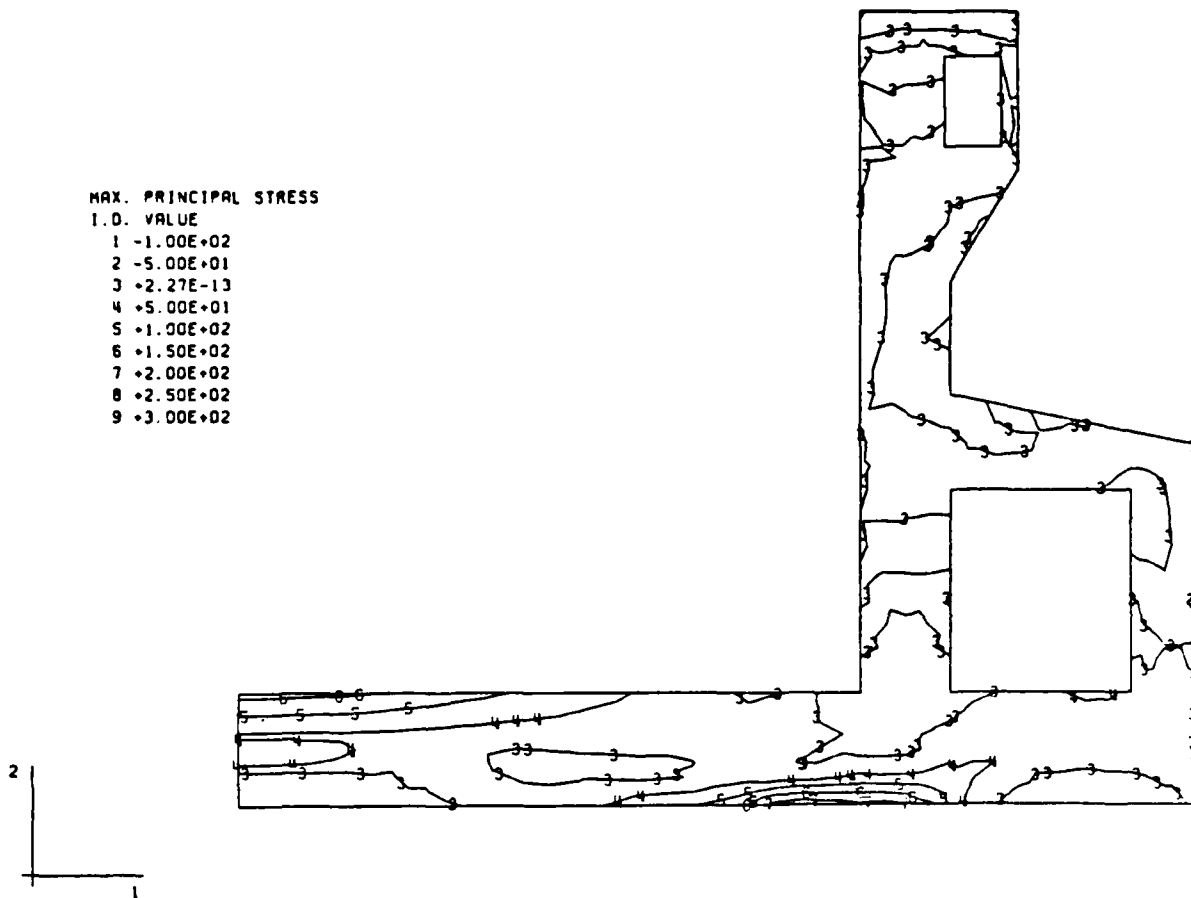
MAX. PRINCIPAL STRESS
 I.D. VALUE
 1 -1.00E+02
 2 -5.00E+01
 3 -2.27E+13
 4 +5.00E+01
 5 +1.00E+02
 6 +1.50E+02
 7 +2.00E+02
 8 +2.50E+02
 9 +3.00E+02



LIFTS - M13 - COARSE MODEL
 STEP 20 INCREMENT 1 ABAQUS VERSION 4.5-147

Figure 19c. Maximum principal stress (tensile) contours in structure 5 days after placement of lift 5, gravity loading only, no creep, using program ABAQUS with first grid

MAX. PRINCIPAL STRESS
 I.D. VALUE
 1 -1.00E+02
 2 -5.00E+01
 3 +2.27E-13
 4 +5.00E+01
 5 +1.00E+02
 6 +1.50E+02
 7 +2.00E+02
 8 +2.50E+02
 9 +3.00E+02



LIFT9 - M13 - COARSE MODEL
 STEP 36 INCREMENT 2 ABAQUS VERSION 4-5-147

Figure 19d. Displaced structure 7 days after lift 9 is placed, gravity loading only, no creep, using program ABAQUS (UMAT 1) with first grid

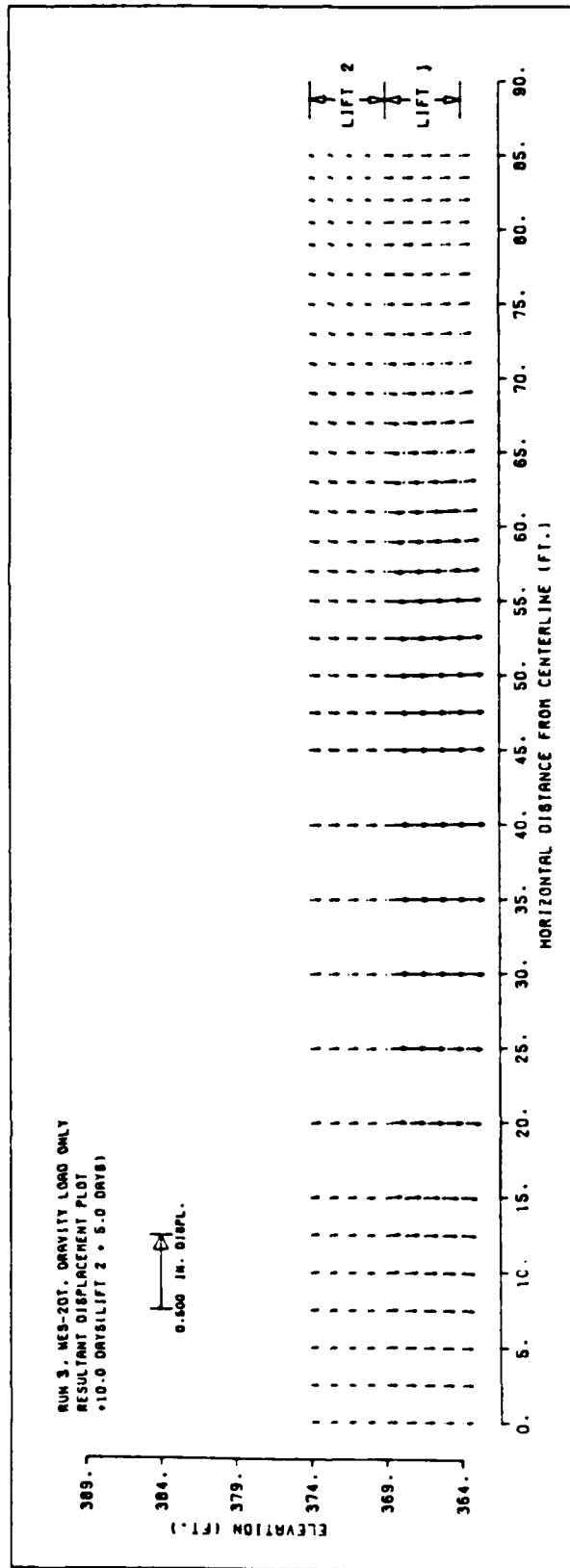


Figure 20a. Displacement of structure 5 days after lift 2 is placed, gravity load only, no creep, using WES-2DT program.

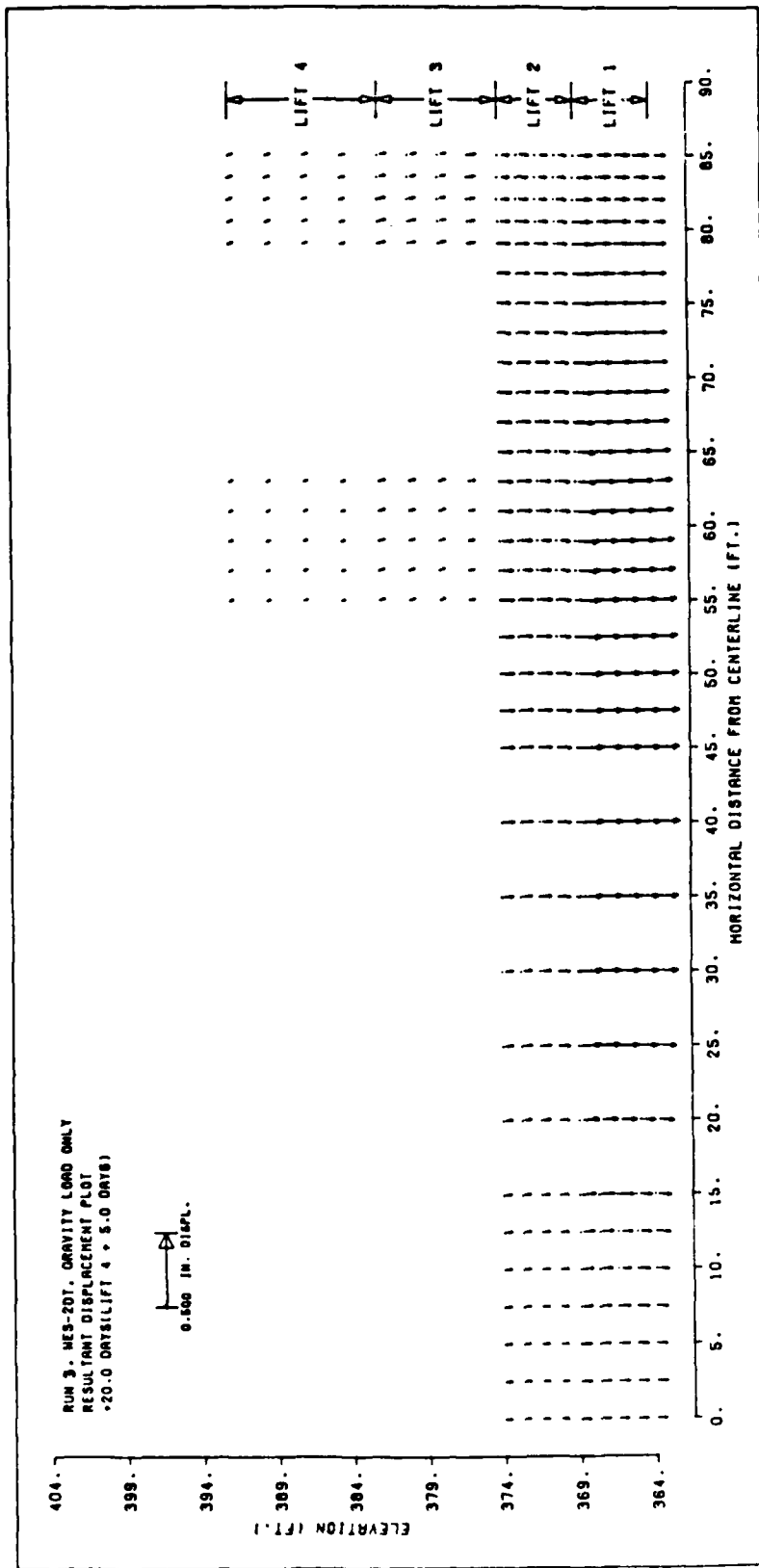


Figure 20b. Displacement of structure 5 days after lift 4 is placed, gravity load only, no creep, using WES-2DT program.

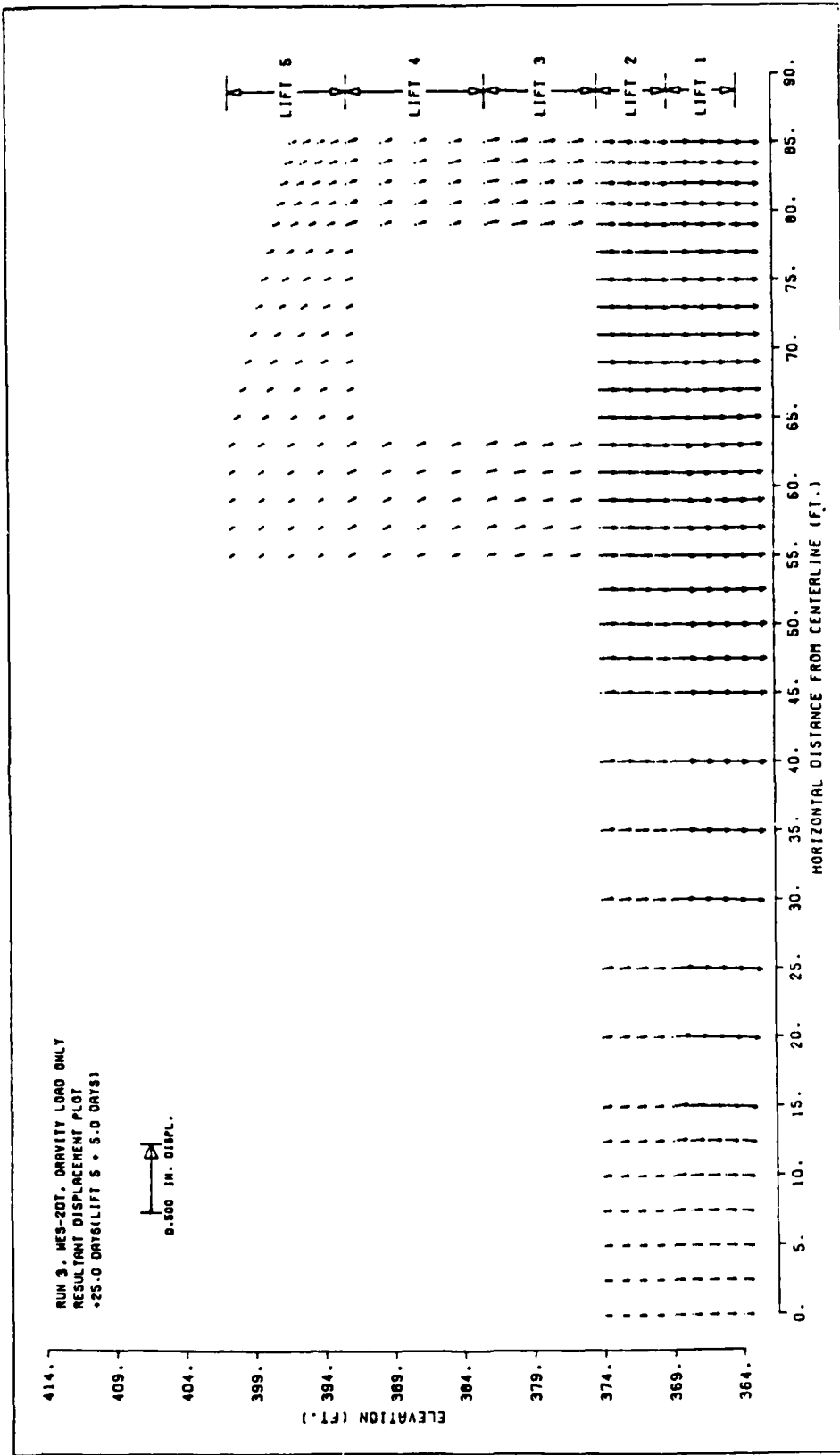


Figure 20c. Displacement of structure 5 days after lift 5 is placed, gravity load only, no creep, using WES-2DT program.

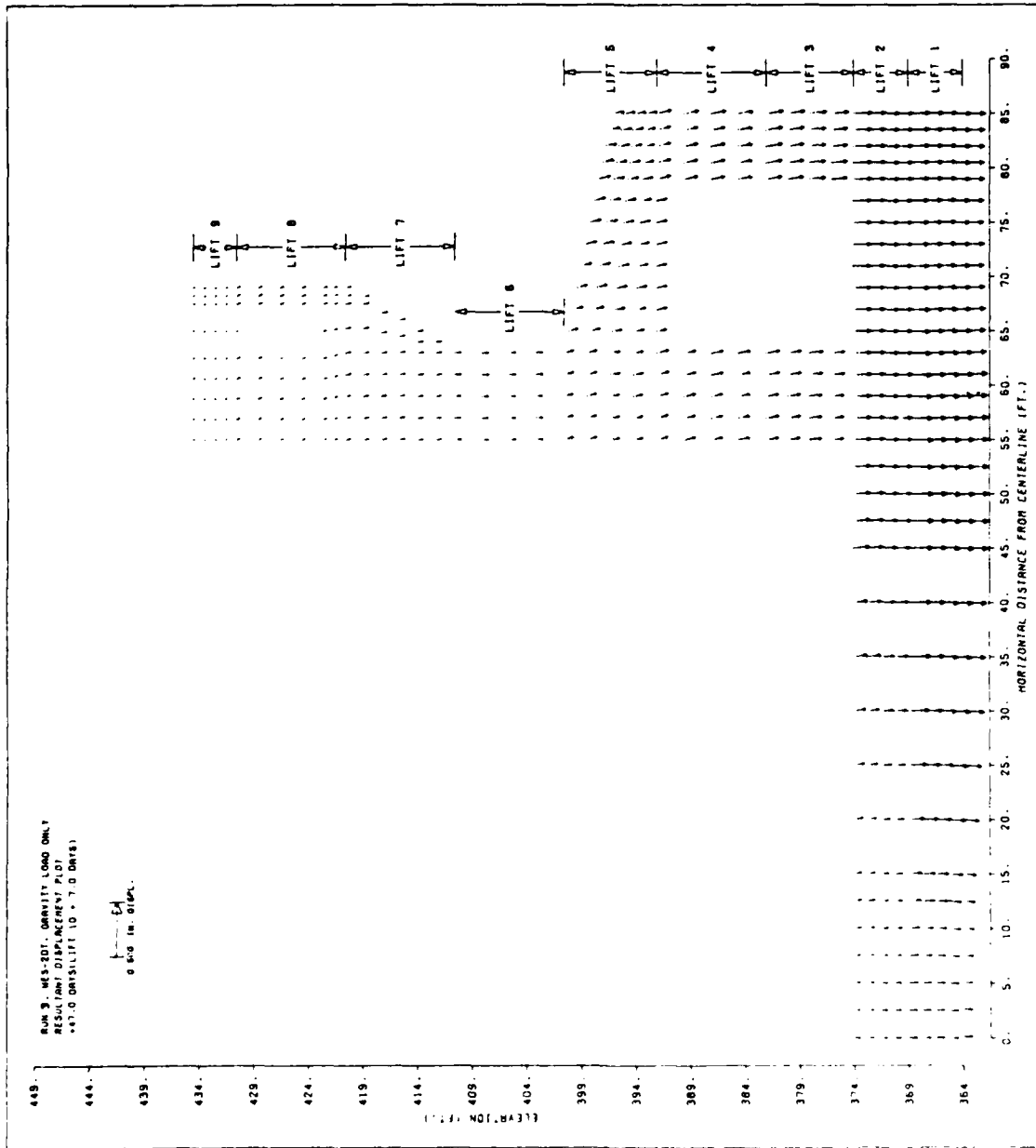


Figure 20d. Displacement of structure 7 days after lift 9 is placed, gravity load only, no creep, using WES-2DT program.

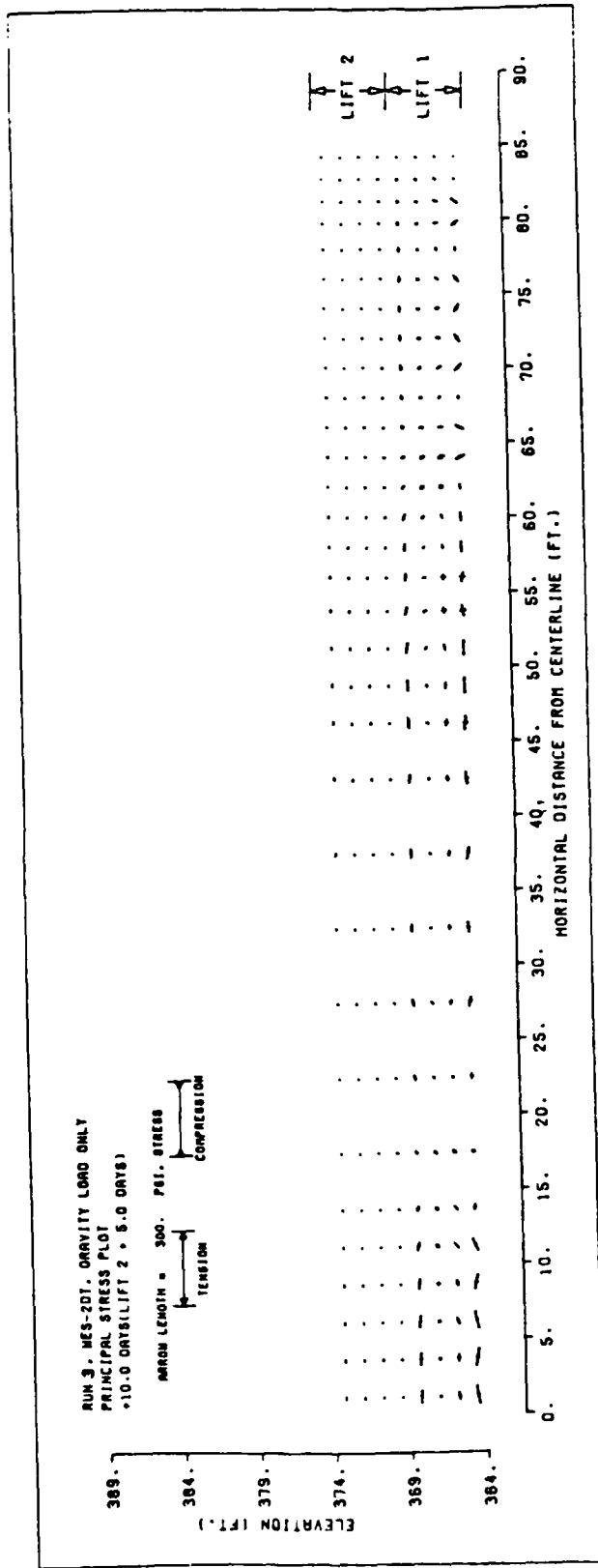


Figure 21a. Principal stress distribution in structure 5 days after lift 2 is placed, gravity loading only, no creep, using WES-2DT program.

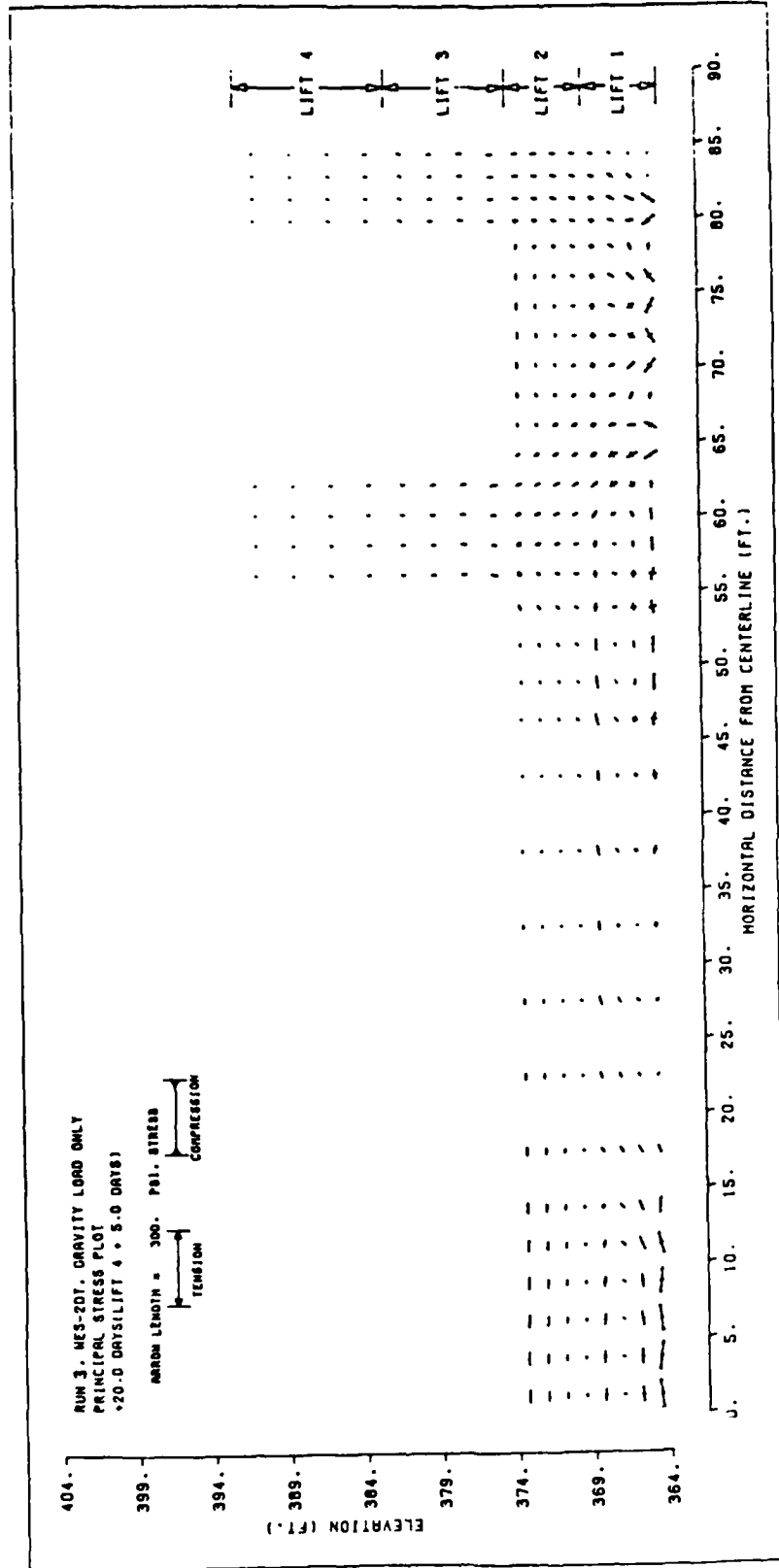


Figure 21b. Principal stress distribution in structure WES-2DT 5 days after lift 4 is placed, gravity loading only, no creep, using WES-2DT program.

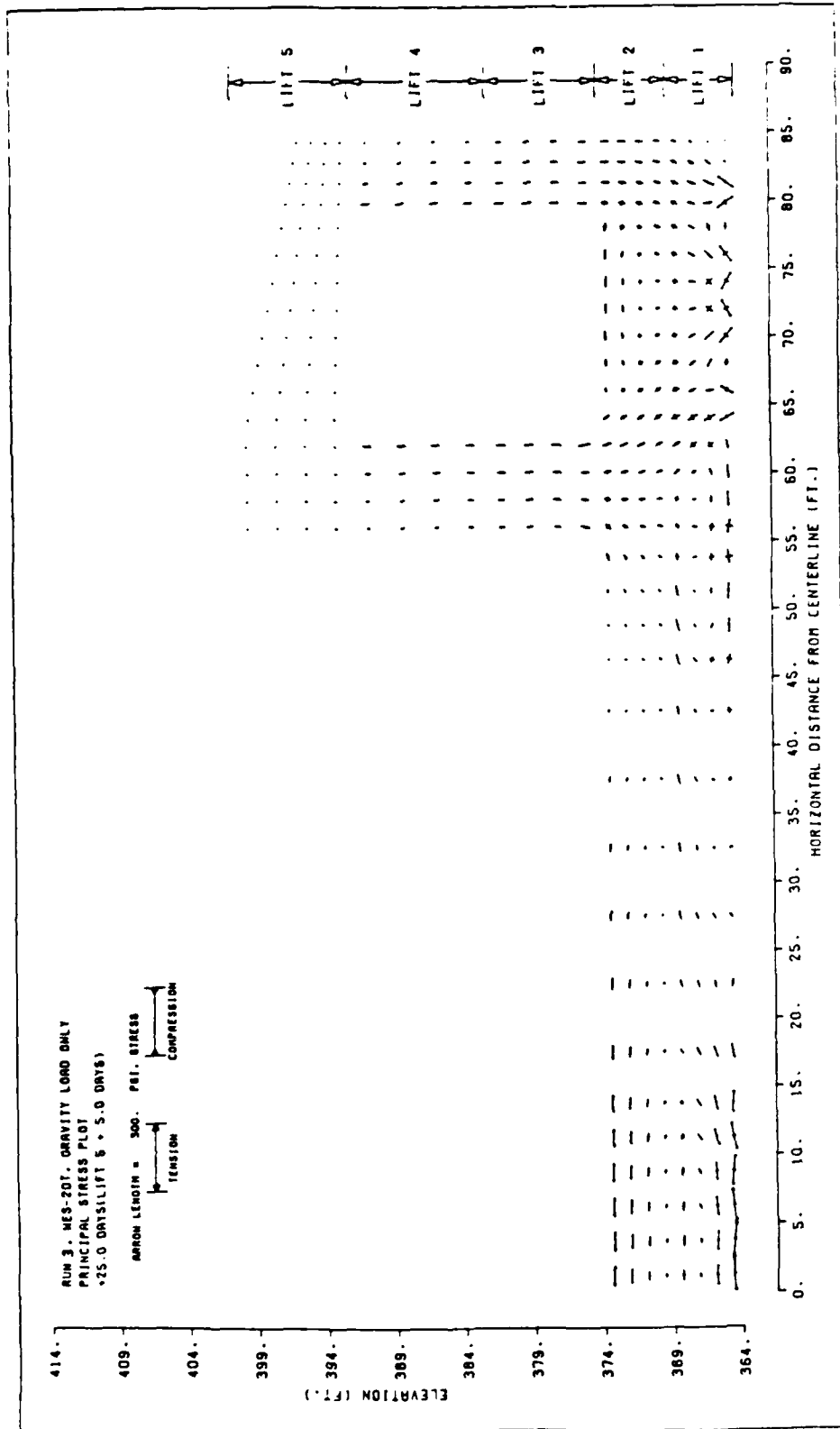


Figure 2lc. Principal stress distribution in structure 5 days after lift 5 is placed, gravity loading only, no creep, using WES-2DT program.

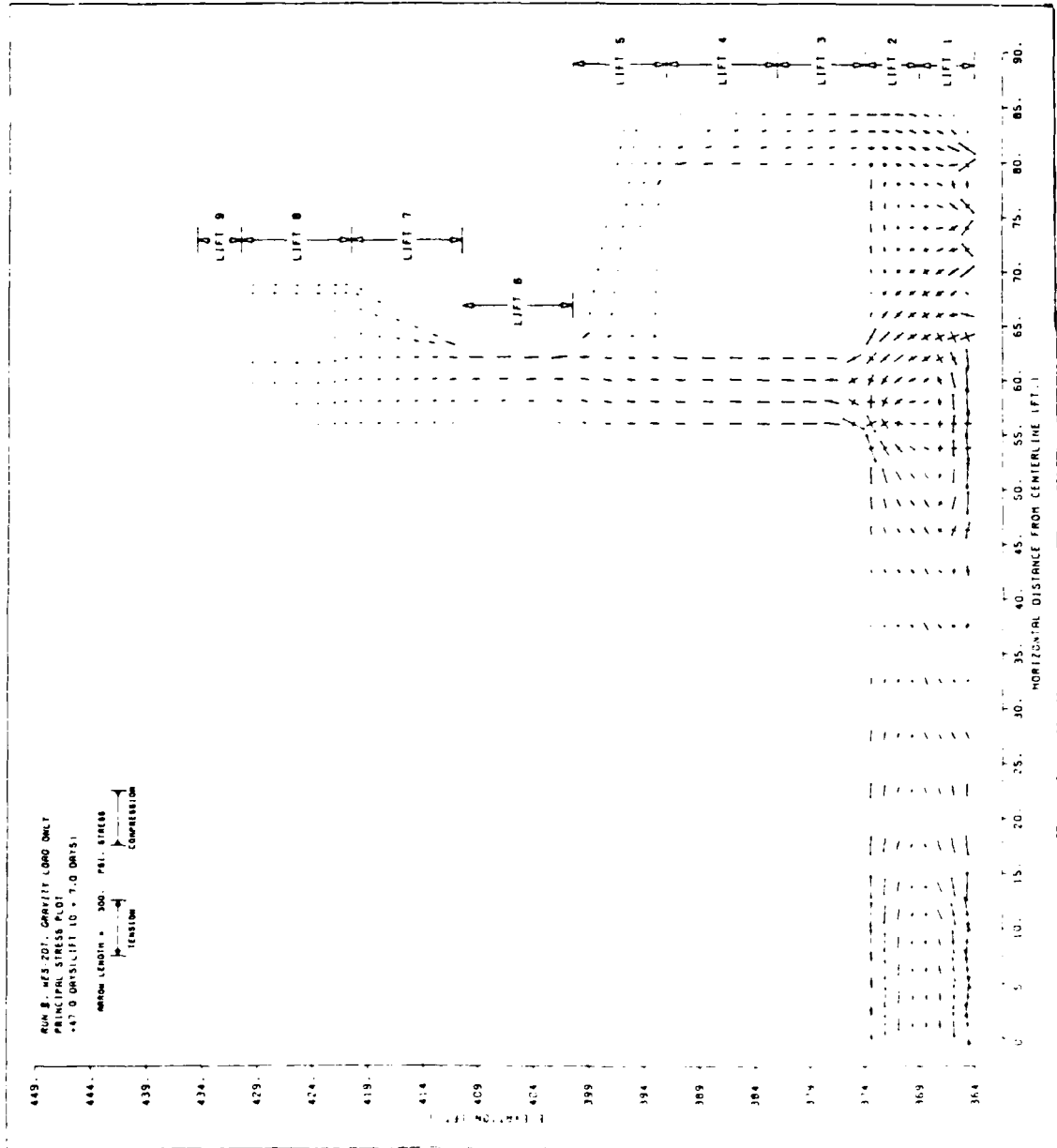


Figure 2ld. Principal stress distribution in structure 7 days after lift 9 is placed, gravity loading only, no creep, using WES-2DT program.

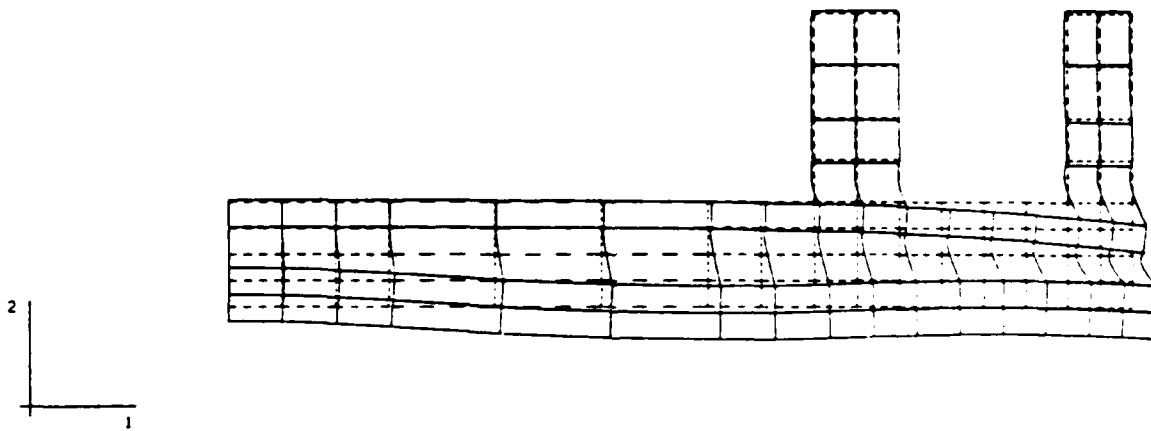
DISPL.
MAG. FACTOR = +2.5E+02
SOLID LINES - DISPLACED MESH
DASHED LINES - ORIGINAL MESH



LIFT2 - M13 - COARSE MODEL
STEP 8 INCREMENT 1 ABAQUS VERSION 4-5-147

Figure 22a. Displaced structure 5 days after lift 2 is placed, thermal and gravity loading, no creep, using program ABAQUS with first grid (UMAT 1)

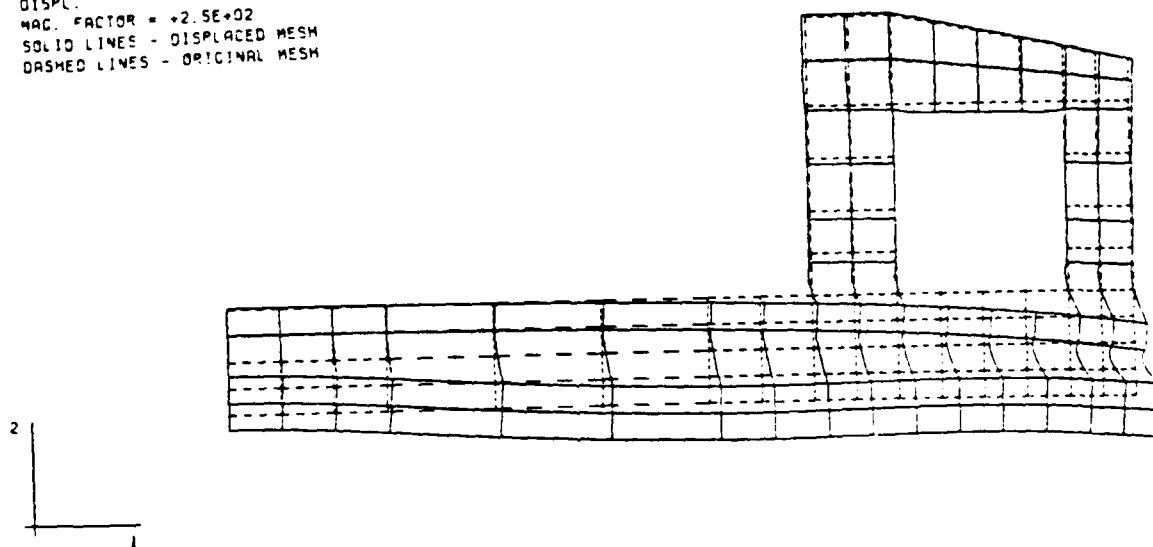
DISPL.
MAC. FACTOR = +2.5E+02
SOLID LINES - DISPLACED MESH
DASHED LINES - ORIGINAL MESH



LIFT4 - M13 - COARSE MODEL
STEP 16 INCREMENT 1 ABAQUS VERSION 4-5-147

Figure 22b. Displaced structure 5 days after lift 4 is placed, thermal and gravity loading, no creep, using program ABAQUS with first grid (UMAT 1)

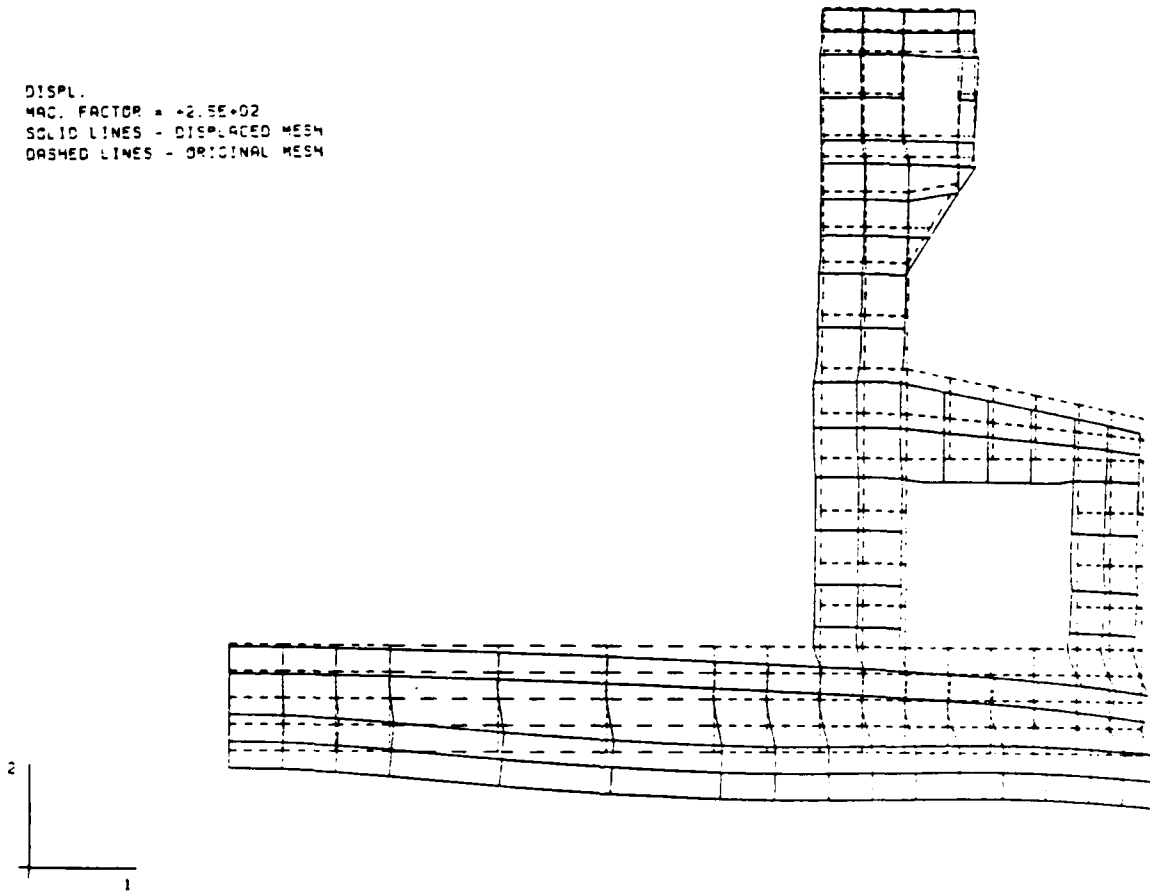
DISPL.
MAG. FACTOR = +2.5E+02
SOLID LINES - DISPLACED MESH
DASHED LINES - ORIGINAL MESH



LIFT5 - M13 - COARSE MODEL
STEP 20 INCREMENT 1 ABAQUS VERSION 4-5-147

Figure 22c. Displaced structure 5 days after lift 5 is placed, thermal and gravity loading, no creep, using program ABAQUS with first grid (UMAT 1)

DISPL.
MAC. FACTOR = +2.5E+02
SOLID LINES - DISPLACED MESH
DASHED LINES - ORIGINAL MESH



LIFT9 - M13 - COARSE MODEL
STEP 35 INCREMENT 2 ABAQUS VERSION 4-5-147

Figure 22d. Displaced structure 7 days after lift 10 is placed, thermal and gravity loading, no creep, using program ABAQUS with first grid (UMAT 1)

MAX. PRINCIPAL STRESS

I.D.	VALUE
1	-1.00E+02
2	-5.00E+01
3	-2.27E-13
4	+5.00E+01
5	+1.00E+02
6	+1.50E+02
7	+2.00E+02
8	+2.50E+02
9	+3.00E+02



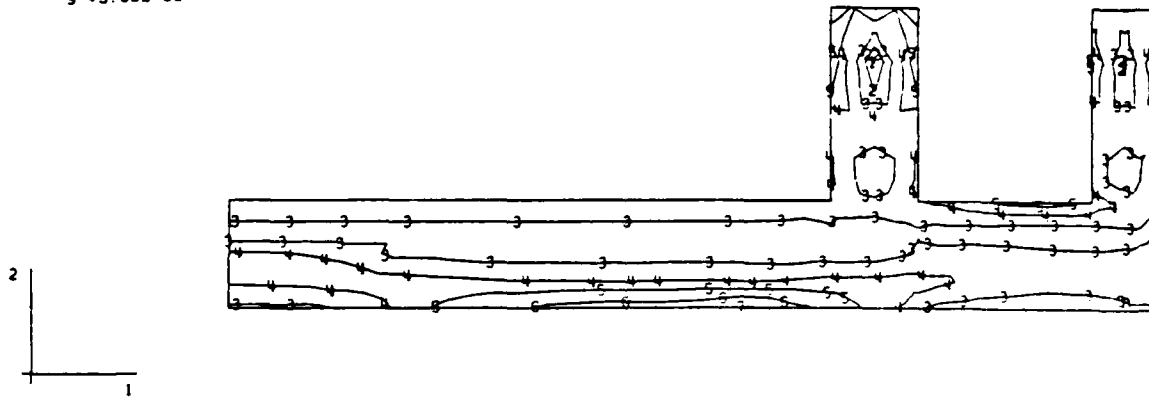
LIFT2 - M13 - COARSE MODEL

STEP 8 INCREMENT 1

ABAQUS VERSION 4-5-147

Figure 23a. Maximum principal stress (tensile) contours in structure 5 days after placement of lift 2, thermal and gravity loading, no creep, using program ABAQUS with first grid

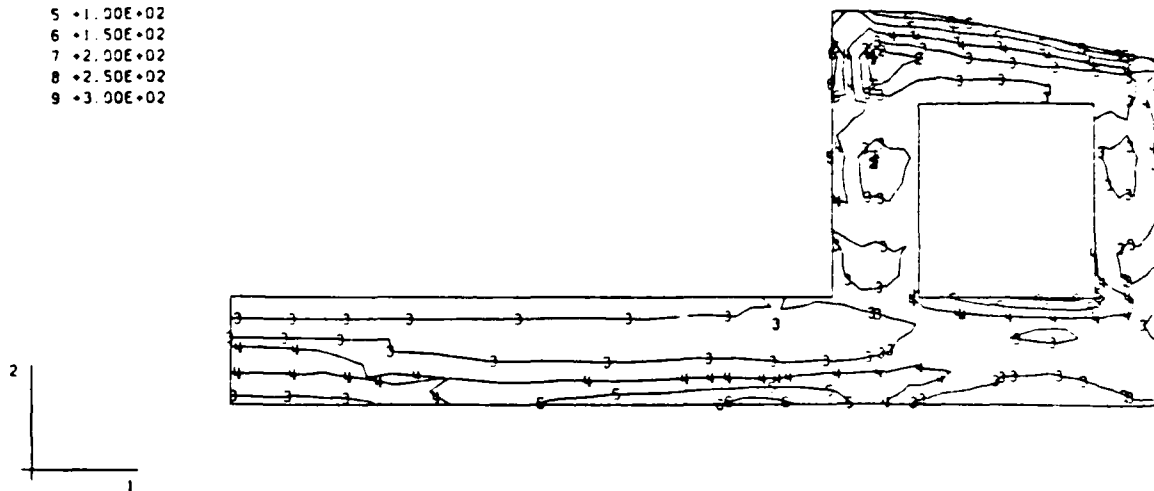
MAX. PRINCIPAL STRESS
 I.D. VALUE
 1 -1.00E+02
 2 -5.00E+01
 3 -2.27E-13
 4 +5.00E+01
 5 +1.00E+02
 6 +1.50E+02
 7 +2.00E+02
 8 +2.50E+02
 9 +3.00E+02



LIFT4 - M13 - COARSE MODEL
 STEP 16 INCREMENT 1 ABAQUS VERSION 4-5-147

Figure 23b. Maximum principal stress (tensile) contours in structure 5 days after placement of lift 4, thermal and gravity loading, no creep, using program ABAQUS with first grid

MAX. PRINCIPAL STRESS
 I.D. VALUE
 1 -1.00E+02
 2 -5.00E+01
 3 +2.27E-13
 4 +5.00E+01
 5 +1.00E+02
 6 +1.50E+02
 7 +2.00E+02
 8 +2.50E+02
 9 +3.00E+02

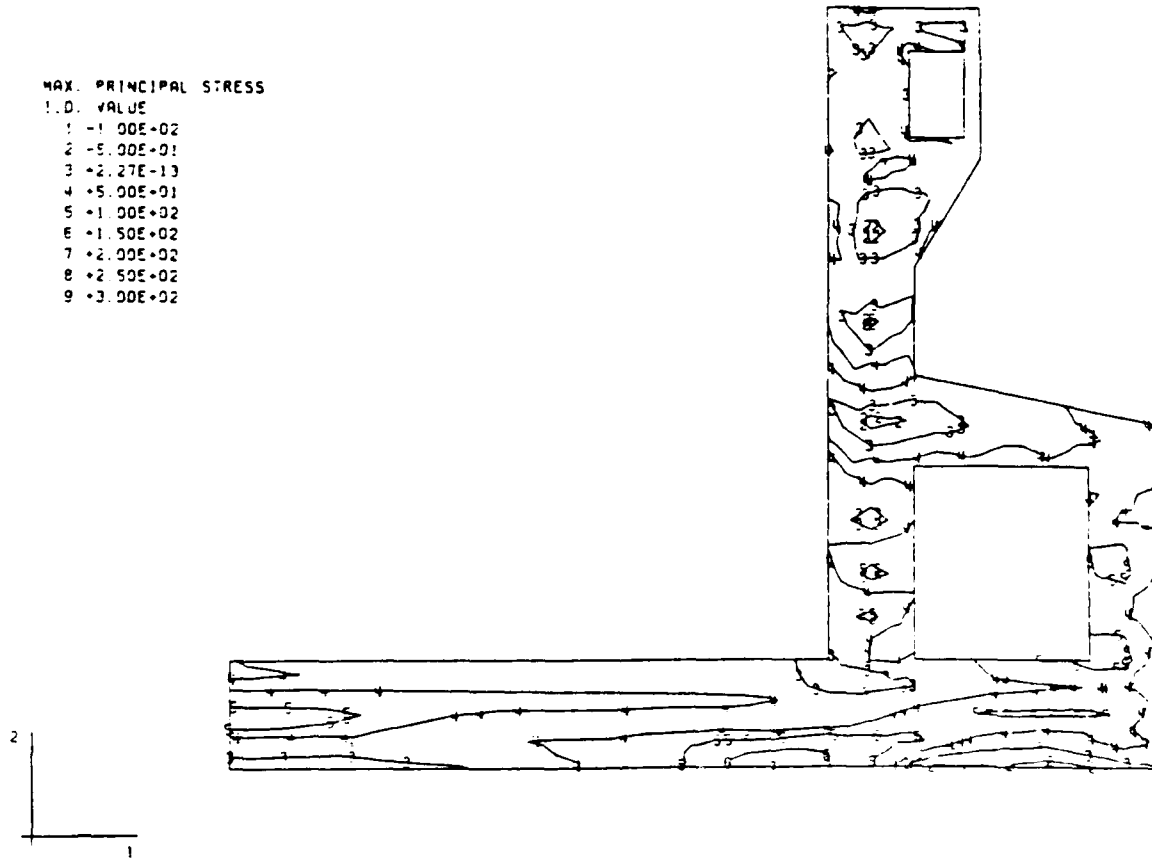


LIFT5 - M13 - COARSE MODEL
 STEP 20 INCREMENT 1 ABAQUS VERSION 4-5-147

Figure 23c. Maximum principal stress (tensile) contours in structure 5 days after placement of lift 5, thermal and gravity loading, no creep, using program ABAQUS with first grid

MAX. PRINCIPAL STRESS

- I.D. VALUE
1 -1.00E-02
2 -5.00E-01
3 +2.27E-13
4 +5.00E+01
5 +1.00E+02
6 +1.50E+02
7 +2.00E+02
8 +2.50E+02
9 +3.00E+02



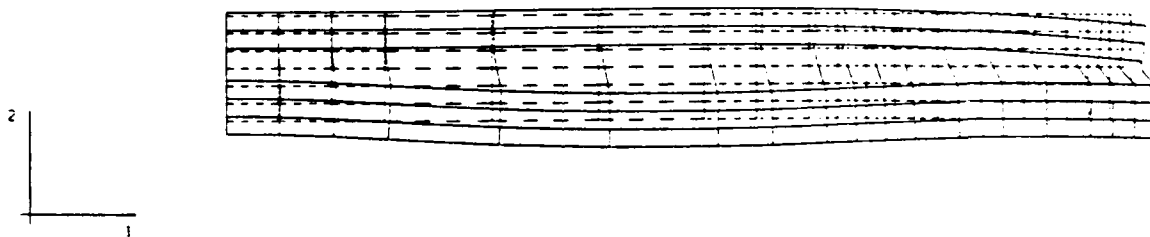
LIFT9 - M13 - COARSE MODEL

STEP 36 INCREMENT 2

ABAQUS VERSION 4-5-147

Figure 23d. Maximum principal stress (tensile) contours in structure 7 days after placement of lift 9, thermal and gravity loading, no creep, using program ABAQUS with first grid

DISPL.
MAG. FACTOR = +2.5E+02
SOLID LINES - DISPLACED MESH
DASHED LINES - ORIGINAL MESH



LIFT2 - M13 - FINE MODEL
STEP 8 INCREMENT 1 ABAQUS VERSION 4-5-147

Figure 24a. Displaced structure 5 days after lift 2 is placed, thermal and gravity loading, no creep, using program ABAQUS with second grid

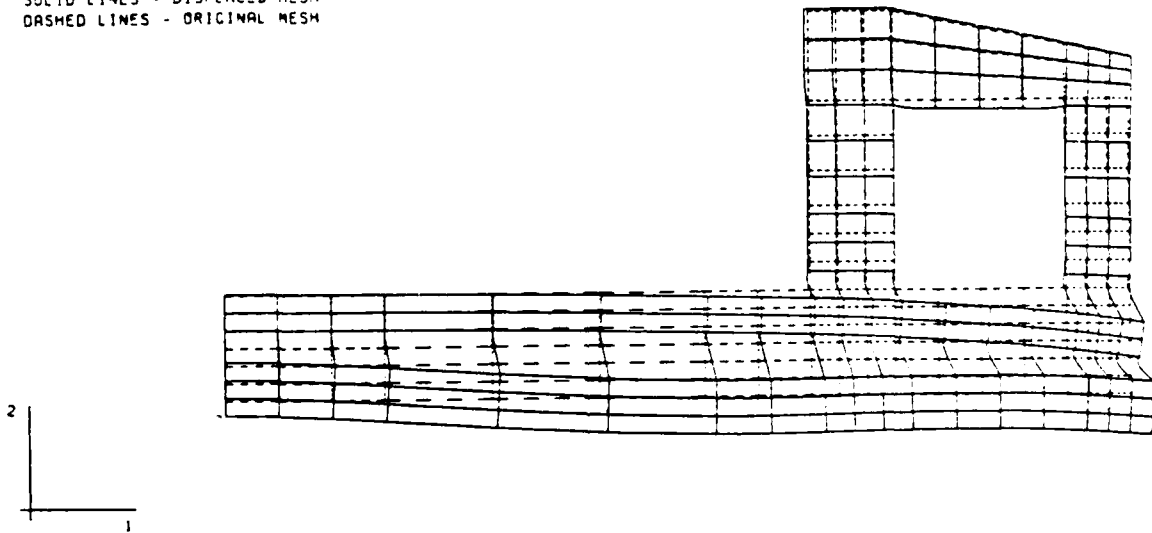
DISPL.
MAG. FACTOR = 42.5E+02
SOLID LINES - DISPLACED MESH
DASHED LINES - ORIGINAL MESH



LIFT4 - M13 - FINE MODEL
STEP 16 INCREMENT 1 ABAQUS VERSION 4.5-147

Figure 24b. Displaced structure 5 days after lift 4 is placed, thermal and gravity loading, no creep, using program ABAQUS with second grid

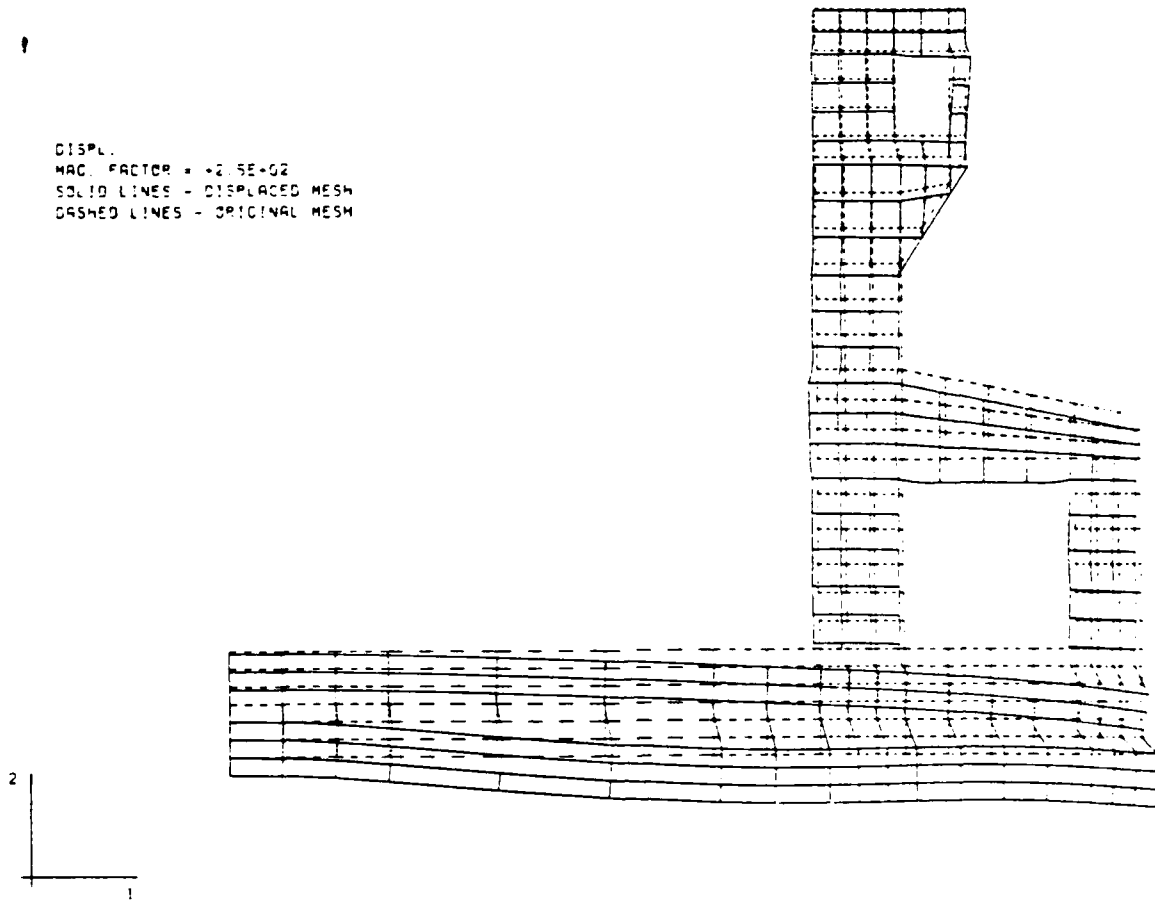
DISPL.
MAC. FACTOR = +2.5E+02
SOLID LINES - DISPLACED MESH
DASHED LINES - ORIGINAL MESH



LIFT5 - M13 - FINE MODEL
STEP 20 INCREMENT 1 ABAQUS VERSION 4-5-147

Figure 24c. Displaced structure 5 days after lift 5 is placed, thermal and gravity loading, no creep, using program ABAQUS with second grid

DISPL.
MAG. FACTOR = +2.5E+02
SOLID LINES - DISPLACED MESH
DASHED LINES - ORIGINAL MESH



LIFT9 - M13 - FINE MODEL
STEP 36 INCREMENT 2 ABAQUS VERSION 4.5-147

Figure 24d. Displaced structure 7 days after lift 9 is placed, thermal and gravity loading, no creep, using program ABAQUS with second grid

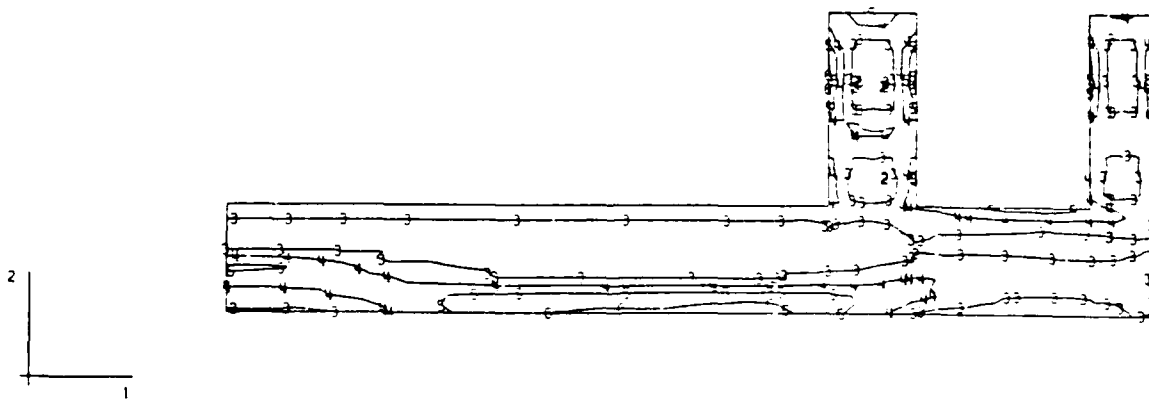
MAX. PRINCIPAL STRESS
 I. D. VALUE
 1 -1.00E+02
 2 -5.00E+01
 3 +2.27E-13
 4 +5.00E+01
 5 +1.00E+02
 6 +1.50E+02
 7 +2.00E+02
 8 +2.50E+02
 9 +3.00E+02



LIFT2 - M13 - FINE MODEL
 STEP 8 INCREMENT 1 ABAQUS VERSION 4-5-147

Figure 25a. Maximum principal stress (tensile) contours in structure 5 days after placement of lift 2, thermal and gravity loading, no creep, using program ABAQUS with second grid

MAX. PRINCIPAL STRESS
 I.D. VALUE
 1 -1.00E+02
 2 -5.00E+01
 3 +2.27E-13
 4 +5.00E+01
 5 +1.00E+02
 6 +1.50E+02
 7 +2.00E+02
 8 +2.50E+02
 9 +3.00E+02

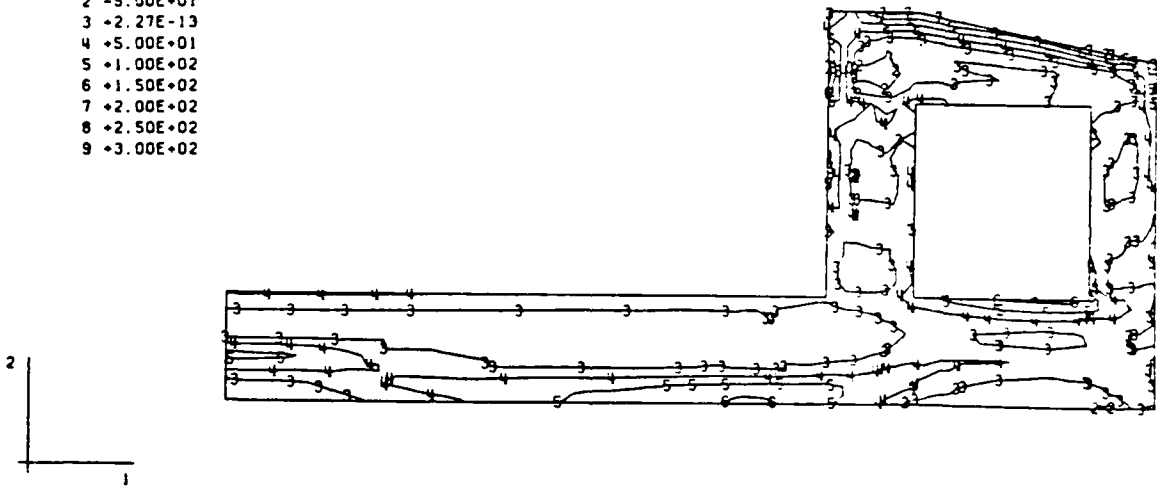


LIFT4 - M13 - FINE MODEL
 STEP 16 INCREMENT 1 ABAQUS VERSION 4.5-147

Figure 25b. Maximum principal stress (tensile) contours in structure 5 days after placement of lift 4, thermal and gravity loading, no creep, using program ABAQUS with second grid

MAX. PRINCIPAL STRESS

I.D.	VALUE
1	-1.00E+02
2	-5.00E+01
3	+2.27E-13
4	+5.00E+01
5	+1.00E+02
6	+1.50E+02
7	+2.00E+02
8	+2.50E+02
9	+3.00E+02



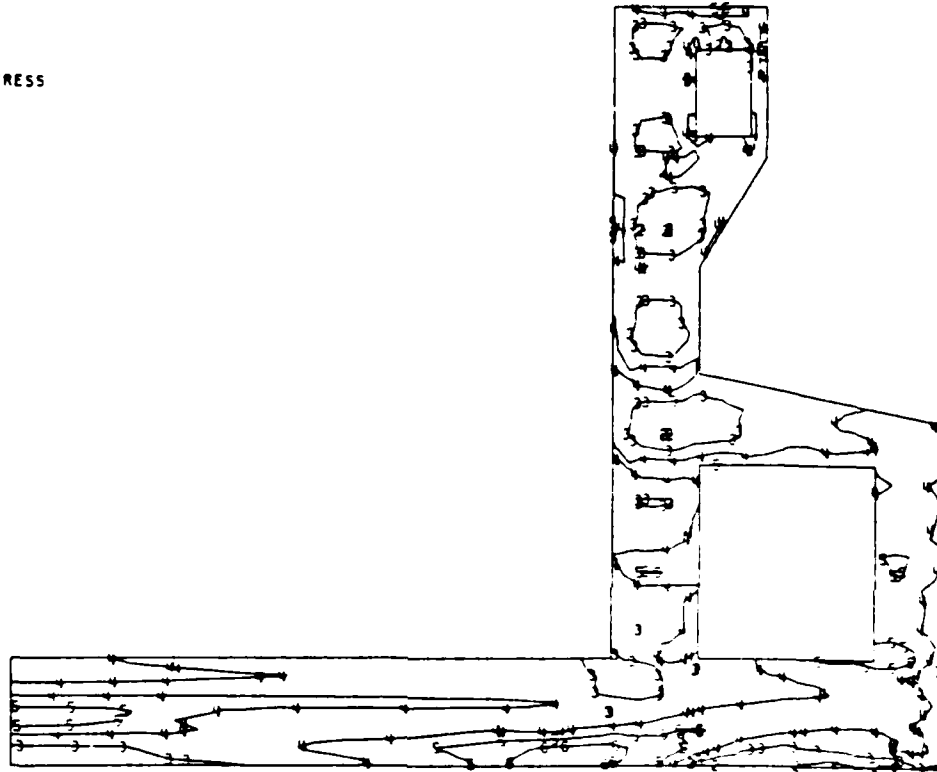
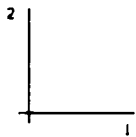
LIFT5 - M13 - FINE MODEL
STEP 20 INCREMENT 1 ABAQUS VERSION 4.5-147

Figure 25c. Maximum principal stress (tensile) contours in structure 5 days after placement of lift 5, thermal and gravity loading, no creep, using program ABAQUS with second grid

MAX. PRINCIPAL STRESS

I. O. VALUE

- 1 -1.00E+02
- 2 -5.00E+01
- 3 -2.27E-13
- 4 +5.00E+01
- 5 +1.00E+02
- 6 -1.50E+02
- 7 +2.00E+02
- 8 +2.50E+02
- 9 +3.00E+02



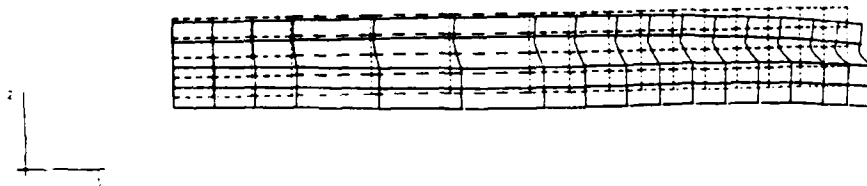
LIFT9 - M13 - FINE MODEL

STEP 36 INCREMENT 2

ABAQUS VERSION 4.5-147

Figure 25d. Maximum principal stress (tensile) contours in structure 7 days after placement of lift 9, thermal and gravity loading, no creep, using program ABAQUS with second grid

DISPL.
MAG. FACTOR = +2.5E+02
SOLID LINES - DISPLACED MESH
DASHED LINES - ORIGINAL MESH



LIFT2 - M10 - COARSE MODEL -NEW UMAT, NOSHINK, NOCREEP, E(T)=CONST.
STEP 8 INCREMENT 1 ABAQUS VERSION 4-5-147

Figure 26a. Displaced structure 5 days after placement of lift 2, E constant with temperature, using ABAQUS (UMAT2).

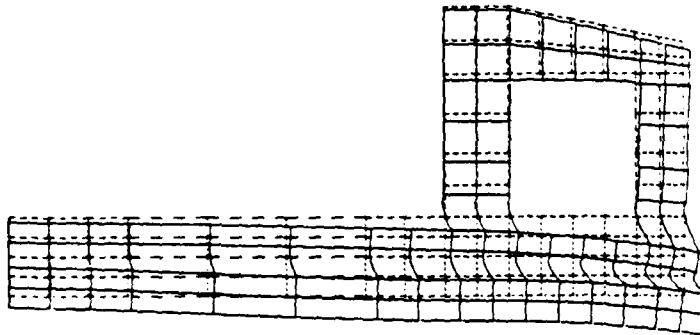
DISPL.
MAG. FACTOR = +2.5E+02
SOLID LINES - DISPLACED MESH
DASHED LINES - ORIGINAL MESH



LIFT4 - M13 - COARSE MODEL -NEW UMAT,NOSHRINK,NOCREEP,E(T)=CONST.
STEP 10 INCREMENT 1 ABAQUS VERSION 4.5-147

Figure 26b. Displaced structure 5 days after placement of lift 4, E constant with temperature, using ABAQUS (UMAT2).

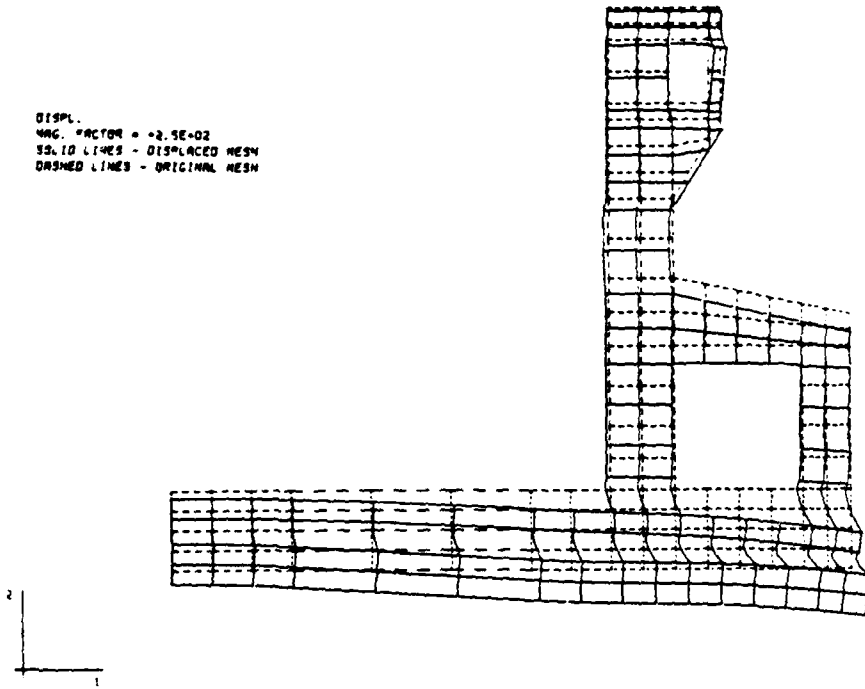
DISPL.
MAG. FACTOR = +2.5E+02
SOLID LINES - DISPLACED MESH
DASHED LINES - ORIGINAL MESH



LIFTS - M13 - COARSE MODEL -NEW UMAT,NOSHRINK,NOCREEP,E(T)=CONST.
STEP 20 INCREMENT 1 ABAQUS VERSION 4.5-147

Figure 26c. Displaced structure 5 days after placement of lift 5, E constant with temperature, using ABAQUS (UMAT2).

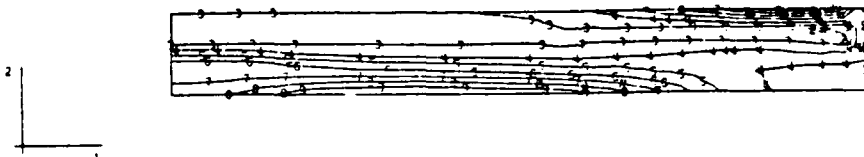
DISPL.
MAG. FACTOR = +2.5E+02
SOLID LINES - DISPLACED MESH
DASHED LINES - ORIGINAL MESH



LIFT9 - M13 - COARSE MODEL -NEW UMAT,NOSHRINK,NOCREEP,E(T)=CONST.
STEP 30 INCREMENT 2 ABAQUS VERSION 4.5-147

Figure 26d. Displaced structure 7 days after placement of lift 9, E constant with temperature, using ABAQUS (UMAT2).

MAX. PRINCIPAL STRESS
 I.D. VALUE
 1 -1.00E+02
 2 -5.00E+01
 3 -2.27E-13
 4 +5.00E+01
 5 +1.00E+02
 6 +1.50E+02
 7 +2.00E+02
 8 +2.50E+02
 9 +3.00E+02



LIFT2 - M13 - COARSE MODEL -NEW UMAT,NOSHRINK,NOCREEP,E(T)=CONST.
 STEP 8 INCREMENT 1 ABAQUS VERSION 4.5-147

Figure 27a. Maximum principal stress contours 5 days after placement of lift 2, E constant with temperature, using ABAQUS (UMAT2).

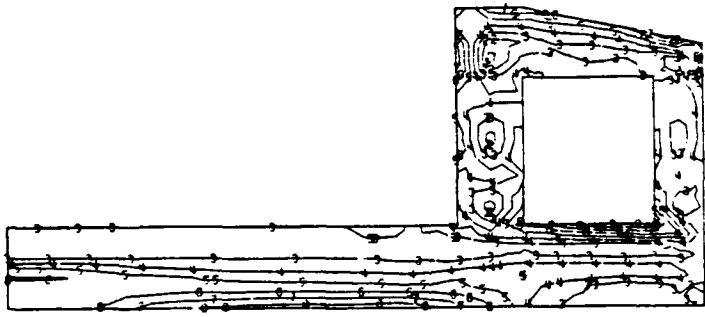
MAX. PRINCIPAL STRESS
 I.D. VALUE
 1 -1.20E+02
 2 -5.20E+01
 3 -2.27E+13
 4 +5.20E+01
 5 +1.20E+02
 6 +1.50E+02
 7 +2.20E+02
 8 +2.50E+02
 9 +3.20E+02



LIFT4 - M13 - COARSE MODEL -NEW UMAT, NUSHRINK, NOCREEP, E(T) =CONST.
 STEP 16 INCREMENT 1 ABAQUS VERSION 4.5-147

Figure 27b. Maximum principal stress contours 5 days after placement of lift 4, E constant with temperature, using ABAQUS (UMAT2).

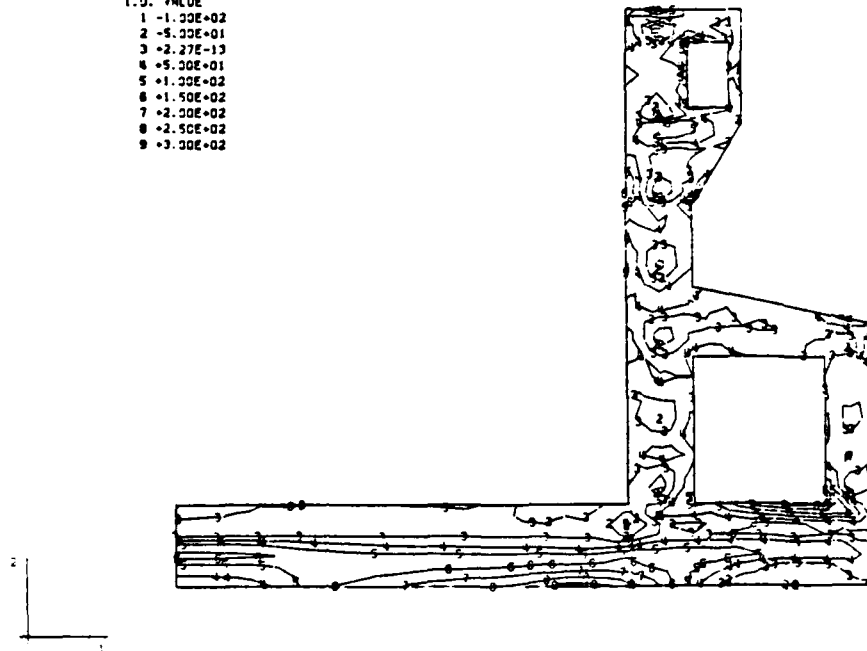
MAX. PRINCIPAL STRESS
 I.D. VALUE
 1 -1.00E+02
 2 -5.00E+01
 3 -2.47E+13
 4 +5.00E+01
 5 +1.00E+02
 6 +1.50E+02
 7 +2.00E+02
 8 +2.50E+02
 9 +3.00E+02



LIFTS - M13 - COARSE MODEL -NEW UMAT,NOSHRINK,NOCREEP,E(T)=CONST.
 STEP 20 INCREMENT 1 ABAQUS VERSION 4.5-147

Figure 27c. Maximum principal stress contours 5 days after placement of lift 5, E constant with temperature, using ABAQUS (UMAT2).

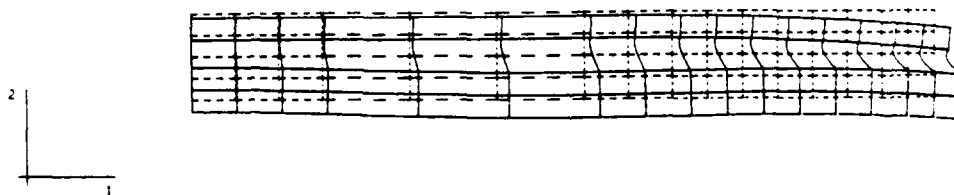
MAX. PRINCIPAL STRESS
 I.D. VALUE
 1 -1.20E+02
 2 -5.20E+01
 3 -2.27E+19
 4 +5.20E+01
 5 +1.20E+02
 6 +1.50E+02
 7 +2.20E+02
 8 +2.50E+02
 9 +3.20E+02



LIFT9 - M13 - COARSE MODEL -NEW UMAT,NOSHRINK,NOCREEP,E(T)=CONST.
 STEP 30 INCREMENT 2 ABAQUS VERSION 4.5-147

Figure 27d. Maximum principal stress contours 7 days after placement of lift 9, E constant with temperature, using ABAQUS (UMAT2).

DISPL.
MAG. FACTOR = +2.5E+02
SOLID LINES - DISPLACED MESH
DASHED LINES - ORIGINAL MESH



LIFT2 - M13 - COARSE MODEL -NEW UMAT,NO SHRINK,NO CREEP
STEP 8 INCREMENT 1 ABAQUS VERSION 4.5-147

Figure 28a. Displaced structure 5 days after placement of lift 2, E is a function of temperature, using ABAQUS (UMAT2).

DISPL.
MAC. FACTOR = +2.5E+02
SOLID LINES - DISPLACED MESH
DASHED LINES - ORIGINAL MESH

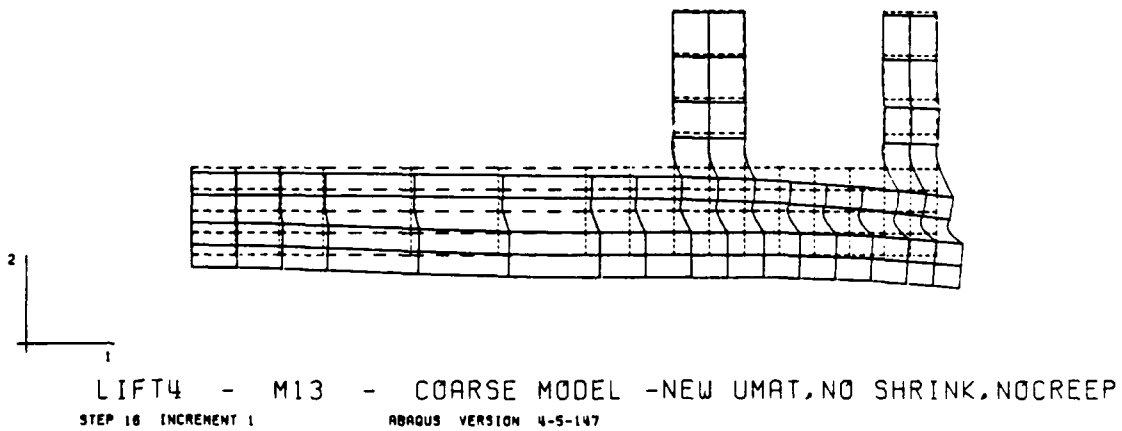


Figure 28b. Displaced structure 5 days after placement of lift 4, E is a function of temperature, using ABAQUS (UMAT2).

DISPL.
MAG. FACTOR = +2.5E+02
SOLID LINES - DISPLACED MESH
DASHED LINES - ORIGINAL MESH

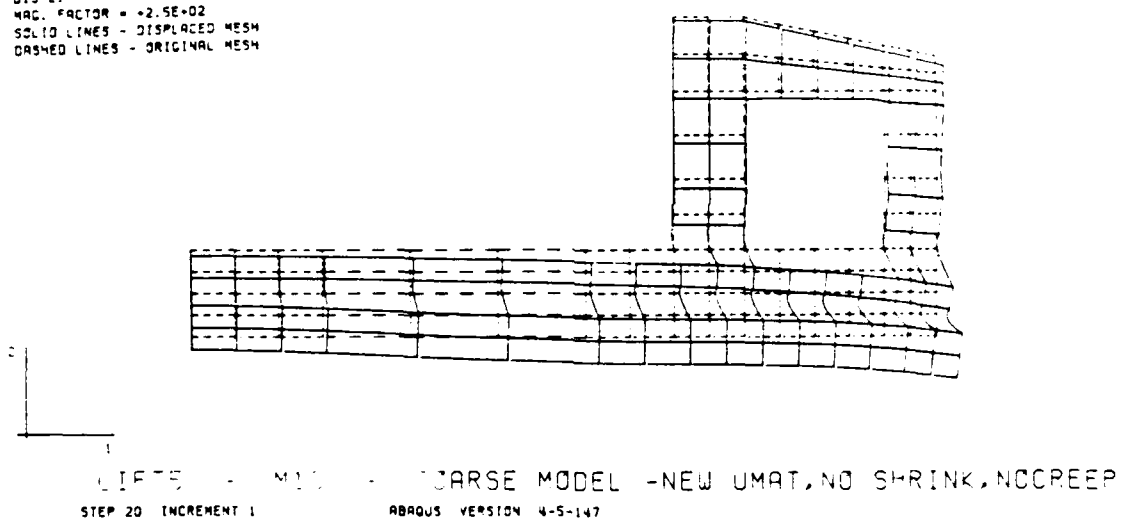
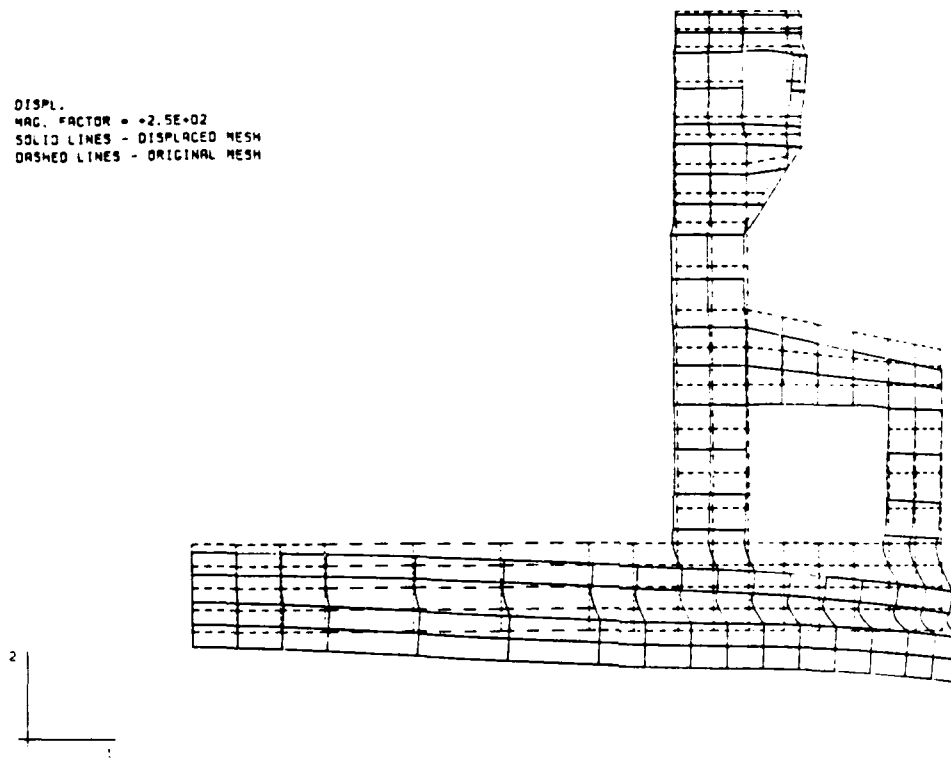


Figure 28c. Displaced structure 5 days after placement of lift 5, E is a function of temperature, using ABAQUS (UMAT2).

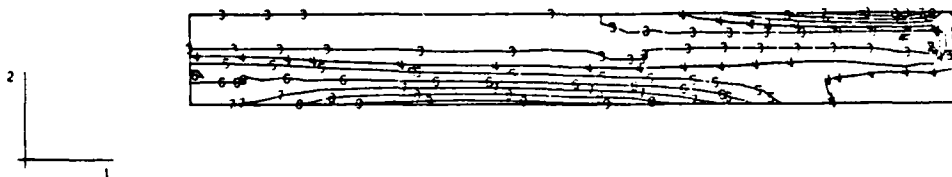
DISPL.
MAG. FACTOR = +2.5E+02
SOLID LINES - DISPLACED MESH
DASHED LINES - ORIGINAL MESH



LIFT9 - M13 - COARSE MODEL -NEW UMAT,NO SHRINK,NO CREEP
STEP 36 INCREMENT 2 ABAQUS VERSION 4.5-147

Figure 28d. Displaced structure 7 days after placement of lift 9, E is a function of temperature, using ABAQUS (UMAT2).

MAX. PRINCIPAL STRESS
 I.D. VALUE
 1 -1.00E+02
 2 -5.00E+01
 3 +2.27E-13
 4 +5.00E+01
 5 +1.00E+02
 6 +1.50E+02
 7 +2.00E+02
 8 +2.50E+02
 9 +3.00E+02

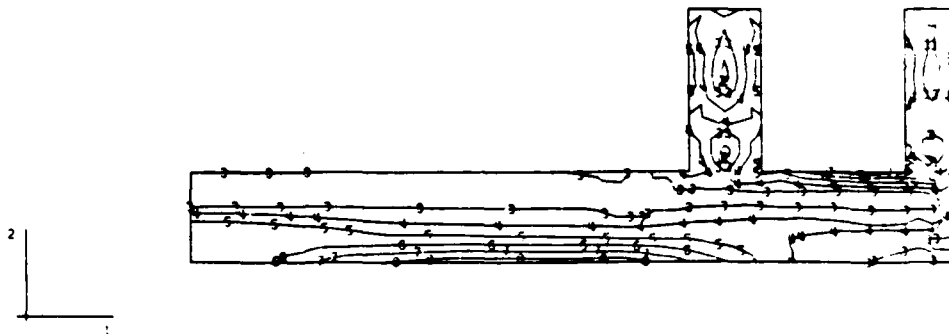


LIFT2 - M13 - COARSE MODEL -NEW UMAT,NO SHRINK,NO CREEP
 STEP 8 INCREMENT 1 ABAQUS VERSION 4.5-147

Figure 29a. Maximum principal stress contours 5 days after placement of lift 2, E is a function of temperature, using ABAQUS (UMAT2).

MAX. PRINCIPAL STRESS
 I.O. VALUE
 1 -1.00E+02
 2 -5.00E+01
 3 +2.2

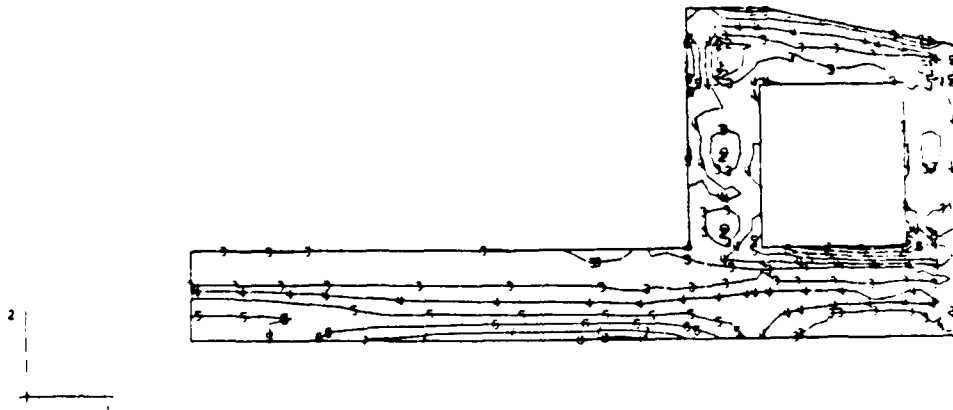
02
 7 +2.00E+02
 8 +2.50E+02
 9 +3.00E+02



LIFT4 - MODEL - COARSE MODEL -NEW UMAT,NO SHRINK,NO CREEP
 STEP 10 INCREMENT 1 ABAQUS VERSION 4.5-147

Figure 29b. Maximum principal stress contours 5 days after placement of lift 4, E is a function of temperature, using ABAQUS (UMAT2).

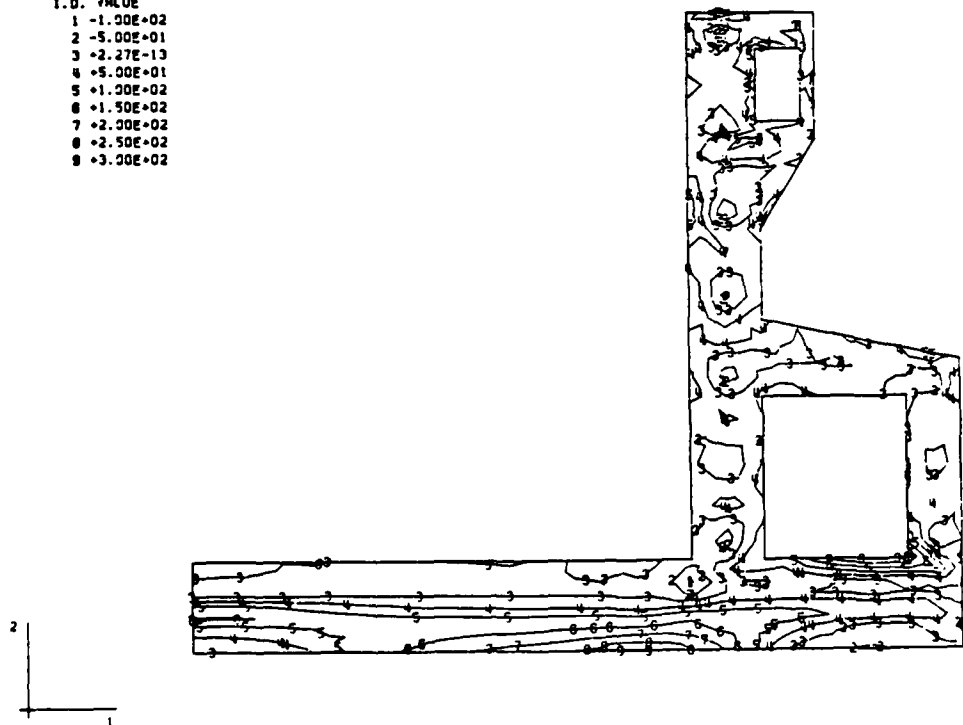
MAX PRINCIPAL STRESS
 I.D. VALUE
 1 -1.00E+02
 2 -5.00E+01
 3 -2.27E+13
 4 +5.00E+01
 5 +1.00E+02
 6 +1.50E+02
 7 +2.00E+02
 8 +2.50E+02
 9 +3.00E+02



LIFT5 - M13 - COARSE MODEL -NEW UMAT,NO SHRINK,NO CREEP
 STEP 20 INCREMENT 1 ABAQUS VERSION 4.5-147

Figure 29c. Maximum principal stress contours 5 days after placement of lift 5, E is a function of temperature, using ABAQUS (UMAT2).

MAX. PRINCIPAL STRESS
 I.D. VALUE
 1 -1.00E+02
 2 -5.00E+01
 3 -2.27E-13
 4 +5.00E+01
 5 +1.00E+02
 6 +1.50E+02
 7 +2.00E+02
 8 +2.50E+02
 9 +3.00E+02



LIFT9 - M13 - COARSE MODEL -NEW UMAT,NO SHRINK,NO CREEP
 STEP 36 INCREMENT 2 ABAQUS VERSION 4.5-147

Figure 29d. Maximum principal stress contours 7 days after placement of lift 9, E is a function of temperature, using ABAQUS (UMAT2).

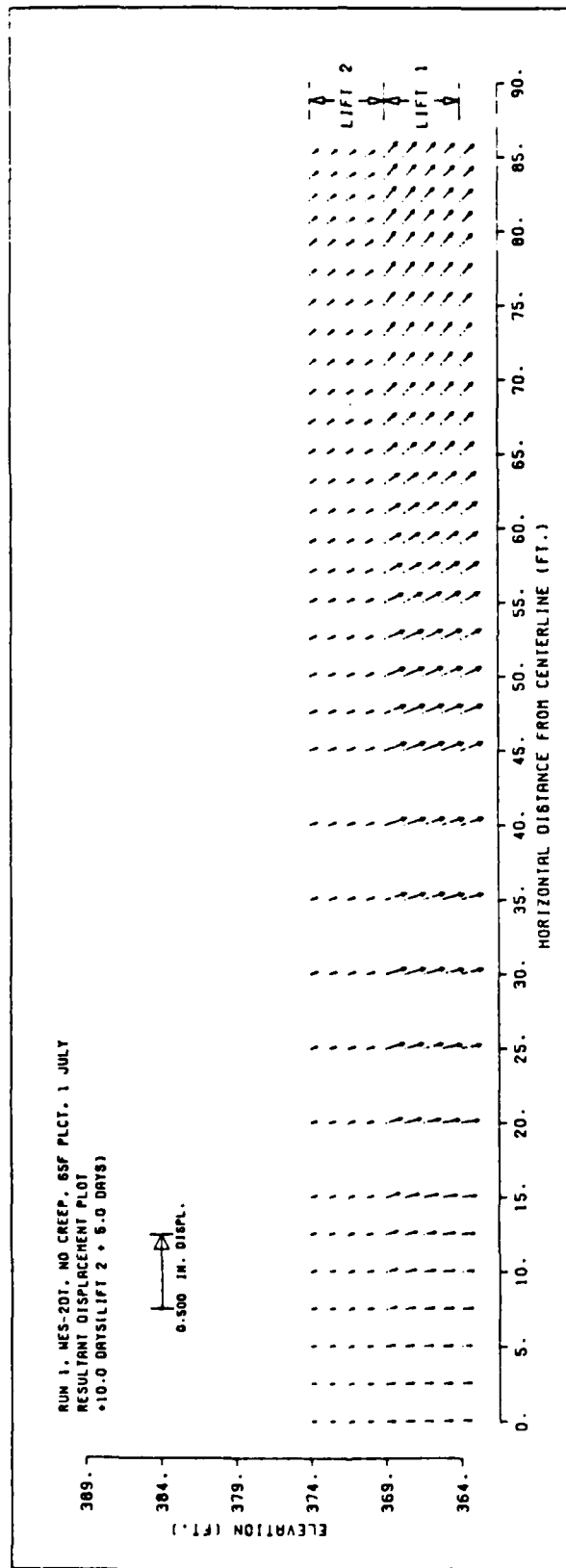


Figure 30a. Displacement of structure 5 days after lift 2 is placed thermal and gravity loading, no creep, using WES -2DT

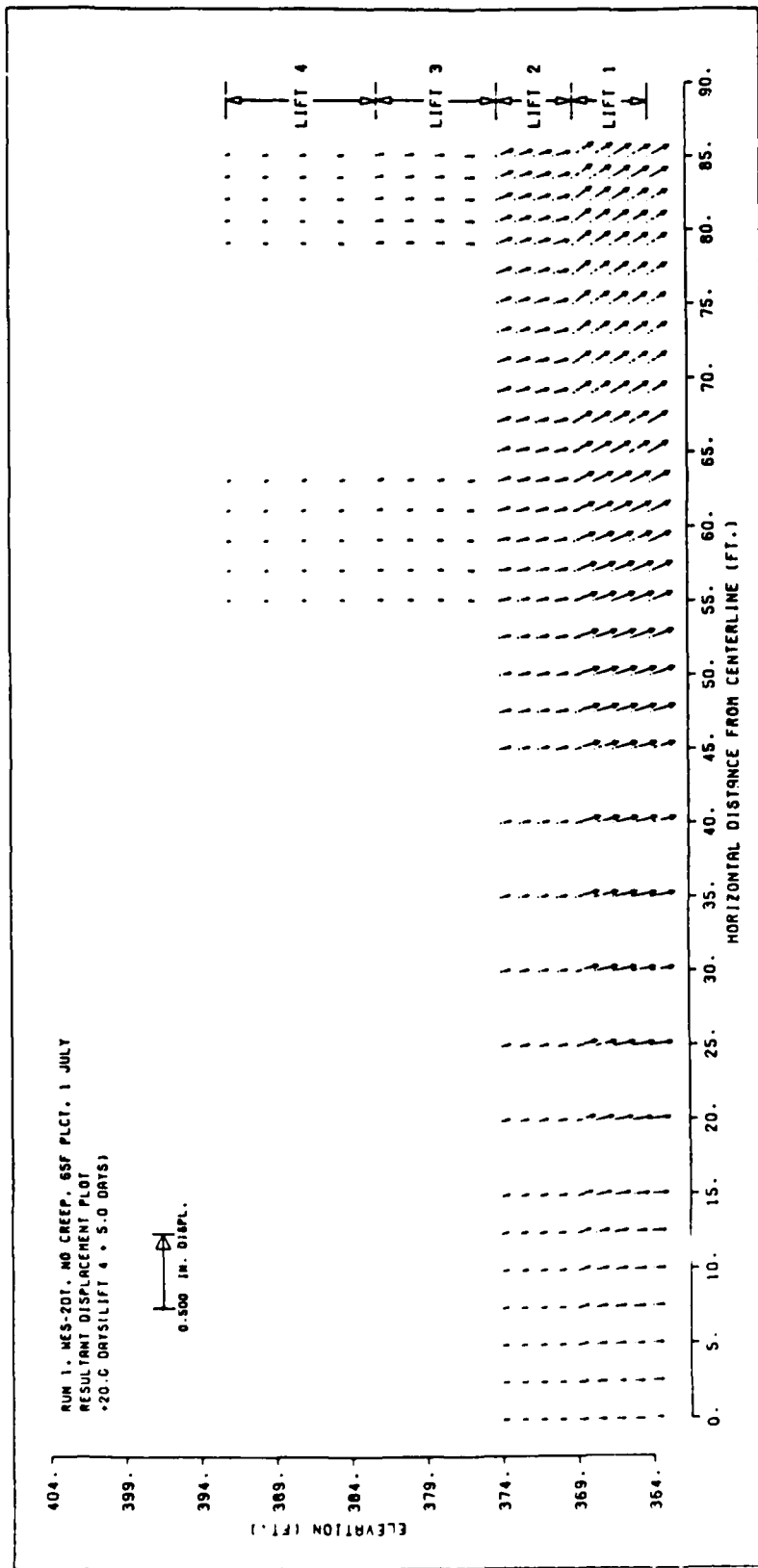


Figure 30b. Displacement of structure 5 days after lift 4 is placed thermal and gravity loading, no creep using WES-2DT program.

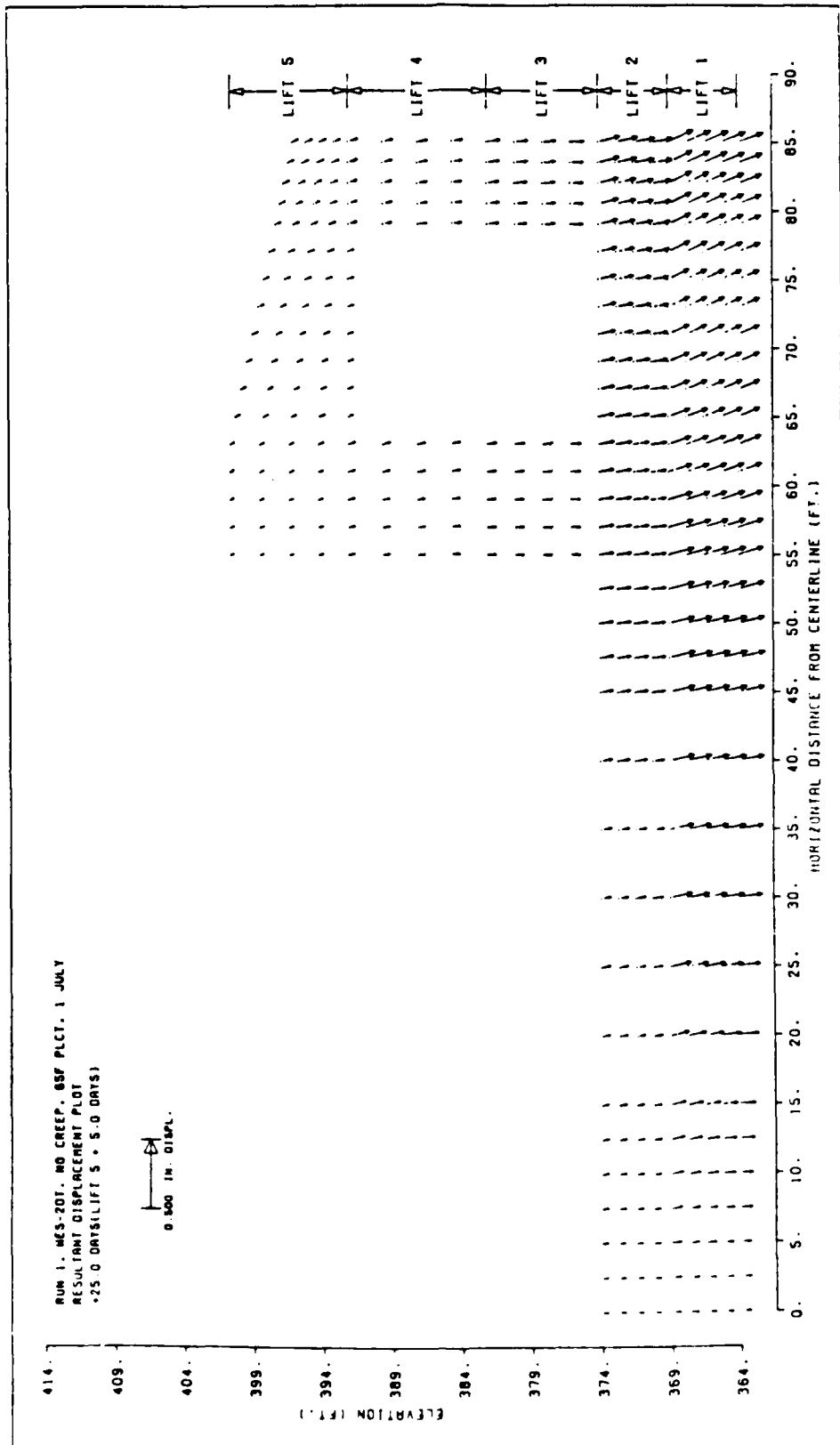


Figure 30c. Displacement of structure 5 days after lift 5 is placed, thermal and gravity loading, no creep, using WES-2DT program.

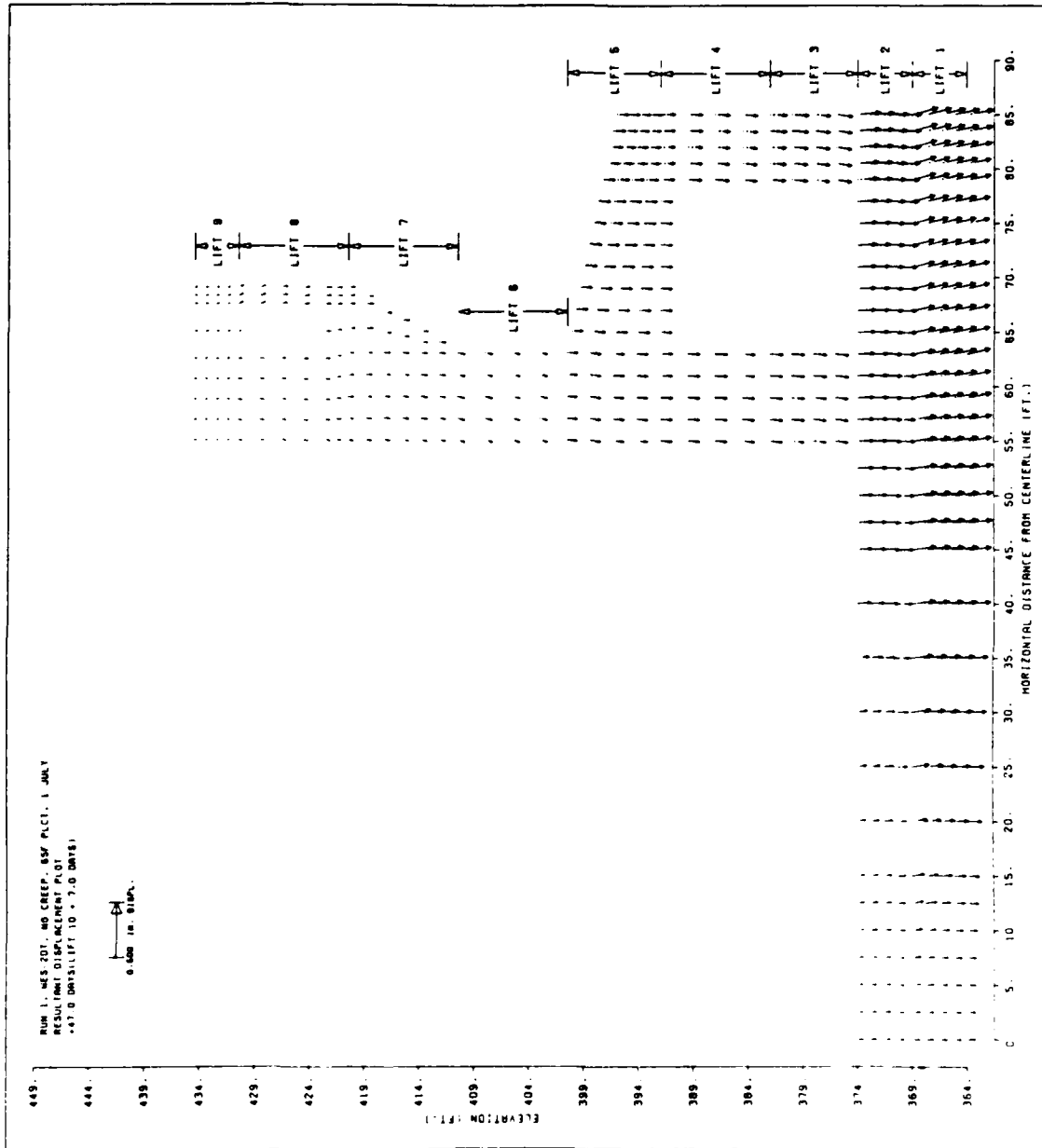


Figure 30d. Displacement of structure 7 days after lift 9 is placed thermal and gravity loading no creep using WES-2DT program.

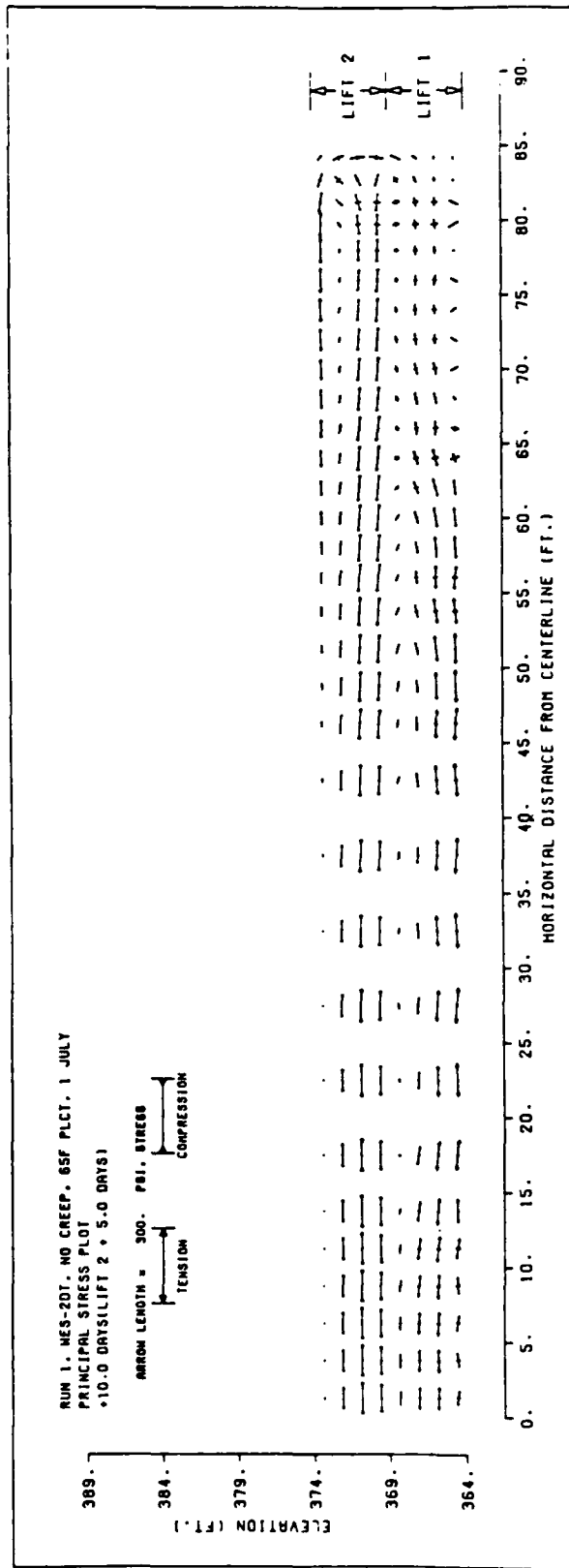


Figure 3la. Principal stress distribution in structure 5 days after lift 2 is placed, thermal and gravity loading, no creep, using WES-2DT program.

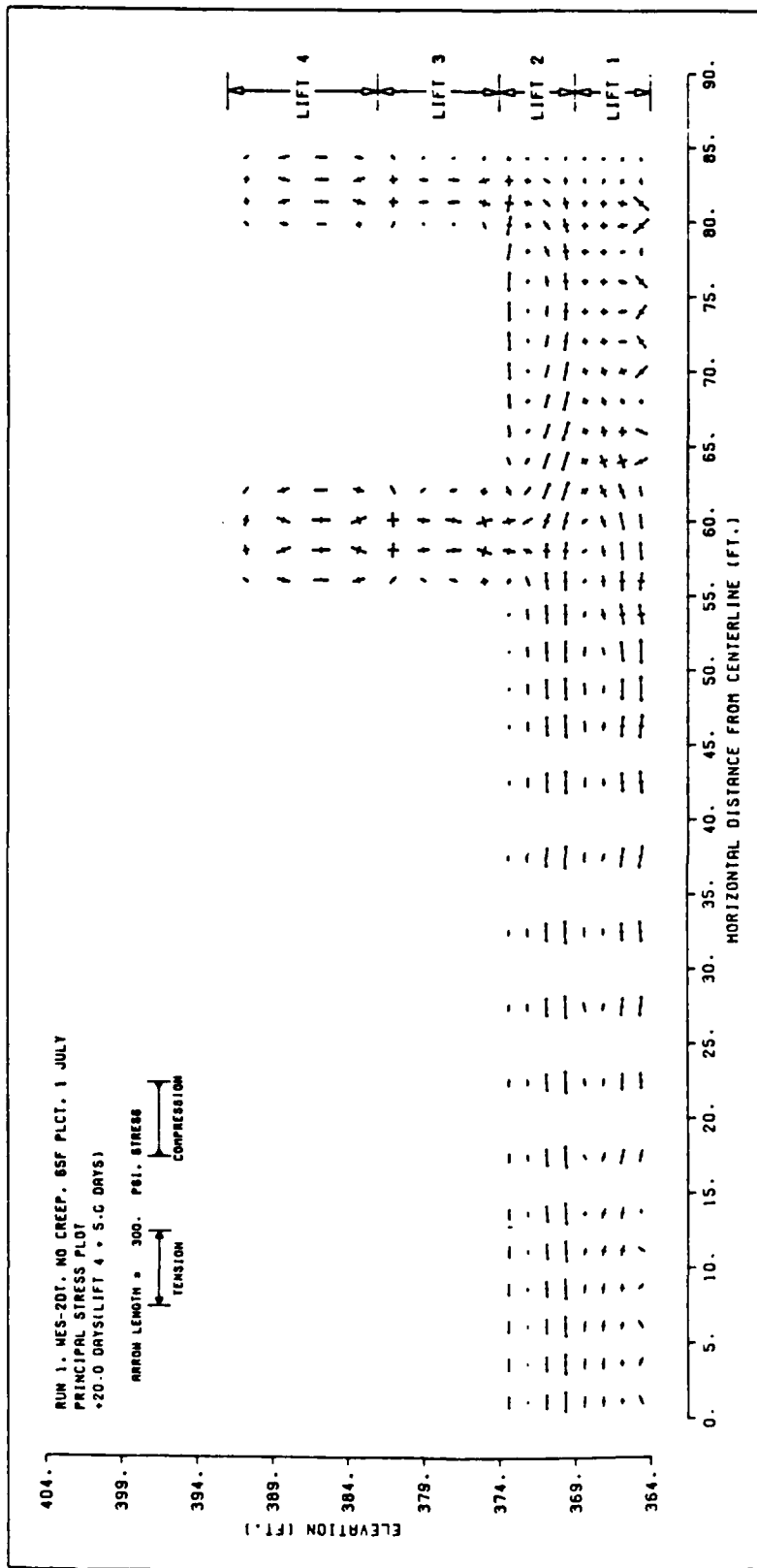


Figure 3lb. Principal stress distribution in structure 5 days after lift 4 is placed, thermal and gravity loading, no creep, using WES-2DT program.

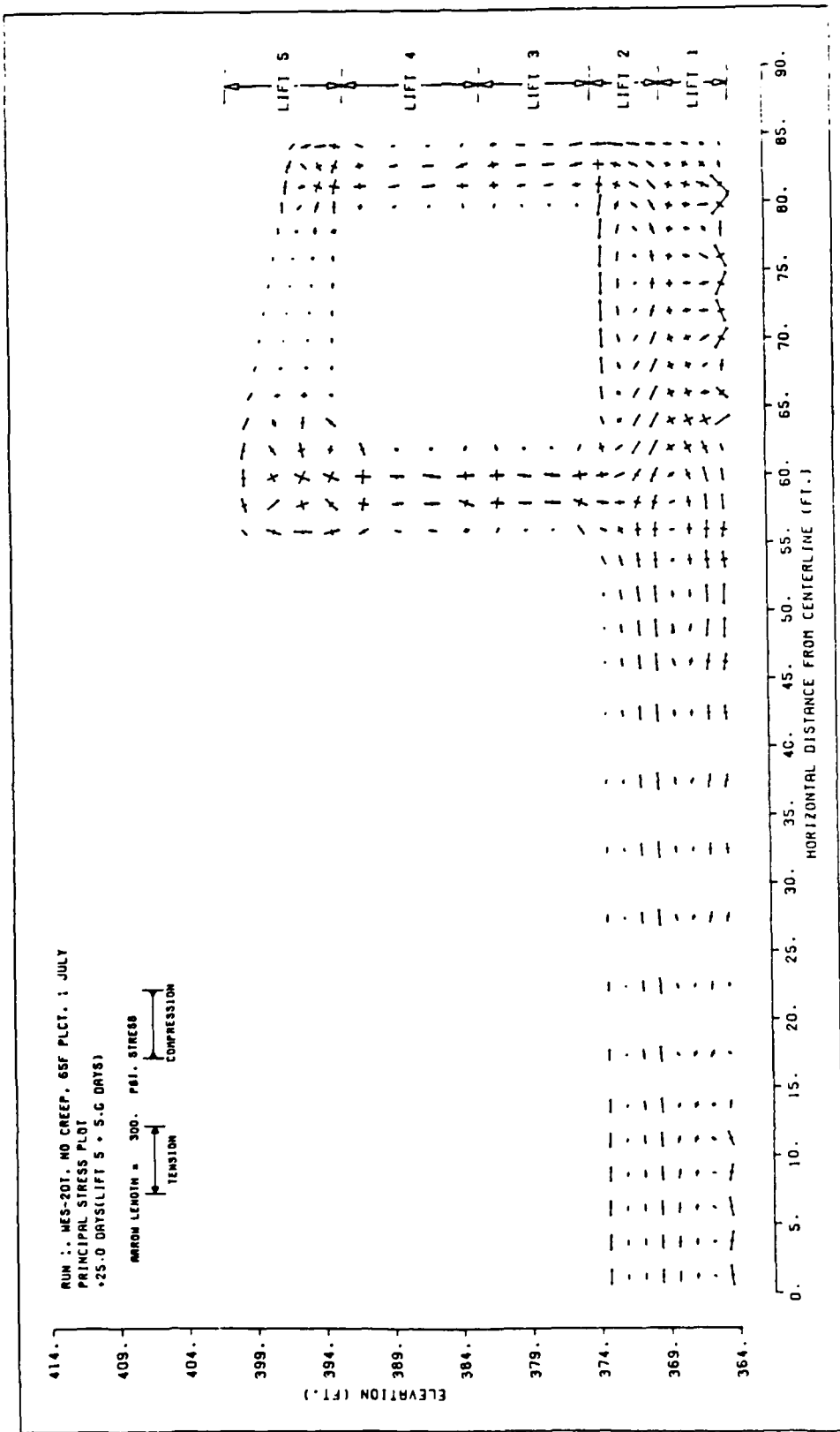


Figure 3lc. Principal stress distribution in structure 5 day after lift 5 is placed, thermal and gravity loading, no creep, using WES-2DT program.

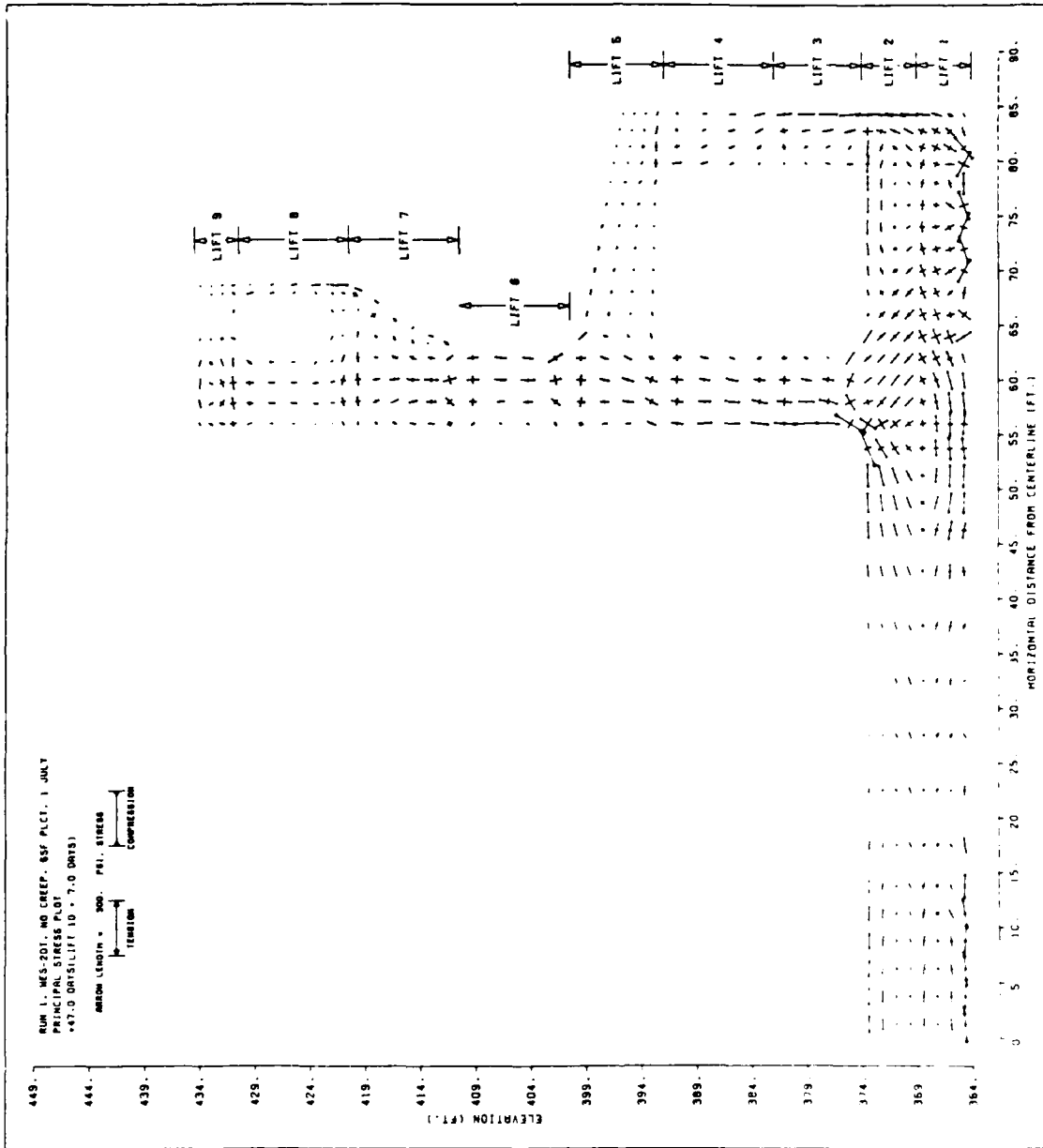
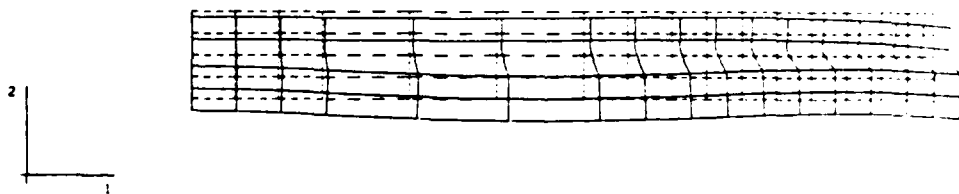


Figure 3ld. Principal stress distribution in structure 7 days after lift 9 is placed, thermal and gravity loading, no creep using WES-2DT program.

DISPL.
MAG. FACTOR = +2.5E+02
SOLID LINES - DISPLACED MESH
DASHED LINES - ORIGINAL MESH



LIFT2 - M13 - COARSE MODEL -NEW UMAT, NO SHRINK, NO CREEP
STEP 8 INCREMENT 1 ABAQUS VERSION 4.5-147

Figure 32a. Displaced structure 5 days after placement of lift 2 including creep, using ABAQUS.

DISPL.
MAG. FACTOR = +2.5E+02
SOLID LINES - DISPLACED MESH
DASHED LINES - ORIGINAL MESH

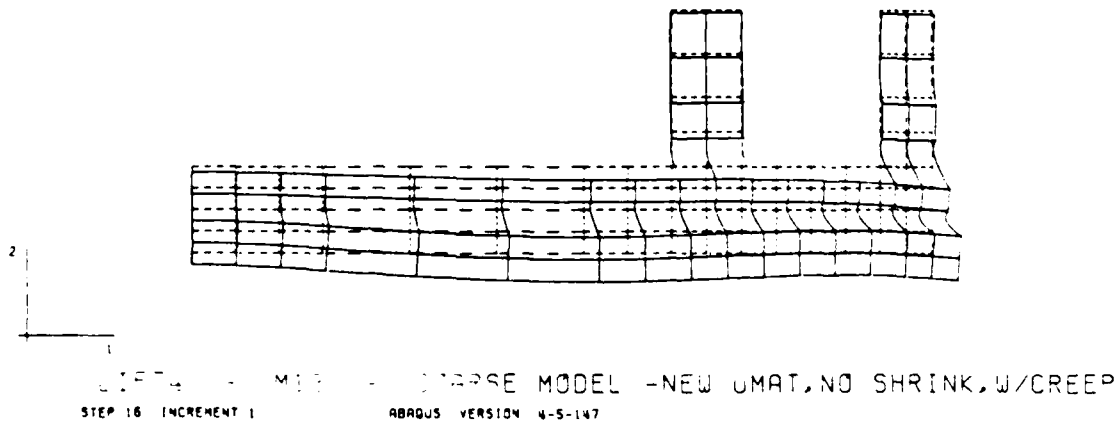
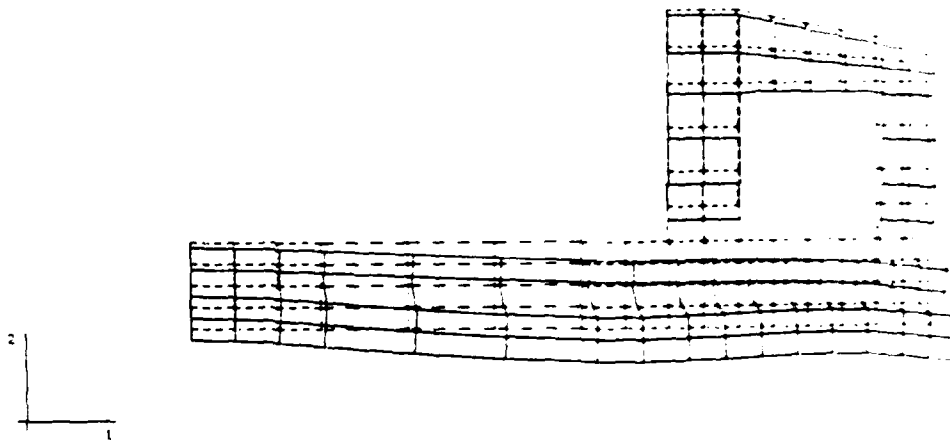


Figure 32b. Displaced structure 5 days after placement of lift 4 including creep, using ABAQUS.

DISPL.
MAG. FACTOR = +2.5E+02
SOLID LINES - DISPLACED MESH
DASHED LINES - ORIGINAL MESH



LIFTS - MID - COARSE MODEL - NEL - MAPPING - ORIGINAL MESH
STEP 20 INCREMENT 1 ABAQUS VERSION 4.5-147

Figure 32c. Displaced structure 5 days after placement of lift structure
creep, using ABAQUS

DISP:
MAG. FACTOR = +2.5E-02
SOLID LINES - DISPLACED MESH
DASHED LINES - ORIGINAL MESH

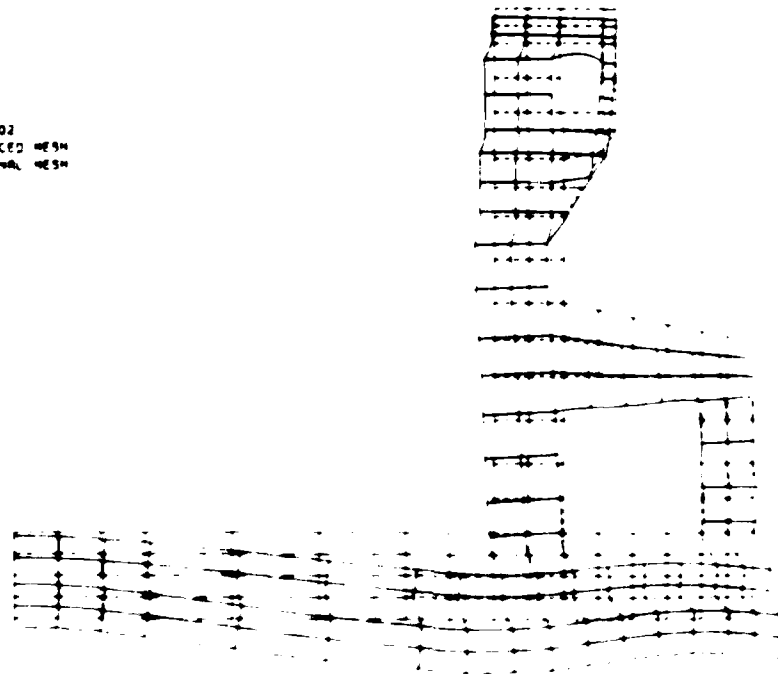


Figure 11. Displacement of structure under effect of internal pressure of
ring using FEM.

408 PRINCIPAL STRESS
 1 0.00E+00
 2 1.00E+02
 3 5.00E+01
 4 2.00E+01
 5 1.00E+02
 6 1.00E+02
 7 2.00E+01
 8 5.00E+01
 9 1.00E+02

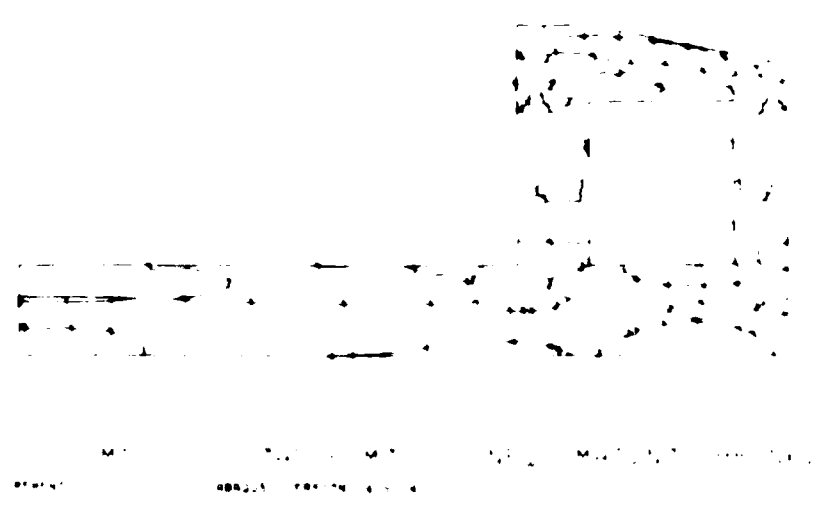


Figure 10. Maximum principal stress contours (kips/in²) after placement of
 lift including hoop stress at 100% MAT.

604 - Run 2, WES 2DT w/ CREEP, 80W PLCT, 1 JULY
 RESOLUTION: 1/8 INCH PER FOOT
 5000 DAYS (1/4 x 50 DAYS)

0.000 to 0.001
 0.000 to 0.001

399 -
 394 -
 389 -
 384 -
 379 -
 374 -
 369 -
 364 -

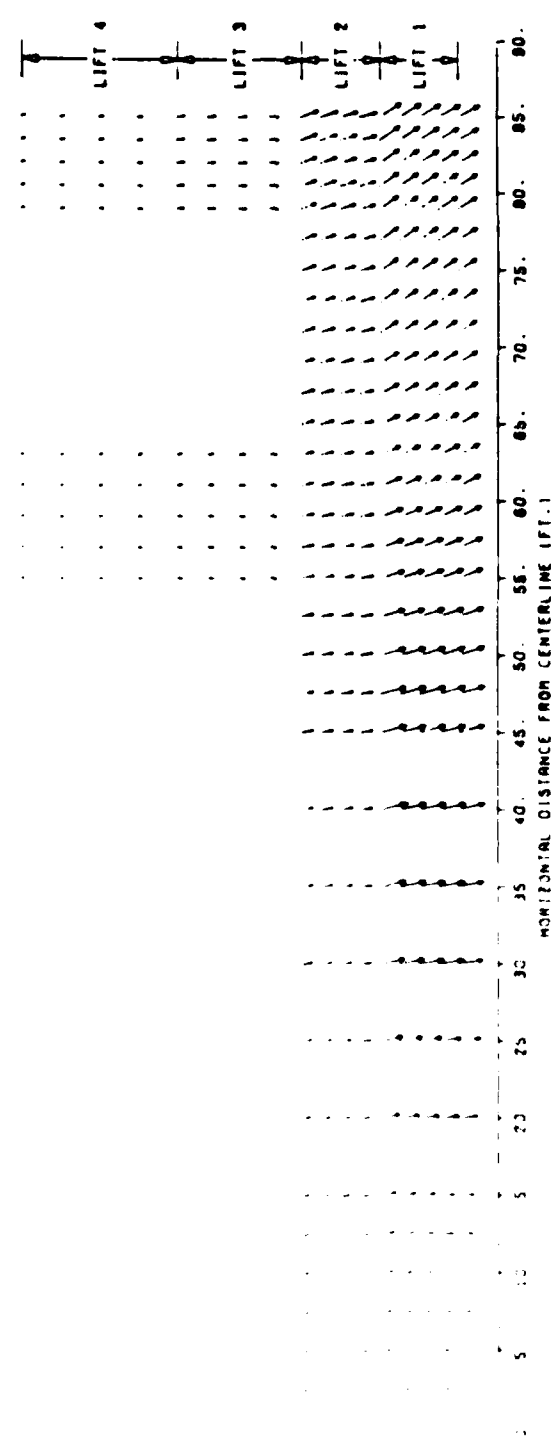


Figure 2 - Displacement of structure 5 days after lift 4 is placed, thermal and gravity creep, using WES-2DT program

6.4
 629
 604
 399
 394
 389
 384
 379
 374
 369
 364

64
 0.000 in diam.

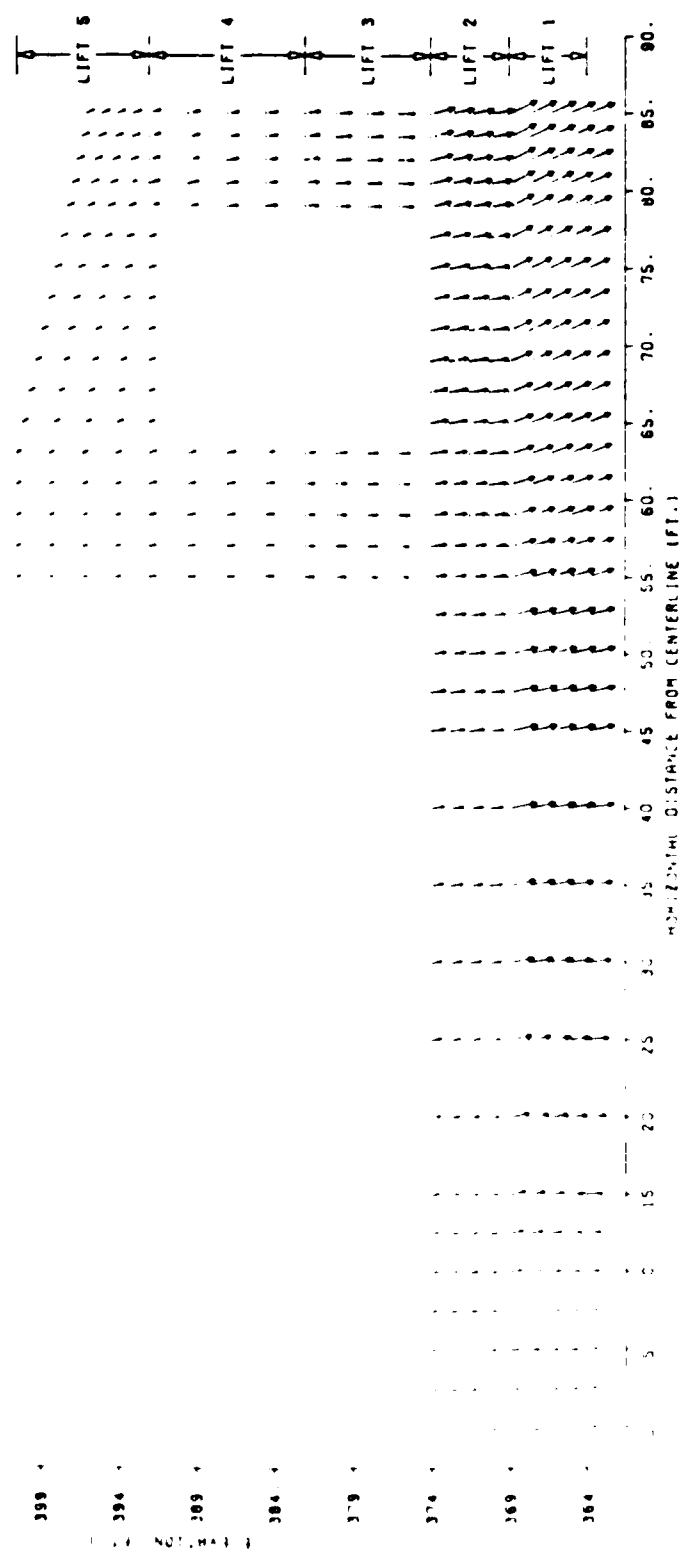


Figure 1. Displacement of structure 5 days after lift 5 is placed, thermal and gravity loading, creep, using WES-2DF program.

488 8.4.7 WES 2DT W. CREEP 0.5F PLCT 1.0ANT
 489 RESULTING 2.5F INCREMENT 4.0
 490 10.0 DAYS 1.0E-02 1.0E-01 0.001E-01

491 1. 5F
 492 2. 50E 10. 500E

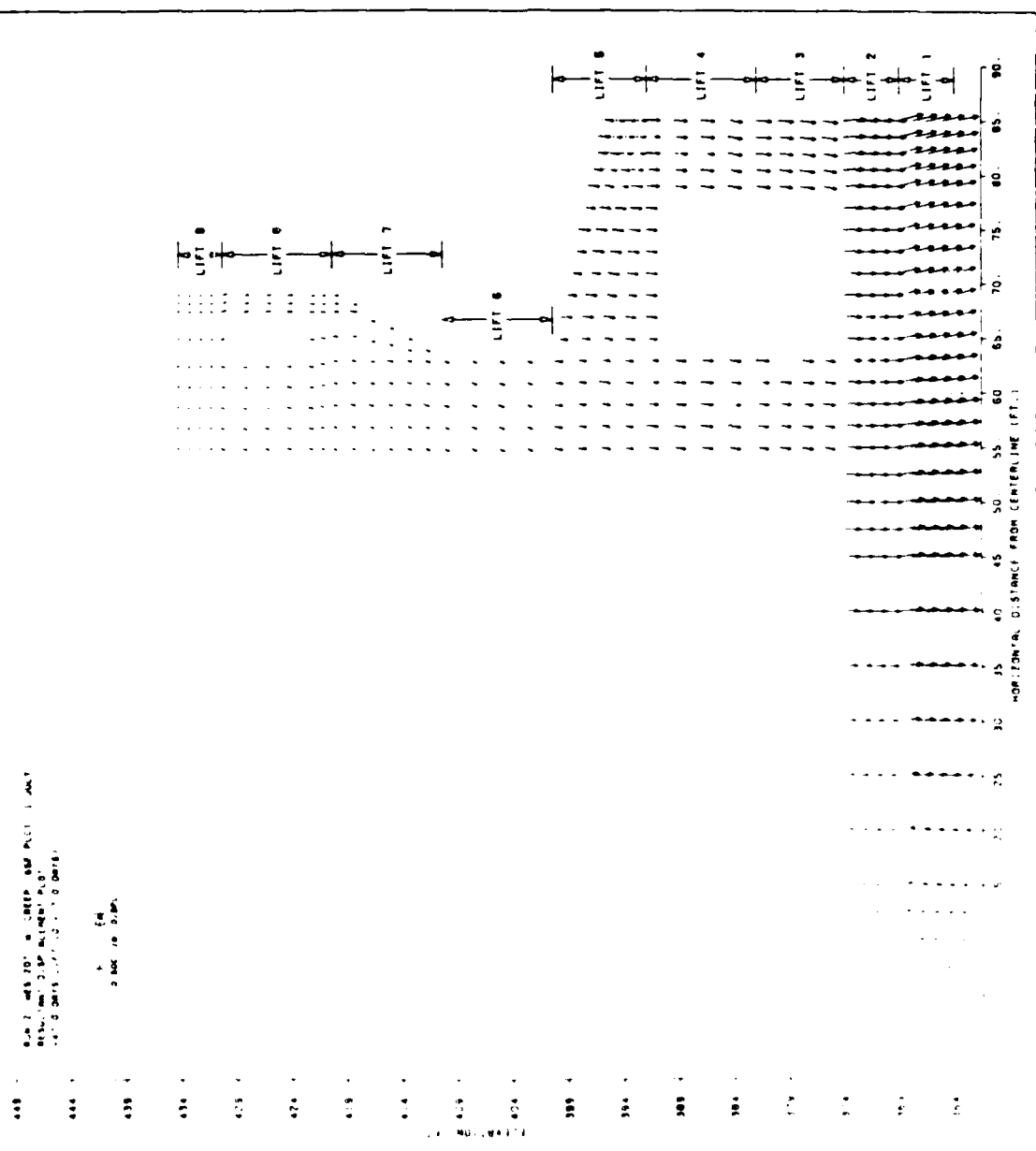


Figure 31d. Displacement of structure 7 days after lift 9 is placed, thermal and gravity loading, creep, using WES-2DT program.

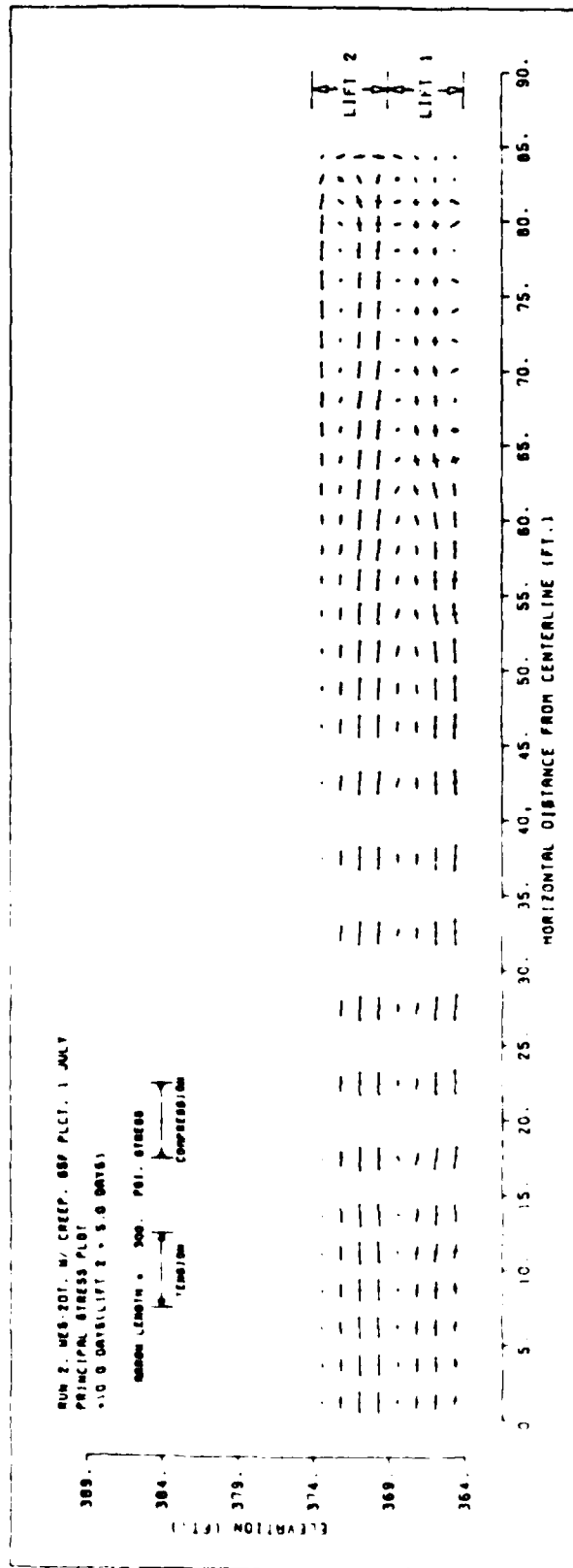


Figure 6d. Principal stress distribution in structure 5 days after lift 2 is placed, (normal and gravity loading, with creep, using WES-2DT program.

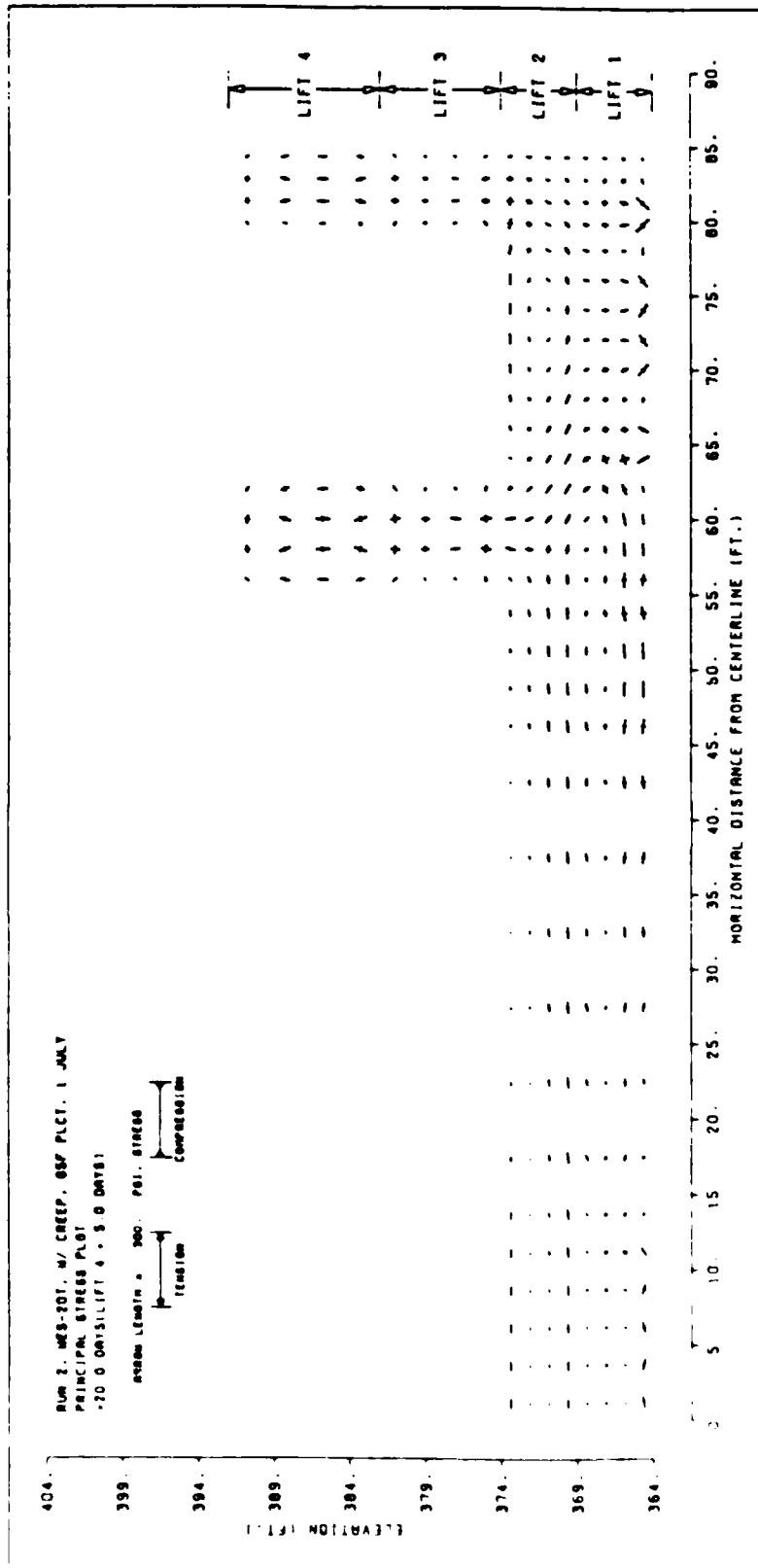


Figure 5(b). Principal stress distribution in structure 5 days after lift 4 is placed, thermal and gravity loading, with creep, using WES-2DT program.

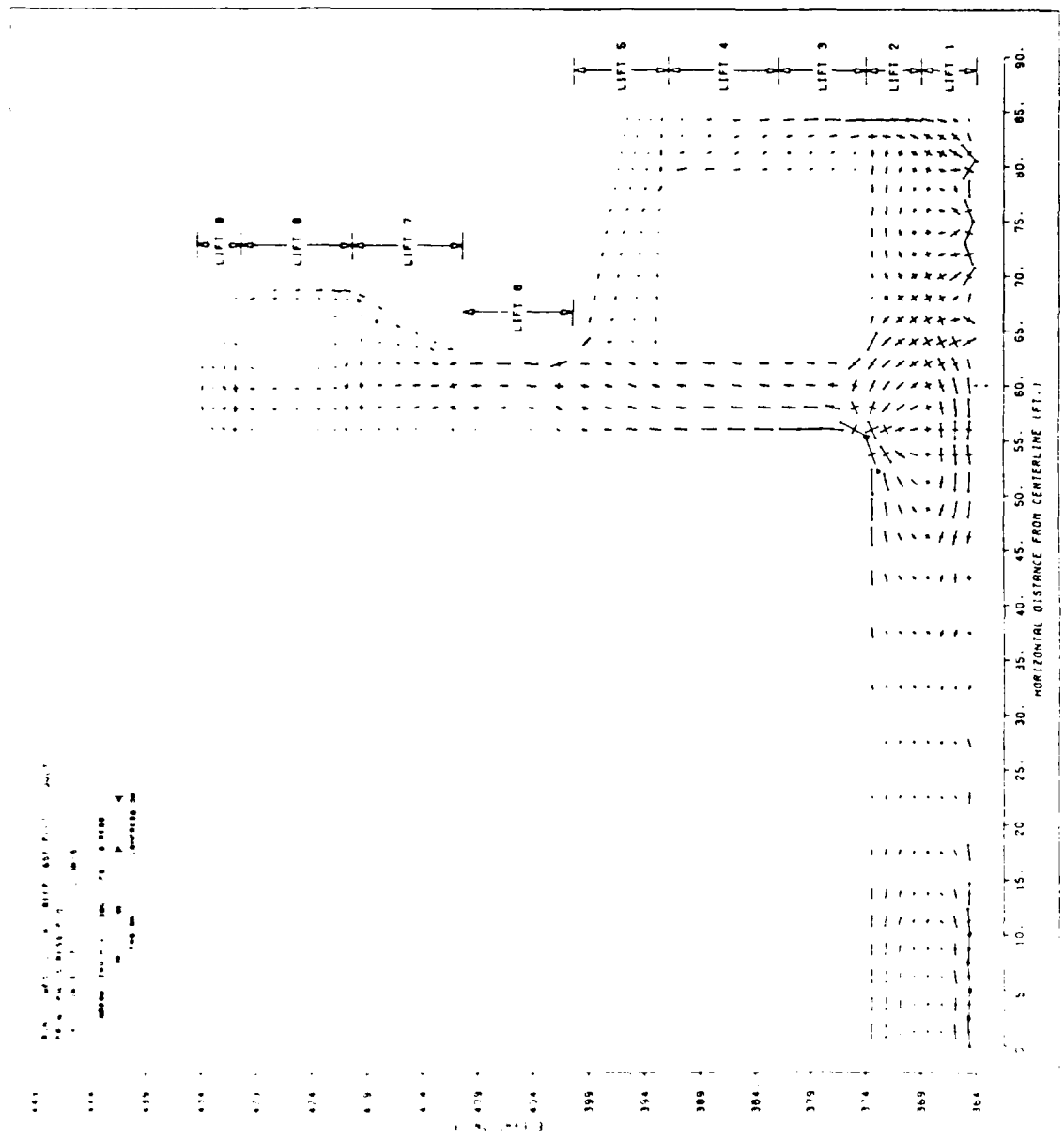


Figure 35d. Principal stress distribution in structure 7 days after lift 9 placed, thermal and gravity loading, with creep, using WES-2DT program.

DISP:
MAG. FACTOR = 42.8E+02
SOLID LINES - DISPLACED MESH
DASHED LINES - ORIGINAL MESH

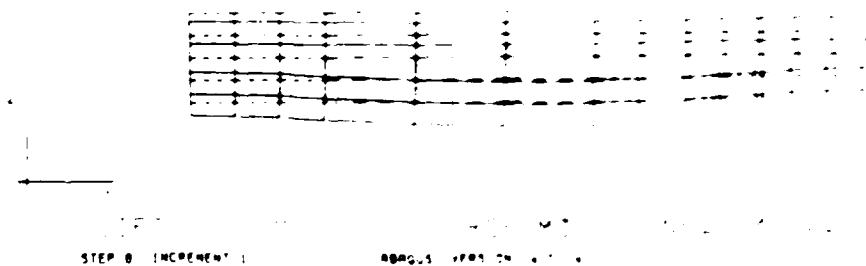
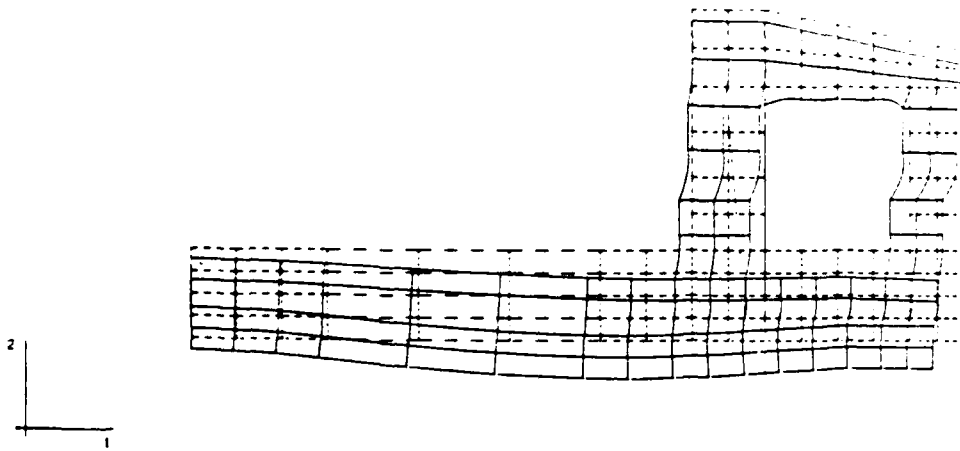


Figure 36a. Displaced structure after creep and shrinkage using 1967

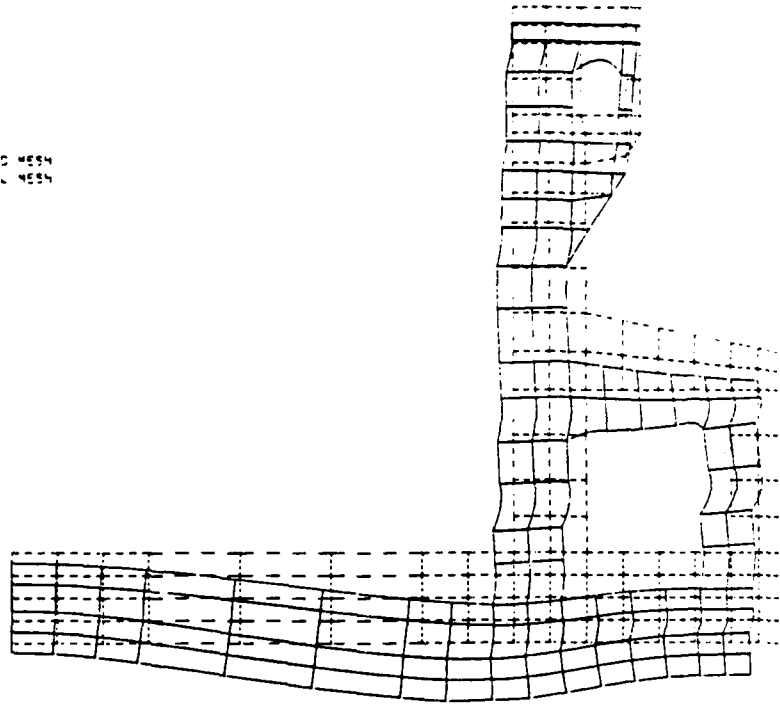
DISPL.
SCALE FACTOR = +2.5E-02
SOLID LINES - DISPLACED MESH
DASHED LINES - ORIGINAL MESH



LIFT5 - M13 - COARSE MODEL -NEW UMAT,W/SHRINK,W/CREEP
STEP 20 INCREMENT 1 ABAQUS VERSION 4-5-147

Figure 36c. Displaced structure 5 days after placement of lift 5 including creep and shrinkage, using ABAQUS.

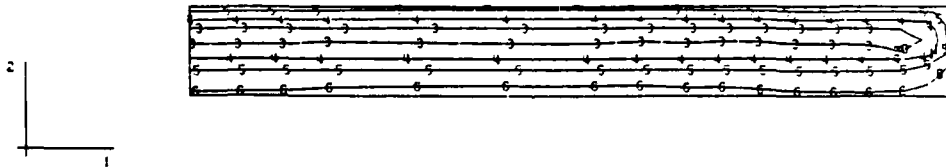
DISPL.
MAG. FACTOR = +2.5E+02
SOLID LINES = DISPLACED MESH
DASHED LINES = ORIGINAL MESH



DISPLACEMENT OF COURSE MODEL -NEW UMAT, W/SHRINK, W/CREEP
STEP 36 INCREMENT 2 ABAQUS VERSION 4.5-147

Figure 36d. Displaced structure 7 days after placement of lift 9 including creep and shrinkage, using ABAQUS.

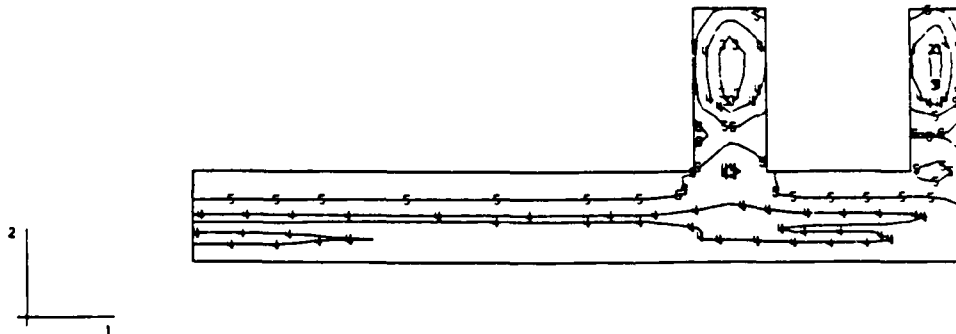
MAX. PRINCIPAL STRESS
 I.D. VALUE
 1 -1.00E+02
 2 -5.00E+01
 3 -2.27E-13
 4 +5.00E+01
 5 +1.00E+02
 6 +1.50E+02
 7 +2.00E+02
 8 +2.50E+02
 9 +3.00E+02



LIFT2 - M13 - COARSE MODEL -NEW UMAT,W/SHRINK,W/CREEP
 STEP 8 INCREMENT 1 ABAQUS VERSION 4-5-147

Figure 37a. Maximum principal stress contours 5 days after placement of lift 2 including creep and shrinkage, using ABAQUS (UMAT2).

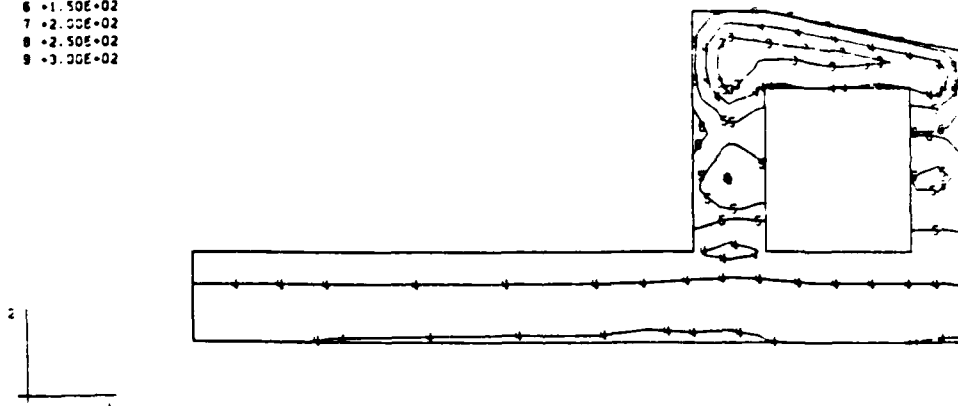
MAX. PRINCIPAL STRESS
 I.D. VALUE
 1 -1.00E+02
 2 -5.00E-01
 3 -2.27E-13
 4 +5.00E-01
 5 +1.00E+02
 6 +1.50E+02
 7 +2.00E+02
 8 +2.50E+02
 9 +3.00E+02



LIFT4 - MID - COARSE MODEL -NEW UMAT,W/SHRINK,W/CREEP
 STEP 18 INCREMENT 1 ABAQUS VERSION 4-5-147

Figure 37b. Maximum principal stress contours 5 days after placement of lift 4 including creep and shrinkage, using ABAQUS (UMAT2).

MAX. PRINCIPAL STRESS
 I.D. VALUE
 1 -1.00E+02
 2 -5.00E+01
 3 -2.27E+13
 4 +5.00E+01
 5 +1.00E+02
 6 +1.50E+02
 7 +2.00E+02
 8 +2.50E+02
 9 +3.00E+02



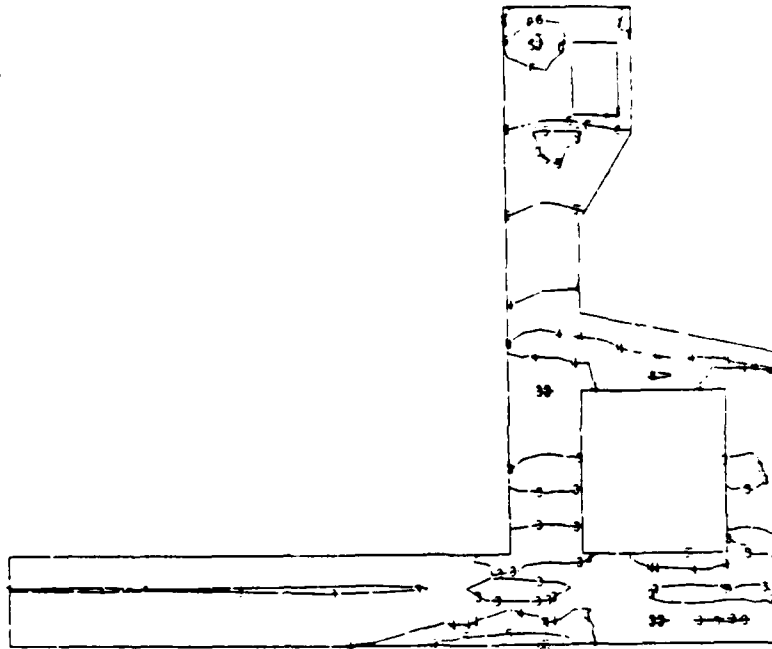
LIFT5 - M13 - COARSE MODEL -NEW UMAT,W/SHRINK,W/CREEP
 STEP 20 INCREMENT 1 ABAQUS VERSION 4-5-147

Figure 37c. Maximum principal stress contours 5 days after placement of lift 5 including creep and shrinkage, using ABAQUS (UMAT2).

```

MAX. PRINCIPAL STRESS
10 VALUE
1 1.122E+02
2 5.222E+01
3 2.47E+01
4 4.822E+01
5 4.122E+01
6 4.122E+02
7 4.122E+02
8 4.122E+02
9 4.122E+02

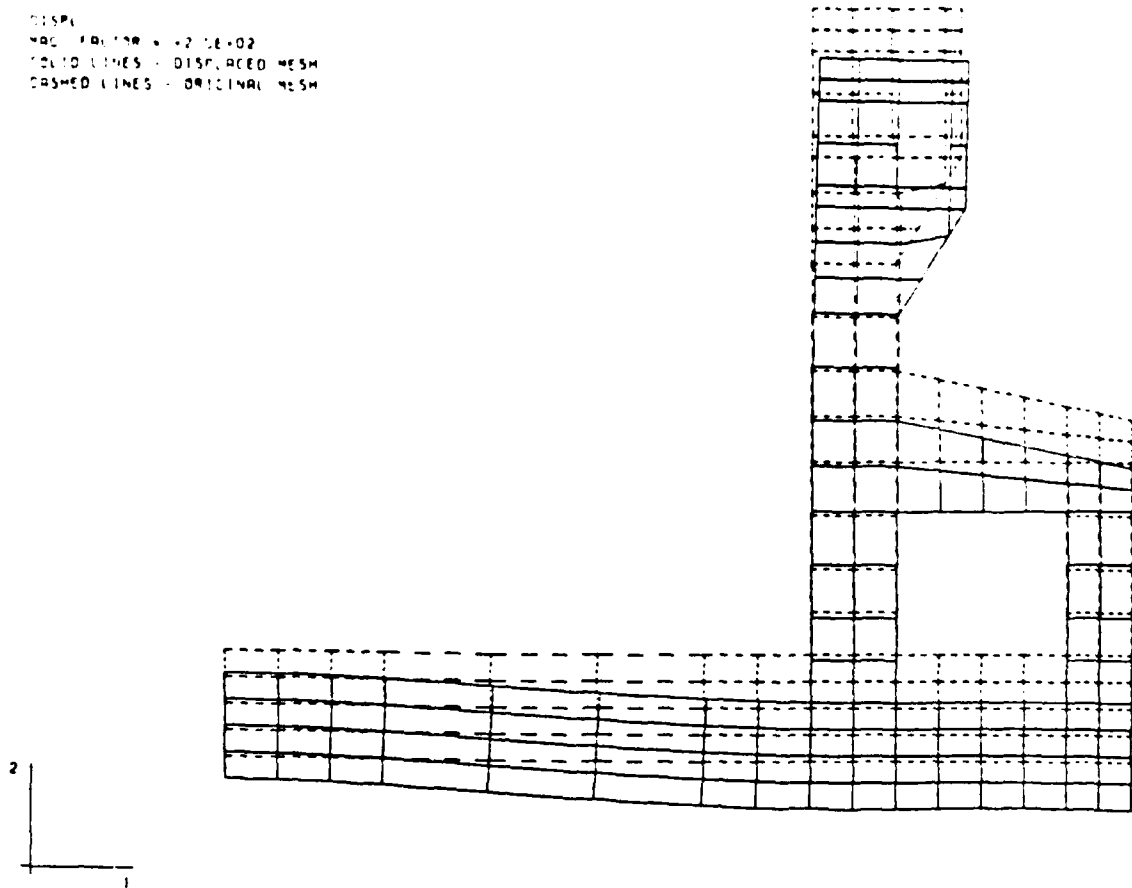
```



LIFT9 - M13 - COARSE MODEL -NEW UMAT,W/SHRINK,W/CREEP
 STEP 30 INCREMENT 2 ABAQUS VERSION 4-5-147

Figure 37d. Maximum principal stress contours 7 days after placement of lift 9 including creep and shrinkage, using ABAQUS (UMAT2).

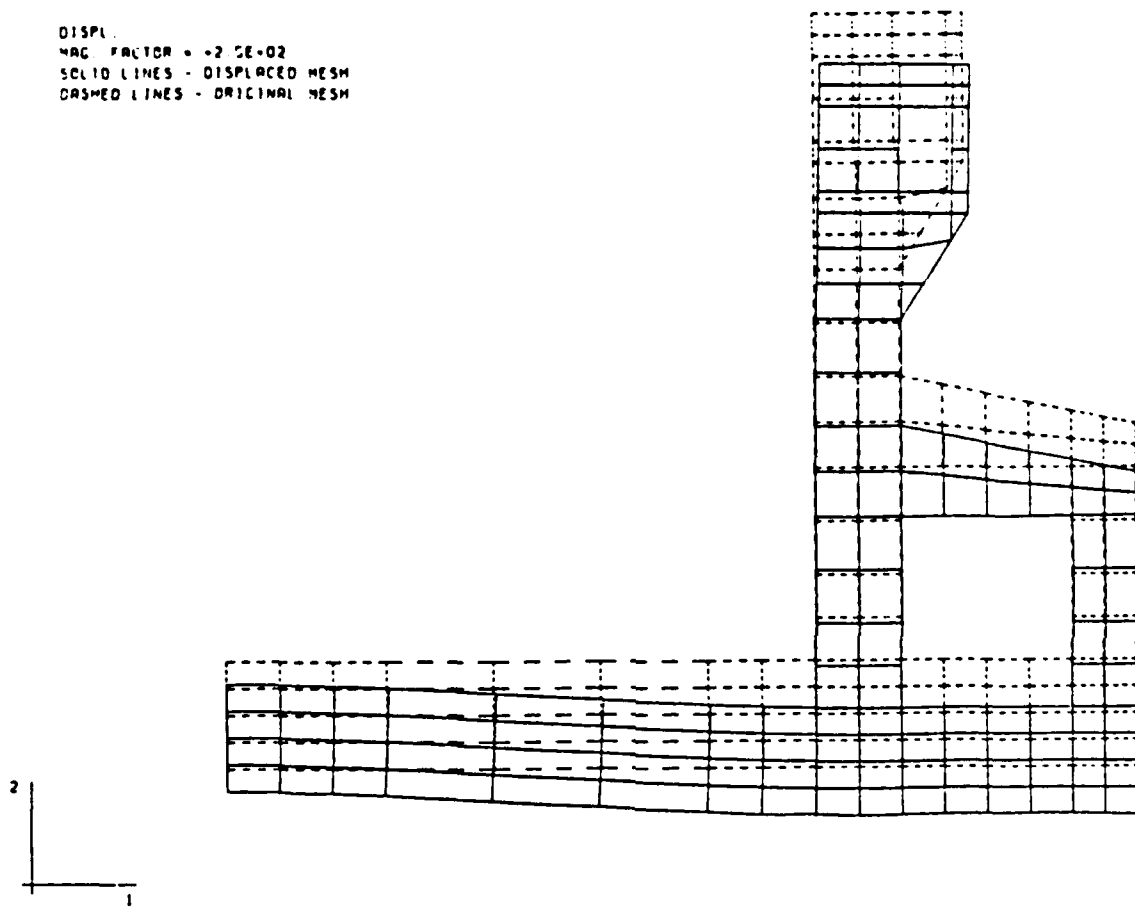
DISPL
 MAG. FACTOR = +2.0E+02
 SOLID LINES = DISPLACED MESH
 DASHED LINES = ORIGINAL MESH



ENTIRE STRUCTURE - M13 - 3D MODEL - E=3.12E6 - NODE PLANE 1
 STEP 1 INCREMENT 1 ARADIS VERSION 4.6-107 1

Figure 38a. Displaced structure for 3-dimensional analysis of Monolith 13 at node plane 1 (centerline).

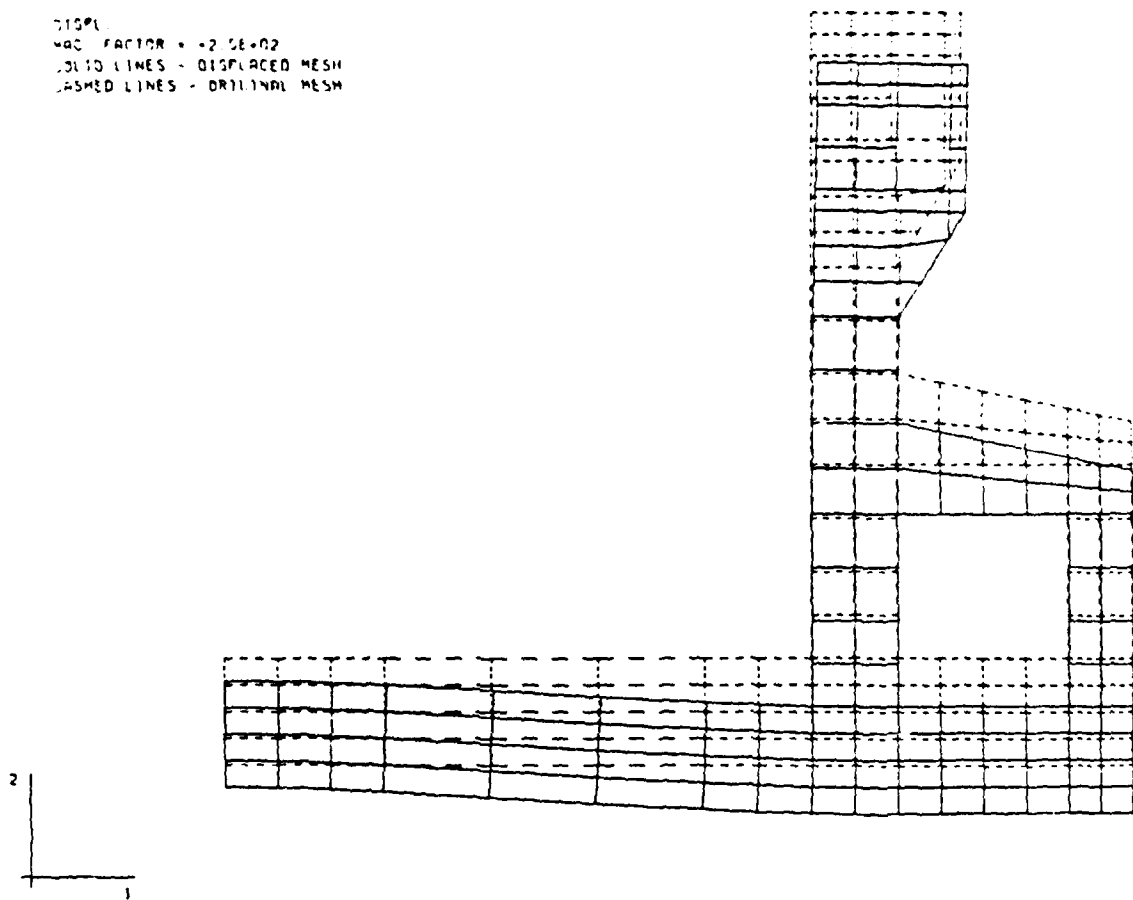
DISPL.
MAG. FACTOR = +2.0E+02
SOLID LINES - DISPLACED MESH
DASHED LINES - ORIGINAL MESH



ENTIRE STRUCTURE -- M13 -- 3D MODEL -- E=3.12E6 -- NODE PLANE 2
STEP 1 INCREMENT 1 ABAQUS VERSION 4.5-147

Figure 38b. Displaced structure for 3-dimensional analysis of Monolith 13 at node plane 2.

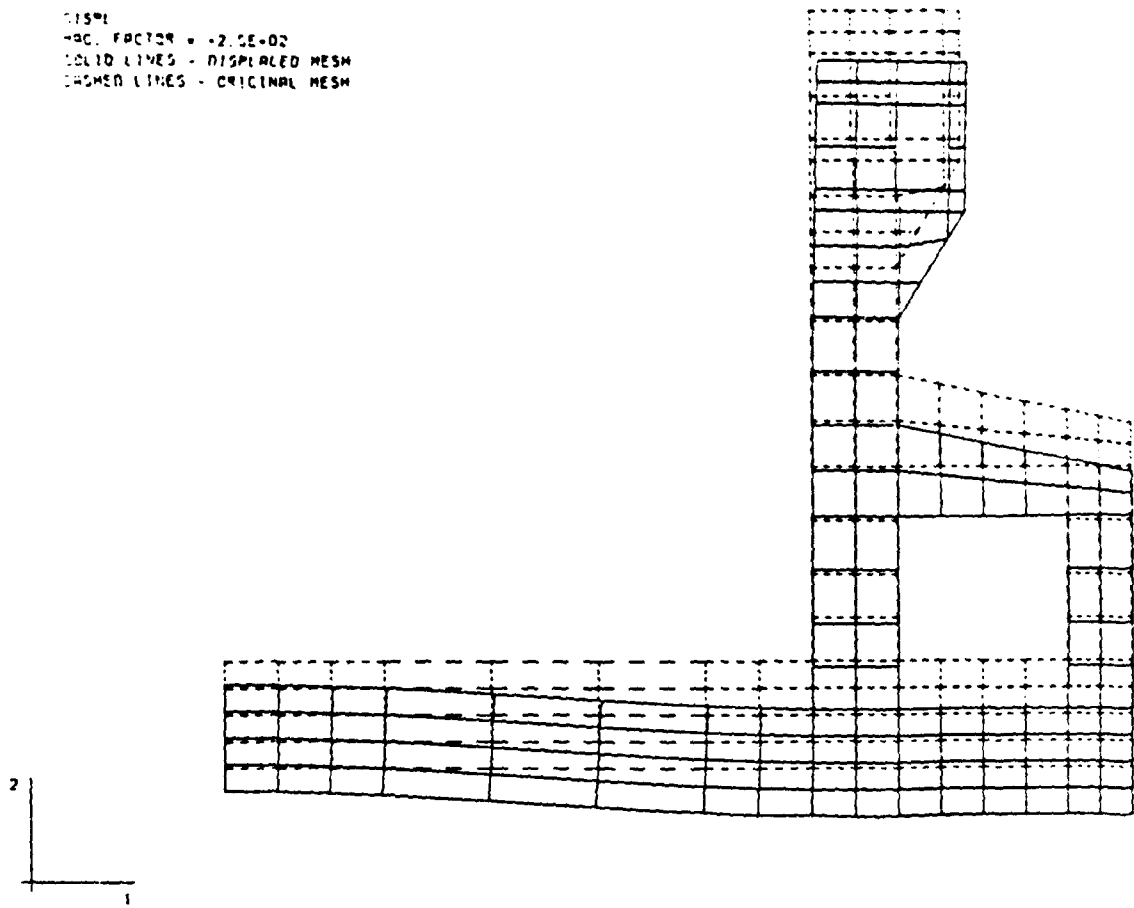
DISPL
MAG. FACTOR = +2.5E+02
SOLID LINES = DISPLACED MESH
DASHED LINES = ORIGINAL MESH



ENTIRE STRUCTURE - M13 - 3D MODEL - E=3.12E6 - NODE PLANE 3
STEP 1 INCREMENT 1 ABAQUS VERSION 4-5-147 3

Figure 38c. Displaced structure for 3-dimensional analysis of Monolith 13 at node plane 3.

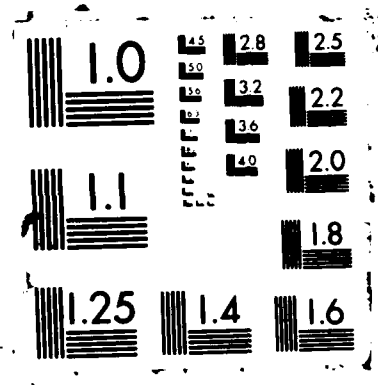
DISP
-SC. FACTOR = 2.0E+02
SOLID LINES - DISPLACED MESH
DASHED LINES - ORIGINAL MESH



ENTIRE STRUCTURE - M13 - 3D MODEL - E=3.12E6 - NODE PLANE
STEP 1 INCREMENT 1 ABAQUS VERSION 4.5-147

4

Figure 38d. Displaced structure for 3-dimensional analysis of Monolith 13 at node plane 4.



Presentation of Results

Two-dimensional
temperature analysis

94. Two-dimensional temperature analyses of monolith L-17 were also performed using both the ABAQUS and WES2DT programs. The 2-D FE models used by ABAQUS (Figure 7d) and WES2DT (Figure 7e) were based upon a cross-section taken at Station 26 + 13 which contained the smallest amount of internal voids. This cross-section was expected to experience the largest temperature rise in the monolith. The WES2DT grid only modeled the structure through lift 13. During the temperature analysis, the top surface of lift 13 was insulated after the time of placement of lift 14 to simulate the effects of the additional concrete. The gravity loading effects past lift 14 were modeled with pressure loads applied to the top of lift 13 to simulate placement of lifts 14 through 16 during the incremental construction stress analysis. Figures 39a thru 39e show results from the ABAQUS program at five stages of construction. Results from the WES2DT program are shown in Figures 40a thru 40d for the same first four of five stages of construction used for presenting ABAQUS data. The presentation of WES2DT temperature results beyond the time of placing lift 13 was omitted.

Three dimensional
temperature analysis

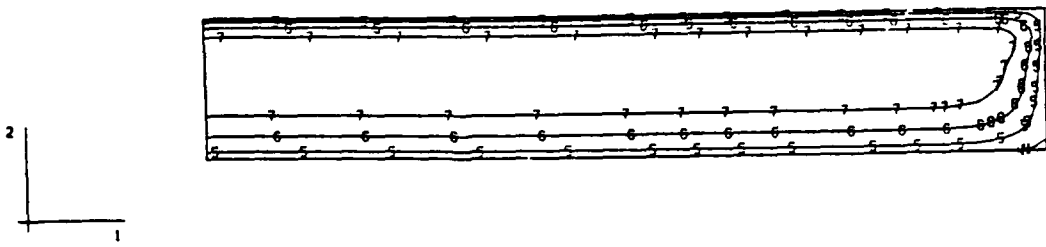
95. Although a 3-D FE model of L-17 (Figure 7e) for use with the ABAQUS program was completed, the analysis could not be run. The temperature analysis was not made due to problems with the ABAQUS program in handling the required number of element sets and the excessive costs of making the computer runs.

Discussion of Results

Two-dimensional temperature analysis

96. The results from ABAQUS and WES2DT show very good agreement. The temperature contours, Figures 39 and 40, give the same trends and are in the identical locations for times through placement of lift 13. Slightly larger areas are shown for the 100° F contours from ABAQUS in Figures 39b and 39d than from WES2DT in Figures 40b and 40d. The ABAQUS analysis shows the maximum temperature of 105° - 110° F occurs after placement of lift 16 in the center of the massive wall section. Since the WES2DT model only extended through lift 13 the corresponding value is not given.

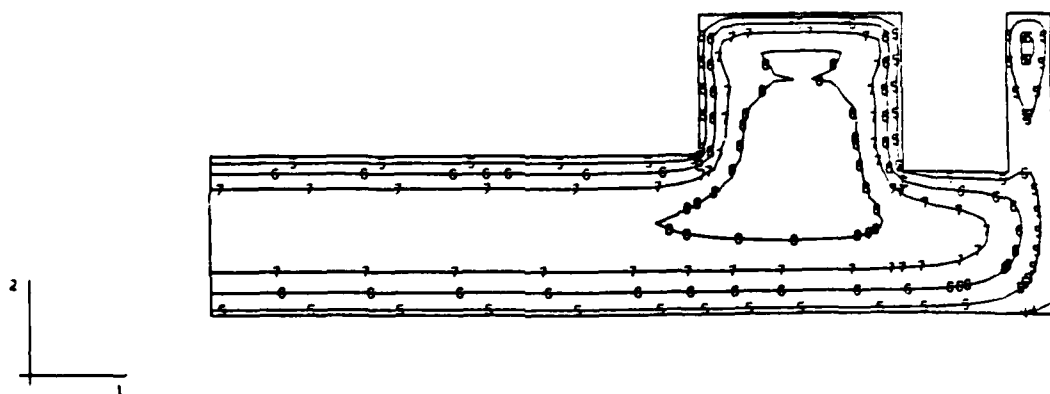
TEMP.
 I.D. VALUE
 1 +6.50E+01
 2 +7.50E+01
 3 +7.50E+01
 4 +8.00E+01
 5 +8.50E+01
 6 +9.00E+01
 7 +9.50E+01
 8 +1.00E+02
 9 +1.25E+02
 10 +1.10E+02
 11 +1.15E+02



LIFT4 - M17 - 2D MODEL
 STEP 8 INCREMENT 6 ABAQUS VERSION 4-5-147

Figure 39a. Temperature contours calculated using ABAQUS in Monolith 17 at 5 days after placement of lift 4.

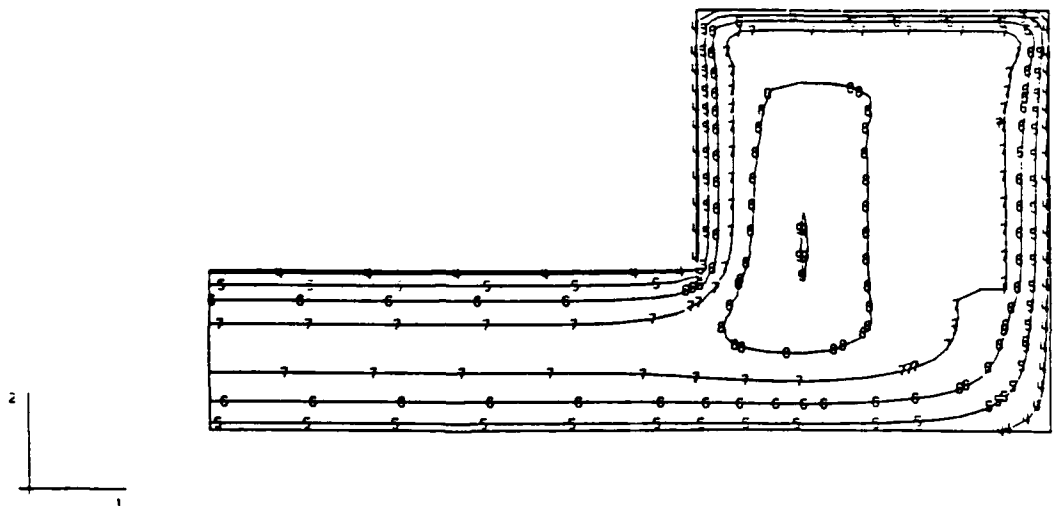
TEMP.
 I.D. VALUE
 1 +6.50E+01
 2 +7.00E+01
 3 +7.50E+01
 4 +8.00E+01
 5 +8.50E+01
 6 +9.00E+01
 7 +9.50E+01
 8 +1.00E+02
 9 +1.05E+02
 10 +1.10E+02
 11 +1.15E+02



LIFT7 - M17 - 2D MODEL
 STEP 14 INCREMENT 6 ABAQUS VERSION 4-5-147

Figure 39b. Temperature contours calculated using ABAQUS in Monolith 17 at 5 days after placement of lift 7.

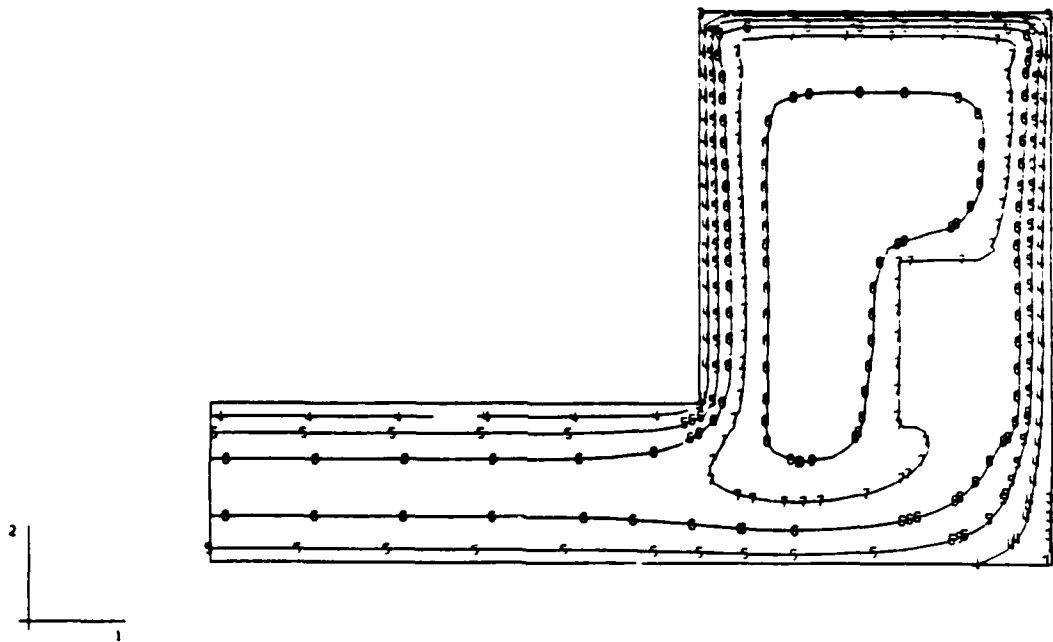
TEMP.
 I.D. VALUE
 1 +6.50E+01
 2 +7.00E+01
 3 +7.50E+01
 4 +8.00E+01
 5 +8.50E+01
 6 +9.00E+01
 7 +9.50E+01
 8 +1.00E+02
 9 +1.05E+02
 10 +1.10E+02
 11 +1.15E+02



LIFT10 - M17 - 2D MODEL
 STEP 20 INCREMENT 8 ABAQUS VERSION 4-5-147

Figure 39c. Temperature contours calculated using ABAQUS in Monolith 17 at 5 days after placement of lift 10.

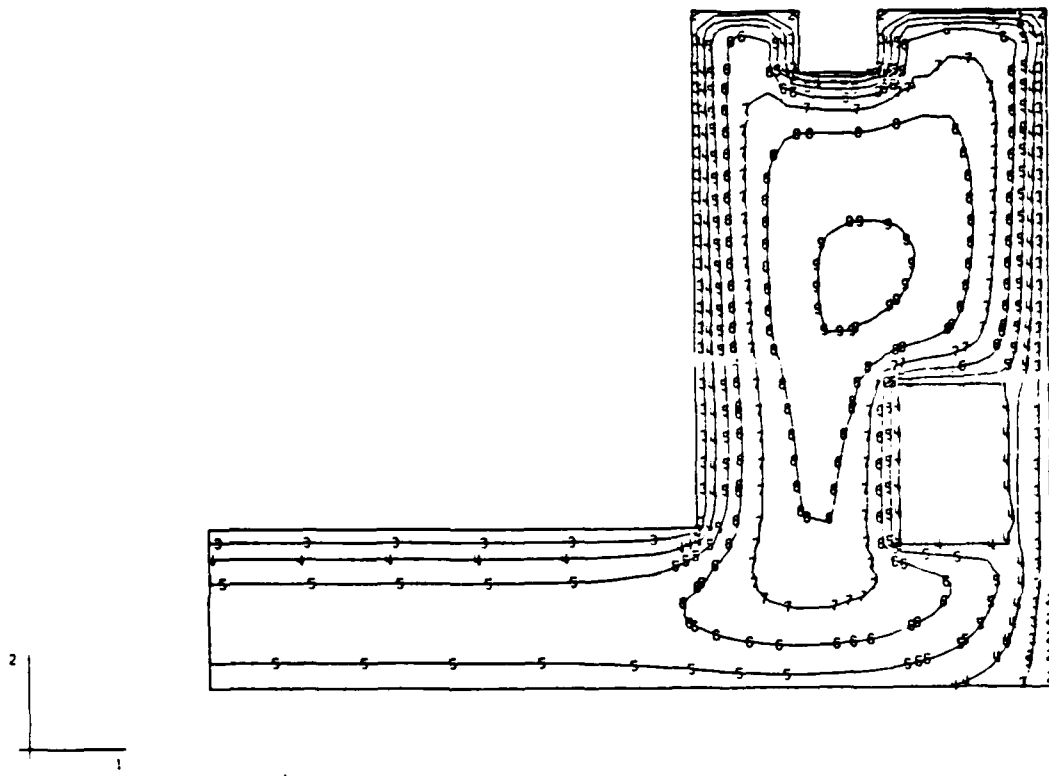
TEMP.
 I.D. VALUE
 1 +6.50E+01
 2 +7.00E+01
 3 +7.50E+01
 4 +8.00E+01
 5 +8.50E+01
 6 +9.00E+01
 7 +9.50E+01
 8 +1.00E+02
 9 +1.05E+02
 10 +1.10E+02
 11 +1.15E+02



LIFT13 - M17 - 2D MODEL
 STEP 26 INCREMENT 8 ABAQUS VERSION 4-5-147

Figure 39d. Temperature contours calculated using ABAQUS in Monolith 17 at 5 days after placement of lift 13.

TEMP.
 I.D. VALUE
 1 +6.50E+01
 2 +7.00E+01
 3 +7.50E+01
 4 +8.00E+01
 5 +8.50E+01
 6 +9.00E+01
 7 +9.50E+01
 8 +1.00E+02
 9 +1.05E+02
 10 +1.10E+02
 11 +1.15E+02



LIFT16 - M17 - 2D MODEL
 STEP 32 INCREMENT 6 ABAQUS VERSION 4-5-147

Figure 39e. Temperature contours calculated using ABAQUS in Monolith 17 at 5 days after placement of lift 16.

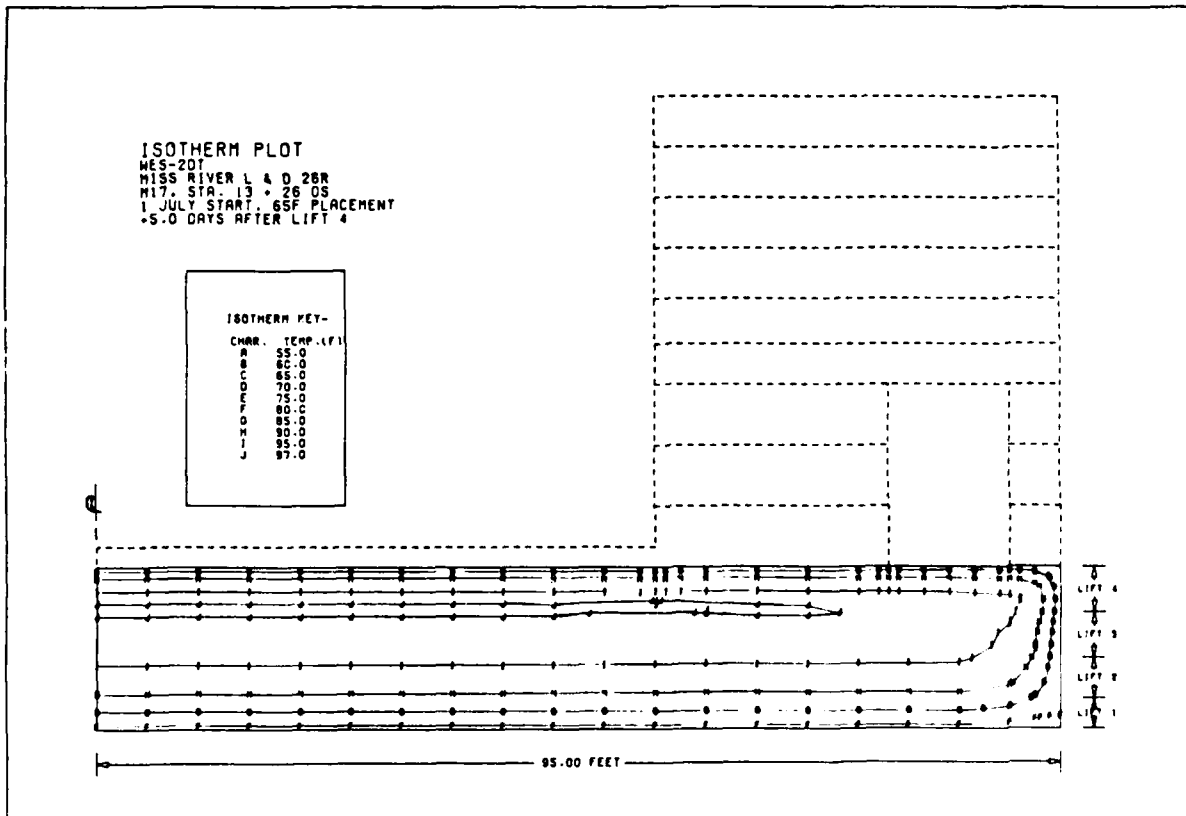


Figure 40a. Temperature contours calculated using WES2DT in Monolith 17 at 5 days after placement of lift 4.

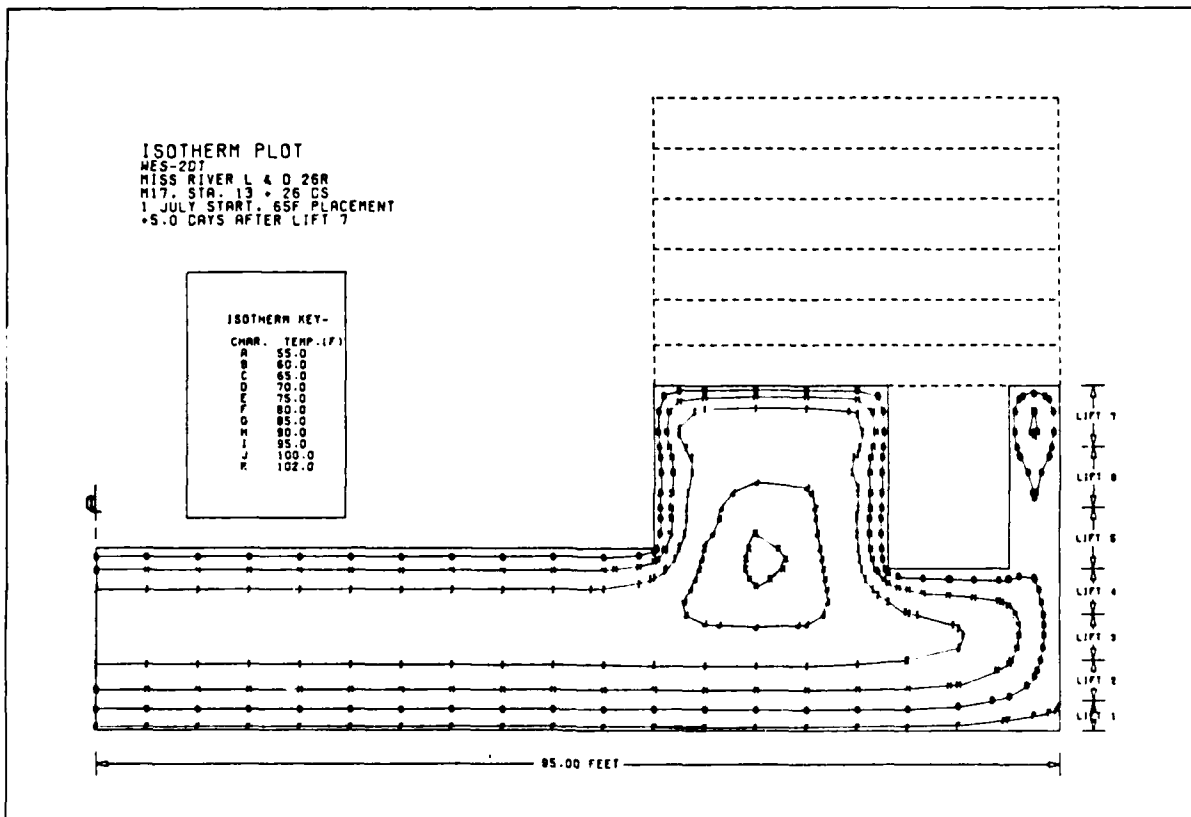


Figure 40b. Temperature contours calculated using WES2DT in Monolith 17 at 5 days after placement of lift 7.

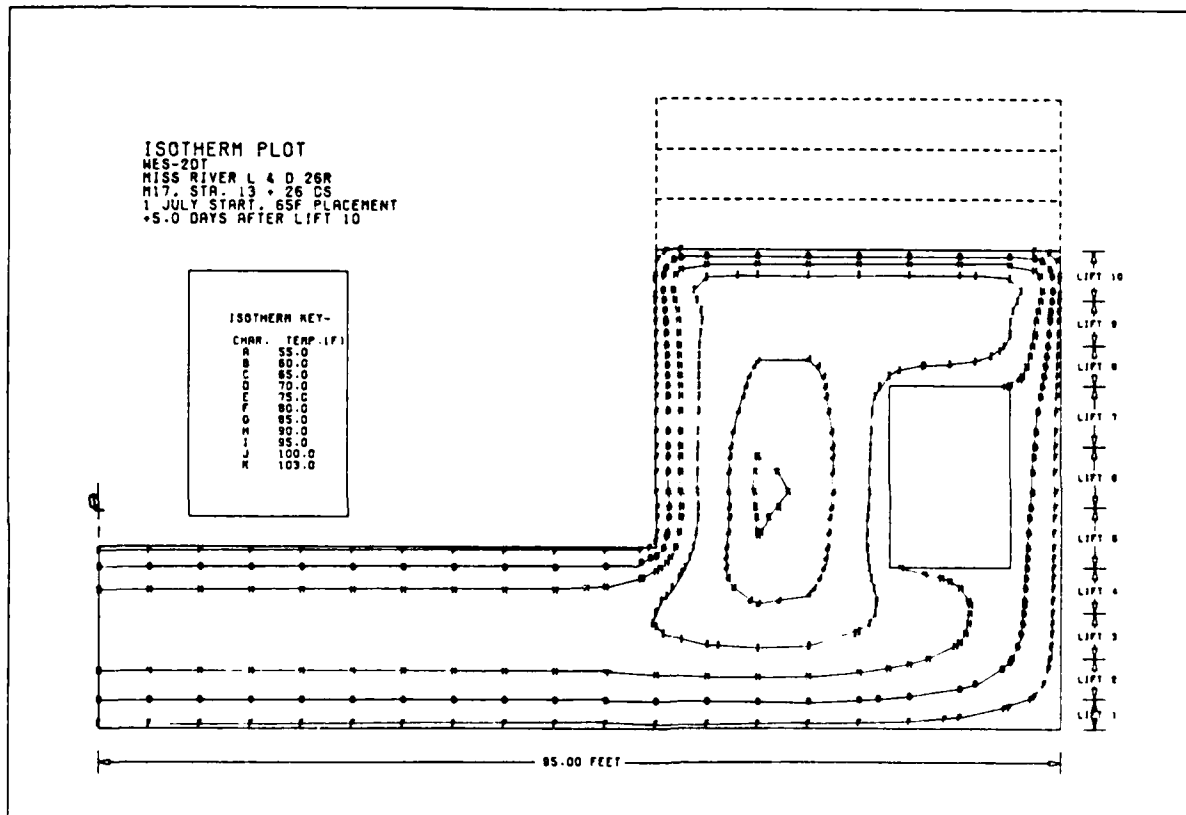


Figure 40c. Temperature contours calculated using WES2DT in Monolith 17 at 5 days after placement of lift 10.

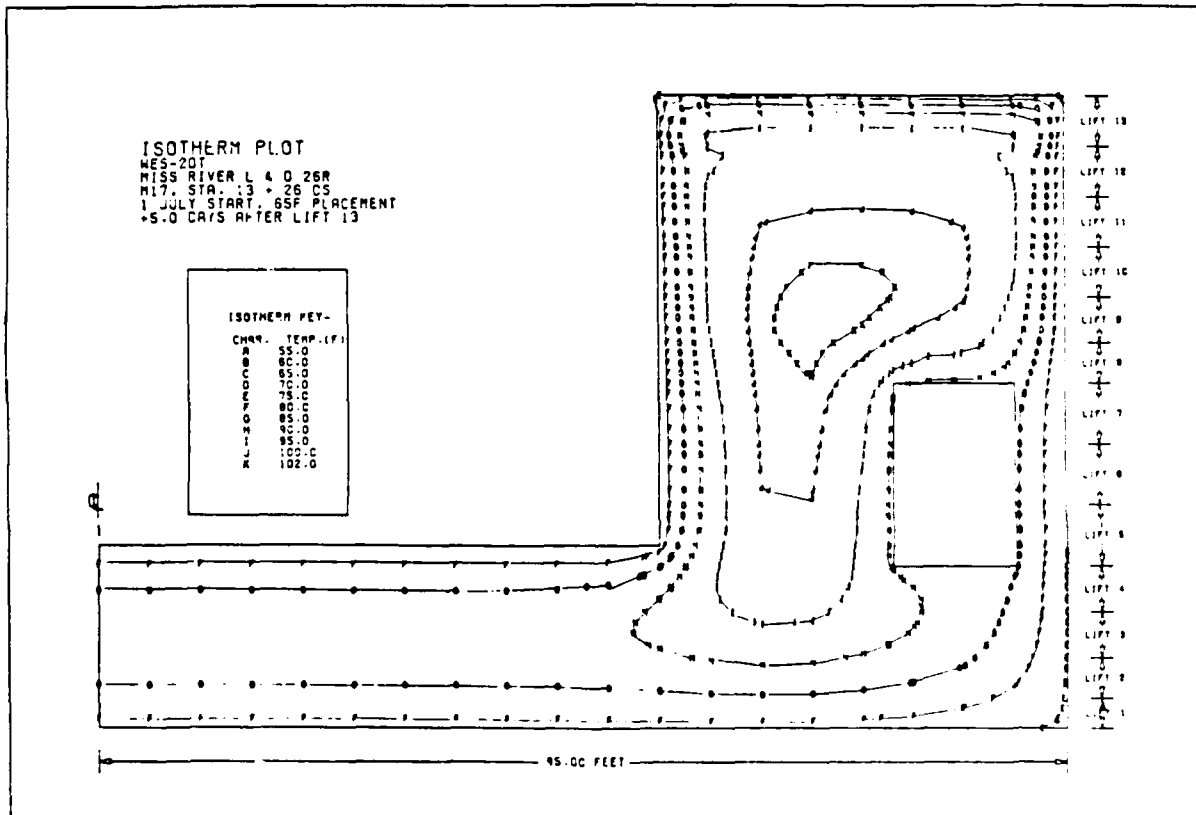


Figure 40d. Temperature contours calculated using WES2DT in Monolith 17 at 5 days after placement of lift 13.

Presentation of Results

Two-dimensional
gravity loading

97. The ABAQUS program was used to perform the 2-D stress analysis of monolith L-17 for both instantaneous gravity turn-on of the entire structure and an incremental construction build-up sequence of the structure. Figures 41a and 41b show the displaced structure and maximum principal (tensile) stress contours, respectively, for the gravity turn-on analysis for a Young's Modulus (E) of 3.12×10^6 psi. Figures 42a and 42b give the same results for $E = 4.80 \times 10^6$ psi. These modulus values correspond to the ACI modified and normal compressive strength of the concrete at 28 days, respectively. Figures 43a thru 43c and 44a thru 44c show the displaced structure and maximum principal stress contours, respectively, for three stages of construction using incremental construction sequencing. This incremental construction analysis uses the material modulus calculation routine UMAT1.

98. WES2DT was used to make an incremental construction analysis. As described in paragraph 94, a FE model was prepared through lift 13. Gravity loads for lifts 14 through 17 were simulated by applying appropriate surface pressures to the top of lift 13. Figures 45a thru 45c and 46a thru 46c show the displacement vector plots and principal stress vector plots, respectively, from this analysis. Figures 45c and 46c represent the conditions at 5 days after lift 16 is placed which corresponds to ABAQUS analyses output in Figures 43c and 44c. All subsequent plots of WES2DT results will be similarly shown.

Two-dimensional
gravity and thermal loading

99. The ABAQUS program was used to perform the 2-D stress analysis including gravity and temperature loading using the modulus routine UMAT1. The

displaced structure plots are given in Figures 47a thru 47c. The maximum principal stress contours are given in Figures 48a thru 48c. The modulus subroutine UMAT2 (concrete aging creep model) was used with ABAQUS to make an analysis with gravity and thermal loading. The displaced structure and maximum principal stress contours are given in Figures 49a thru 49c and 50a thru 50c, respectively. A WES2DT analysis was not made for this same gravity and temperature loading only.

Two-dimensional gravity and thermal loading including creep

100. ABAQUS was used in incremental construction analyses of the structure with the modulus subroutine UMAT2 including creep. Displaced-structure plots are shown in Figures 51a thru 51c. Maximum principal stress contours are shown in Figures 52a thru 52c. WES2DT was also used to make the same analysis. Figures 53a thru 53c show resultant displacement vectors and Figures 54a thru 54c show principal stress vectors from the WES2DT analysis.

Two-dimensional gravity and thermal loading including creep and shrinkage

101. ABAQUS was used to make this analysis also with modulus subroutine UMAT2. Displaced-structure plots for this analysis are shown in Figures 55a thru 55c. Maximum principal stress contours are shown in Figures 56a thru 56c.

Discussion of Results

Gravity turn-on analyses

102. Comparisons of gravity turn-on analyses of monolith L-17 made with $E = 3.12 \times 10^6$ psi and $E = 4.8 \times 10^6$ psi seen in Figures 41 and 42, respectively, showed both the displacements and stresses to be in close agreement. Maximum principal stresses are slightly higher for $E = 4.8 \times 10^6$ psi as expected especially in the top, center of the base slab.

Incremental construction
with gravity loading only
ABAQUS versus WES2DT

103. Incremental construction analyses of monolith L-17 with gravity loading only were conducted with ABAQUS and WES2DT. Comparison of displacement results in Figures 43 and 45 show the results to be very similar. The largest deflections in the base slab occur all along its entire length except near the center of the wall zone after placement of the first four lifts (Figures 43a and 45a). This is because the loading is uniform and the pile support is stronger under the wall. As concrete in the lower wall region was placed, deflections in the base slab became more uniform (Figures 43b and 45b). As wall placement continued, displacements of the slab under the wall increased and maximum displacements in the slab shifted outward toward the edge of the monolith (Figures 43c and 45c).

104. Stress comparisons between the ABAQUS and WES2DT programs required comparing principal stress in contour and vector plots (Figures 44 and 46), respectively, as was described earlier in discussion of L-13. Maximum tensile stresses were generally in the same locations of the models with both programs.

Gravity turn-on versus
incremental construction

105. Comparisons between whole-structure gravity turn-on and incremental construction simulation with gravity loading only with ABAQUS showed predictable results. In both analyses, the maximum displacements of the base occurred after the simulation reached full height. Displacements were less at the centerline of the slab and greatest near the outer edge of the monolith under the wall. Actually, displacements at the outer edge were greater in the incremental construction analysis. As was demonstrated in the L-13 analyses, the displacements within the base slab and wall were characteristically different in gravity turn-on and incremental construction analyses. During increme-

ntal construction, each successive lift is placed up to its planned elevation. Therefore, the displacement of the top of each lift decreases at higher elevations in the structure. Conversely, in the gravity turn-on analysis, the maximum displacement occurs at the top of the wall because all displacements accumulate at the highest elevation. These results have thus exhibited known modes of displacement for gravity turn-on and incremental construction analyses.

106. Stress contours resulting from ABAQUS calculations of gravity turn-on and incremental construction were very similar as expected. Stress values within the base slab were slightly higher for the gravity turn-on analysis which used $E = 4.8 \times 10^6$ psi and for incremental construction analysis because E values were more similar while the wall was placed.

Two-dimensional gravity and thermal loading

107. When thermal effects due to heat of hydration of cement were added to the loading, the predominant changes in the response of the structure were, as with L-13 analyses, an elongation of the base slab and a downward curvature of the outer end of the base slab. However, in L-17 the curvature phenomenon continued into the wall. These effects were observed from the both the ABAQUS and WES2DT results. This response is illustrated by comparing Figures 47, 49, 51, and 53. Elongation of the slab is due to thermal expansion relative to the centerline. As described in paragraph 76, the curvature occurs as a result of differential thermal expansion between a new lift and previous lifts. In FE analyses of monolith L-13, the differential expansion phenomenon only occurred in the two lifts of the base slab. None of the higher lifts was sufficiently long for any observable curvature to result. In monolith L-17, however, there are four full and one partial full-width lifts in the base and nine full-width lifts in the wall. The differential thermal expansion of all these lifts

contributes to a curvature in both the base slab and wall.

108. The addition of thermal loading caused an increase in maximum principal (tensile) stresses along the bottom of the base slab near the centerline and on the top surface of the base slab near the outer edge through placement of lift 4. The maximum principal stress response was similar up to this stage of simulated construction from use of both modulus subroutines UMAT1 and UMAT2 (Figures 48a and 50a). The increases in tensile stresses due to thermal loading in the areas cited above were more than 300 psi and 100 psi, respectively. Results from use of UMAT1 and UMAT2 began to differ by the time lift 16 in the wall was placed. With UMAT1, the zone of maximum tensile stress continued to be located along the bottom of the base slab near the centerline. With UMAT2, however, the zone of maximum tensile stress shifted to the top of the base slab near the centerline. This difference in maximum principal stress response is again attributed to the higher values of E within the first day with UMAT2.

109. The addition of thermal loading also increased the level of maximum principal (tensile) stresses in the wall. Tensile stresses increased from near zero with gravity loading only to about 200 psi on the top surface of lift 8 with both UMAT1 and UMAT2. As lifts 9 through 16 were added, maximum principal stresses in the upper, massive portion of the wall appeared to coincide with lift interfaces in a vertically, alternating pattern of higher and lower stress contours (Figures 48c and 50c). It is believed that the higher tensile stress levels that exist on the top surface of each new lift are "locked in" as a result of placement of the successive lift. Lower levels of maximum tensile stresses in these areas were generated in the UMAT2 analysis. This situation may be attributed to the higher, early-age E values used by the subroutine UMAT2. It is believed that different stress fields are developed when the values of E change during the same time that a temperature change is ongoing

in the concrete. The higher initial E in UMAT2 prevents this same reaction. A comparable WES2DT analysis with gravity and thermal loading, but without creep was not conducted.

Two-dimensional gravity and thermal loading including creep

110. Analyses of L-17 which included gravity and thermal loading with creep were conducted using both ABAQUS-UMAT2 and WES2DT. The effects of creep, as on monolith L-13, changed the displaced response of the monolith. When ABAQUS results using UMAT2 with creep were compared with those without creep, it was seen that creep decreases the curvature of the outer, bottom of the base (Figures 49 and 51). Outward expansion of the base slab and wall increased with creep, the direct result of displaced relaxation of the lower lifts to the elongating force supplied by the thermally expanding subsequent lifts. It seems reasonable certain that this effect is exaggerated due to the higher, early-age E values used by UMAT2. With creep, the concrete appeared to displace in an exaggerated manner in certain locations. This was the case for the increased vertical displacement of the outer edge of the floor slab (Figures 49c and 51c).

111. The displacement trends produced by ABAQUS and WES2DT did not compare (Figures 51 and 53) as well as was seen earlier with results from L-13. Again this may be partially due to the different plane strain formulations used in the two programs that was discussed earlier. The larger mass of this monolith increased internal temperatures. Therefore, increased potential existed for differential expansion. It has been seen that this differential caused generalized curvature of the monolith. However, the combined effects of high early-age E , higher creep potential than used by WES2DT, increased member stiffness due to size, and higher temperature rise caused larger lateral expansion. Actually, the displacements from the WES2DT analysis more closely

matched the ABAQUS-UMAT2 analysis without creep. This may indicate that the amount of creep in the ABAQUS-UMAT2 analysis is excessive.

112. When comparing the ABAQUS-UMAT2 maximum principal stress plots without creep (Figures 50) to maximum principal stress plots with creep (Figure 52), the following observations were made. The relaxation of stresses due to creep with ABAQUS-UMAT2 reduced peak principal stresses in the base slab from 300 psi (Figure 50a) to 100 psi (Figure 52a) at five days after placement of lift 4. At 5 days after placement of lift 7, peak principal stresses in the base slab were reduced from around 300 psi (Figure 50b) without creep to 50 psi with creep (Figure 52b). Maximum principal stresses in the vicinity of lift 13 at 5 days after placement of lift 16 were 100 psi without creep and near zero psi with creep. In contrast, maximum principal stresses in the base slab from WES2DT with creep were about 225 psi at 5 days after placement of lift 4, and approximately 175 psi at 5 days after placement of lift 7. Although WES2DT was not run without creep for L-17, the very large relaxation of stresses due to creep with ABAQUS-UMAT2 and the higher stresses with creep from WES2DT act to confirm the apparent excessive creep from UMAT2. This is the same conclusion as reached in paragraph 82 for the analyses of L-13. It is expected that incorporating into UMAT2 a corrected E versus time modulus model that better represents the 1- to 2-day values and comparable creep data as were used in the WES2DT analysis, lower initial stress levels and less creep relaxation would result from ABAQUS analyses.

Two-dimensional gravity and thermal loading including creep and shrinkage

113. An ABAQUS analysis was conducted on L-17 using UMAT2 with gravity and thermal loading including creep and shrinkage. The addition of this auto-genous shrinkage caused similar, noticeably different results as was seen earlier in L-13. Comparison of ABAQUS analyses with creep, but with and with-

out shrinkage showed both different displacement and principal stress response. Comparison of displaced grids (Figures 51 and 55) for analyses with and without shrinkage, respectively, shows that the addition of shrinkage greatly reduced the thermal elongation of successive lifts in the base slab and reduced the differential thermal expansion between these lifts. The result was greatly reduced downward curvature of the outer end of the base slab and a general shortening of the slab. Shrinkage did cause the wall to attain a curvature vertically along both the inner and outer surfaces (Figure 55c).

114. Comparison of maximum principal stresses showed that at 5 days after placement of lift 4, peak values were nearly the same as without shrinkage. However, the location of maximum stresses changed from the bottom of the base slab without shrinkage to the top of the slab with shrinkage applied. Maximum principal stresses also increased in the wall, especially at times shortly after placement. This is seen in comparisons of maximum principal stresses in Figures 52b - 52c and 56b - 56c. Stresses in the last two lifts placed with shrinkage are clearly higher. Shrinkage provides an additive effect to thermal stresses that result from internal restraint.

Pile loads

115. As stated earlier, the distribution of the pile loads along the bottom of the base slab is principally dependent upon the base slab deflections. Table 9 gives the vertical pile loads from the different ABAQUS and WES2DT analyses and those supplied by the St. Louis District.

116. The ABAQUS results for a gravity turn-on analysis using an ACI-modified modulus value is in close agreement with the St. Louis District results. The discrepancies can be attributed to minor cross-sectional differences in the two cases. An ABAQUS analysis was also made using the unmodified modulus value since the remaining incremental analysis would also

Table 7. Vertical Pile Loads for Monolith 17
(5 Days after placement of last lift)

Pile No	St. Louis District	GRAVITY TURN-ON		GRAVITY ONLY		GRAVITY & THERMAL LOADS			GRAVITY & THERMAL LOADS		
		ABAQUS		ABAQUS (UMAT1)	WES2DT	ABAQUS		ABAQUS	(W/CREEP)		(W/CREEP & SHRINK.) ABAQUS
		E1	E2			(UMAT1)	(UMAT2)		ABAQUS	WES2DT	
1	92.0	94.2	100.6	99.6	92.8	85.9	86.2	62.4	78.9	67.2	
2	92.5	95.8	101.8	102.2	94.5	88.3	87.6	78.7	79.3	82.3	
3	92.8	97.3	103.3	105.8	99.0	91.2	88.6	76.8	80.3	79.2	
4	151.1	162.5	171.2	177.4	165.0	152.2	144.9	147.3	165.1	146.7	
5	158.2	167.7	176.4	182.9	171.9	155.4	145.0	131.7	170.1	128.1	
6	168.6	178.0	185.4	192.6	180.9	162.1	147.7	171.8	176.3	161.2	
7	172.6	186.8	193.6	201.1	192.0	167.3	148.1	160.2	183.6	146.4	
8	185.8	200.9	205.9	214.5	205.0	176.4	151.2	211.6	191.8	194.6	
9	192.8	212.5	216.6	225.9	219.5	183.9	152.0	201.8	200.8	187.8	
10	207.3	229.8	231.4	241.7	235.3	195.4	156.4	258.0	210.0	254.6	
11	216.2	243.8	244.5	254.2	251.6	204.4	160.3	249.4	219.3	256.1	
12	231.7	261.2	260.0	267.9	267.6	214.7	169.3	274.0	228.0	293.0	
13	241.3	278.9	276.1	279.3	281.9	225.5	184.1	292.1	378.0	323.1	
14	256.0	295.7	291.7	287.4	293.1	239.0	208.2	297.5	402.0	337.1	
15	266.9	313.6	308.1	295.4	301.3	263.3	250.0	319.4	219.0	360.0	
16	279.0	324.5	320.0	302.4	313.9	301.2	309.1	280.6	245.4	303.5	
17	291.1	340.4	335.2	320.0	332.1	366.2	399.8	304.0	282.5	309.5	
18	303.2	359.8	352.7	348.9	359.4	460.0	523.4	376.1	332.4	348.8	
19	315.3	255.2	247.9	260.1	265.8	388.2	453.2	367.9	265.3	302.3	

NOTE - All pile loads are in KIPS/PILE

GRAVITY TURN-ON

- Instantaneous placement of entire structure in one step
- Incremental construction of structure in lifts with only gravity applied

GRAVITY ONLY

- Incremental construction of structure in lifts with gravity and temperature loading
- Pile loads supplied by St. Louis District (E = 3,120,000 psi)

GRAVITY AND THERMAL LOADS

- ABAQUS results using E = 3,120,000 psi (28-day strength modified by ACI code)
- ABAQUS results using E = 4,800,000 psi (28-day strength)
- Original modulus calculation routine modified for use with ABAQUS in this study, only considers aging of the concrete
- New modulus routine which can include aging, creep, shrinkage and E as a function of temperature

St. Louis District

E1

E2

UMAT1

UMAT2

use unmodified values. As in the L-13 runs, this stiffer concrete slightly redistributed the pile loads with the higher values being located under the wall. Maximum loads were approximately 350 kips/pile.

117. When the lock was constructed incrementally using ABAQUS and WES2DT with only gravity loading, a slight redistribution of pile loads took place. Smaller loads were located under the wall and larger loads were located under the chamber section of the slab. These shifts in loads were less than 20 kips/pile with very good agreement between ABAQUS and WES2DT. The maximum pile loads occurred at the same location with only a slight decrease in magnitude when compared with gravity turn-on analyses.

118. As thermal loading was added, the pile loads shifted more to the wall area with both UMAT1 and UMAT2 modulus subroutines. With UMAT1 the maximum pile load was 460 kips/pile while with UMAT2 it was 520 kips/pile. These maximum loads occurred at the second pile in from the outer edge of the monolith in both cases.

119. When creep was considered in the analysis, the ABAQUS and WES2DT programs gave similar results except for piles 10 - 15. This is principally due to the WES2DT analysis using a smeared pile stiffness over a given area while ABAQUS used discrete piles. ABAQUS and WES2DT produced larger pile loads under the inner wall area while having lower values under the wall toward the outer edge. The maximum values from ABAQUS was 376 kips/pile and again occurred at the second pile from the outer edge of the monolith. The WES2DT results gave the maximum load in pile 14 under the inner wall. However, this is misleading since an artificially high stiffness was used at this location because it was at the intersection of two zones of the smeared pile stiffnesses.

120. When shrinkage was added to the analysis with ABAQUS, the loads were redistributed. There was a slight increase in loads under the chamber

area, a significant increase in loads under the wall, and a decrease in loads at the outer edge. The maximum pile load occurred under the wall with a value of 360 kips/pile. However, the previous location of maximum pile load still carried a load of 350 kips/pile. Therefore, other locations can be considered critical.

Cracking potential

121. Comparisons of results were also made to evaluate the potential for cracking of concrete in the L-17 analyses reported herein. Modulus of rupture test results cited in paragraph 90 were again used as a simple cracking threshold for tensile stress. As a review, the modulus rupture values used were 124 psi, 280 psi, 320 psi, and 464 psi at 1-, 3-, 7-, and 28-days age, respectively. The following conclusions are made regarding cracking potential in monolith L-17.

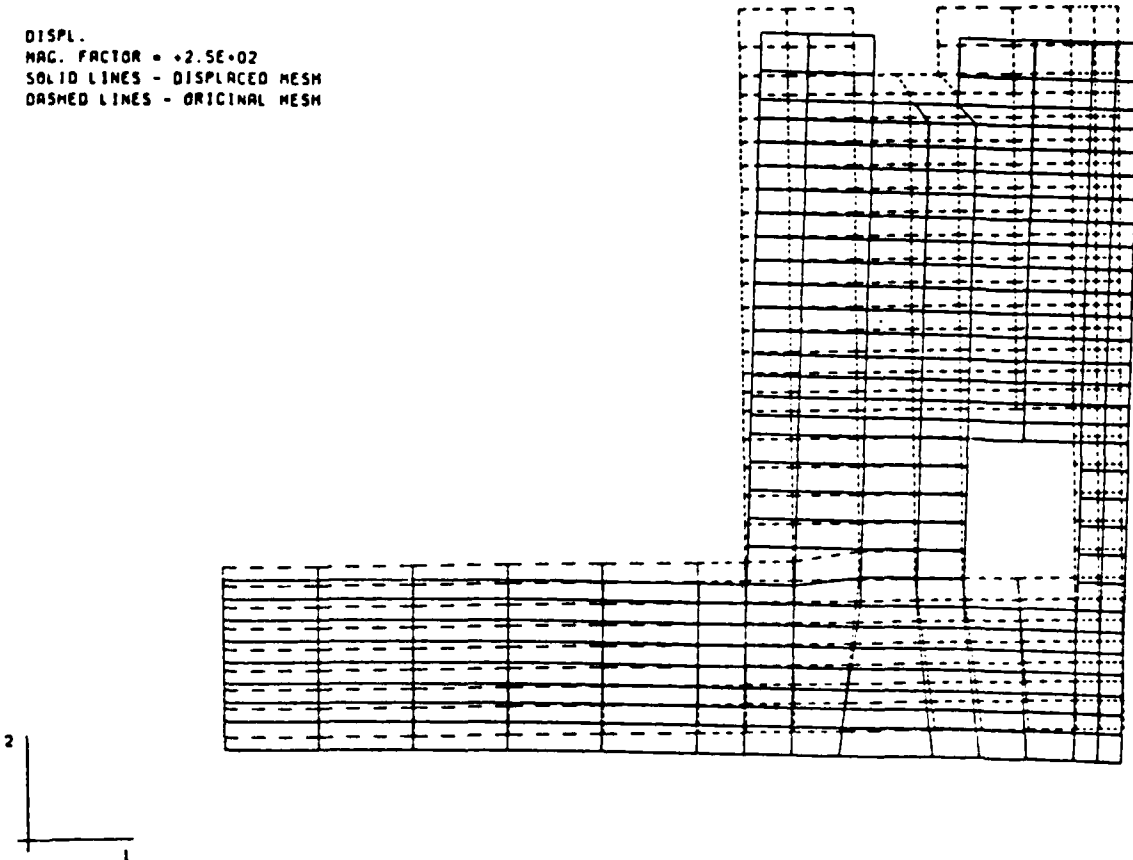
122. First, maximum principal stresses computed in WES2DT analyses which included gravity and thermal loading with creep reached 225 psi in the bottom of the base slab (lift 1). These stresses developed over a period of more than 21 days as a reaction to thermal expansion of lifts 2 through 5. Consequently, the peak value was not reached until the concrete in lift 1 was more than 21 days old and had attained a modulus of rupture of about 425 psi. Thus the maximum tensile stress was less than 55 percent of tensile stress capacity.

123. Secondly, maximum principal tensile stresses computed in ABAQUS analyses using UMAT1, which employed the identical modulus versus time relationship as WES2DT analyses, reached 300 psi in the top of the base slab by 5 days after placement of lift 7 and 250 psi in several locations in the wall (Figure 48). The 300 psi level occurred in concrete that was at least 15 days old and the 250 psi values developed around 5 days after placement. Even

without the benefit of creep stress relief, which should relax stresses by 20-40 percent, these peak tensile stresses are only around 80 percent of modulus of rupture attained at the concrete age when maximum tensile stresses occurred.

124. Finally, maximum principal tensile stresses computed in ABAQUS analyses using UMAT2, which contained an excessively high modulus function for the first day or so of age, reached 300 psi in the bottom of the base slab by 21 days after placement of lift 1. Stresses were only about 100 psi in the same location and time when creep was applied. Stresses in the wall without creep reached around 200 psi and with creep were about 100 psi (Figures 50 and 52). Considering that the computed early-age stresses were probably high due to the higher initial modulus used in UMAT2, it is probable that stress values generated by ABAQUS will be less than shown here. This reinforces the conclusion reached with the WES2DT analyses that peak tensile stresses are less than 55 percent of modulus of rupture in this structure.

DISPL.
MAG. FACTOR = +2.5E+02
SOLID LINES - DISPLACED MESH
DASHED LINES - ORIGINAL MESH

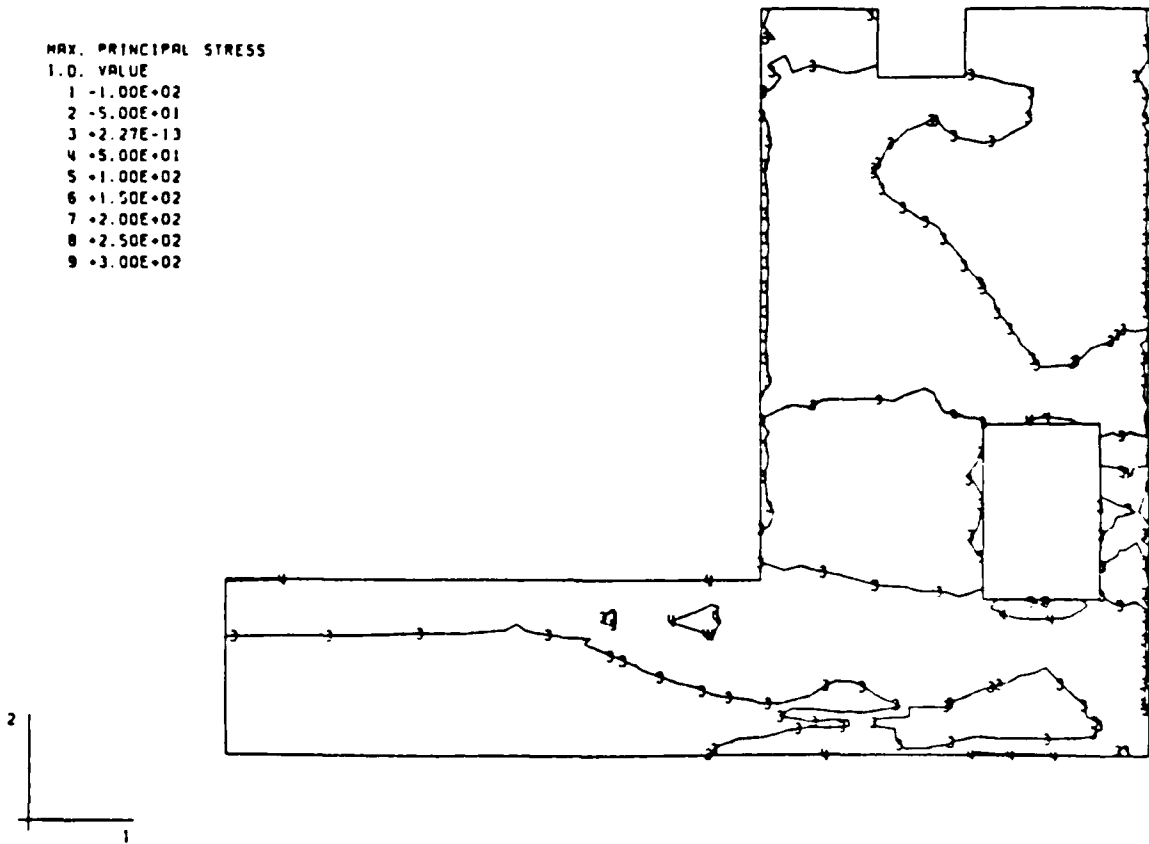


ENTIRE STRUCTURE - M13 - 2D MODEL - E=3.12E6
STEP 1 INCREMENT 1 ABAQUS VERSION 4.5-147

Figure 41a. Displaced structure from gravity turn-on analysis,
E = 3.12×10^6 psi

MAX. PRINCIPAL STRESS

- I.D. VALUE
1 -1.00E+02
2 -5.00E+01
3 +2.27E-13
4 +5.00E+01
5 +1.00E+02
6 +1.50E+02
7 +2.00E+02
8 +2.50E+02
9 +3.00E+02

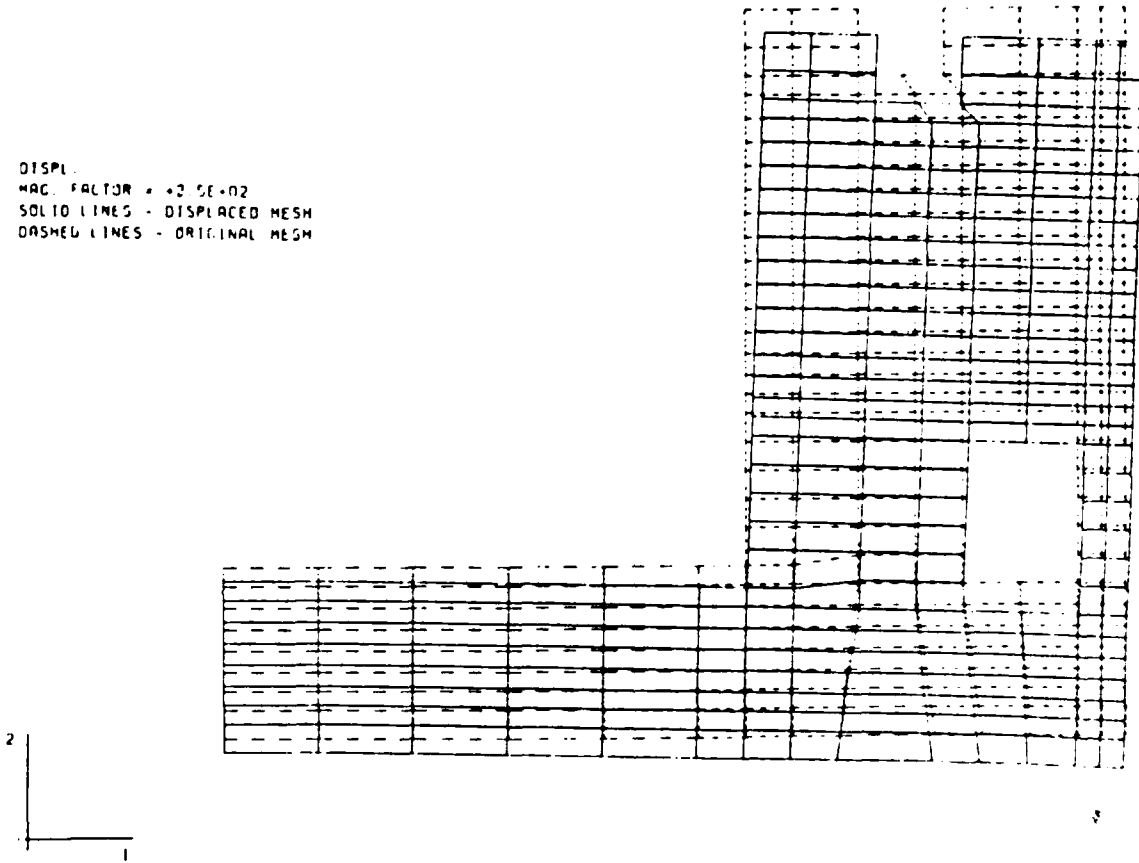


ENTIRE STRUCTURE - M13 - 20 MODEL - E 3.12E6

PBAQUS VERSION 4-5-197

Figure 41b. Maximum principal stress contours for gravity turn-on analysis.
 $E = 3.12 \times 10^6$ psi

DISPL.
MAG. FACTOR = +2.5E+02
SOLID LINES - DISPLACED MESH
DASHED LINES - ORIGINAL MESH

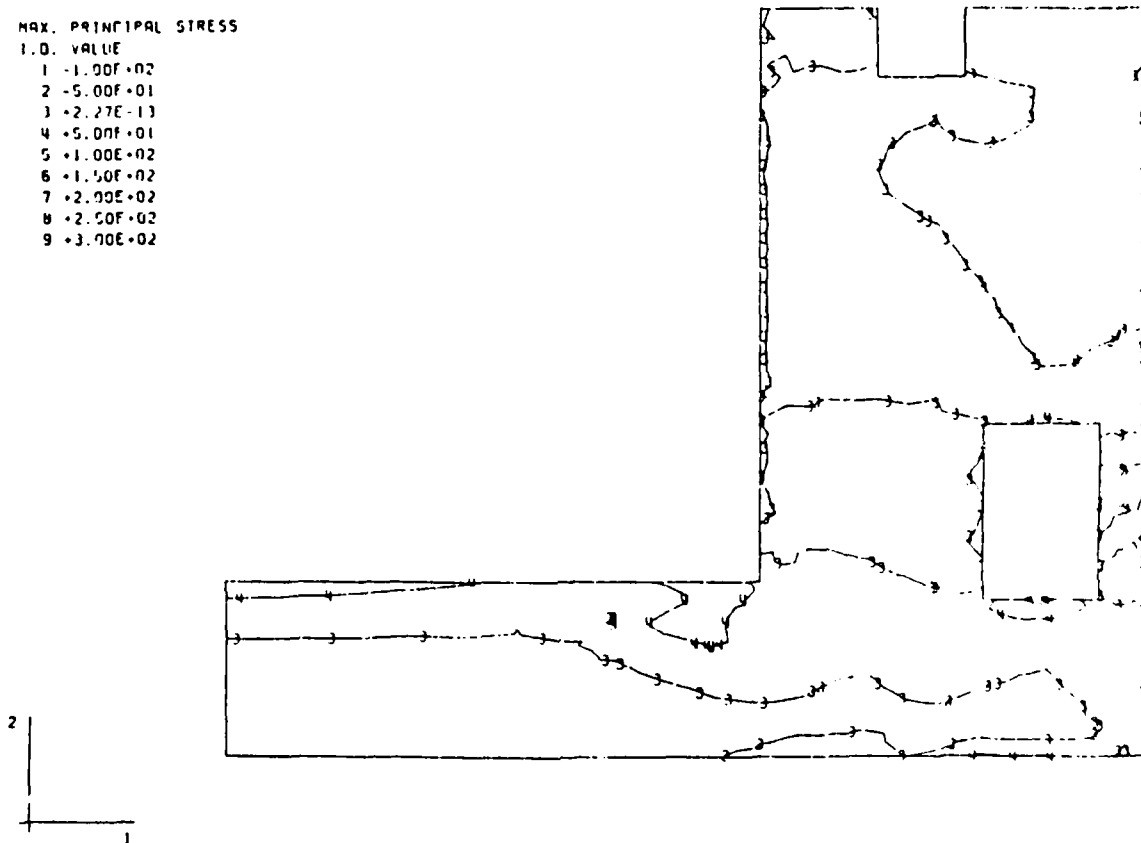


ENTIRE STRUCTURE - M13 - 2D MODEL - E=4.8E6
STEP 1 INCREMENT 1 ABAQUS VERSION 4.5-147

Figure 42a. Displaced structure from gravity turn-on analysis.
 $E = 4.8 \times 10^6$ psi

MAX. PRINCIPAL STRESS

I.D.	VALUE
1	-1.00E+02
2	-5.00E+01
3	2.27E-13
4	5.00E+01
5	1.00E+02
6	1.50E+02
7	2.00E+02
8	2.50E+02
9	3.00E+02



ENTIRE STRUCTURE - M13 - 2D MODEL - E=4.8E6
STEP 1 INCREMENT 1 ABAQUS VERSION 4-5-147

Figure 42b. Maximum principal stress contours for gravity turn-on analysis.
E = 4.8×10^6 psi

DISPL.
MAG. FACTOR = +2.5E+02
SOLID LINES - DISPLACED MESH
DASHED LINES - ORIGINAL MESH

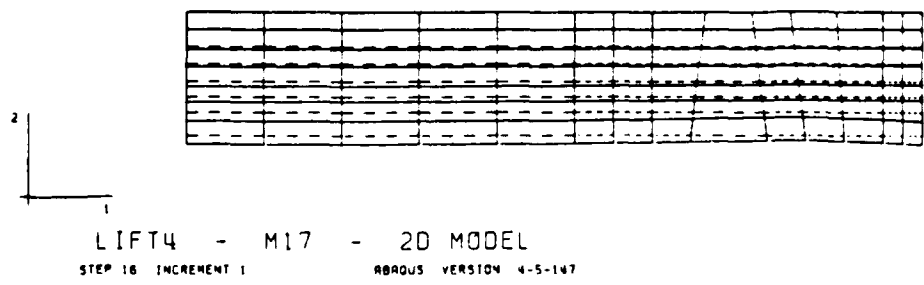


Figure 43a. Displaced structure 5 days after placement of lift 4, gravity loading only, using ABAQUS.

DISPL.
MAG. FACTOR = +2.5E+02
SOLID LINES - DISPLACED MESH
DASHED LINES - ORIGINAL MESH

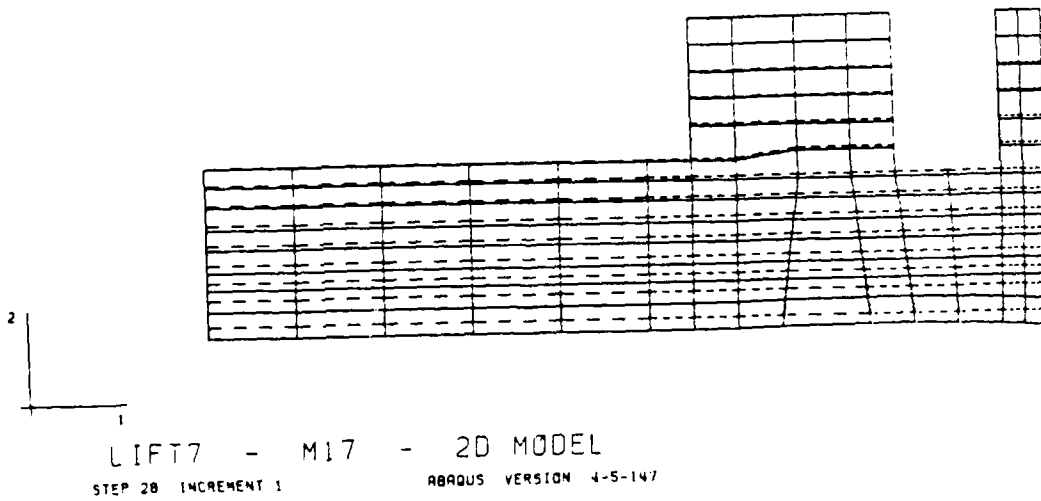
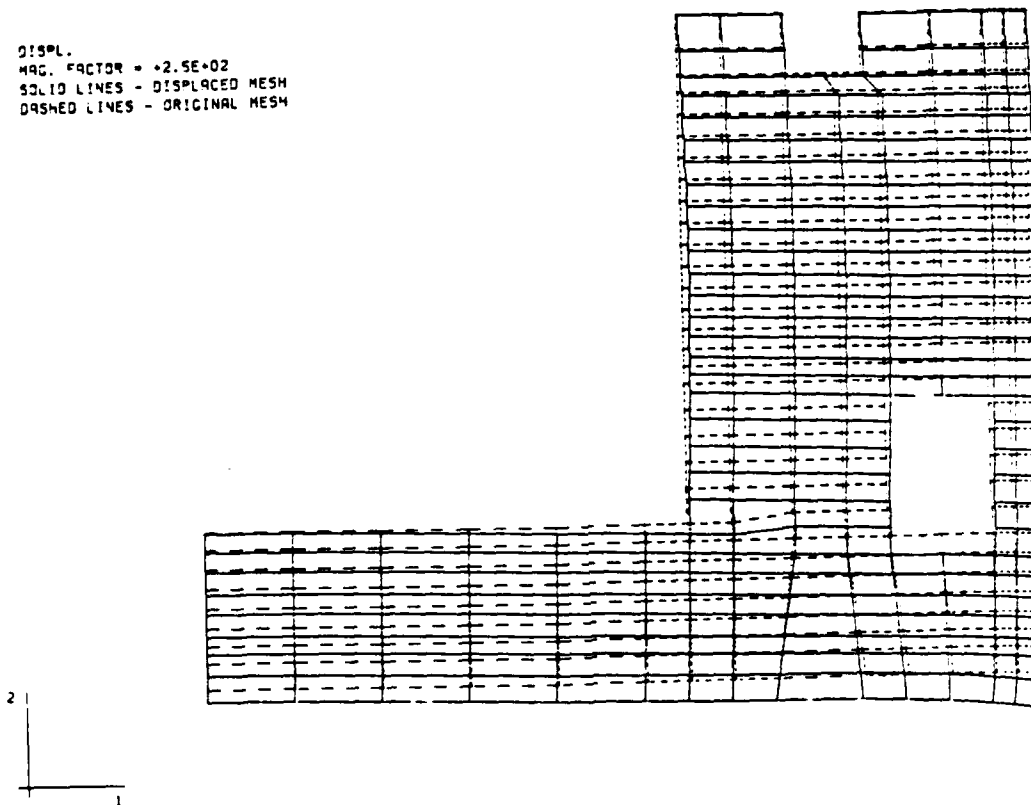


Figure 43b. Displaced structure 5 days after placement of lift 7, gravity loading only, using ABAQUS.

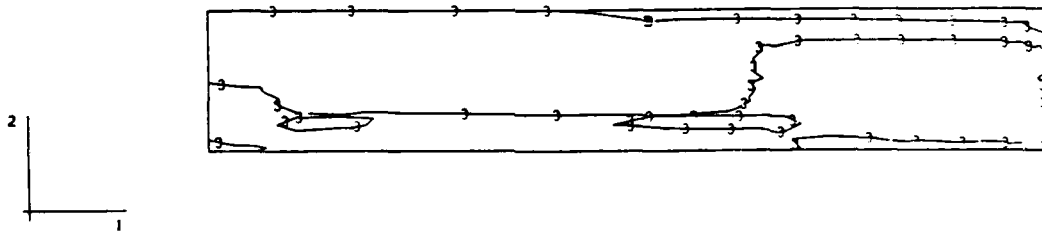
DISPL.
MAG. FACTOR = +2.5E+02
SOLID LINES - DISPLACED MESH
DASHED LINES - ORIGINAL MESH



LIFT16 - M17 - 2D MODEL
STEP 64 INCREMENT 1 ABAQUS VERSION 4.5-147

Figure 43c. Displaced structure 5 days after placement of lift 16, gravity loading only, using ABAQUS.

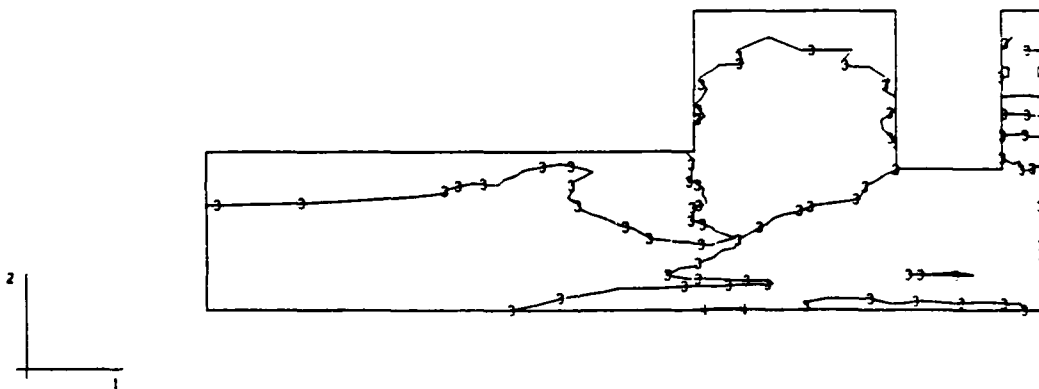
MAX. PRINCIPAL STRESS
 I.D. VALUE
 1 -1.00E+02
 2 -5.00E+01
 3 +2.27E-13
 4 +5.00E+01
 5 +1.00E+02
 6 +1.50E+02
 7 +2.00E+02
 8 +2.50E+02
 9 +3.00E+02



LIFT4 - M17 - 2D MODEL
 STEP 16 INCREMENT 1 ABAQUS VERSION 4-5-147

Figure 44a. Maximum principal stress contours 5 days after placement of lift 4, gravity loading only, using ABAQUS.

MAX. PRINCIPAL STRESS
 I.D. VALUE
 1 -1.00E+02
 2 -5.00E+01
 3 -2.27E+13
 4 +5.00E+01
 5 +1.00E+02
 6 +1.50E+02
 7 +2.00E+02
 8 +2.50E+02
 9 +3.00E+02

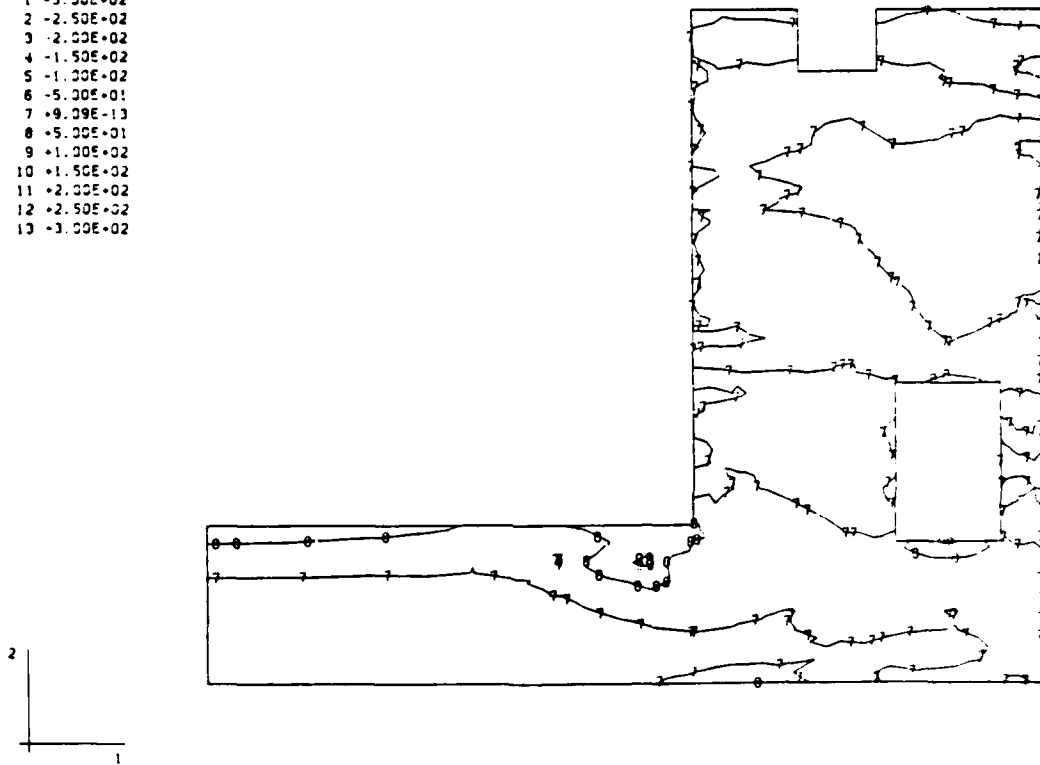


LIFT7 - M17 - 2D MODEL
 STEP 20 INCREMENT 1 ABAQUS VERSION 4-5-147

Figure 44b. Maximum principal stress contours 5 days after placement of lift 7, gravity loading only, using ABAQUS.

MAX. PRINCIPAL STRESS

I.D.	VALUE
1	-3.00E-02
2	-2.50E-02
3	-2.00E-02
4	-1.50E-02
5	-1.00E-02
6	-5.00E-01
7	+9.09E-13
8	+5.00E-01
9	+1.00E-02
10	+1.50E-02
11	+2.00E-02
12	+2.50E-02
13	+3.00E-02



LIFT16 - M17 - 2D MODEL

STEP 64 INCREMENT 1

ABAQUS VERSION 4-5-147

Figure 44c. Maximum principal stress contours 5 days after placement of lift 16, gravity loading only, using ABAQUS.

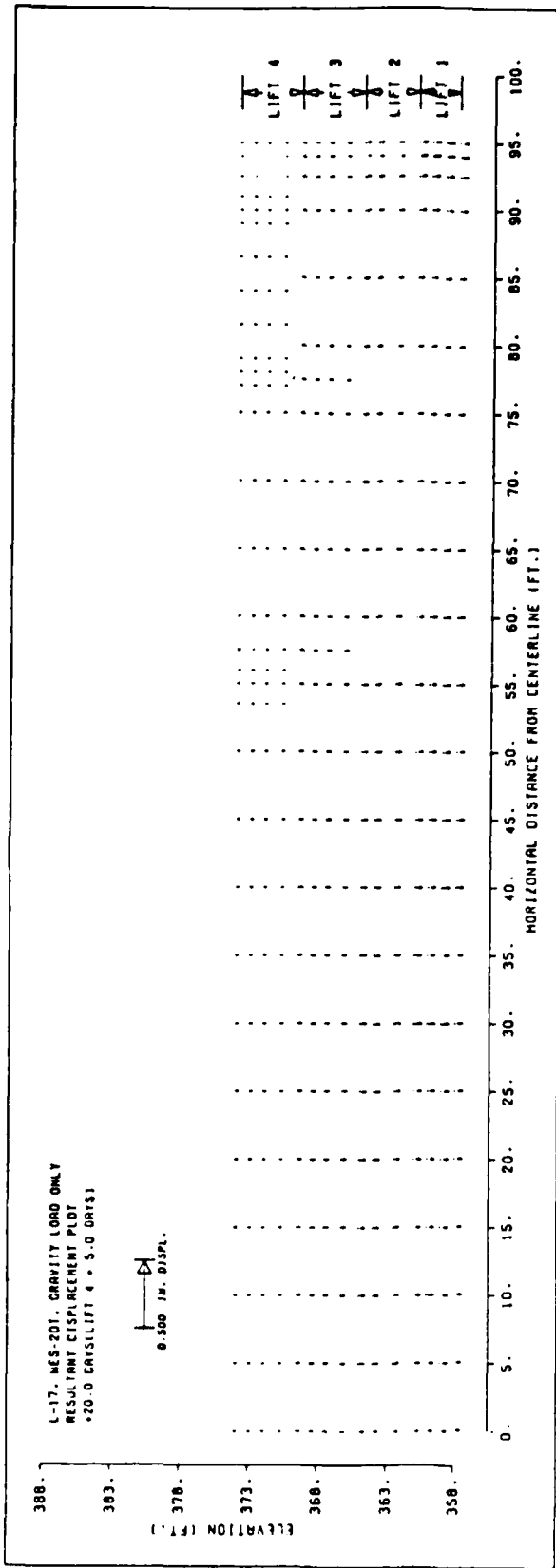


Figure 45a. Resultant displacement vector plot of structure 5 days after lift 4 is placed, gravity only, using WES2DT.

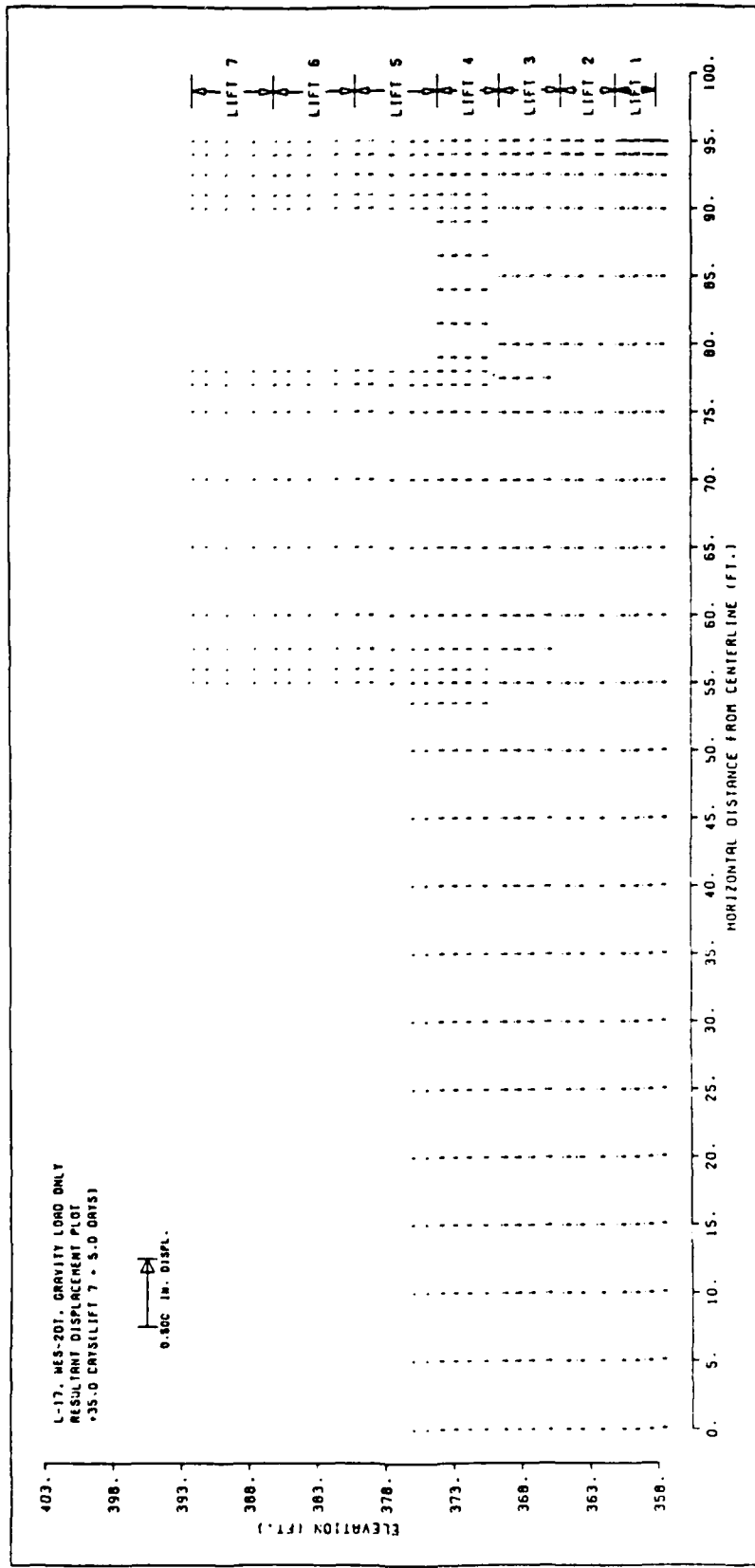


Figure 45b. Resultant displacement vector plot of structure 5 days after lift 7 is placed, gravity only, using WES2DT.

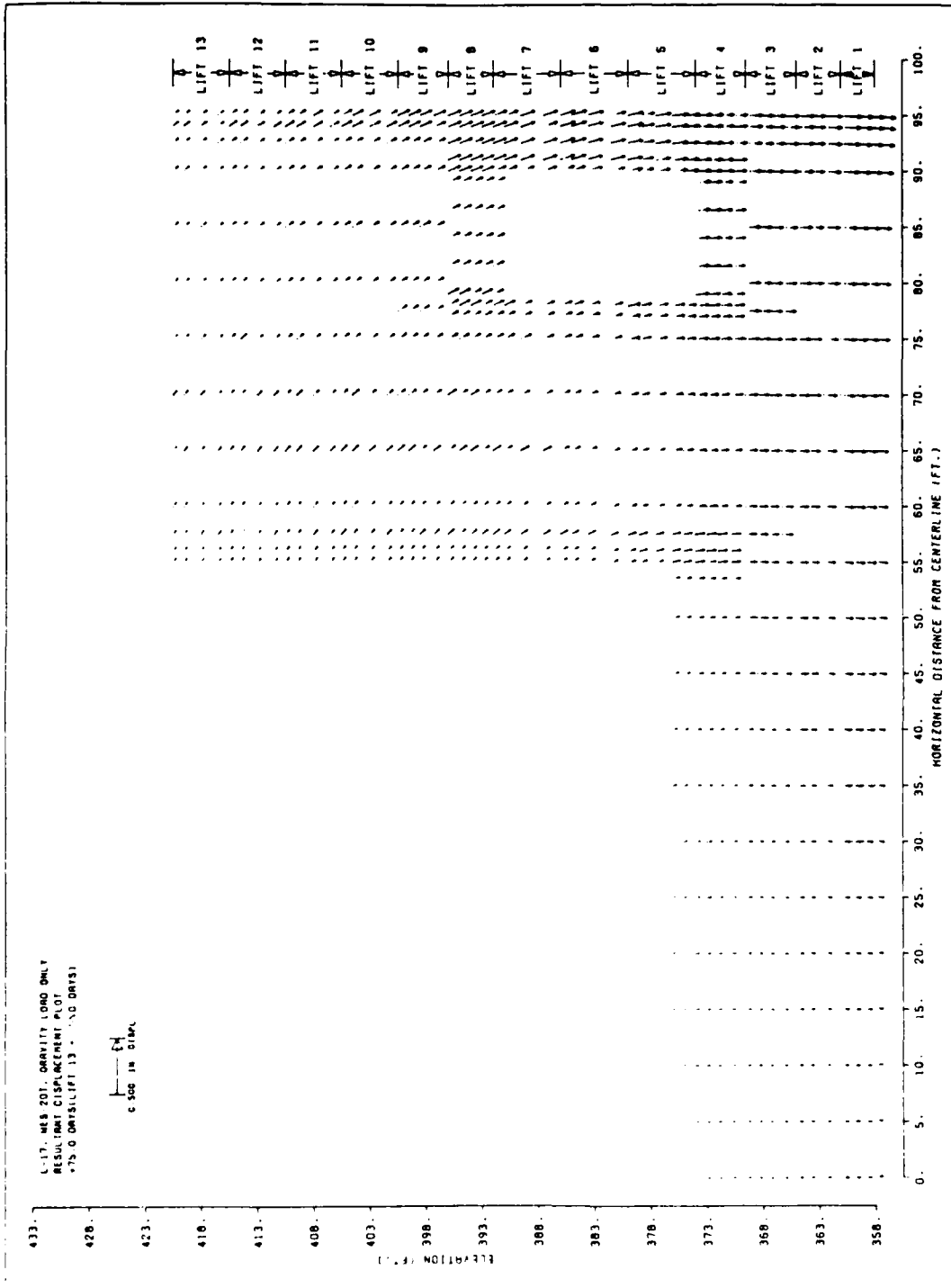


Figure 45c. Resultant displacement vector plot of structure 201 after lift 13 is placed, gravity only, using WES2DT. (This corresponds to 5 days after lift 16 is placed).

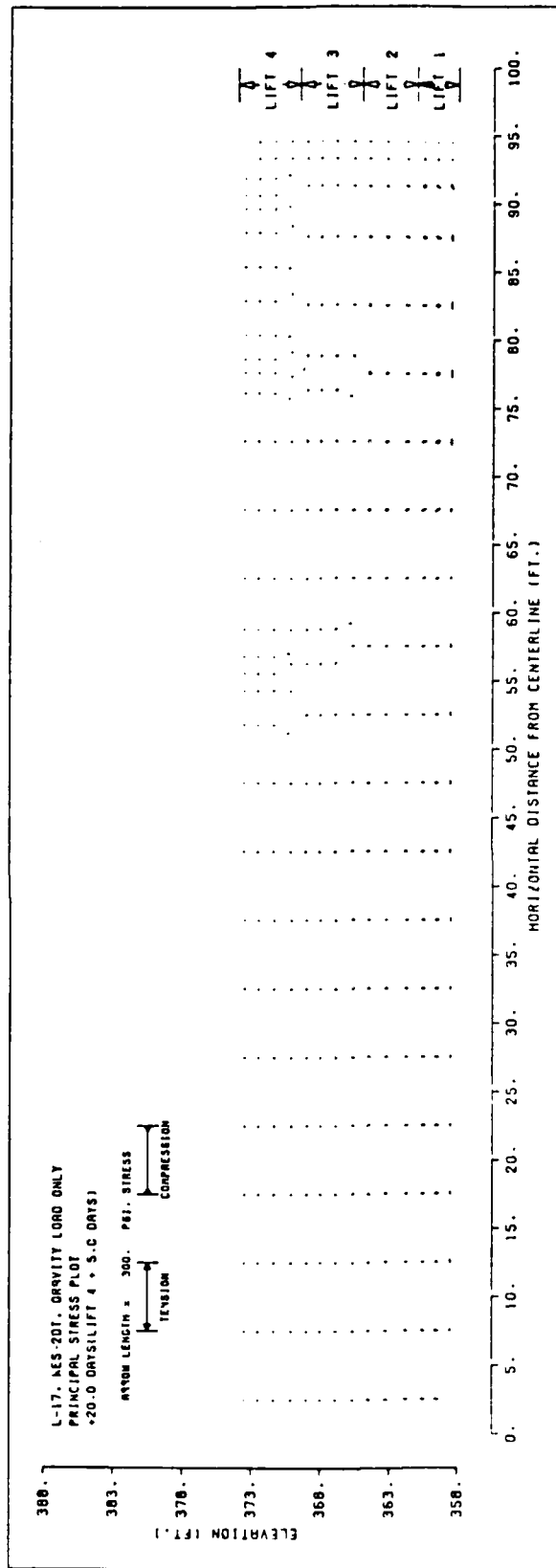


Figure 46a. Principal stress contours of structures 5 days after lift 4 is placed, gravity loading only, using WES2DT.

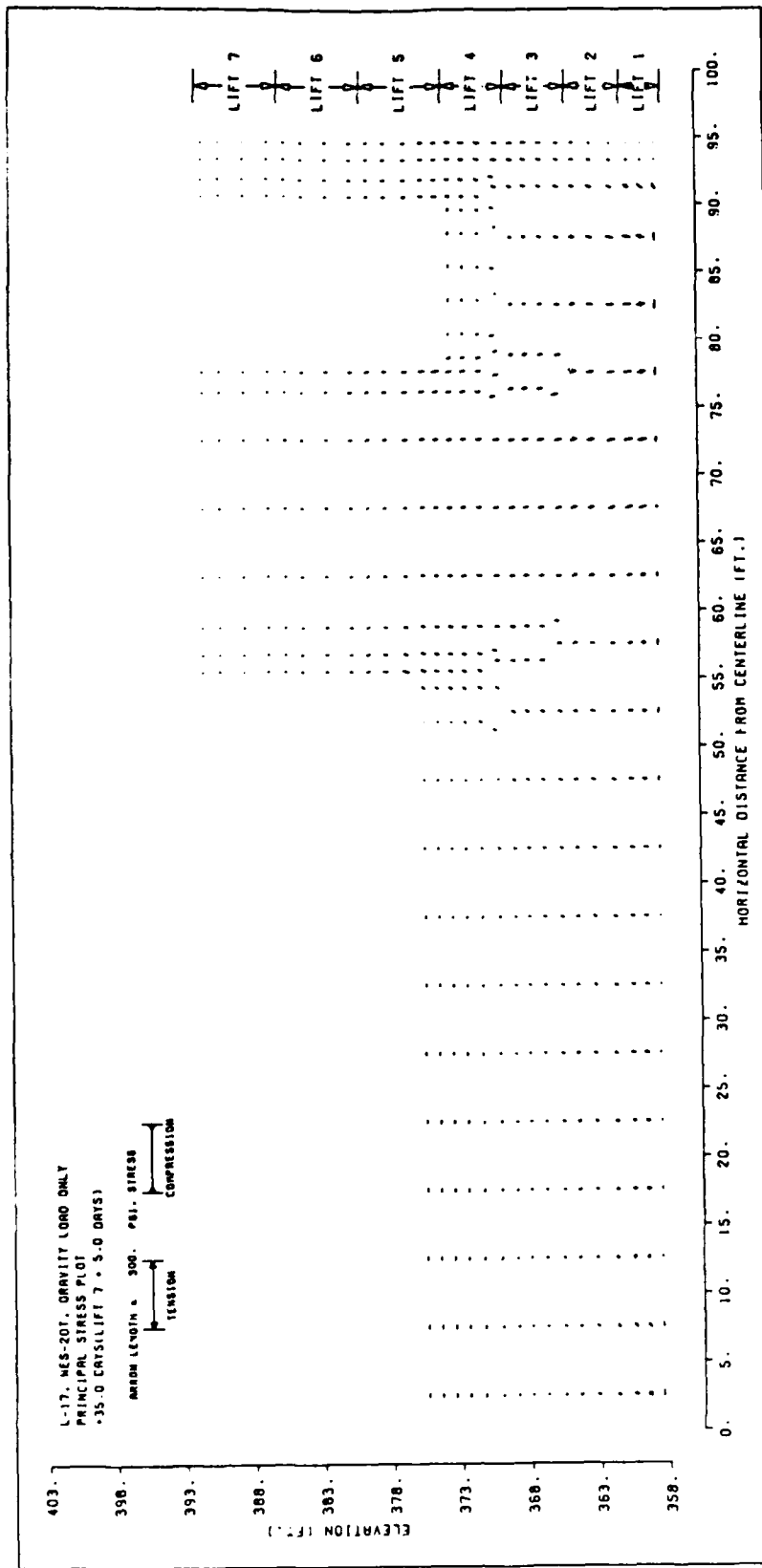


Figure 46b. Principal stress contours of structure 5 days after lift 7 is placed, gravity loading only, using WES2DT.

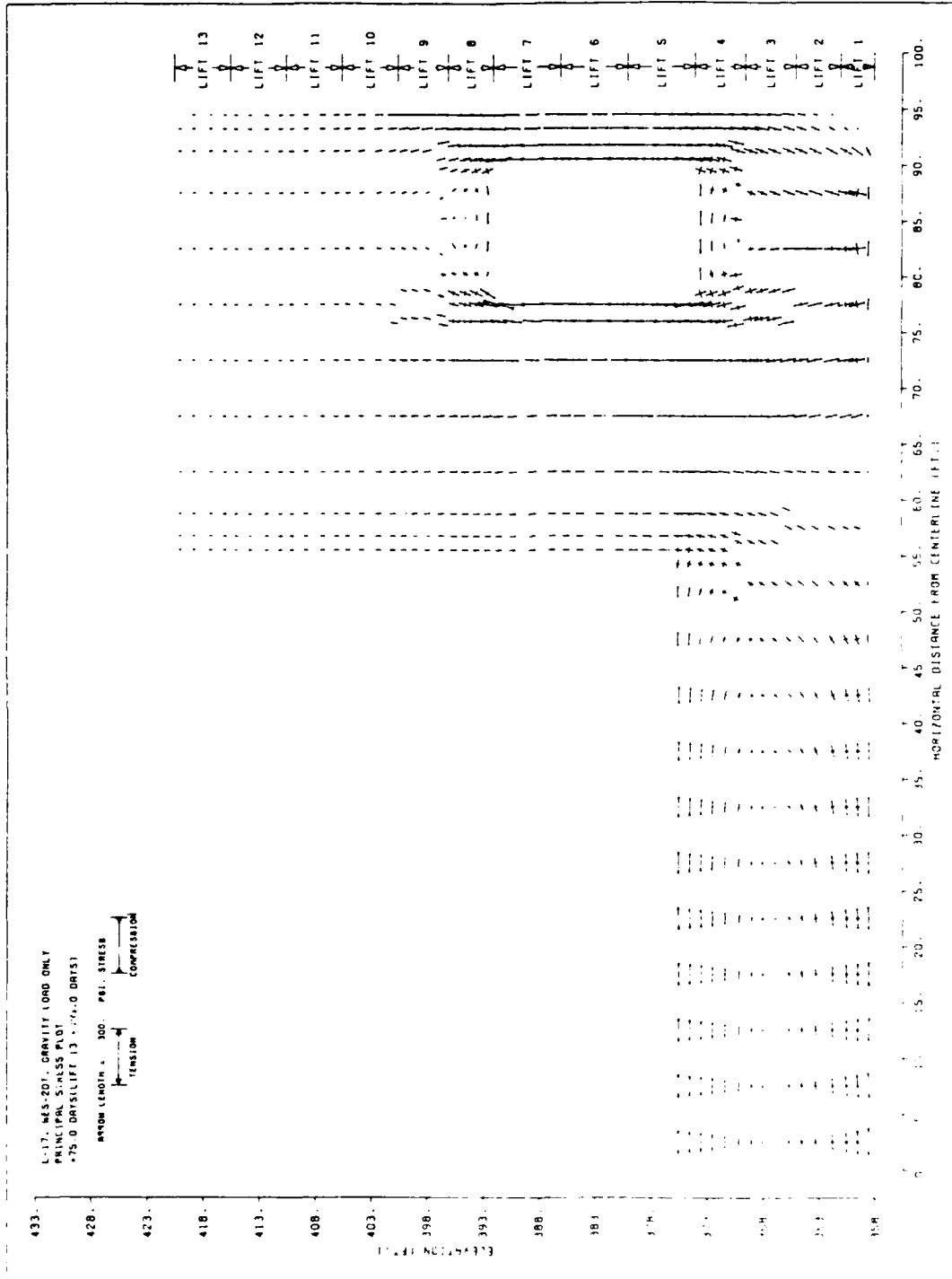
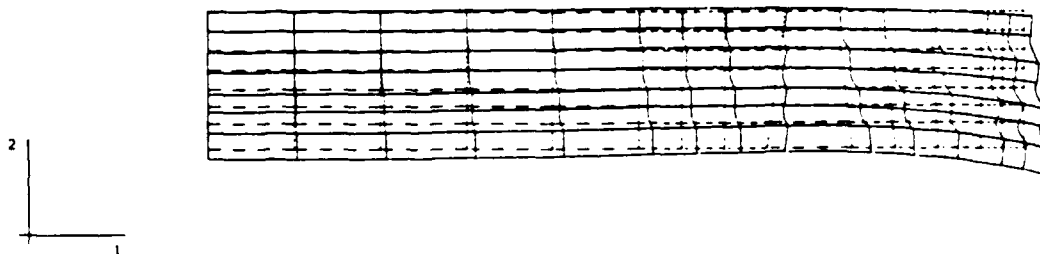


Figure 46c. Principal stress contours of structure 20 days after lift 13 is placed, gravity loading only, using WES2DT. (This corresponds to 5 days after lift 16 is placed).

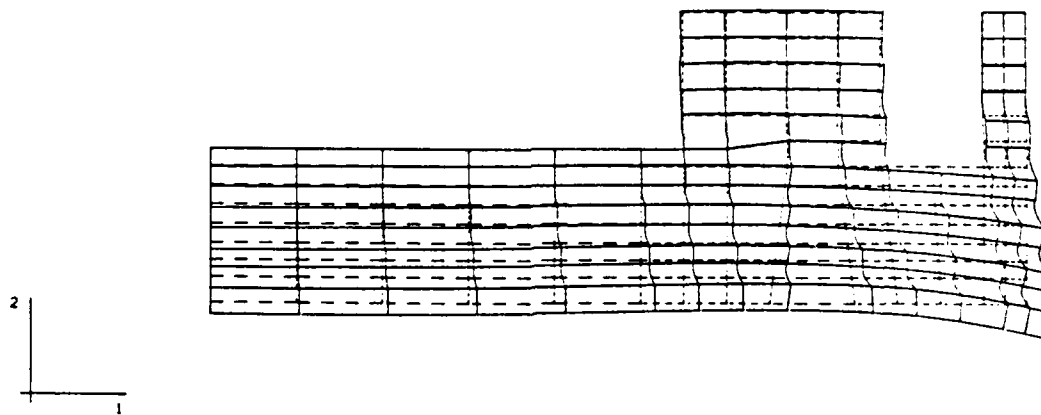
DISPL.
MAG. FACTOR = +2.5E+02
SOLID LINES - DISPLACED MESH
DASHED LINES - ORIGINAL MESH



LIFT4 - M17 - 2D MODEL
STEP 16 INCREMENT 1 ABAQUS VERSION 4.5-147

Figure 47a. Displaced structure 5 days after placement of lift 4, gravity and temperature loading, using ABAQUS (UMAT1).

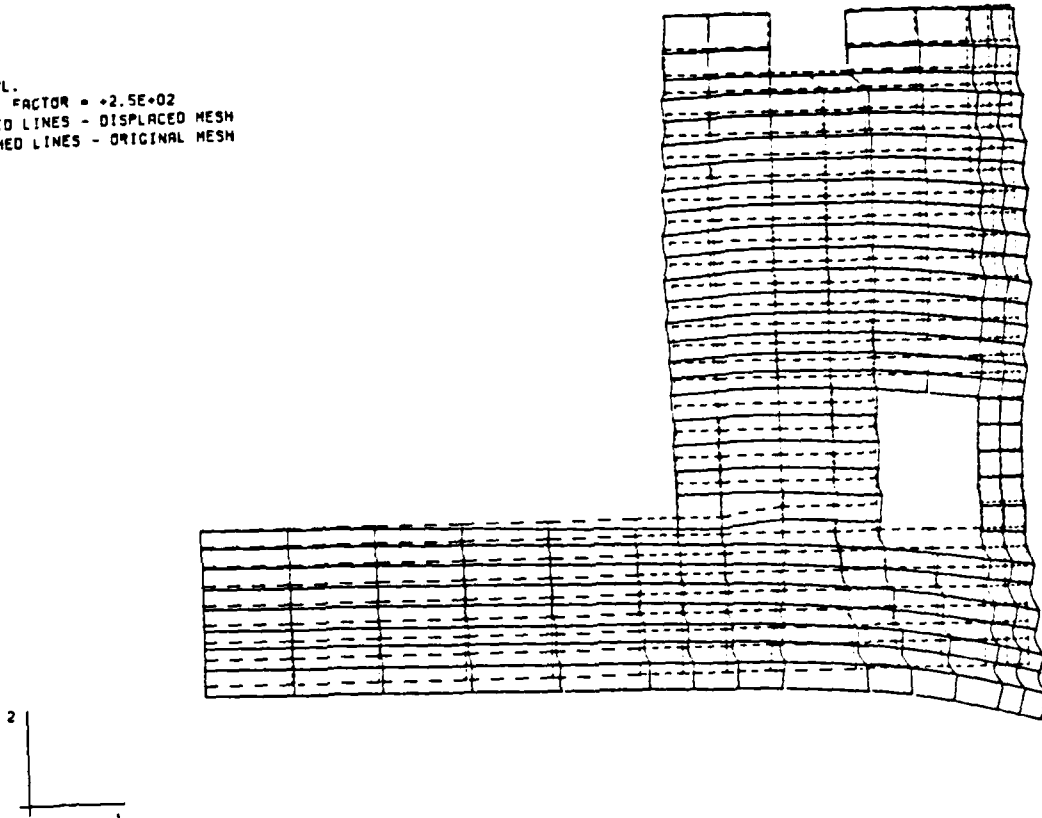
DISPL.
MAG. FACTOR = +2.5E+02
SOLID LINES - DISPLACED MESH
DASHED LINES - ORIGINAL MESH



LIFT7 - M17 - 2D MODEL
STEP 20 INCREMENT 1 ABAQUS VERSION 4-5-147

Figure 47b. Displaced structure 5 days after placement of lift 7, gravity and temperature loading, using ABAQUS (UMAT1).

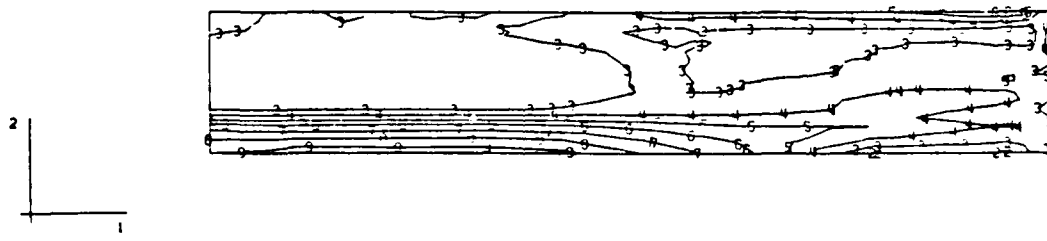
DISPL.
MAG. FACTOR = +2.5E+02
SOLID LINES - DISPLACED MESH
DASHED LINES - ORIGINAL MESH



LIFT16 - M17 - 2D MODEL
STEP 64 INCREMENT 1 ABAQUS VERSION 4.5-147

Figure 47c. Displaced structure 5 days after placement of lift 16, gravity and temperature loading, using ABAQUS (UMAT1).

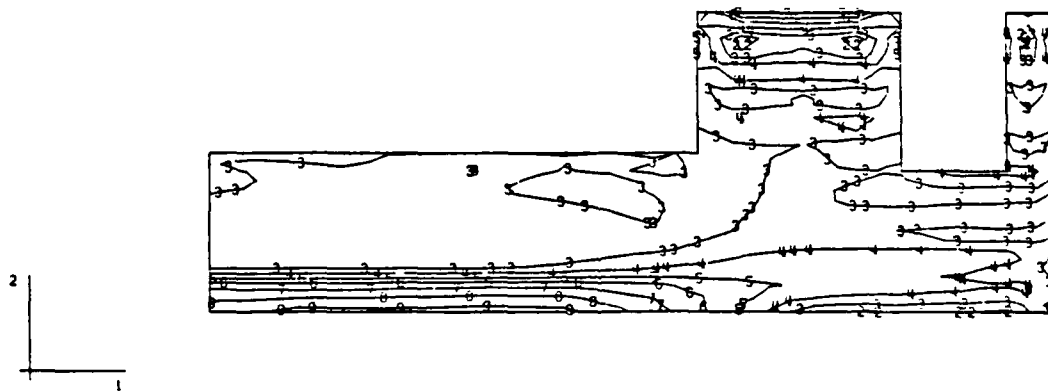
MAX. PRINCIPAL STRESS
 I.D. VALUE
 1 -1.00E+02
 2 -5.00E+01
 3 +2.27E-13
 4 +5.00E+01
 5 +1.00E+02
 6 +1.50E+02
 7 +2.00E+02
 8 +2.50E+02
 9 +3.00E+02



LIFT4 - M17 - 2D MODEL
 STEP 16 INCREMENT 1 ABAQUS VERSION 4-5-147

Figure 48a. Maximum principal stress contours 5 days after placement of lift 4, gravity and temperature loading, using ABAQUS (UMAT1).

MAX. PRINCIPAL STRESS
 I. O. VALUE
 1 -1.00E+02
 2 -5.00E+01
 3 +2.27E-13
 4 +5.00E+01
 5 +1.00E+02
 6 +1.50E+02
 7 +2.00E+02
 8 +2.50E+02
 9 +3.00E+02

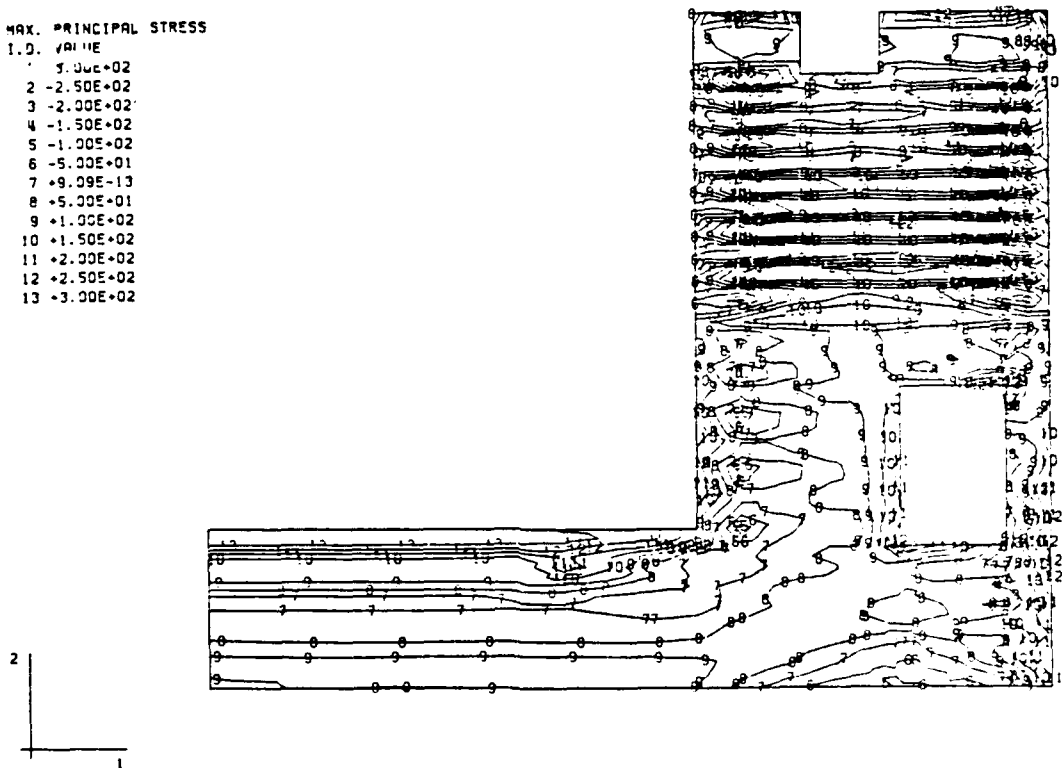


LIFT7 - M17 - 2D MODEL
 STEP 28 INCREMENT 1 ABAQUS VERSION 4-5-147

Figure 48b. Maximum principal stress contours 5 days after placement of lift 7, gravity and temperature loading, using ABAQUS (UMAT1).

MAX. PRINCIPAL STRESS
 I.D. VALUE

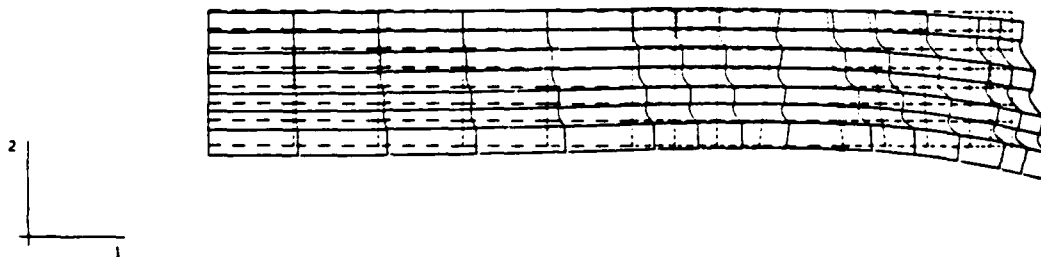
1	5.00E+02
2	-2.50E+02
3	-2.00E+02
4	-1.50E+02
5	-1.00E+02
6	-5.00E+01
7	+9.09E-13
8	+5.00E+01
9	+1.00E+02
10	+1.50E+02
11	+2.00E+02
12	+2.50E+02
13	+3.00E+02



LIFT16 - M17 - 2D MODEL
 STEP 64 INCREMENT 1 ABAQUS VERSION 4.5-147

Figure 48c. Maximum principal stress contours 5 days after placement of lift 16, gravity and temperature loading, using ABAQUS (UMAT1).

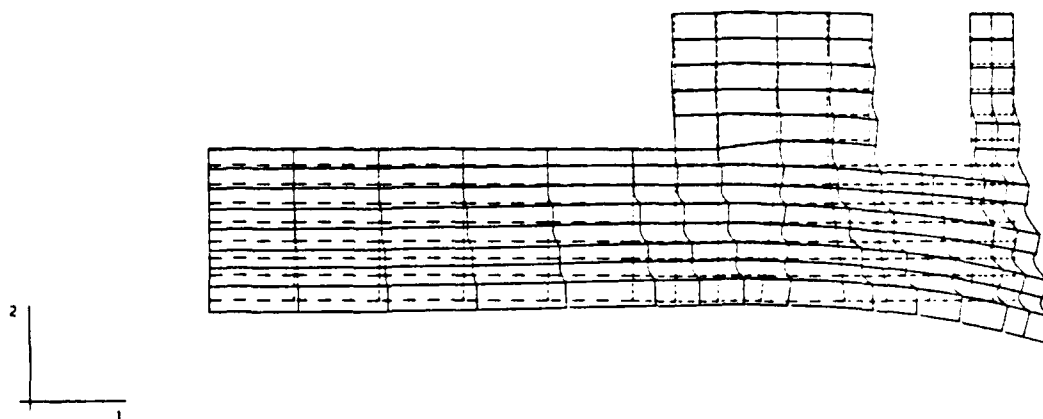
DISPL.
MAC. FACTOR = +2.5E+02
SOLID LINES - DISPLACED MESH
DASHED LINES - ORIGINAL MESH



LIFT4 - M17 - 2D MODEL, NEW UMAT, NOCREEP, NO SHRINK
STEP 16 INCREMENT 1 ABAQUS VERSION 4-5-147

Figure 49a. Displaced structure 5 days after placement of lift 4, gravity and temperature loading, using ABAQUS (UMAT2).

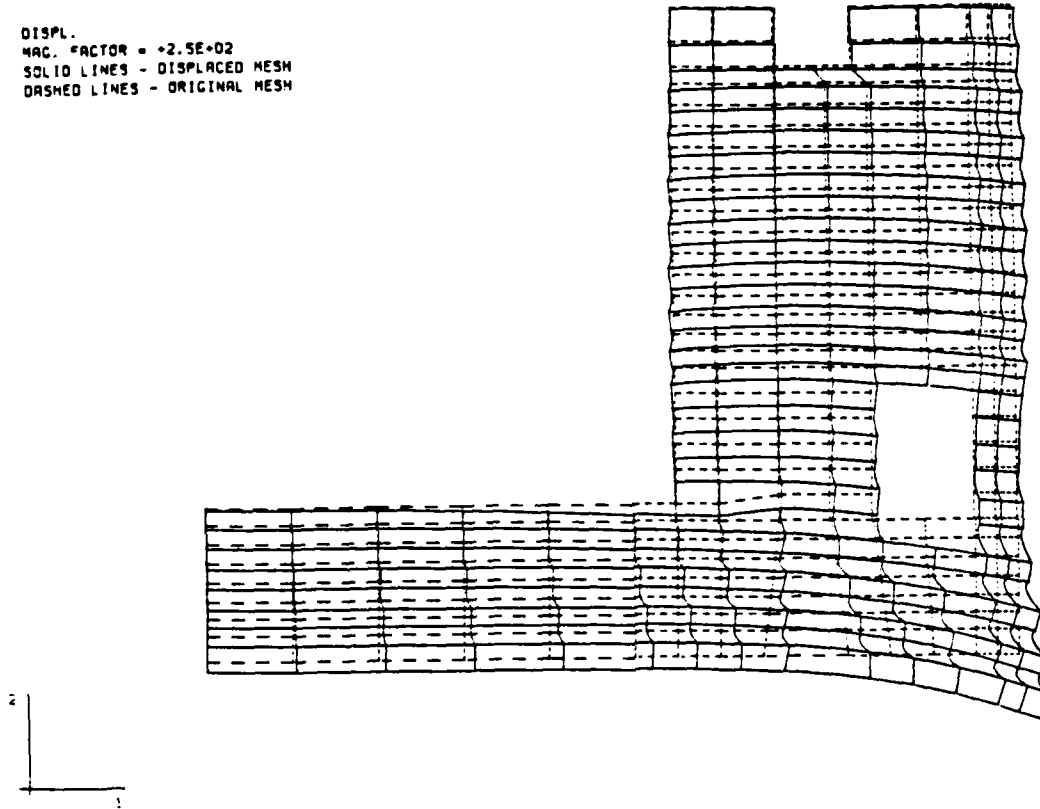
DISPL.
MAG. FACTOR = +2.5E+02
SOLID LINES - DISPLACED MESH
DASHED LINES - ORIGINAL MESH



LIFT7 - M17 - 2D MODEL, NEW UMAT, NO CREEP, NO SHRINK
STEP 28 INCREMENT 1 ABAQUS VERSION 4-5-147

Figure 49b. Displaced structure 5 days after placement of lift 7, gravity and temperature loading, using ABAQUS (UMAT2).

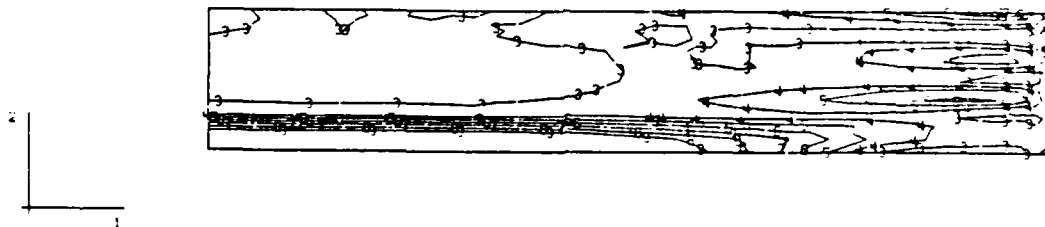
DISPL.
MAG. FACTOR = +2.5E+02
SOLID LINES - DISPLACED MESH
DASHED LINES - ORIGINAL MESH



LIFT16 - M17 - 2D MODEL, NEW UMAT, NO CREEP, NO SHRINK
STEP 64 INCREMENT 1 ABAQUS VERSION 4-5-147

Figure 49c. Displaced structure 5 days after placement of lift 16, gravity and temperature loading, using ABAQUS (UMAT2).

MAX. PRINCIPAL STRESS
 I.D. VALUE
 1 -1.00E+02
 2 -5.00E+01
 3 -2.27E-13
 4 +5.00E+01
 5 +1.00E+02
 6 +1.50E+02
 7 +2.00E+02
 8 +2.50E+02
 9 +3.00E+02

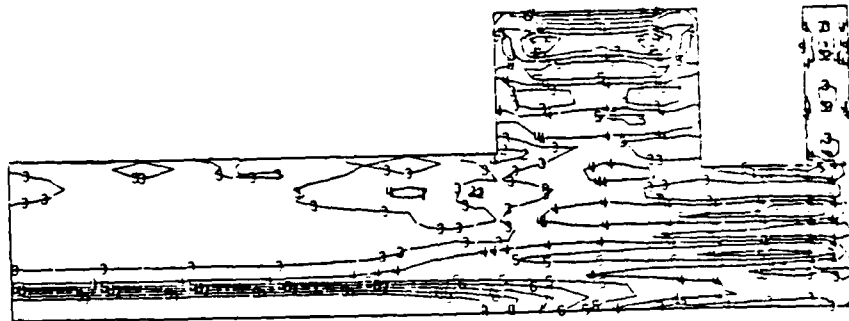


LIFT4 - M17 - 2D MODEL, NEW UMAT, NO CREEP, NO SHRINK
 STEP 16 INCREMENT 1 ABAQUS VERSION 4-5-147

Figure 50a. Maximum principal stress contours 5 days after placement of lift 4, gravity and temperature loading, using ABAQUS (UMAT2).

MAX. PRINCIPAL STRESS

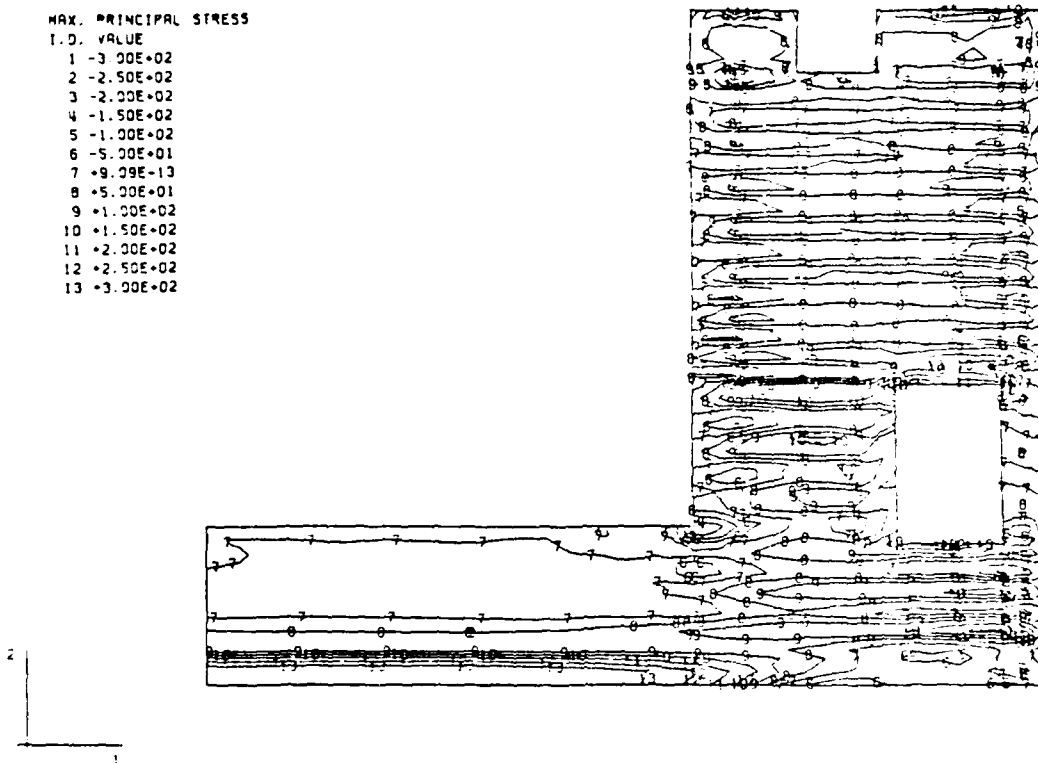
I.D.	VALUE
1	-1.00E+02
2	-5.00E+01
3	-2.27E+13
4	+5.00E+01
5	+1.00E+02
6	+1.50E+02
7	+2.00E+02
8	+2.50E+02
9	+3.00E+02



LIFT7 - M17 - 2D MODEL, NEW UMAT, NO CREEP, NO SHRINK
STEP 28 INCREMENT 1 ABAQUS VERSION 4.5-147

Figure 50b. Maximum principal stress contours 5 days after placement of lift 7, gravity and temperature loading, using ABAQUS (UMAT2).

MAX. PRINCIPAL STRESS
 I.D. VALUE
 1 -3.00E+02
 2 -2.50E+02
 3 -2.00E+02
 4 -1.50E+02
 5 -1.00E+02
 6 -5.00E+01
 7 +9.09E-13
 8 +5.00E+01
 9 +1.00E+02
 10 +1.50E+02
 11 +2.00E+02
 12 +2.50E+02
 13 +3.00E+02



LIFT16 - M17 - 2D MODEL, NEW UMAT, NO CREEP, NO SHRINK
 STEP 64 INCREMENT 1 ABAQUS VERSION 4-5-147

Figure 50c. Maximum principal stress contours 5 days after placement of lift 16, gravity and temperature loading, using ABAQUS (UMAT2).

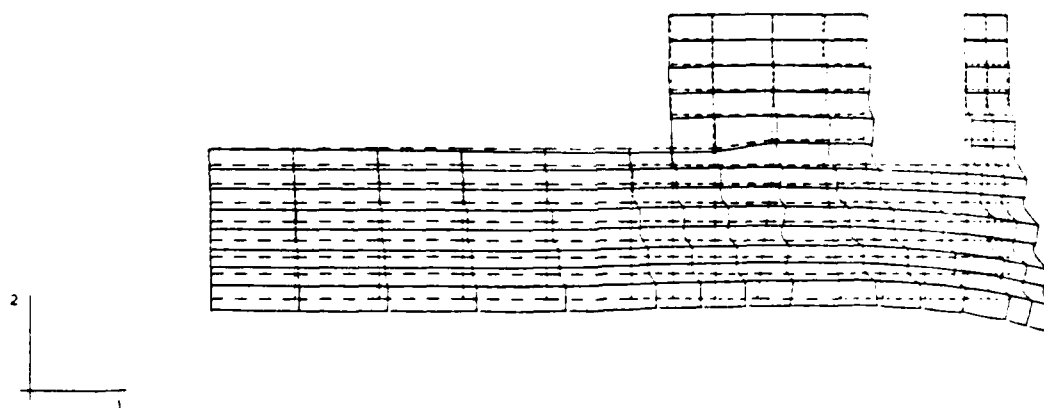
DISPL.
MAG. FACTOR = +2.5E+02
SOLID LINES - DISPLACED MESH
DASHED LINES - ORIGINAL MESH



LIFT4 - M17 - 2D MODEL, NEW UMAT, W/ CREEP, NOSHINK
STEP 16 INCREMENT 1 ABAQUS VERSION 4.5-147

Figure 51a. Displaced structure 5 days after placement of lift 4, gravity and temperature loading with creep, using ABAQUS (UMAT2).

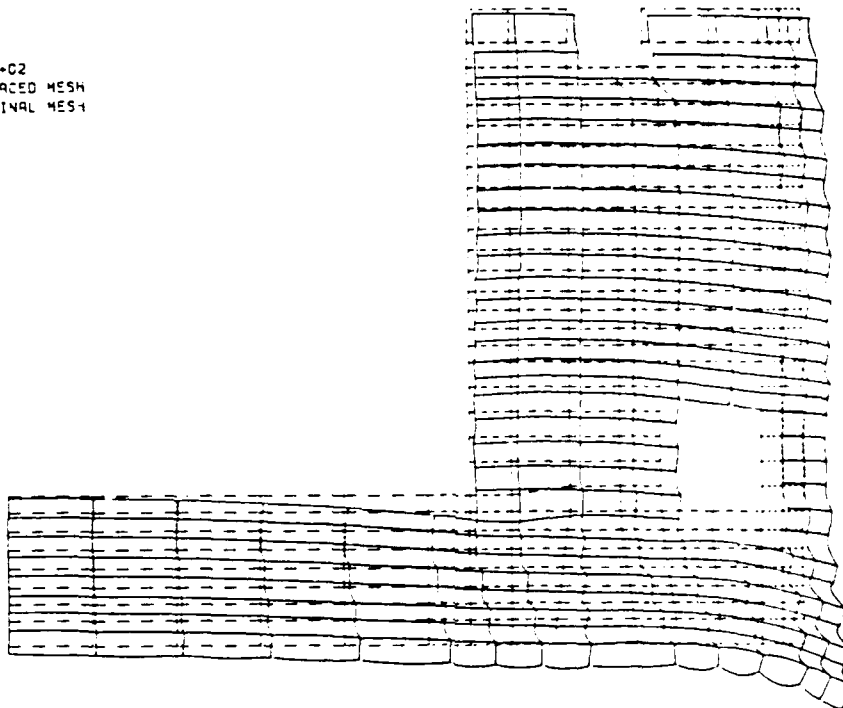
DISPL.
MAG. FACTOR = +2.5E+02
SOLID LINES - DISPLACED MESH
DASHED LINES - ORIGINAL MESH



LIFT7 - M17 - 2D MODEL, NEW UMAT, W/CREEP, NO SHRINK
STEP 28 INCREMENT 1 ABAQUS VERSION 4.5-147

Figure 51b. Displaced structure 5 days after placement of lift 7, gravity and temperature loading with creep, using ABAQUS (UMAT2).

DISPL.
MAG. FACTOR = +2.5E+02
SOLID LINES - DISPLACED MESH
DASHED LINES - ORIGINAL MESH



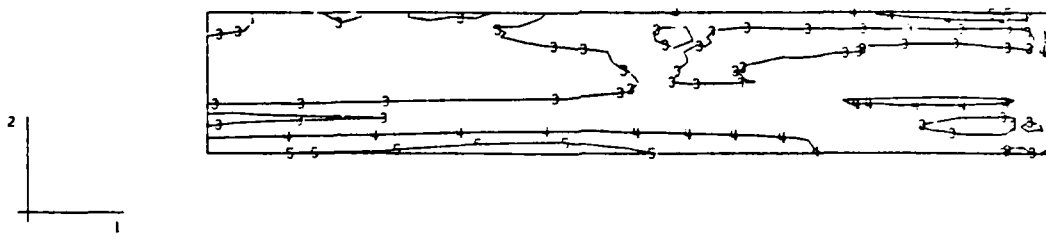
LIFT16 - M17 - 2D MODEL, NEW UMAT, U/CREEP, NOSHRINK
STEP 64 INCREMENT 1 ABAQUS VERSION 4.5-147

Figure 51c. Displaced structure 5 days after placement of lift 16, gravity and temperature loading with creep, using ABAQUS (UMAT2).

MAX. PRINCIPAL STRESS

I.D. VALUE

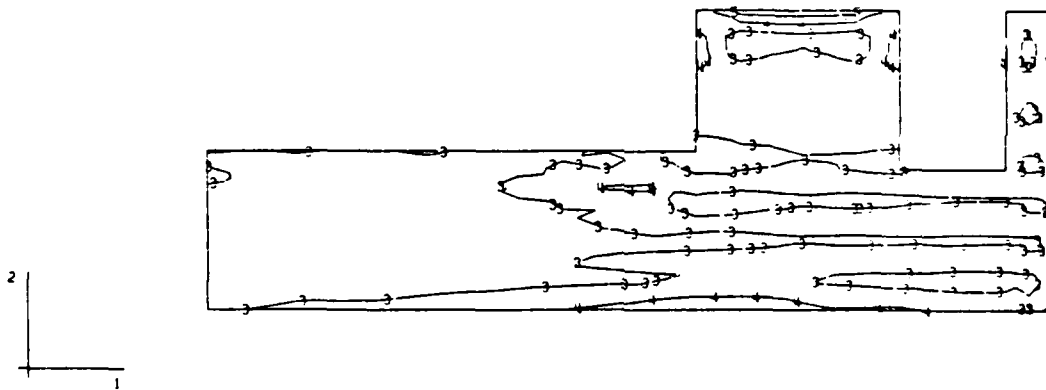
1	-1.00E+02
2	-5.00E+01
3	-2.27E+10
4	+5.00E+01
5	+1.00E+02
6	+1.50E+02
7	+2.00E+02
8	+2.50E+02
9	+3.00E+02



LIFT4 - M17 - 2D MODEL, NEW UMAT, W/CREEP, NOSHRINK
STEP 16 INCREMENT 1 ABAQUS VERSION 4-5-147

Figure 52a. Maximum principal stress contours 5 days after placement of lift 4, gravity and temperature loading with creep, using ABAQUS (UMAT2).

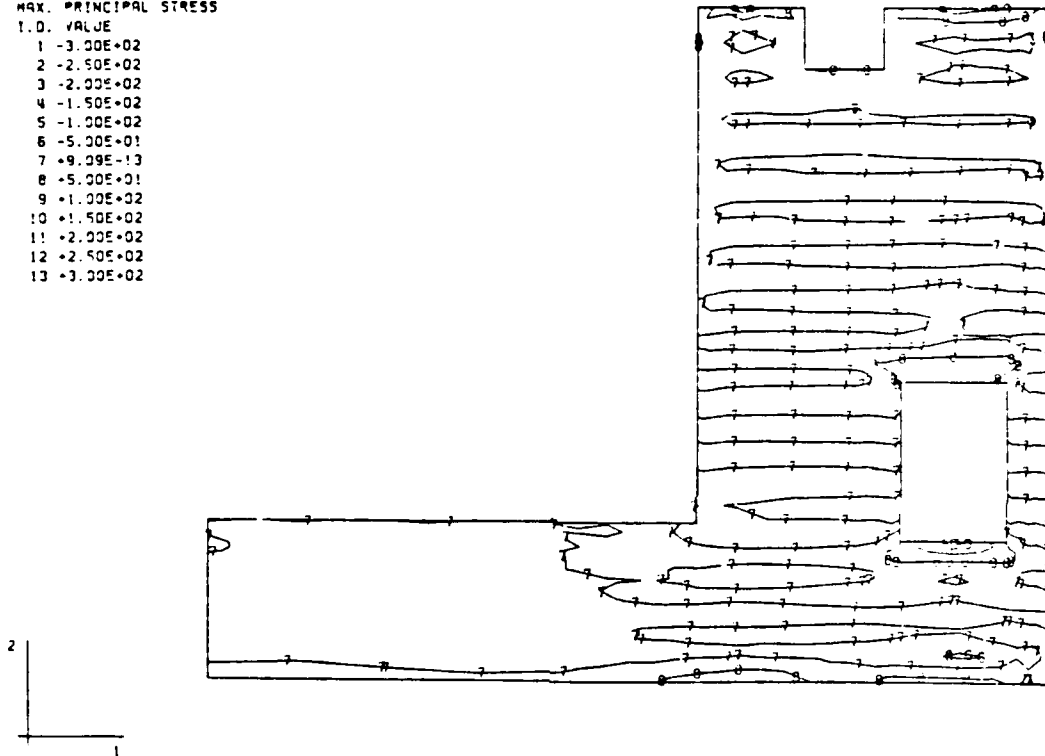
MAX. PRINCIPAL STRESS
 I.D. VALUE
 1 -1.00E+02
 2 -5.00E+01
 3 -2.27E+13
 4 +5.00E+01
 5 +1.00E+02
 6 +1.50E+02
 7 +2.00E+02
 8 +2.50E+02
 9 +3.00E+02



LIFT7 - M17 - 2D MODEL, NEW UMAT, W/CRFEP, NOSHRINK
 STEP 28 INCREMENT 1 ABAQUS VERSION 4-5-147

Figure 52b. Maximum principal stress contours 5 days after placement of lift 7, gravity and temperature loading with creep, using ABAQUS (UMAT2).

MAX. PRINCIPAL STRESS
 I.D. VALUE
 1 -3.00E+02
 2 -2.50E+02
 3 -2.00E+02
 4 -1.50E+02
 5 -1.00E+02
 6 -5.00E+01
 7 +9.09E-13
 8 +5.00E+01
 9 +1.00E+02
 10 +1.50E+02
 11 +2.00E+02
 12 +2.50E+02
 13 +3.00E+02



LIFT16 - M17 - 2D MODEL, NEW UMAT, W/CREEP, NOSHINK
 STEP 64 INCREMENT 1 ABAQUS VERSION 4.5-147

Figure 52c. Maximum principal stress contours 5 days after placement of lift 16, gravity and temperature loading with creep, using ABAQUS (UMAT2).

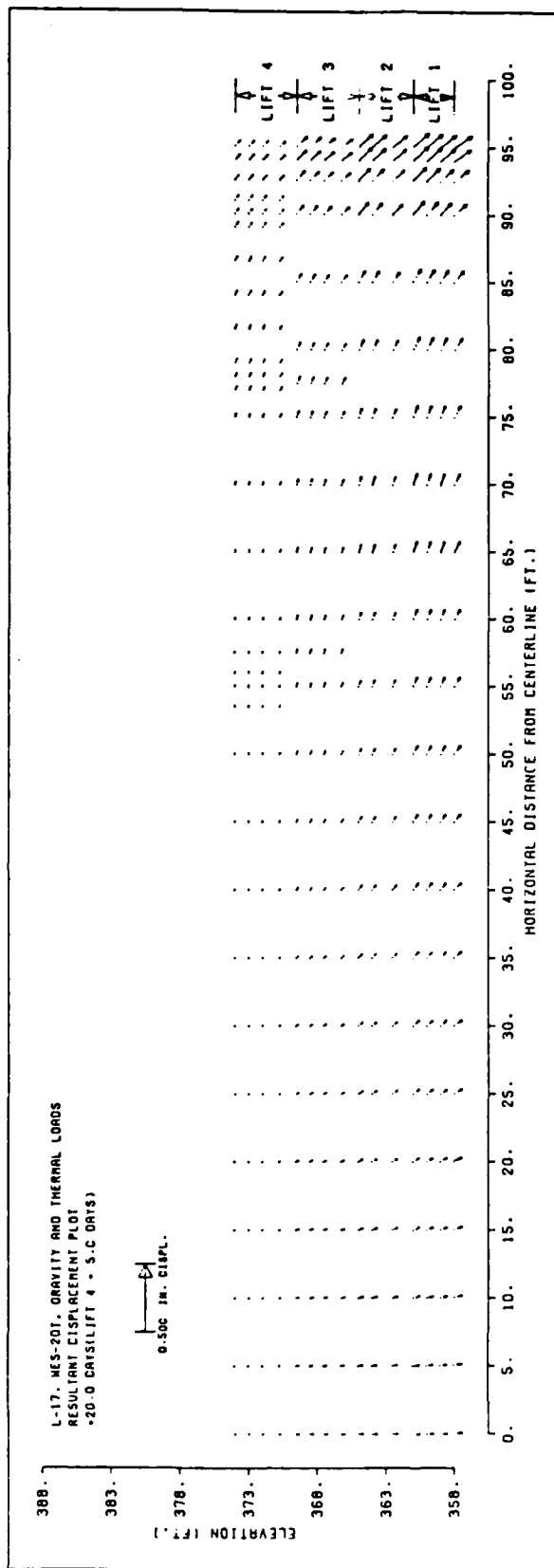


Figure 53a. Resultant displacement vector plot of structure 5 days after placement of lift 4, gravity and temperature loading including creep, using WES2DT.

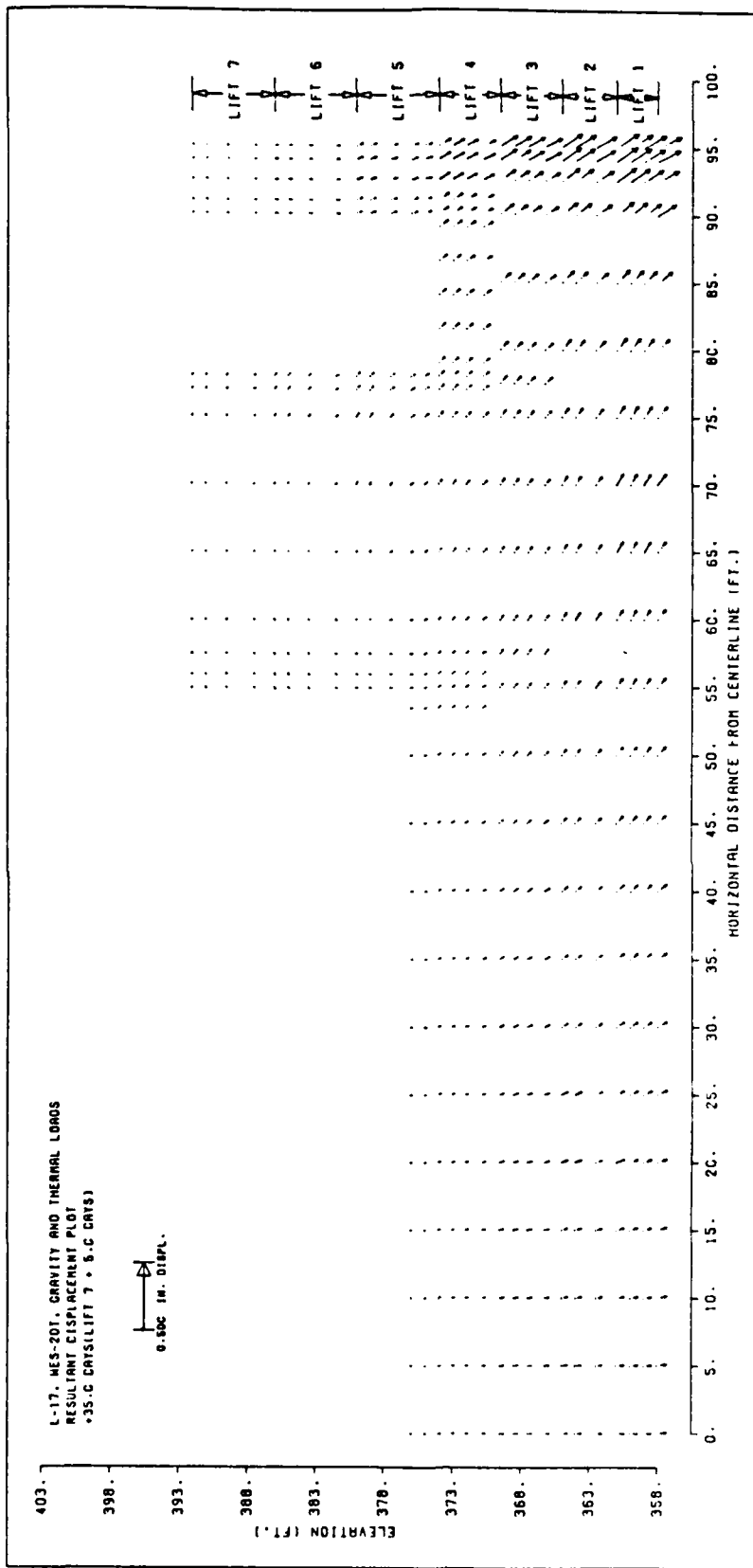


Figure 53b. Resultant displacement vector plot of structure 5 days after placement of lift 7, gravity and temperature loading including creep, using WES2DT.

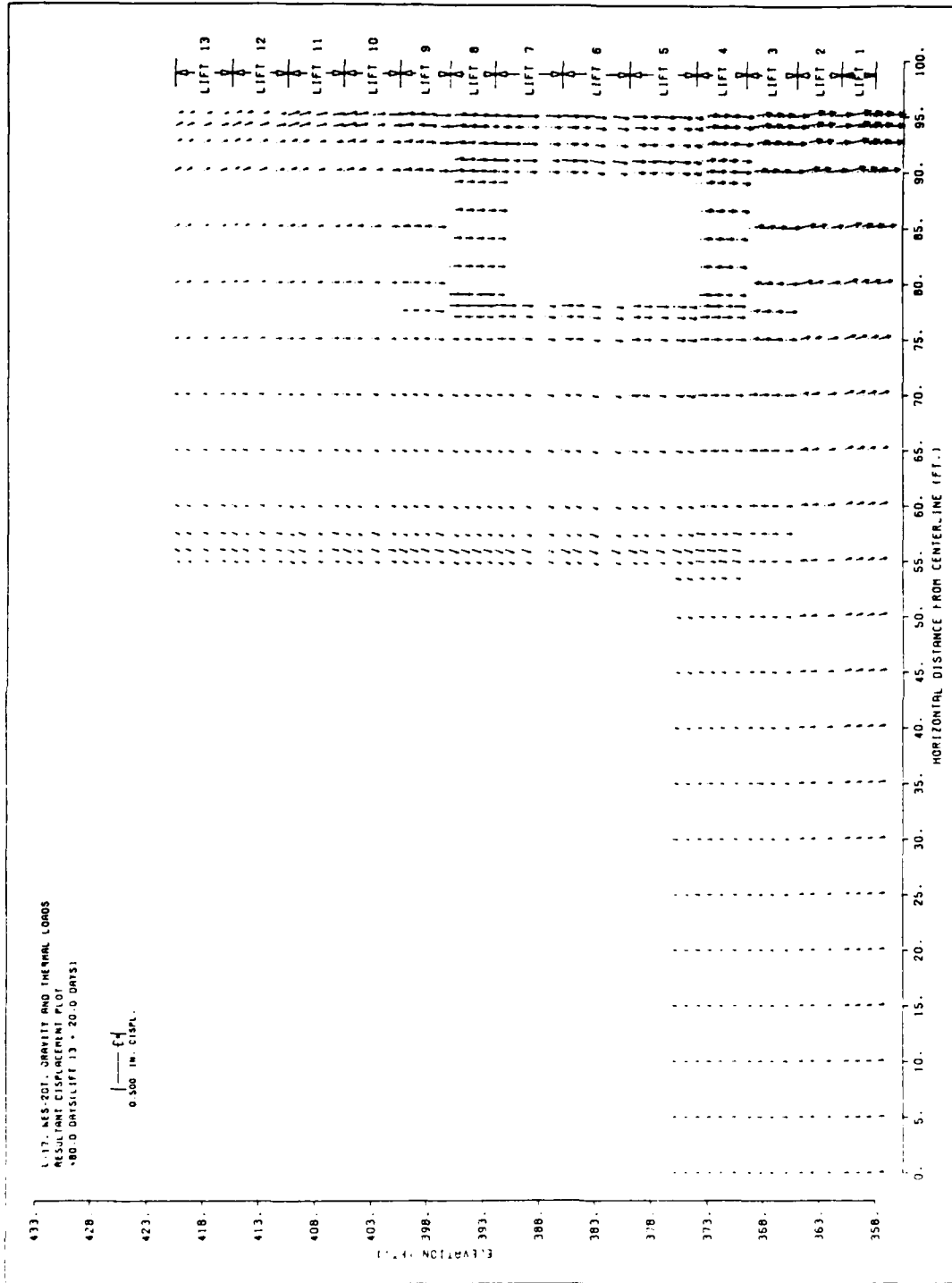


Figure 53c. Resultant displacement vector plot of structure 20 days after placement of lift 13, gravity and temperature loading including creep, using WES2DT. (This corresponds to 5 days after lift 16 is placed).

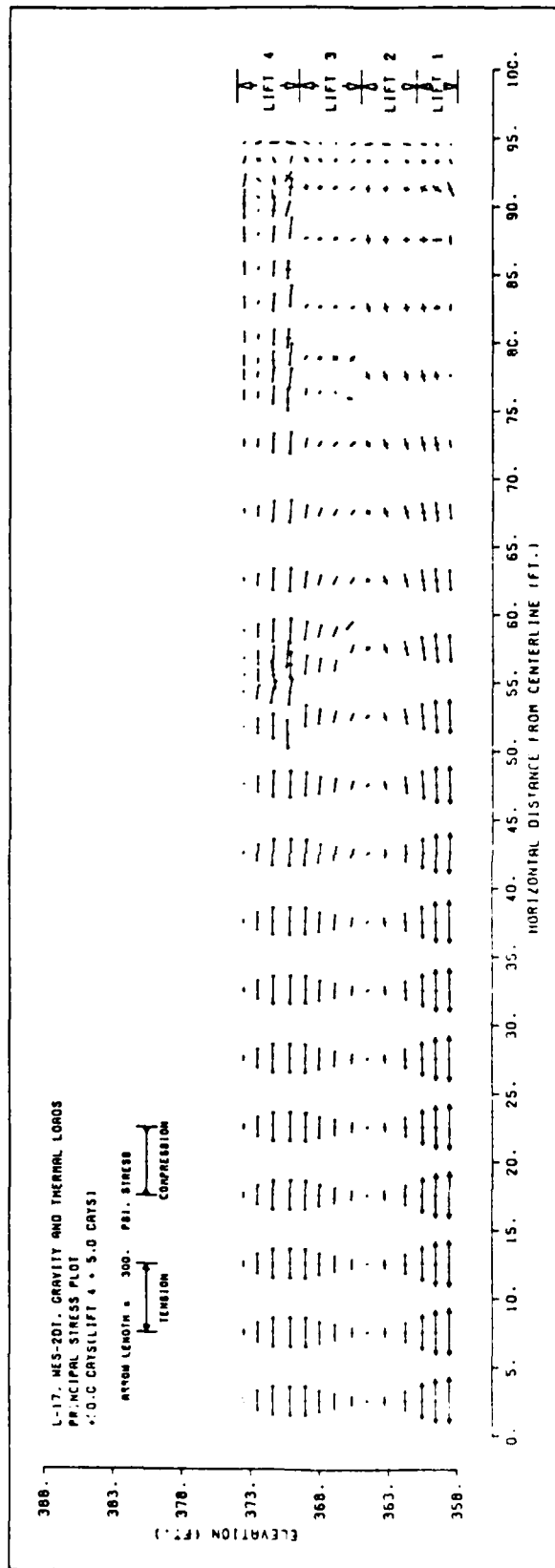


Figure 54a. Principal stress contours of structure 5 days after lift 4 is placed, gravity and temperature loading including creep, using WES2DT.

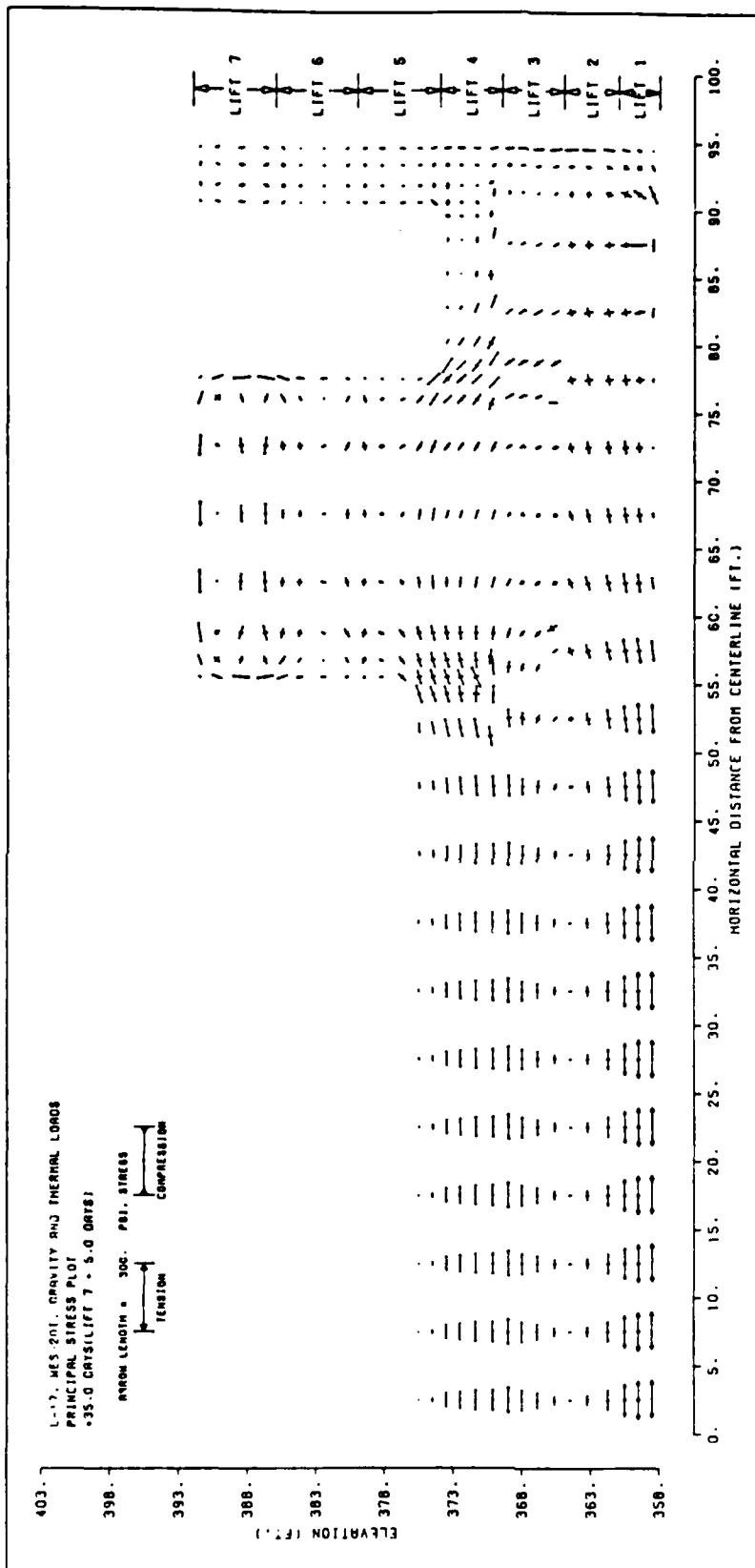


Figure 54b. Principal stress contours of structure 5 days after lift 7 is placed, gravity and temperature loading including creep, using WES2DT.

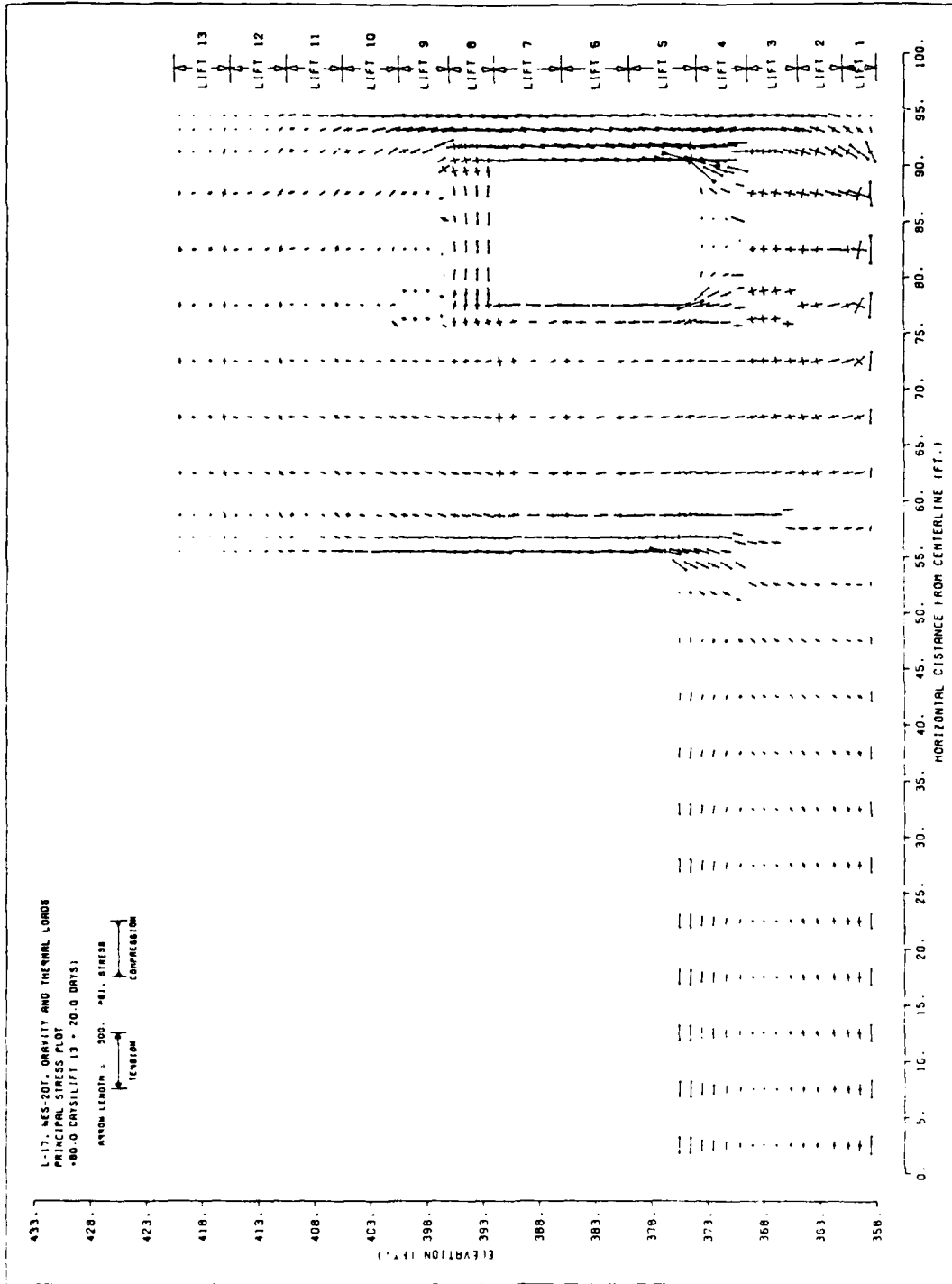
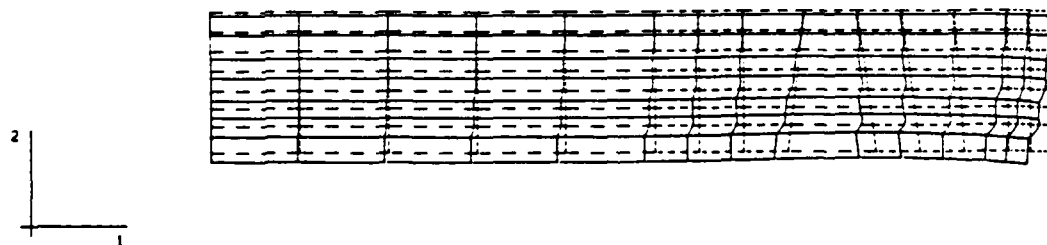


Figure 54c. Principal stress contours of structure 20 days after lift 13 is placed, gravity and temperature loading including creep, using WES2DT.

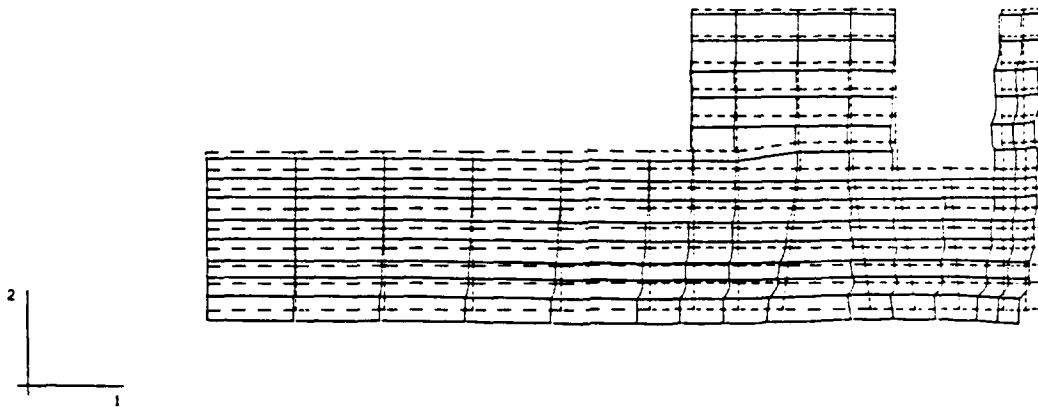
DISPL.
MAG. FACTOR = +2.5E+02
SOLID LINES - DISPLACED MESH
DASHED LINES - ORIGINAL MESH



LIFT4 - M17 - 2D MODEL, NEW UMAT, W/ CREEP, W/ SHRINK
STEP 16 INCREMENT 1 ABAQUS VERSION 4-5-147

Figure 55a. Displaced structure 5 days after placement of lift 4, gravity and temperature loading with creep and shrinkage, using ABAQUS (UMAT2).

DISPL.
MAG. FACTOR = +2.5E+02
SOLID LINES - DISPLACED MESH
DASHED LINES - ORIGINAL MESH



LIFT7 - M17 - 2D MODEL, NEW UMAT, W/ CREEP, W/ SHRINK
STEP 28 INCREMENT 1 ABAQUS VERSION 4.5-147

Figure 55b. Displaced structure 5 days after placement of lift 7, gravity and temperature loading with creep and shrinkage, using ABAQUS (UMAT2).

DISPL.
MAG. FACTOR = +2.5E+02
SOLID LINES - DISPLACED MESH
DASHED LINES - ORIGINAL MESH

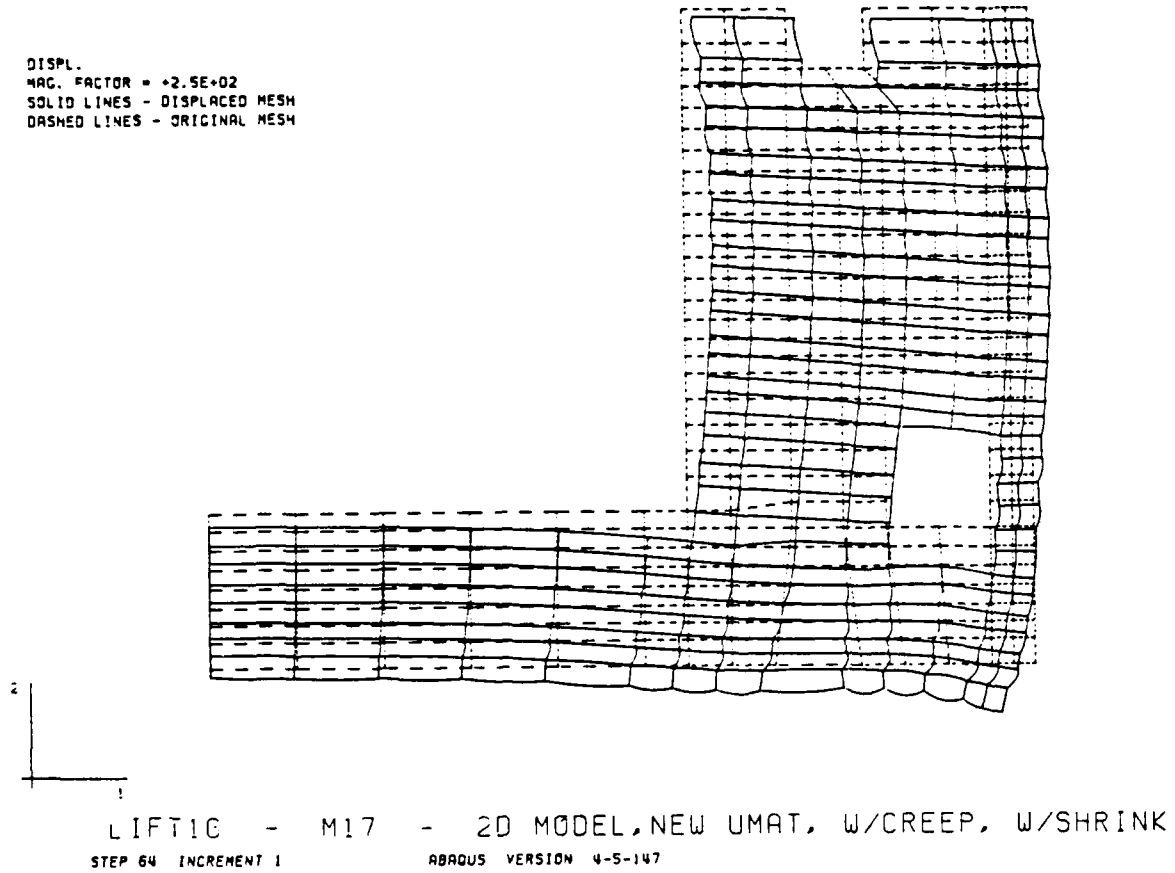
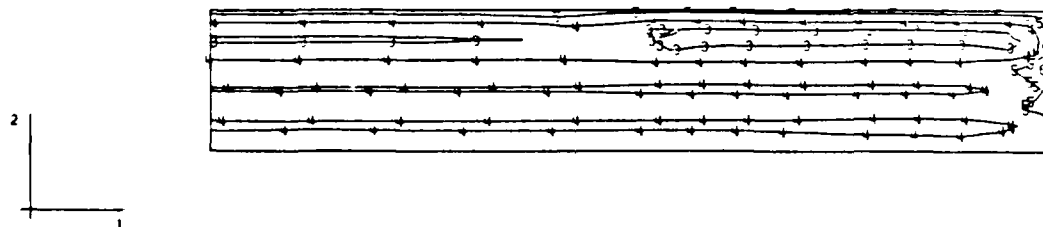


Figure 55c. Displaced structure 5 days after placement of lift 16, gravity and temperature loading with creep and shrinkage, using ABAQUS (UMAT2).

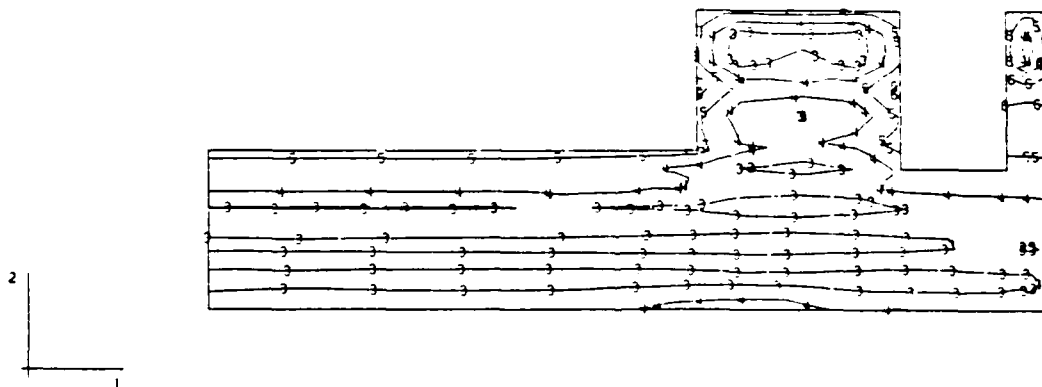
MAX. PRINCIPAL STRESS
 I.D. VALUE
 1 -1.00E+02
 2 -5.00E+01
 3 -2.27E-13
 4 +5.00E+01
 5 +1.00E+02
 6 +1.50E+02
 7 +2.00E+02
 8 +2.50E+02
 9 +3.00E+02



LIFT4 - M17 - 2D MODEL, NEW UMAT, W/CREEP, W/SHRINK
 STEP 16 INCREMENT 1 ABAQUS VERSION 4-5-147

Figure 56a. Maximum principal stress contours 5 days after placement of lift 4, gravity and temperature loading with creep and shrinkage, using ABAQUS (UMAT2).

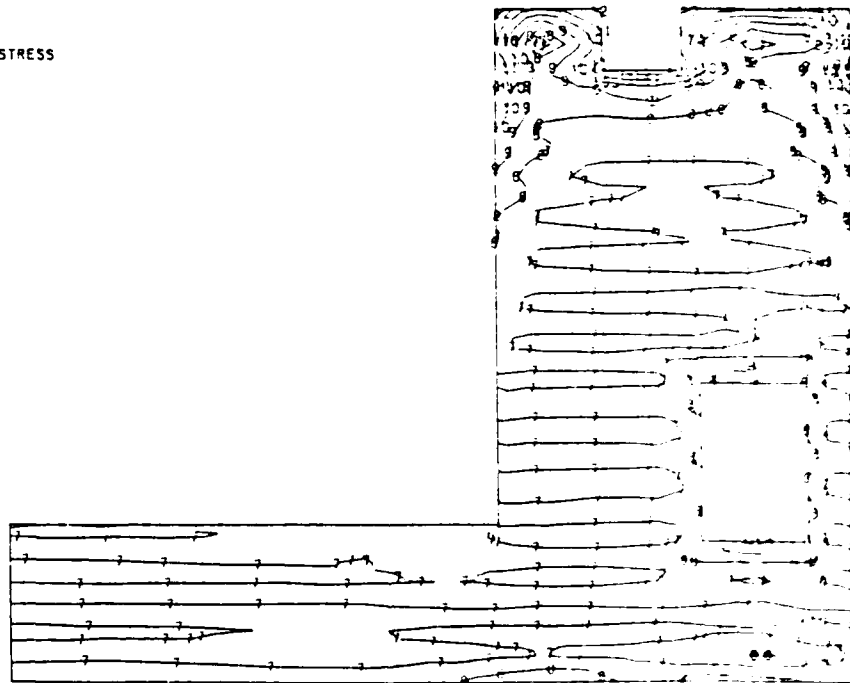
MAX. PRINCIPAL STRESS
 I.D. VALUE
 1 -1.00E+02
 2 -5.00E+01
 3 -2.27E+13
 4 +5.00E+01
 5 +1.00E+02
 6 +1.50E+02
 7 +2.00E+02
 8 +2.50E+02
 9 +3.00E+02



LIFT7 - M17 - 2D MODEL, NEW UMAT, W/ CREEP, W/ SHRINK
 STEP 20 INCREMENT 1 ABAQUS VERSION 4-5-147

Figure 56b. Maximum principal stress contours 5 days after placement of lift 7, gravity and temperature loading with creep and shrinkage, using ABAQUS (UMAT2).

MAX. PRINCIPAL STRESS
 I.D. VALUE
 1 -3.00E+02
 2 -2.50E+02
 3 -2.00E+02
 4 -1.50E+02
 5 -1.00E+02
 6 -5.00E+01
 7 +9.09E-13
 8 +5.00E+01
 9 +1.00E+02
 10 +1.50E+02
 11 +2.00E+02
 12 +2.50E+02
 13 +3.00E+02



LIFT16 - M17 - 2D MODEL, NEW UMAT, 2-DIMENSIONAL
 STEP 64 INCREMENT 1 ABAQUS VERSION 4.5-147

Figure 56c. Maximum principal stress contours 5 days after placement of lift 16, gravity and temperature loading with creep and shrinkage using ABAQUS (UMAT2).

PART XI: CONCLUSIONS AND RECOMMENDATIONS

125. Throughout the course of this study, the ABAQUS computer program seemed to adequately capture the behavior of the lock monoliths during construction. Options existed in the program to adequately model the phenomena that occurs during the incremental construction process. While at the present time there is a need to refine the aging creep model used during this study, it does appear that an adequate two-dimensional incremental construction thermal stress analysis can be accomplished using this computer program.

126. Accuracy and precision of results in finite element thermal stress analysis of mass concrete structures are strongly dependent on the accuracy and precision of material properties test results such as moduli, specific creep, shrinkage, etc., which are used as input to the numerical model in the computer program. For the aging creep numerical model used in ABAQUS in this study, it is clear that the early-age E versus time values are higher than those values for the Lock and Dam 26(R) concrete being modeled. This led to calculation of excessive thermal stresses and creep relaxation at early time. A better representation for the modulus should be developed and verified for concrete similar to that used in Lock and Dam 26(R).

127. Distribution of pile loads beneath the lock sections is significantly affected by the assumptions made in the analysis (i.e., gravity turn on incremental construction with temperature, age, creep, shrinkage, etc.). It was found that the distribution of pile loads beneath the lock sections at early age is significantly affected by the assumptions made in the analysis. With all the assumptions made in the analysis, the distribution of pile loads beneath the lock sections is significantly affected by the assumptions made in the analysis. The distribution of pile loads beneath the lock sections is significantly affected by the assumptions made in the analysis.

necessary to perform an incremental construction analysis, preferably with an aging creep model, in some instances, if practical.

128. Incremental construction models better simulate actual field construction conditions than simple gravity turn-on analyses in producing realistic construction-related stresses. It was found that the interaction of the many mechanisms at work during construction can produce results that are not obtainable by simple analysis methods. More research is required in this area to delineate the extent to which incremental construction analyses should be required in structural design. It has become evident that the effects of the construction process should be considered in the design process, because cracking in mass concrete structures during the construction phase may alter design considerations.

129. As pointed out in paragraph 95, the costs of performing the three-dimensional incremental construction temperature and thermal stress analyses was prohibitive. The ABAQUS three-dimensional computer runs were made using a commercial computer service. It became apparent that using commercial computer services to perform three-dimensional analyses was not economically feasible at the present time. Alternative computer resources at government-owned installations, in which the ABAQUS computer program was installed and running, were located and also found to be too costly to use.

The ABAQUS is now available on several "super-mini" computers at the Army Corps of Engineers, Vicksburg District, Vicksburg, Mississippi.

The Corps of Engineers is currently conducting a study to determine the feasibility of using the ABAQUS computer program for the analysis of concrete structures during construction.

The study will be completed by the end of the fiscal year 1980.

three-dimensional analyses of incremental construction problems. This formulation was developed in a modern, general purpose heat transfer and structural analysis code. Every effort was made to ensure that the analysis concept was effective, rational, and consistent. With this requirement in mind it soon became apparent that effective modeling of key parameters affecting final stresses in incrementally constructed mass concrete structures were pushed far beyond the current state of the art. These key parameters include: early age (1 day, 2 day, ...) properties such as shrinkage, creep, material aging, and cracking strength. Also, the concept of the incremental formulation itself presents some unusual, subtle problems.

132. Currently, research programs are underway to better define and verify these parameters through carefully planned theoretical, computational, and experimental research programs. The intent of this research is to provide effective and efficient design and analysis guidance to the field engineers in the area of mass concrete construction. The approach taken here is a cooperative research effort among research and design staffs at District and Division Offices, major universities, private engineering firms, and Corp's laboratories.

REFERENCES

1. Fong, H. H., "A Comparison of Eight General Purpose Finite Element Computer Programs," Structural Mechanics Software Series - V. (e. W. D. Pilke), University Press of Virginia, Charlottesville, Virginia, 1983.
2. Wilson, E. L., "The Determination of Temperatures Within Mass Concrete Structures," Report No. 68-17, Dec 1968, Structural Engineering Laboratory, University of California, Berkeley, California.
3. Sandhu, R. S., Wilson, E. L., and Raphael J. M., "Two Dimensional Stress Analysis with Incremental Construction and Creep," Report No. 67-34, Dec 1967, Structural Engineering Laboratory, University of California, Berkeley, California.
4. McCoy, E. E., "Laboratory Tests of Concrete and Reinforcing Steel, Port Allen Lock," Miscellaneous Paper No. 6-297, Dec 1958, U. S. Army Engineer Waterways Experiment Station, CE, Vicksburg, Mississippi.
5. McHenry, Douglas, "A New Aspect of Creep in Concrete and Its Application to Design," Proceedings, American Society for Testing and Materials, Vol 43, 1943, pp 1069-1087.
6. King, I. P., "Finite Element Analysis of Two-Dimensional Time-Dependent Stress Problems," Report No. 65-1, Jan 1965, Structural Engineering Laboratory, University of California, Berkeley, California.
7. Norman, C. D., Campbell, R. L., Garner, S. B. "Rehabilitation of Navigation Lock Walls, Report 2, Analysis of Concrete Cracking in Lockwall Resurfacing," Technical Report REMR-CS-7, In publication, U. S. Army Engineer Waterways Experiment Station, CE, Vicksburg, Mississippi.

APPENDIX A: ABAQUS TWO-DIMENSIONAL NODE FILE
USED FOR MONOLITH L-17

NODE NO.	X	Y	Z	NODE NO.	X	Y	Z	NODE NO.	X	Y	Z
51	360.000	4236.000	0.000	101	660.000	4296.000	0.000	151	895.500	4332.000	0.000
52	420.000	4236.000	0.000	102	690.000	4296.000	0.000	152	925.500	4332.000	0.000
53	480.000	4236.000	0.000	103	720.000	4296.000	0.000	153	955.500	4332.000	0.000
54	540.000	4236.000	0.000	104	750.000	4296.000	0.000	154	986.625	4332.000	0.000
55	600.000	4236.000	0.000	105	780.000	4296.000	0.000	155	1017.750	4332.000	0.000
56	660.000	4236.000	0.000	106	840.000	4296.000	0.000	156	1048.875	4332.000	0.000
57	720.000	4236.000	0.000	107	900.000	4296.000	0.000	157	1080.000	4332.000	0.000
58	780.000	4236.000	0.000	108	930.000	4296.000	0.000	158	1095.000	4332.000	0.000
59	840.000	4236.000	0.000	109	960.000	4296.000	0.000	159	1110.000	4332.000	0.000
60	900.000	4236.000	0.000	110	990.000	4296.000	0.000	160	1125.000	4332.000	0.000
61	960.000	4236.000	0.000	111	1020.000	4296.000	0.000	161	1140.000	4332.000	0.000
62	1020.000	4236.000	0.000	112	1050.000	4296.000	0.000	162	0.000	4344.000	0.000
63	1080.000	4236.000	0.000	113	1080.000	4296.000	0.000	163	120.000	4344.000	0.000
64	1140.000	4236.000	0.000	114	1095.000	4296.000	0.000	164	240.000	4344.000	0.000
65	1200.000	4236.000	0.000	115	1110.000	4296.000	0.000	165	360.000	4344.000	0.000
66	1260.000	4236.000	0.000	116	1125.000	4296.000	0.000	166	480.000	4344.000	0.000
67	1320.000	4236.000	0.000	117	1140.000	4296.000	0.000	167	600.000	4344.000	0.000
68	1380.000	4236.000	0.000	118	0.000	4314.000	0.000	168	660.000	4344.000	0.000
69	1440.000	4236.000	0.000	119	120.000	4314.000	0.000	169	720.000	4344.000	0.000
70	1500.000	4236.000	0.000	120	240.000	4314.000	0.000	170	786.000	4344.000	0.000
71	1560.000	4236.000	0.000	121	360.000	4314.000	0.000	171	894.000	4344.000	0.000
72	1620.000	4236.000	0.000	122	480.000	4314.000	0.000	172	954.000	4344.000	0.000
73	1680.000	4236.000	0.000	123	600.000	4314.000	0.000	173	1017.000	4344.000	0.000
74	1740.000	4236.000	0.000	124	660.000	4314.000	0.000	174	1080.000	4344.000	0.000
75	1800.000	4236.000	0.000	125	720.000	4314.000	0.000	175	1110.000	4344.000	0.000
76	1860.000	4236.000	0.000	126	782.250	4314.000	0.000	176	1140.000	4344.000	0.000
77	1920.000	4236.000	0.000	127	897.750	4314.000	0.000	177	0.000	4356.000	0.000
78	1980.000	4236.000	0.000	128	977.750	4314.000	0.000	178	60.000	4356.000	0.000
79	2040.000	4236.000	0.000	129	1018.875	4314.000	0.000	179	120.000	4356.000	0.000
80	2100.000	4236.000	0.000	130	1080.000	4314.000	0.000	180	180.000	4356.000	0.000
81	2160.000	4236.000	0.000	131	1110.000	4314.000	0.000	181	240.000	4356.000	0.000
82	2220.000	4236.000	0.000	132	1140.000	4314.000	0.000	182	300.000	4356.000	0.000
83	2280.000	4236.000	0.000	133	0.000	4312.000	0.000	183	360.000	4356.000	0.000
84	2340.000	4236.000	0.000	134	60.000	4312.000	0.000	184	420.000	4356.000	0.000
85	2400.000	4236.000	0.000	135	120.000	4312.000	0.000	185	480.000	4356.000	0.000
86	2460.000	4236.000	0.000	136	180.000	4312.000	0.000	186	540.000	4356.000	0.000
87	2520.000	4236.000	0.000	137	240.000	4312.000	0.000	187	600.000	4356.000	0.000
88	2580.000	4236.000	0.000	138	300.000	4312.000	0.000	188	630.000	4356.000	0.000
89	2640.000	4236.000	0.000	139	360.000	4312.000	0.000	189	660.000	4356.000	0.000
90	2700.000	4236.000	0.000	140	420.000	4312.000	0.000	190	690.000	4356.000	0.000
91	2760.000	4236.000	0.000	141	480.000	4312.000	0.000	191	720.000	4356.000	0.000
92	2820.000	4236.000	0.000	142	540.000	4312.000	0.000	192	753.750	4356.000	0.000
93	2880.000	4236.000	0.000	143	600.000	4312.000	0.000	193	787.500	4356.000	0.000
94	2940.000	4236.000	0.000	144	660.000	4312.000	0.000	194	840.000	4356.000	0.000
95	3000.000	4236.000	0.000	145	690.000	4312.000	0.000	195	892.500	4356.000	0.000
96	3060.000	4236.000	0.000	146	690.000	4312.000	0.000	196	922.500	4356.000	0.000
97	3120.000	4236.000	0.000	147	720.000	4312.000	0.000	197	952.500	4356.000	0.000
98	3180.000	4236.000	0.000	148	752.750	4312.000	0.000	198	984.375	4356.000	0.000
99	3240.000	4236.000	0.000	149	784.500	4312.000	0.000	199	1016.250	4356.000	0.000
100	3300.000	4236.000	0.000	150	840.000	4312.000	0.000	200	1048.125	4356.000	0.000

STRESS ANALYSIS REPORT

MODE NO.	X	Y	Z	MODE NO.	X	Y	Z	MODE NO.	X	Y	Z
351	1110.000	4461.000	0.000	351	720.000	4420.500	0.000	301	720.000	4420.500	0.000
352	1140.000	4447.500	0.000	302	795.563	4420.500	0.000	302	795.563	4420.500	0.000
353	0.000	4461.000	0.000	303	854.438	4420.500	0.000	303	854.438	4420.500	0.000
354	60.000	4461.000	0.000	304	944.438	4420.500	0.000	304	944.438	4420.500	0.000
355	120.000	4461.000	0.000	305	1012.219	4420.500	0.000	305	1012.219	4420.500	0.000
356	180.000	4461.000	0.000	306	1580.000	4420.500	0.000	306	1580.000	4420.500	0.000
357	240.000	4461.000	0.000	307	1110.000	4420.500	0.000	307	1110.000	4420.500	0.000
358	300.000	4461.000	0.000	308	1140.000	4420.500	0.000	308	1140.000	4420.500	0.000
359	360.000	4461.000	0.000	309	0.000	4434.000	0.000	309	0.000	4434.000	0.000
360	420.000	4461.000	0.000	310	60.000	4434.000	0.000	310	60.000	4434.000	0.000
361	480.000	4461.000	0.000	311	120.000	4434.000	0.000	311	120.000	4434.000	0.000
362	540.000	4461.000	0.000	312	180.000	4434.000	0.000	312	180.000	4434.000	0.000
363	600.000	4461.000	0.000	313	240.000	4434.000	0.000	313	240.000	4434.000	0.000
364	630.000	4461.000	0.000	314	300.000	4434.000	0.000	314	300.000	4434.000	0.000
365	660.000	4461.000	0.000	315	360.000	4434.000	0.000	315	360.000	4434.000	0.000
366	690.000	4461.000	0.000	316	420.000	4434.000	0.000	316	420.000	4434.000	0.000
367	720.000	4461.000	0.000	317	480.000	4434.000	0.000	317	480.000	4434.000	0.000
368	760.313	4461.000	0.000	318	540.000	4434.000	0.000	318	540.000	4434.000	0.000
369	800.625	4461.000	0.000	319	600.000	4434.000	0.000	319	600.000	4434.000	0.000
370	840.000	4461.000	0.000	320	630.000	4434.000	0.000	320	630.000	4434.000	0.000
371	879.375	4461.000	0.000	321	660.000	4434.000	0.000	321	660.000	4434.000	0.000
372	909.375	4461.000	0.000	322	690.000	4434.000	0.000	322	690.000	4434.000	0.000
373	939.375	4461.000	0.000	323	720.000	4434.000	0.000	323	720.000	4434.000	0.000
374	974.532	4461.000	0.000	324	758.625	4434.000	0.000	324	758.625	4434.000	0.000
375	1009.688	4461.000	0.000	325	797.250	4434.000	0.000	325	797.250	4434.000	0.000
376	1044.844	4461.000	0.000	326	840.000	4434.000	0.000	326	840.000	4434.000	0.000
377	1080.000	4461.000	0.000	327	882.750	4434.000	0.000	327	882.750	4434.000	0.000
378	1095.000	4461.000	0.000	328	912.750	4434.000	0.000	328	912.750	4434.000	0.000
379	1110.000	4461.000	0.000	329	942.750	4434.000	0.000	329	942.750	4434.000	0.000
380	1125.000	4461.000	0.000	330	977.063	4434.000	0.000	330	977.063	4434.000	0.000
381	1140.000	4461.000	0.000	331	1011.375	4434.000	0.000	331	1011.375	4434.000	0.000
382	0.000	4474.500	0.000	332	1045.688	4434.000	0.000	332	1045.688	4434.000	0.000
383	120.000	4474.500	0.000	333	1080.000	4434.000	0.000	333	1080.000	4434.000	0.000
384	240.000	4474.500	0.000	334	1095.000	4434.000	0.000	334	1095.000	4434.000	0.000
385	360.000	4474.500	0.000	335	1110.000	4434.000	0.000	335	1110.000	4434.000	0.000
386	480.000	4474.500	0.000	336	1125.000	4434.000	0.000	336	1125.000	4434.000	0.000
387	600.000	4474.500	0.000	337	1140.000	4434.000	0.000	337	1140.000	4434.000	0.000
388	660.000	4474.500	0.000	338	0.000	4447.500	0.000	338	0.000	4447.500	0.000
389	720.000	4474.500	0.000	339	120.000	4447.500	0.000	339	120.000	4447.500	0.000
390	802.313	4474.500	0.000	340	240.000	4447.500	0.000	340	240.000	4447.500	0.000
391	877.688	4474.500	0.000	341	360.000	4447.500	0.000	341	360.000	4447.500	0.000
392	937.688	4474.500	0.000	342	480.000	4447.500	0.000	342	480.000	4447.500	0.000
393	1008.844	4474.500	0.000	343	600.000	4447.500	0.000	343	600.000	4447.500	0.000
394	1080.000	4474.500	0.000	344	660.000	4447.500	0.000	344	660.000	4447.500	0.000
395	1110.000	4474.500	0.000	345	720.000	4447.500	0.000	345	720.000	4447.500	0.000
396	1140.000	4474.500	0.000	346	798.938	4447.500	0.000	346	798.938	4447.500	0.000
397	0.000	4488.000	0.000	347	881.063	4447.500	0.000	347	881.063	4447.500	0.000
398	60.000	4488.000	0.000	348	941.063	4447.500	0.000	348	941.063	4447.500	0.000
399	120.000	4488.000	0.000	349	1010.532	4447.500	0.000	349	1010.532	4447.500	0.000
400	180.000	4488.000	0.000	350	1080.000	4447.500	0.000	350	1080.000	4447.500	0.000

Node No.	X	Y	Z	Node No.	X	Y	Z	Node No.	X	Y	Z	Node No.	X	Y	Z
631	720.000	4716.000	0.000	651	1140.000	4752.000	0.000	701	1110.000	4806.000	0.000	751	1080.000	4866.000	0.000
632	804.000	4716.000	0.000	652	660.000	4765.500	0.000	702	1125.000	4806.000	0.000	752	1095.000	4866.000	0.000
633	876.000	4716.000	0.000	653	720.000	4765.500	0.000	703	1140.000	4806.000	0.000	753	1110.000	4866.000	0.000
634	936.000	4716.000	0.000	654	804.000	4765.500	0.000	704	660.000	4821.000	0.000	754	1125.000	4866.000	0.000
635	1008.000	4716.000	0.000	655	876.000	4765.500	0.000	705	720.000	4821.000	0.000	755	1140.000	4866.000	0.000
636	1080.000	4716.000	0.000	656	936.000	4765.500	0.000	706	804.000	4821.000	0.000	756	660.000	4881.000	0.000
637	1152.000	4716.000	0.000	657	1008.000	4765.500	0.000	707	876.000	4821.000	0.000	757	720.000	4881.000	0.000
638	1224.000	4716.000	0.000	658	1080.000	4765.500	0.000	708	936.000	4821.000	0.000	758	804.000	4881.000	0.000
639	1308.000	4716.000	0.000	659	1140.000	4765.500	0.000	709	1008.000	4821.000	0.000	759	876.000	4881.000	0.000
640	1380.000	4716.000	0.000	660	1140.000	4765.500	0.000	710	1080.000	4821.000	0.000	760	936.000	4881.000	0.000
641	1464.000	4716.000	0.000	661	660.000	4779.000	0.000	711	1110.000	4821.000	0.000	761	1008.000	4881.000	0.000
642	1548.000	4716.000	0.000	662	690.000	4779.000	0.000	712	1140.000	4821.000	0.000	762	1080.000	4881.000	0.000
643	1632.000	4716.000	0.000	663	720.000	4779.000	0.000	713	660.000	4836.000	0.000	763	1110.000	4881.000	0.000
644	1716.000	4716.000	0.000	664	762.000	4779.000	0.000	714	690.000	4836.000	0.000	764	1140.000	4881.000	0.000
645	1800.000	4716.000	0.000	665	804.000	4779.000	0.000	715	720.000	4836.000	0.000	765	660.000	4896.000	0.000
646	1884.000	4716.000	0.000	666	840.000	4779.000	0.000	716	762.000	4836.000	0.000	766	690.000	4896.000	0.000
647	1968.000	4716.000	0.000	667	876.000	4779.000	0.000	717	804.000	4836.000	0.000	767	720.000	4896.000	0.000
648	2052.000	4716.000	0.000	668	906.000	4779.000	0.000	718	840.000	4836.000	0.000	768	762.000	4896.000	0.000
649	2136.000	4716.000	0.000	669	936.000	4779.000	0.000	719	876.000	4836.000	0.000	769	804.000	4896.000	0.000
650	2220.000	4716.000	0.000	670	972.000	4779.000	0.000	720	906.000	4836.000	0.000	770	840.000	4896.000	0.000
651	2304.000	4716.000	0.000	671	1008.000	4779.000	0.000	721	936.000	4836.000	0.000	771	876.000	4896.000	0.000
652	2388.000	4716.000	0.000	672	1044.000	4779.000	0.000	722	972.000	4836.000	0.000	772	906.000	4896.000	0.000
653	2472.000	4716.000	0.000	673	1080.000	4779.000	0.000	723	1008.000	4836.000	0.000	773	936.000	4896.000	0.000
654	2556.000	4716.000	0.000	674	1095.000	4779.000	0.000	724	1044.000	4836.000	0.000	774	972.000	4896.000	0.000
655	2640.000	4716.000	0.000	675	1110.000	4779.000	0.000	725	1080.000	4836.000	0.000	775	1008.000	4896.000	0.000
656	2724.000	4716.000	0.000	676	1125.000	4779.000	0.000	726	1095.000	4836.000	0.000	776	1044.000	4896.000	0.000
657	2808.000	4716.000	0.000	677	1140.000	4779.000	0.000	727	1110.000	4836.000	0.000	777	1080.000	4896.000	0.000
658	2892.000	4716.000	0.000	678	660.000	4792.500	0.000	728	1125.000	4836.000	0.000	778	1095.000	4896.000	0.000
659	2976.000	4716.000	0.000	679	720.000	4792.500	0.000	729	1140.000	4836.000	0.000	779	1110.000	4896.000	0.000
660	3060.000	4716.000	0.000	680	804.000	4792.500	0.000	730	660.000	4851.000	0.000	780	1125.000	4896.000	0.000
661	3144.000	4716.000	0.000	681	876.000	4792.500	0.000	731	720.000	4851.000	0.000	781	1140.000	4896.000	0.000
662	3228.000	4716.000	0.000	682	936.000	4792.500	0.000	732	804.000	4851.000	0.000	782	660.000	4911.000	0.000
663	3312.000	4716.000	0.000	683	1008.000	4792.500	0.000	733	876.000	4851.000	0.000	783	720.000	4911.000	0.000
664	3396.000	4716.000	0.000	684	1080.000	4792.500	0.000	734	936.000	4851.000	0.000	784	804.000	4911.000	0.000
665	3480.000	4716.000	0.000	685	1110.000	4792.500	0.000	735	1008.000	4851.000	0.000	785	876.000	4911.000	0.000
666	3564.000	4716.000	0.000	686	1140.000	4806.000	0.000	736	1080.000	4851.000	0.000	786	936.000	4911.000	0.000
667	3648.000	4716.000	0.000	687	660.000	4806.000	0.000	737	1110.000	4851.000	0.000	787	1008.000	4911.000	0.000
668	3732.000	4716.000	0.000	688	690.000	4806.000	0.000	738	1140.000	4851.000	0.000	788	1080.000	4911.000	0.000
669	3816.000	4716.000	0.000	689	720.000	4806.000	0.000	739	660.000	4866.000	0.000	789	1110.000	4911.000	0.000
670	3900.000	4716.000	0.000	690	762.000	4806.000	0.000	740	690.000	4866.000	0.000	790	1140.000	4911.000	0.000
671	3984.000	4716.000	0.000	691	804.000	4806.000	0.000	741	720.000	4866.000	0.000	791	660.000	4926.000	0.000
672	4068.000	4716.000	0.000	692	840.000	4806.000	0.000	742	762.000	4866.000	0.000	792	690.000	4926.000	0.000
673	4152.000	4716.000	0.000	693	876.000	4806.000	0.000	743	804.000	4866.000	0.000	793	720.000	4926.000	0.000
674	4236.000	4716.000	0.000	694	906.000	4806.000	0.000	744	840.000	4866.000	0.000	794	762.000	4926.000	0.000
675	4320.000	4716.000	0.000	695	936.000	4806.000	0.000	745	876.000	4866.000	0.000	795	804.000	4926.000	0.000
676	4404.000	4716.000	0.000	696	972.000	4806.000	0.000	746	906.000	4866.000	0.000	796	840.000	4926.000	0.000
677	4488.000	4716.000	0.000	697	1008.000	4806.000	0.000	747	936.000	4866.000	0.000	797	876.000	4926.000	0.000
678	4572.000	4716.000	0.000	698	1044.000	4806.000	0.000	748	972.000	4866.000	0.000	798	906.000	4926.000	0.000
679	4656.000	4716.000	0.000	699	1080.000	4806.000	0.000	749	1008.000	4866.000	0.000	799	936.000	4926.000	0.000
680	4740.000	4716.000	0.000	700	1095.000	4806.000	0.000	750	1044.000	4866.000	0.000	800	972.000	4926.000	0.000

Node No.	X	Y	Z	Node No.	X	Y	Z	Node No.	X	Y	Z	Node No.	X	Y	Z
851	936.000	4986.000	0.000	901	876.000	5046.000	0.000	951	804.000	5106.000	0.000	1000	690.000	5166.000	0.000
852	972.000	4986.000	0.000	902	906.000	5046.000	0.000	952	840.000	5106.000	0.000				
853	1008.000	4986.000	0.000	903	936.000	5046.000	0.000	953	876.000	5106.000	0.000				
854	1044.000	4986.000	0.000	904	972.000	5046.000	0.000	954	906.000	5106.000	0.000				
855	1080.000	4986.000	0.000	905	1008.000	5046.000	0.000	955	936.000	5106.000	0.000				
856	1095.000	4986.000	0.000	906	1044.000	5046.000	0.000	956	972.000	5106.000	0.000				
857	1110.000	4986.000	0.000	907	1080.000	5046.000	0.000	957	1008.000	5106.000	0.000				
858	1125.000	4986.000	0.000	908	1095.000	5046.000	0.000	958	1044.000	5106.000	0.000				
859	1140.000	4986.000	0.000	909	1110.000	5046.000	0.000	959	1080.000	5106.000	0.000				
860	660.000	5001.000	0.000	910	1125.000	5046.000	0.000	960	1095.000	5106.000	0.000				
861	720.000	5001.000	0.000	911	1140.000	5046.000	0.000	961	1110.000	5106.000	0.000				
862	804.000	5001.000	0.000	912	660.000	5061.000	0.000	962	1125.000	5106.000	0.000				
863	876.000	5001.000	0.000	913	720.000	5061.000	0.000	963	1140.000	5106.000	0.000				
864	936.000	5001.000	0.000	914	804.000	5061.000	0.000	964	660.000	5118.000	0.000				
865	1008.000	5001.000	0.000	915	876.000	5061.000	0.000	965	720.000	5118.000	0.000				
866	1080.000	5001.000	0.000	916	936.000	5061.000	0.000	966	804.000	5118.000	0.000				
867	1110.000	5001.000	0.000	917	1008.000	5061.000	0.000	967	867.000	5118.000	0.000				
868	1140.000	5001.000	0.000	918	1080.000	5061.000	0.000	968	924.000	5118.000	0.000				
869	660.000	5016.000	0.000	919	1110.000	5061.000	0.000	969	1008.000	5118.000	0.000				
870	690.000	5016.000	0.000	920	1140.000	5061.000	0.000	970	1080.000	5118.000	0.000				
871	720.000	5016.000	0.000	921	660.000	5076.000	0.000	971	1110.000	5118.000	0.000				
872	762.000	5016.000	0.000	922	690.000	5076.000	0.000	972	1140.000	5118.000	0.000				
873	804.000	5016.000	0.000	923	720.000	5076.000	0.000	973	660.000	5130.000	0.000				
874	840.000	5016.000	0.000	924	762.000	5076.000	0.000	974	690.000	5130.000	0.000				
875	876.000	5016.000	0.000	925	804.000	5076.000	0.000	975	720.000	5130.000	0.000				
876	906.000	5016.000	0.000	926	840.000	5076.000	0.000	976	762.000	5130.000	0.000				
877	936.000	5016.000	0.000	927	876.000	5076.000	0.000	977	804.000	5130.000	0.000				
878	972.000	5016.000	0.000	928	906.000	5076.000	0.000	978	831.000	5130.000	0.000				
879	1044.000	5016.000	0.000	929	936.000	5076.000	0.000	979	858.000	5130.000	0.000				
880	1044.000	5016.000	0.000	930	972.000	5076.000	0.000	980	885.000	5130.000	0.000				
881	1080.000	5016.000	0.000	931	1008.000	5076.000	0.000	981	912.000	5130.000	0.000				
882	1044.000	5016.000	0.000	932	1044.000	5076.000	0.000	982	954.000	5130.000	0.000				
883	1110.000	5016.000	0.000	933	1080.000	5076.000	0.000	983	1008.000	5130.000	0.000				
884	1125.000	5016.000	0.000	934	1095.000	5076.000	0.000	984	1044.000	5130.000	0.000				
885	1140.000	5016.000	0.000	935	1110.000	5076.000	0.000	985	1080.000	5130.000	0.000				
886	660.000	5031.000	0.000	936	1125.000	5076.000	0.000	986	1095.000	5130.000	0.000				
887	720.000	5031.000	0.000	937	1140.000	5076.000	0.000	987	1110.000	5130.000	0.000				
888	804.000	5031.000	0.000	938	660.000	5091.000	0.000	988	1125.000	5130.000	0.000				
889	876.000	5031.000	0.000	939	720.000	5091.000	0.000	989	1140.000	5130.000	0.000				
890	936.000	5031.000	0.000	940	804.000	5091.000	0.000	990	660.000	5148.000	0.000				
891	1008.000	5031.000	0.000	941	876.000	5091.000	0.000	991	720.000	5148.000	0.000				
892	1080.000	5031.000	0.000	942	936.000	5091.000	0.000	992	804.000	5148.000	0.000				
893	1110.000	5031.000	0.000	943	1008.000	5091.000	0.000	993	858.000	5148.000	0.000				
894	1125.000	5031.000	0.000	944	1080.000	5091.000	0.000	994	912.000	5148.000	0.000				
895	660.000	5046.000	0.000	945	1110.000	5091.000	0.000	995	1008.000	5148.000	0.000				
896	690.000	5046.000	0.000	946	1140.000	5091.000	0.000	996	1080.000	5148.000	0.000				
897	720.000	5046.000	0.000	947	660.000	5106.000	0.000	997	1110.000	5148.000	0.000				
898	762.000	5046.000	0.000	948	690.000	5106.000	0.000	998	1140.000	5148.000	0.000				
899	804.000	5046.000	0.000	949	720.000	5106.000	0.000	999	660.000	5166.000	0.000				
900	840.000	5046.000	0.000	950	762.000	5106.000	0.000	1000	690.000	5166.000	0.000				

NUCLE NO	X	Y	Z
1001	720 000	5166 000	0 000
1002	762 000	5166 000	0 000
1003	804 000	5166 000	0 000
1004	846 000	5166 000	0 000
1005	888 000	5166 000	0 000
1006	930 000	5166 000	0 000
1007	972 000	5166 000	0 000
1008	1014 000	5166 000	0 000
1009	1056 000	5166 000	0 000
1010	1098 000	5166 000	0 000
1011	1140 000	5166 000	0 000
1012	1182 000	5166 000	0 000
1013	1224 000	5166 000	0 000
1014	1266 000	5166 000	0 000
1015	1308 000	5166 000	0 000
1016	1350 000	5166 000	0 000
1017	1392 000	5166 000	0 000
1018	1434 000	5166 000	0 000
1019	1476 000	5166 000	0 000
1020	1518 000	5166 000	0 000
1021	1560 000	5166 000	0 000
1022	1602 000	5166 000	0 000
1023	1644 000	5166 000	0 000
1024	1686 000	5166 000	0 000
1025	1728 000	5166 000	0 000
1026	1770 000	5166 000	0 000
1027	1812 000	5166 000	0 000
1028	1854 000	5166 000	0 000
1029	1896 000	5166 000	0 000
1030	1938 000	5166 000	0 000
1031	1980 000	5166 000	0 000
1032	2022 000	5166 000	0 000
1033	2064 000	5166 000	0 000
1034	2106 000	5166 000	0 000
1035	2148 000	5166 000	0 000
1036	2190 000	5166 000	0 000
1037	2232 000	5166 000	0 000
1038	2274 000	5166 000	0 000
1039	2316 000	5166 000	0 000
1040	2358 000	5166 000	0 000
1041	2400 000	5166 000	0 000
1042	2442 000	5166 000	0 000
1043	2484 000	5166 000	0 000
1044	2526 000	5166 000	0 000
1045	2568 000	5166 000	0 000
1046	2610 000	5166 000	0 000
1047	2652 000	5166 000	0 000
1048	2694 000	5166 000	0 000
1049	2736 000	5166 000	0 000
1050	2778 000	5166 000	0 000
1051	2820 000	5166 000	0 000
1052	2862 000	5166 000	0 000
1053	2904 000	5166 000	0 000
1054	2946 000	5166 000	0 000
1055	2988 000	5166 000	0 000
1056	3030 000	5166 000	0 000
1057	3072 000	5166 000	0 000
1058	3114 000	5166 000	0 000
1059	3156 000	5166 000	0 000
1060	3198 000	5166 000	0 000
1061	3240 000	5166 000	0 000
1062	3282 000	5166 000	0 000
1063	3324 000	5166 000	0 000
1064	3366 000	5166 000	0 000
1065	3408 000	5166 000	0 000
1066	3450 000	5166 000	0 000
1067	3492 000	5166 000	0 000
1068	3534 000	5166 000	0 000
1069	3576 000	5166 000	0 000
1070	3618 000	5166 000	0 000
1071	3660 000	5166 000	0 000
1072	3702 000	5166 000	0 000
1073	3744 000	5166 000	0 000
1074	3786 000	5166 000	0 000
1075	3828 000	5166 000	0 000
1076	3870 000	5166 000	0 000
1077	3912 000	5166 000	0 000
1078	3954 000	5166 000	0 000
1079	3996 000	5166 000	0 000
1080	4038 000	5166 000	0 000
1081	4080 000	5166 000	0 000
1082	4122 000	5166 000	0 000
1083	4164 000	5166 000	0 000
1084	4206 000	5166 000	0 000
1085	4248 000	5166 000	0 000
1086	4290 000	5166 000	0 000
1087	4332 000	5166 000	0 000
1088	4374 000	5166 000	0 000
1089	4416 000	5166 000	0 000
1090	4458 000	5166 000	0 000
1091	4500 000	5166 000	0 000
1092	4542 000	5166 000	0 000
1093	4584 000	5166 000	0 000
1094	4626 000	5166 000	0 000
1095	4668 000	5166 000	0 000
1096	4710 000	5166 000	0 000
1097	4752 000	5166 000	0 000
1098	4794 000	5166 000	0 000
1099	4836 000	5166 000	0 000
1100	4878 000	5166 000	0 000

APPENDIX B: ABAQUS TWO-DIMENSIONAL ELEMENT FILE
USED FOR MONOLITH L-17

ELE NO.	N1	N2	N3	N4	N5	N6	N7	N8
301	973	975	1001	999	974	991	1000	990
302	975	977	1003	1001	976	992	1002	991
303*	977	979	1005	1003	978	993	1004	992
304*	979	981	1007	1005	980	994	1006	993
305	981	983	1009	1007	982	995	1008	994
306	983	985	1011	1009	984	996	1010	995
307	985	987	1013	1011	986	997	1012	996
308	987	989	1015	1013	988	998	1014	997
309	999	1001	1027	1025	1000	1017	1026	1016
310	1001	1003	1029	1027	1002	1018	1028	1017
311*	1003	1005	1031	1029	1004	1019	1030	1018
312*	1005	1007	1033	1031	1006	1020	1032	1019
313	1007	1009	1035	1033	1008	1021	1034	1020
314	1009	1011	1037	1035	1010	1022	1036	1021
315	1011	1013	1039	1037	1012	1023	1038	1022
316	1013	1015	1041	1039	1014	1024	1040	1023

APPENDIX 1 ABAQUS TWO-DIMENSIONAL THERMAL ANALYSIS
INPUT FILE FOR MONOLITH L-17

```

*HEADING
L-17 2D MODEL, THERMAL ANALYSIS OF GATE MONOLITH - INCLUDES AIR ELEMENTS
*NODE, INPUT=15
<Inserts node file here
*ELEMENT, TYPE=DC2DB, INPUT=16
<Inserts element file here
137,138,145,146
*ELSET, ELSET=AIR6
153,154,161,162
*ELSET, ELSET=AIR7
169,170,177,178
*ELSET, ELSET=AIRESL
AIR5, AIR6, AIR7
*ELSET, ELSET=AIR15
303, 304
*ELSET, ELSET=AIR
311, 312
*ELSET, ELSET=AIRESL
AIRESL, AIR15, AIR16
*ELSET, ELSET=SOILT, GENERATE
15, 28, 1
*ELSET, ELSET=SOILB, GENERATE
1, 14, 1
*ELSET, ELSET=SOIL
SOILT, SOILB
*ELSET, ELSET=LIFT1, GENERATE
29, 42, 1
*ELSET, ELSET=LIFTIR
42
*ELSET, ELSET=LIFT2B, GENERATE
43, 56, 1
*ELSET, ELSET=LIFT2T, GENERATE
57, 70, 1
*ELSET, ELSET=LIFT2
LIFT2B, LIFT2T
*ELSET, ELSET=LIFT2R
56, 70
*ELSET, ELSET=LIFT3B, GENERATE
71, 84, 1
*ELSET, ELSET=LIFT3T, GENERATE
85, 98, 1
*ELSET, ELSET=LIFT3
LIFT3B, LIFT3T
*ELSET, ELSET=LIFT3R
84, 98
*ELSET, ELSET=LIFT4B, GENERATE
99, 112, 1
*ELSET, ELSET=LIFT4T, GENERATE
113, 126, 1
*ELSET, ELSET=LIFT4IF
123, 124

```

```

*ELSET, ELSET=LIFT6
LIFT6B, LIFT6T
112, 126
*ELSET, ELSET=LIFT5F, GENERATE
127, 132
*ELSET, ELSET=LIFT5WB
134, 133, 135, 136, 137, 140
*ELSET, ELSET=LIFT5B
LIFT5F, LIFT5WB
*ELSET, ELSET=LIFT5T
141, 142, 143, 144, 147, 148
*ELSET, ELSET=LIFT5
LIFT5B, LIFT5T
*ELSET, ELSET=LIFT5IR
136, 144
*ELSET, ELSET=LIFT5IL
139, 147
*ELSET, ELSET=LIFT5R
140, 148
*ELSET, ELSET=LIFT5L
141
*ELSET, ELSET=LIFT6B
149, 150, 151, 152, 155, 156
*ELSET, ELSET=LIFT6T
157, 158, 159, 160, 163, 164
*ELSET, ELSET=LIFT6
LIFT6B, LIFT6T
*ELSET, ELSET=LIFT6IR
152, 160
*ELSET, ELSET=LIFT6IL
155, 163
*ELSET, ELSET=LIFT6R
156, 164
*ELSET, ELSET=LIFT6L
149, 157
*ELSET, ELSET=LIFT7B
165, 166, 167, 168, 171, 172
*ELSET, ELSET=LIFT7T
173, 174, 175, 176, 179, 180
*ELSET, ELSET=LIFT7
LIFT7B, LIFT7T
*ELSET, ELSET=LIFT7IR
168, 176
*ELSET, ELSET=LIFT7IL
171, 179
*ELSET, ELSET=LIFT7R
172, 180
*ELSET, ELSET=LIFT7L
165, 173

```

<Continue element set definition

```

*ELSET, ELSET=LIFT8B, GENERATE
181, 188, 1
*ELSET, ELSET=LIFT8T, GENERATE
189, 196, 1
*ELSET, ELSET=LIFT8
LIFT8B, LIFT8T
*ELSET, ELSET=LIFT8R
188, 196
*ELSET, ELSET=LIFT8L
181, 189
*ELSET, ELSET=LIFT8IB
185, 186
*ELSET, ELSET=LIFT9B, GENERATE
197, 204, 1
*ELSET, ELSET=LIFT9T, GENERATE
205, 212, 1
*ELSET, ELSET=LIFT9
LIFT9B, LIFT9T
*ELSET, ELSET=LIFT9R
204, 212
*ELSET, ELSET=LIFT9L
197, 205
*ELSET, ELSET=LIFT10B, GENERATE
213, 220, 1
*ELSET, ELSET=LIFT10T, GENERATE
221, 228, 1
*ELSET, ELSET=LIFT10
LIFT10B, LIFT10T
*ELSET, ELSET=LIFT10R
220, 228
*ELSET, ELSET=LIFT10L
213, 221
*ELSET, ELSET=LIFT11B, GENERATE
229, 236, 1
*ELSET, ELSET=LIFT11T, GENERATE
237, 244, 1
*ELSET, ELSET=LIFT11
LIFT11B, LIFT11T
*ELSET, ELSET=LIFT11R
236, 244
*ELSET, ELSET=LIFT11L
229, 237
*ELSET, ELSET=LIFT12B, GENERATE
245, 252, 1
*ELSET, ELSET=LIFT12T, GENERATE
253, 260, 1
*ELSET, ELSET=LIFT12
LIFT12B, LIFT12T
*ELSET, ELSET=LIFT12R
252, 260

```

Page 3 of 17

<Continue element set definition

```

*ELSET, ELSET=LIFT12L
245, 253
*ELSET, ELSET=LIFT13B, GENERATE
261, 268, 1
*ELSET, ELSET=LIFT13T, GENERATE
269, 276, 1
*ELSET, ELSET=LIFT13
LIFT13B, LIFT13T
*ELSET, ELSET=LIFT13R
268, 276
*ELSET, ELSET=LIFT13L
261, 269
*ELSET, ELSET=LIFT14B, GENERATE
277, 284, 1
*ELSET, ELSET=LIFT14T, GENERATE
285, 292, 1
*ELSET, ELSET=LIFT14
LIFT14B, LIFT14T
*ELSET, ELSET=LIFT14R
284, 292
*ELSET, ELSET=LIFT14L
277, 285
*ELSET, ELSET=LIFT15B, GENERATE
293, 300, 1
*ELSET, ELSET=LIFT15T
301, 302, 305, 306, 307, 308
*ELSET, ELSET=LIFT15
LIFT15B, LIFT15T
*ELSET, ELSET=LIFT15R
302
*ELSET, ELSET=LIFT15L
305
*ELSET, ELSET=LIFT15R
300, 308
*ELSET, ELSET=LIFT15L
293, 301
*ELSET, ELSET=LIFT15IP
295, 296
*ELSET, ELSET=LIFT16
309, 310, 313, 314, 315, 316
*ELSET, ELSET=LIFT16R
310
*ELSET, ELSET=LIFT16IL
313
*ELSET, ELSET=LIFT16R
316
*ELSET, ELSET=LIFT16L
*ELSET, ELSET=CONCE1
LIFT2, LIFT3, LIFT4, LIFT5
*ELSET, ELSET=CONCE2

```

Page 4 of 17

<Concrete elements sets completed


```

*END STEP
*STEP
PLACE LIFT3 - DAY 11.12 (REL 1.2)
*HEAT TRANSFER
6.48
*MODEL CHANGE INCLUDE
LIFT3
*FILM AMPLITUDE-AMB OP-NEW
LIFT3R.F2..0 0283
LIFT3T.F3..0 0283
LIFT3R.F2..0 00588
*PLOT.FREQ-2
LIFT3 - M17 - 2D MODEL
*DETAIL
-0 001.4295 99.0.1140 01.4434 01.0
*CONTOUR
100.11.65.115.
*END STEP
*STEP
LIFT3 - DAY 13.14.15 (REL 3.4.5) REMOVE L3 ENT FORMS
*HEAT TRANSFER
12.72
*FILM AMPLITUDE AMB
LIFT3R.F2..0 0283
*END STEP
*STEP
PLACE LIFT4 - DAY 16.17 (REL 1.2)
*HEAT TRANSFER
6.48
*MODEL CHANGE INCLUDE
LIFT4
*FILM AMPLITUDE AMB OP-NEW
LIFT4R.F2..0 0283
LIFT4T.F3..0 0283
LIFT4R.F2..0 00588
*PLOT.FREQ-2
LIFT4 - M17 - 2D MODEL
*DETAIL
-0 001.4295 99.0.1140 01.4488 01.0
*CONTOUR
100.11.65.115.
*END STEP
*STEP
LIFT4 - DAY 18.19.20 (REL 3.4.5) REMOVE L4 ENT FORMS
*HEAT TRANSFER
12.72
*FILM AMPLITUDE-AMB
LIFT4R.F2..0 0283
*END STEP

```

```

*HEAT TRANSFER
6.48
*MODEL CHANGE INCLUDE
LIFT5
*FILM AMPLITUDE-AMB OP-NEW
LIFT5R.F2..0 0283
LIFT5T.F3..0 0283
LIFT5R.F2..0 00588
*PLOT.FREQ-2
LIFT5 - M17 - 2D MODEL
*DETAIL
-0 001.4295 99.0.1140 01.4542 01.0
*CONTOUR
100.11.65.115.
*END STEP
*STEP
LIFT5 - DAY 21.22.23 (REL 3.4.5) REMOVE L5 ENT FORMS
*HEAT TRANSFER
12.72
*FILM AMPLITUDE AMB
LIFT5R.F2..0 0283
LIFT5T.F3..0 0283
LIFT5R.F2..0 00588
*PLOT.FREQ-2
LIFT5 - M17 - 2D MODEL
*DETAIL
-0 001.4295 99.0.1140 01.4596 01.0
*CONTOUR
100.11.65.115.
*END STEP
*STEP
PLACE LIFT6 - DAY 24.25 (REL 1.2)
*HEAT TRANSFER
6.48
*MODEL CHANGE INCLUDE
LIFT6
*FILM AMPLITUDE AMB OP-NEW
LIFT6R.F2..0 0283
LIFT6T.F3..0 0283
LIFT6R.F2..0 00588
*PLOT.FREQ-2
LIFT6 - M17 - 2D MODEL
*DETAIL
-0 001.4295 99.0.1140 01.4650 01.0
*CONTOUR
100.11.65.115.
*END STEP
*STEP
LIFT6 - DAY 26.27.28 (REL 3.4.5) REMOVE L6 ENT FORMS
*HEAT TRANSFER
12.72
*FILM AMPLITUDE-AMB
LIFT6R.F2..0 0283
*END STEP

```



```

LIFT6 - M17 - 2D MODEL
*DETAIL
-0 001.4295 99.0 1140 01.4632 01.0
*CONTOUR
100.11.65.115.
*END STEP
LIFT6 - DAY 28.29.30 (REL 3.4.5) REMOVE L6 EXT & L3 5 INT FORMS
*HEAT TRANSFER
12.72
*FILM,AMPLITUDE=AMB
LIFT6R.F2.,0 0283
LIFT6L.F4.,0 0283
LIFT6IR.F2.,0 0176
LIFT6IL.F4.,0 0176
*END STEP
*STEP
PLACE LIFT7 - DAYS 31.32 (REL 1.2)
*HEAT TRANSFER
6.48
*MODEL CHANGE,INCLUDE
LIFT7
*FILM,AMPLITUDE=AMB,OP=NEW
LIFT6R.F2.,0 0283
LIFT5F.F3.,0 0283
LIFT4IF.F3.,0 01760
LIFT56L.F4.,0 0283
LIFT56JR.F2.,0 01760
LIFT56IL.F4.,0 01760
LIFT7IR.F2.,0 00522
LIFT7IL.F4.,0 00588
LIFT7L.F4.,0 00588
LIFT7T.F3.,0 0283
*PLOT.FREQ=2
LIFT7 - M17 - 2D MODEL
*DETAIL
-0 001.4295 99.0 1140 01.4704 01.0
*CONTOUR
100.11.65.115.
*END STEP
LIFT7 - DAY 33.34.35 (REL 3.4.5) REMOVE L7 EXT FORMS
*HEAT TRANSFER
12.72
*FILM,AMPLITUDE=AMB
LIFT7R.F2.,0 0283
LIFT7L.F4.,0 0283
LIFT7IR.F2.,0 0176
LIFT7IL.F4.,0 0176

```

```

*END STEP
*STEP
PLACE LIFT8 - DAY 36 37 (REL 1.2)
*HEAT TRANSFER
6.48
*MODEL CHANGE,INCLUDE
LIFT8
*FILM,AMPLITUDE=AMB,OP=NEW
LIFT8R.F2.,0 0283
LIFT8L.F4.,0 0283
LIFT8IR.F2.,0 00588
LIFT8IL.F4.,0 00588
LIFT8T.F3.,0 0283
*PLOT.FREQ=2
LIFT8 - M17 - 2D MODEL
*DETAIL
-0 001.4295 99.0 1140 01.4752 01.0
*CONTOUR
100.11.65.115.
*END STEP
*STEP
PLACE LIFT9 - DAY 39.40 (REL 3.4.5) REMOVE L8 EXT FORMS
*HEAT TRANSFER
12.72
*FILM,AMPLITUDE=AMB
LIFT8R.F2.,0 0283
LIFT8L.F4.,0 0283
*END STEP
*STEP
PLACE LIFT9 - DAY 41.42 (REL 1.2)
*HEAT TRANSFER
6.48
*MODEL CHANGE,INCLUDE
LIFT9
*FILM,AMPLITUDE=AMB,OP=NEW
LIFT8R.F2.,0 0283
LIFT8L.F4.,0 0283
LIFT9L.F4.,0 00588
LIFT9R.F2.,0 00588
LIFT9T.F3.,0 0283
*PLOT.FREQ=2
LIFT9 - M17 - 2D MODEL
*DETAIL
-0 001.4295 99.0 1140 01.4808 01.0
*CONTOUR
100.11.65.115.
*END STEP
*STEP

```

```

LIFT9 - DAY 43.45 (REL 3.5) REMOVE L9 EXT FORMS
*HEAT TRANSFER
12.72
*FILM,AMPLITUDE=AMB
LIFT9L,F4,,0.0283
LIFT9R,F2,,0.0283
*END STEP
*STEP
PLACE LIFT10 - DAY 46.47 (REL 1.2)
*HEAT TRANSFER
6.48
*MODEL CHANGE,INCLUDE
LIFT10,
*FILM,AMPLITUDE=AMB,OP=NEW
LIFT10R,F2,,0.0283
LIFT10L,F4,,0.0283
LIFT10L,F4,,0.0283
LIFT10L,F4,,0.00588
LIFT10L,F4,,0.00588
LIFT10L,F3,,0.0283
*PLOT,FREQ=2
LIFT10 - M17 - 2D MODEL
*DETAIL
-0.001,4295,99.0,1140,01,4866,01,0
100,11,65,115,
*CONTOUR
*END STEP
*STEP
LIFT10 - DAY 48.49,50 (REL 3.4,5) REMOVE L10 EXT FORMS
*HEAT TRANSFER
12.72
*FILM,AMPLITUDE=AMB
LIFT10R,F2,,0.0283
LIFT10L,F4,,0.0283
*END STEP
*STEP
PLACE LIFT11 - DAY 51.52 (REL 1.2)
*HEAT TRANSFER
6.48
*MODEL CHANGE,INCLUDE
LIFT11,
*FILM,AMPLITUDE=AMB,OP=NEW
LIFT11R,F2,,0.0283
LIFT11L,F4,,0.0283
LIFT11L,F4,,0.00588
LIFT11L,F4,,0.00588
LIFT11L,F3,,0.0283
*PLOT,FREQ=2
LIFT11 - M17 - 2D MODEL

```

```

*DETAIL
-0.001,4295,99.0,1140,01,4866,01,0
*CONTOUR
100,11,65,115,
*END STEP
*STEP
LIFT12 - DAY 58.59,60 (REL 3.4,5) REMOVE L12 EXT FORMS
*HEAT TRANSFER
12.72
*FILM,AMPLITUDE=AMB
LIFT12R,F2,,0.0283
LIFT12L,F4,,0.0283
*END STEP
*STEP
PLACE LIFT13 - DAY 61.62 (REL 1.2)
*HEAT TRANSFER
6.48
*MODEL CHANGE,INCLUDE
LIFT13,
*FILM,AMPLITUDE=AMB,OP=NEW
LIFT13R,F2,,0.0283
LIFT13L,F3,,0.0283
*PLOT,FREQ=2
LIFT13 - M17 - 2D MODEL
*DETAIL
-0.001,4295,99.0,1140,01,4866,01,0
*CONTOUR
100,11,65,115,
*END STEP
*STEP
LIFT12 - DAY 58.59,60 (REL 3.4,5) REMOVE L12 EXT FORMS
*HEAT TRANSFER
12.72
*FILM,AMPLITUDE=AMB
LIFT12R,F2,,0.0283
LIFT12L,F4,,0.0283
*END STEP
*STEP
PLACE LIFT13 - DAY 61.62 (REL 1.2)
*HEAT TRANSFER
6.48
*MODEL CHANGE,INCLUDE
LIFT13,
*FILM,AMPLITUDE=AMB,OP=NEW
LIFT13R,F2,,0.0283
LIFT13L,F3,,0.0283

```

```

LIFT12L,F4,,0 0283
LIFT13R,F2,,0 00588
LIFT13L,F4,,0 00588
LIFT13T,F3,,0 0283
*PLOT,FREQ=2
LIFT13 - M17 - 2D MODEL
*DETAIL
-0 001,4295 99,0,1140 01,5046 01,0
100,11,65,115,
*CONTOUR
LIFT13 - DAY 63,64,65 (REL 3,4,5) REMOVE L13 EXT FORMS
*END STEP
*HEAT TRANSFER
12,72
*FILM,AMPLITUDE-AMB
LIFT13R,F2,,0 0283
LIFT13L,F4,,0 0283
*END STEP
*STEP
PLACE LIFT14- DAY 66,67 (REL 1,2)
*HEAT TRANSFER
6,48
*MODEL CHANGE,INCLUDE
LIFT14,
*FILM,AMPLITUDE-AMB,OP=NEW
LIFT13R,F2,,0 0283
LIFT13L,F4,,0 0283
LIFT13T,F3,,0 0283
LIFT14R,F2,,0 00588
LIFT14L,F4,,0 00588
LIFT14T,F3,,0 0283
*PLOT,FREQ=2
LIFT14 - M17 - 2D MODEL
*DETAIL
-0 001,4295 99,0,1140 01,5106 01,0
100,11,65,115,
*CONTOUR
LIFT14 - DAY 68,69,70 (REL 3,4,5) REMOVE L14 EXT FORMS
*END STEP
*STEP
LIFT14 - DAY 68,69,70 (REL 3,4,5) REMOVE L14 EXT FORMS
*HEAT TRANSFER
12,72
*FILM,AMPLITUDE-AMB
LIFT14R,F2,,0 0283
LIFT14L,F4,,0 0283
*END STEP
*STEP
PLACE LIFT15- DAY 71,72 (REL 1,2)
*HEAT TRANSFER

```

```

6,48
*MODEL CHANGE,INCLUDE
LIFT15,
*FILM,AMPLITUDE-AMB,OP=NEW
LIFT14R,F2,,0 0283
LIFT14L,F4,,0 0283
LIFT14T,F3,,0 0283
LIFT15L,F4,,0 0283
LIFT15R,F2,,0 0283
LIFT15L,F4,,0 0283
LIFT15R,F2,,0 0283
LIFT15L,F4,,0 0283
LIFT15T,F3,,0 0283
LIFT15I,F3,,0 0283
LIFT15I,R,F2,,0 00588
LIFT15I,L,F4,,0 00588
*PLOT,FREQ=2
LIFT15 - M17 - 2D MODEL
*DETAIL
-0 001,4295 99,0,1140 01,5166 01,0
100,11,65,115,
*CONTOUR
LIFT15 - DAY 73,74,75 (REL 3,4,5) REMOVE L15 EXT FORMS
*END STEP
*STEP
PLACE LIFT16- DAY 76,77 (REL 1,2)
*HEAT TRANSFER
6,48
*MODEL CHANGE,INCLUDE
LIFT16,
*FILM,AMPLITUDE-AMB,OP=NEW
LIFT15R,F2,,0 0283
LIFT15F,F3,,0 0283
LIFT14I,F3,,0 01760
LIFT15L,F4,,0 0283
LIFT15I,F3,,0 0283
LIFT15I,R,F2,,0 0283
LIFT15I,L,F4,,0 0283
LIFT16R,F2,,0 00588
LIFT16L,F4,,0 00588
LIFT16I,F3,,0 0283
LIFT16I,R,F2,,0 005220
LIFT16I,L,F4,,0 005220
*PLOT,FREQ=2

```

LIFT16 - M17 - 2D MODEL
*DETAIL
-0.001,4295 99,0.11*0.01,5214.01,0
*CONTOUR
100,11.65,115,
*END STEP
*STEP
LIFT16 - DAY 78.79,80 (REL.3,4,5) REMOVE L16 EXT FORMS
*HEAT TRANSFER
12.72
*FILM,AMPLITUDE=AMB
LIFT16R.F2.,0.0283
LIFT16L.F4.,0.0283
LIFT16IR.F2.,0.0283
LIFT16IL.F4.,0.0283
*END STEP

APPENDIX C - ABAQUS TWO-DIMENSIONAL STRESS ANALYSIS
INPUT COMMAND FILE USED FOR MODEL 1 (7TH)

```

*HEADIN.
1 17 23 HOPEL. INTERNAL STRESS ANALYSIS WITH SUBROUTINE UMAT
*NODE INPUT IS
*ELEMENT TYPE CPMR, INPUT 16
*ELSET ELSET-LIFT1, GENERATE
29, 42, 1
*ELSET, ELSET-LIFT2, GENERATE
43, 56, 1
*ELSET, ELSET-LIFT3, GENERATE
57, 70, 1
*ELSET, ELSET-LIFT4
LIFT2B, LIFT2T
*ELSET, ELSET-LIFT3B, GENERATE
71, 84, 1
*ELSET, ELSET-LIFT3T, GENERATE
85, 98, 1
*ELSET, ELSET-LIFT3
LIFT3B, LIFT3T
*ELSET, ELSET-LIFT4B, GENERATE
99, 112, 1
*ELSET, ELSET-LIFT4T, GENERATE
113, 126, 1
*ELSET, ELSET-LIFT4
LIFT4B, LIFT4T
*ELSET, ELSET-LIFT5F, GENERATE
127, 132
*ELSET, ELSET-LIFT5R
134, 133, 135, 136, 139, 140
*ELSET, ELSET-LIFT5B
LIFT5F, LIFT5R
*ELSET, ELSET-LIFT5T
141, 142, 143, 144, 147, 148
*ELSET, ELSET-LIFT5
LIFT5B, LIFT5T
*ELSET, ELSET-LIFT6B
149, 150, 151, 152, 155, 156
*ELSET, ELSET-LIFT6T
157, 158, 159, 160, 163, 164
*ELSET, ELSET-LIFT6
LIFT6B, LIFT6T
*ELSET, ELSET-LIFT7B
165, 166, 167, 168, 171, 172
*ELSET, ELSET-LIFT7T
173, 174, 175, 176, 179, 180
*ELSET, ELSET-LIFT7
LIFT7B, LIFT7T
*ELSET, ELSET-LIFT8B, GENERATE
181, 184, 1
*ELSET, ELSET-LIFT8T, GENERATE
185, 188, 1

```

```

*ELSET, ELSET-LIFT9B
189, 192, 1
*ELSET, ELSET-LIFT9T, GENERATE
193, 196, 1
*ELSET, ELSET-LIFT10B, GENERATE
200, 207, 1
*ELSET, ELSET-LIFT10T
LIFT10B, LIFT10T
*ELSET, ELSET-LIFT11B
197, 205
*ELSET, ELSET-LIFT11B, GENERATE
213, 220, 1
*ELSET, ELSET-LIFT11T, GENERATE
221, 228, 1
*ELSET, ELSET-LIFT11
LIFT11B, LIFT11T
*ELSET, ELSET-LIFT12B, GENERATE
229, 236, 1
*ELSET, ELSET-LIFT12T, GENERATE
237, 244, 1
*ELSET, ELSET-LIFT12
LIFT12B, LIFT12T
*ELSET, ELSET-LIFT13B, GENERATE
245, 252, 1
*ELSET, ELSET-LIFT13T, GENERATE
253, 260, 1
*ELSET, ELSET-LIFT13
LIFT13B, LIFT13T
*ELSET, ELSET-LIFT14B, GENERATE
261, 268, 1
*ELSET, ELSET-LIFT14T, GENERATE
269, 276, 1
*ELSET, ELSET-LIFT14
LIFT14B, LIFT14T
*ELSET, ELSET-LIFT15B
293, 294, 297, 298, 299, 300
*ELSET, ELSET-LIFT15F
295, 296
*ELSET, ELSET-LIFT15T
301, 302, 305, 306, 307, 308
*ELSET, ELSET-LIFT15
LIFT15B, LIFT15F, LIFT15T
*ELSET, ELSET-LIFT16
309, 310, 313, 314, 315, 316

```

NO-A103 664

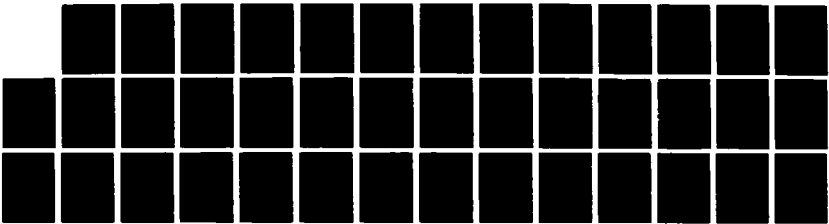
THERMAL STRESS ANALYSES OF MISSISSIPPI RIVER LOCK AND
DAM 26(R)(U) ARMY ENGINEER WATERWAYS EXPERIMENT STATION
VICKSBURG MS STRUCTURES LAB A A BOMBICH ET AL. JUL 87
MES/TR/SL-87-21

4/4

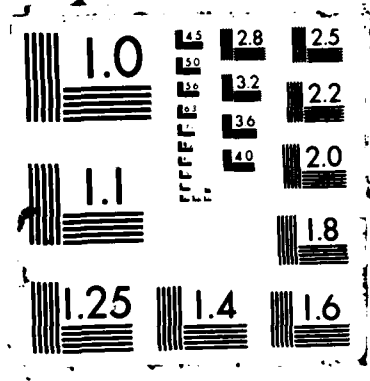
UNCLASSIFIED

F/G 13/13

NL



END
9-87
DTC




```

*ELSET, ELSET=CONCE1
LIFT2, LIFT3, LIFT4, LIFT5
*ELSET, ELSET=CONCE2
LIFT6, LIFT7, LIFT8, LIFT9, LIFT10, LIFT11, LIFT12, LIFT13, LIFT14, LIFT15, LIFT16
*ELSET, ELSET=REMOVEL
CONCE1, CONCE2
*ELSET, ELSET=CONCE
LIFT1, REMOVEL
*ELSET, ELSET=LIFT12
LIFT1, LIFT2
*ELSET, ELSET=LIFT13
LIFT12, LIFT3
*ELSET, ELSET=LIFT14
LIFT13, LIFT4
*ELSET, ELSET=LIFT15
LIFT14, LIFT5
*ELSET, ELSET=LIFT16
LIFT15, LIFT6
*ELSET, ELSET=LIFT17
LIFT16, LIFT7
*ELSET, ELSET=LIFT18
LIFT17, LIFT8
*ELSET, ELSET=LIFT19
LIFT18, LIFT9
*ELSET, ELSET=LIFT110
LIFT19, LIFT10
*ELSET, ELSET=LIFT111
LIFT110, LIFT11
*ELSET, ELSET=LIFT112
LIFT111, LIFT12
*ELSET, ELSET=LIFT113
LIFT112, LIFT13
*ELSET, ELSET=LIFT114
LIFT113, LIFT14
*ELSET, ELSET=LIFT115
LIFT114, LIFT15
*ELSET, ELSET=LIFT116
LIFT115, LIFT16
*SPRING
89, 1, 285, 273
89, 2, 11679, 60
*SPRING
90, 1, 570, 55
90, 2, 23359, 20
*SPRING
91, 1, 285, 27
91, 2, 11679, 60
*SPRING
91, 1, 352, 524
92, 2, 18767, 94

```

<Define element sets that
combine lifts to facilitate
deactivation of unplaced lifts

<Element set for all concrete
elements

<Define element sets to include
all elements at each stage

<Enter x then y stiffnesses
of piles in lb/in

```

*SPRING
93, 1, 352, 52
93, 2, 18767, 94
*SPRING
94, 1, 352, 52
94, 2, 18767, 94
*SPRING
95, 1, 352, 52
95, 2, 18767, 94
*SPRING
96, 1, 352, 52
96, 2, 18767, 94
*SPRING
97, 1, 352, 52
97, 2, 18767, 94
*SPRING
98, 1, 352, 52
98, 2, 18767, 94
*SPRING
99, 1, 352, 52
99, 2, 18767, 94
*SPRING
101, 1, 352, 52
101, 2, 18767, 94
*SPRING
103, 1, 528, 50
103, 2, 18767, 94
*SPRING
105, 1, 528, 50
105, 2, 18767, 94
*SPRING
106, 1, 1057, 02
106, 2, 37535, 94
*SPRING
107, 1, 1057, 02
107, 2, 37535, 94
*SPRING
109, 1, 1057, 02
109, 2, 37535, 94
*SPRING
111, 1, 1057, 02
111, 2, 37535, 94
*SPRING
113, 1, 700, 92
113, 2, 24891, 18
*MPC, USER
101, 592, 591, 595
101, 593, 591, 595
101, 594, 591, 595
*NSET, NSET=CLINE

```

<Continue pile stiffness input

<Enter data required by user
subroutine MPC for formwork
simulation to support concrete
in lift 8 above void
<Node set for centerline nodes


```

72 0.3600000 , 0 17, 96 0.3750000 , 0 17, 120 0.3950000 .
0 17, 144 0.4170000 , 0 17, 240 0.4400000 , 0 17, 336 0
4600000 , 0 17, 504 0.4800000 , 0 17, 672 0.5150000 , 0 17
1344 0.5400000 , 0 17, 2160 0.5800000 , 0 17, 4800 0.6150000 .
0 17, 10800 0.4.5E-06,
*MATERIAL,ELSET=LIFT10
*USER MATERIAL CONSTANTS=67
0 0, 0 17, 0 0, 0 0, 0 17, 6 0, 750000 , 0 17
12 0.1550000 , 0 17, 18 0.2100000 , 0 17, 24 0.2500000 .
0 17, 30 0.2750000 , 0 17, 36 0.2900000 , 0 17, 42 0
3050000 , 0 17, 48 0.3250000 , 0 17, 60 0.3400000 , 0 17
72 0.3600000 , 0 17, 96 0.3750000 , 0 17, 120 0.3950000 .
0 17, 144 0.4170000 , 0 17, 240 0.4400000 , 0 17, 336 0
4600000 , 0 17, 504 0.4800000 , 0 17, 672 0.5150000 , 0 17
1344 0.5400000 , 0 17, 2160 0.5800000 , 0 17, 4800 0.6150000 .
0 17, 10800 0.4.5E-06,
*MATERIAL,ELSET=LIFT11
*USER MATERIAL CONSTANTS=67
0 0, 0 17, 0 0, 0 0, 0 17, 6 0, 750000 , 0 17
12 0.1550000 , 0 17, 18 0.2100000 , 0 17, 24 0.2500000 .
0 17, 30 0.2750000 , 0 17, 36 0.2900000 , 0 17, 42 0
3050000 , 0 17, 48 0.3250000 , 0 17, 60 0.3400000 , 0 17
72 0.3600000 , 0 17, 96 0.3750000 , 0 17, 120 0.3950000 .
0 17, 144 0.4170000 , 0 17, 240 0.4400000 , 0 17, 336 0
4600000 , 0 17, 504 0.4800000 , 0 17, 672 0.5150000 , 0 17
1344 0.5400000 , 0 17, 2160 0.5800000 , 0 17, 4800 0.6150000 .
0 17, 10800 0.4.5E-06,
*MATERIAL,ELSET=LIFT12
*USER MATERIAL CONSTANTS=67
0 0, 0 17, 0 0, 0 0, 0 17, 6 0, 750000 , 0 17
12 0.1550000 , 0 17, 18 0.2100000 , 0 17, 24 0.2500000 .
0 17, 30 0.2750000 , 0 17, 36 0.2900000 , 0 17, 42 0
3050000 , 0 17, 48 0.3250000 , 0 17, 60 0.3400000 , 0 17
72 0.3600000 , 0 17, 96 0.3750000 , 0 17, 120 0.3950000 .
0 17, 144 0.4170000 , 0 17, 240 0.4400000 , 0 17, 336 0
4600000 , 0 17, 504 0.4800000 , 0 17, 672 0.5150000 , 0 17
1344 0.5400000 , 0 17, 2160 0.5800000 , 0 17, 4800 0.6150000 .
0 17, 10800 0.4.5E-06,
*MATERIAL,ELSET=LIFT13
*USER MATERIAL CONSTANTS=67
0 0, 0 17, 0 0, 0 0, 0 17, 6 0, 750000 , 0 17
12 0.1550000 , 0 17, 18 0.2100000 , 0 17, 24 0.2500000 .
0 17, 30 0.2750000 , 0 17, 36 0.2900000 , 0 17, 42 0
3050000 , 0 17, 48 0.3250000 , 0 17, 60 0.3400000 , 0 17
72 0.3600000 , 0 17, 96 0.3750000 , 0 17, 120 0.3950000 .
0 17, 144 0.4170000 , 0 17, 240 0.4400000 , 0 17, 336 0
4600000 , 0 17, 504 0.4800000 , 0 17, 672 0.5150000 , 0 17
1344 0.5400000 , 0 17, 2160 0.5800000 , 0 17, 4800 0.6150000 .
0 17, 10800 0.4.5E-06,

```

```

*MATERIAL,ELSET=LIFT14
*USER MATERIAL CONSTANTS=67
0 0, 0 17, 0 0, 0 0, 0 17, 6 0, 750000 , 0 17
12 0.1550000 , 0 17, 18 0.2100000 , 0 17, 24 0.2500000 .
0 17, 30 0.2750000 , 0 17, 36 0.2900000 , 0 17, 42 0
3050000 , 0 17, 48 0.3250000 , 0 17, 60 0.3400000 , 0 17
72 0.3600000 , 0 17, 96 0.3750000 , 0 17, 120 0.3950000 .
0 17, 144 0.4170000 , 0 17, 240 0.4400000 , 0 17, 336 0
4600000 , 0 17, 504 0.4800000 , 0 17, 672 0.5150000 , 0 17
1344 0.5400000 , 0 17, 2160 0.5800000 , 0 17, 4800 0.6150000 .
0 17, 10800 0.4.5E-06,
*MATERIAL,ELSET=LIFT15
*USER MATERIAL CONSTANTS=67
0 0, 0 17, 0 0, 0 0, 0 17, 6 0, 750000 , 0 17
12 0.1550000 , 0 17, 18 0.2100000 , 0 17, 24 0.2500000 .
0 17, 30 0.2750000 , 0 17, 36 0.2900000 , 0 17, 42 0
3050000 , 0 17, 48 0.3250000 , 0 17, 60 0.3400000 , 0 17
72 0.3600000 , 0 17, 96 0.3750000 , 0 17, 120 0.3950000 .
0 17, 144 0.4170000 , 0 17, 240 0.4400000 , 0 17, 336 0
4600000 , 0 17, 504 0.4800000 , 0 17, 672 0.5150000 , 0 17
1344 0.5400000 , 0 17, 2160 0.5800000 , 0 17, 4800 0.6150000 .
0 17, 10800 0.4.5E-06,
*MATERIAL,ELSET=LIFT16
*USER MATERIAL CONSTANTS=67
0 0, 0 17, 0 0, 0 0, 0 17, 6 0, 750000 , 0 17
12 0.1550000 , 0 17, 18 0.2100000 , 0 17, 24 0.2500000 .
0 17, 30 0.2750000 , 0 17, 36 0.2900000 , 0 17, 42 0
3050000 , 0 17, 48 0.3250000 , 0 17, 60 0.3400000 , 0 17
72 0.3600000 , 0 17, 96 0.3750000 , 0 17, 120 0.3950000 .
0 17, 144 0.4170000 , 0 17, 240 0.4400000 , 0 17, 336 0
4600000 , 0 17, 504 0.4800000 , 0 17, 672 0.5150000 , 0 17
1344 0.5400000 , 0 17, 2160 0.5800000 , 0 17, 4800 0.6150000 .
0 17, 10800 0.4.5E-06,
*NSSET,NSSET=SOIL5,GENERATE
89.117
*NSSET,NSSET=CONCH,GENERATE
118.436
438.461
465.474
476.487
491.500
502.513
517.526
528.539
543.552
554.565
569.578
580.992
994.1003
1020.1029

```

<Node set for top of soil used for initial temperatures
<Node set for all concrete nodes for defining initial temperature in thermal stress analysis

```

1033,1041
*INITIAL CONDITIONS,TYPE=TEMPERATURE <Specify initial temperatures
SOILS,70
UNCON,65
*RESTART WRITE,FREQUENCY=2
*STEP,AMP=STEP
LIFT1 PLACED DAY 1
*STATIC,PTOL=10,DIRECT
6,24
*MODEL CHANGE,REMOVE
REMOVE
*TEMPERATURE,FILE=17,BSTEP=1(INC=1),ESTEP=1(INC=4) <Nodal temps from file 17
*NODE PRINT
2,
*EL PRINT,ELSET=LIFT1
1,1,1,1,
1,1,1,1,
2,2,1,1,2,
*PLOT,FREQ=2
LIFT1 M17 2D MODEL
*DETAIL
-0.01,4295.99,0.1140,01,4332,01,0
*CONTOUR
1,13,300,300
2,13,300,300
3,13,500,100
14,9,100,300
*DISPLACED
1,250
*END STEP
*STEP,AMP=STEP
LIFT1 DAY 2
*STATIC,PTOL=10,DIRECT
12,24
*DLOAD,OP=NEW
LIFT1 BY,0,04714
*TEMPERATURE,FILE=17,BSTEP=1(INC=5),ESTEP=1(INC=8)
*END STEP
*STEP,AMP=STEP
LIFT1 DAY 3
*STATIC,PTOL=10,DIRECT
24,24
*TEMPERATURE,FILE=17,BSTEP=2(INC=2),ESTEP=2(INC=2)
*END STEP
LIFT1 DAYS 4 5
*STEP,AMP=STEP
*STATIC,PTOL=10,DIRECT
48,48
*TEMPERATURE,FILE=17,BSTEP=2(INC=6),ESTEP=2(INC=6)
*END STEP

```

```

*STEP,AMP=STEP
LIFT2 PLACED DAY 6 (REL. DAY 1)
*STATIC,PTOL=10,DIRECT
6,24
*MODEL CHANGE,INCLUDE
LIFT2
*DLOAD
LIFT2B,P1,-4,1828
*TEMPERATURE,FILE=17,BSTEP=3(INC=1),ESTEP=3(INC=4)
*EL PRINT,ELSET=LIFT2
1,1,1,1,
1,1,1,1,
2,2,1,1,2,
*PLOT,FREQ=2
LIFT2 M17 2D MODEL
*DETAIL
-0.01,4295.99,0.1140,01,4380,01,0
*CONTOUR
1,13,300,300
2,13,300,300
3,13,500,100
14,9,100,300
*DISPLACED
1,250
*END STEP
*STEP,AMP=STEP
LIFT2 DAY 7 (REL. DAY 2)
*STATIC,PTOL=10,DIRECT
12,24
*DLOAD,OP=NEW
LIFT2 BY,0,08714
*TEMPERATURE,FILE=17,BSTEP=3(INC=5),ESTEP=3(INC=8)
*END STEP
*STEP,AMP=STEP
LIFT2 DAY 8 (REL. DAY 3)
*STATIC,PTOL=10,DIRECT
24,24
*TEMPERATURE,FILE=17,BSTEP=4(INC=2),ESTEP=4(INC=2)
*END STEP
LIFT2 DAYS 9-10 (REL. DAY 4-5)
*STEP,AMP=STEP
*STATIC,PTOL=10,DIRECT
48,48
*TEMPERATURE,FILE=17,BSTEP=4(INC=6),ESTEP=4(INC=6)
*END STEP
LIFT3 PLACED DAY 11 (REL. DAY 1)
*STATIC,PTOL=10,DIRECT
6,24
*MODEL CHANGE,INCLUDE

```

```

LIFT3
*DLOAD
LIFT3,P1,-4,7056
*TEMPERATURE,FILE=17,BSTEP=5(INC=1),ESTEP=5(INC=4)
*EL PRINT,ELSET=LFT3
1,1,1,1,
1,1,1,1,
2,2,1,2,
*PLOT,FREQ=2
LIFT3 M17 - 2D MODEL
*DETAIL
0 01,4295.99,0,1140 01,4434,01,0
*CONTOUR
1,13,-300,300
2,13,-300,300
3,13,-500,100
14,9,-100,300
*DISPLACED
1,250
*END STEP
*STEP,AMP=STEP
LIFT3,DAY 12 (REL DAY 2)
*STATIC,PTOL=10,DIRECT
12,24
*DLOAD,OP=NEW
LIFT3,BY,-0.08714
*TEMPERATURE,FILE=17,BSTEP=5(INC=5),ESTEP=5(INC=8)
*END STEP
*STEP,AMP=STEP
LIFT3,DAY 13 (REL DAY 3)
*STATIC,PTOL=10,DIRECT
14,24
*TEMPERATURE,FILE=17,BSTEP=6(INC=2),ESTEP=6(INC=2)
*END STEP
*STEP,AMP=STEP
LIFT3,DAYS 14 15 (REL DAY 4-5)
*STATIC,PTOL=10,DIRECT
14,48
*TEMPERATURE,FILE=17,BSTEP=6(INC=6),ESTEP=6(INC=6)
*END STEP
*STEP,AMP=STEP
LIFT4 PLACED DAY 16 (REL DAY 1)
*STATIC,PTOL=10,DIRECT
6,24
*MODEL CHANGE,INCLUDE
LIFT4
LIFT4,P1,-4,7056
*TEMPERATURE,FILE=17,BSTEP=7(INC=1),ESTEP=7(INC=4)
*EL PRINT,ELSET=LFT4

```

```

1,1,1,1,
1,1,1,1,
2,2,1,2,
*PLOT,FREQ=2
LIFT4 - M17 - 2D MODEL
*DETAIL
-0.01,4295.99,0,1140.01,4486.01,0
*CONTOUR
1,13,-300,300
2,13,-300,300
3,13,-500,100
14,9,-100,300
*DISPLACED
1,250
*END STEP
*STEP,AMP=STEP
LIFT4,DAY 17 (REL DAY 2)
*STATIC,PTOL=10,DIRECT
12,24
*DLOAD,OP=NEW
LIFT4,BY,-0.08714
*TEMPERATURE,FILE=17,BSTEP=7(INC=5),ESTEP=7(INC=8)
*END STEP
*STEP,AMP=STEP
LIFT4,DAY 18 (REL DAY 4)
*STATIC,PTOL=10,DIRECT
24,24
*TEMPERATURE,FILE=17,BSTEP=8(INC=2),ESTEP=8(INC=2)
*END STEP
*STEP,AMP=STEP
LIFT4,DAYS 19-20 (REL DAY 4-5)
*STATIC,PTOL=10,DIRECT
48,48
*TEMPERATURE,FILE=17,BSTEP=8(INC=6),ESTEP=8(INC=6)
*END STEP
*STEP,AMP=STEP
LIFT5 PLACED DAY 21 (REL DAY 1)
*STATIC,PTOL=10,DIRECT
6,24
*MODEL CHANGE,INCLUDE
LIFT5
LIFT5,P1,-2,0914
LIFT5,P1,-6,2742
*TEMPERATURE,FILE=17,BSTEP=9(INC=1),ESTEP=9(INC=4)
*EL PRINT,ELSET=LFT5
1,1,1,1,
1,1,1,1,
2,2,1,2,
*PLOT,FREQ=2

```

```

LIFT5 - M17 - 2D MODEL
*DETAIL
0 01.4295 99,0.1140 01.4560 01.0
*CONTOUR
1,13, 300, 300.
2,13, 300, 300.
3,13, 500, 100.
14,9, 100, 300.
*DISPLACED
1,250
*END STEP
*STEP,AMP-STEP
LIFT5, DAY 22 (REL. DAY 2)
*STATIC, PTOL=10, DIRECT
12, 24
*DLOAD, OP=NEW
LIFT5, BY, 0.08714
*TEMPERATURE, FILE=17, BSTEP=9(INC=5), ESTEP=9(INC=8)
*END STEP
*STEP, AMP-STEP
LIFT5, DAY 23 (REL. DAY 4)
*STATIC, PTOL=10, DIRECT
24, 24
*TEMPERATURE, FILE=17, BSTEP=10(INC=2), ESTEP=10(INC=2)
*END STEP
*STEP, AMP-STEP
LIFT5, DAYS 24-25 (REL. DAY 4-5)
*STATIC, PTOL=10, DIRECT
48, 48
*TEMPERATURE, FILE=17, BSTEP=10(INC=6), ESTEP=10(INC=6)
*END STEP
*STEP, AMP-STEP
LIFT6 PLACED DAY 26 (REL. DAY 1)
*STATIC, PTOL=10, DIRECT
6, 24
*MODEL CHANGE, INCLUDE
LIFT6
*DLOAD
LIFT6B, P1, -6.2742
*TEMPERATURE, FILE=17, BSTEP=11(INC=1), ESTEP=11(INC=4)
*EL PRINT, ELSEI=LIFT6
1,1,1,1,
1,1,1,
2,2,1,2,
*PLOT, FREQ=2
LIFT6 - M17 - 2D MODEL
*DETAIL
0 01.4295 99,0.1140 01.4612 01.0
*CONTOUR
1,13, 300, 300.

```

```

2,13, 300, 300.
3,13, 500, 100.
14,9, 100, 300.
*DISPLACED
1,250.
*END STEP
*STEP,AMP-STEP
LIFT6, DAY 27 (REL. DAY 2)
*STATIC, PTOL=10, DIRECT
12, 24
*DLOAD, OP=NEW
LIFT6, BY, 0.08714
*TEMPERATURE, FILE=17, BSTEP=11(INC=5), ESTEP=11(INC=8)
*END STEP
*STEP, AMP-STEP
LIFT6, DAY 28 (REL. DAY 6)
*STATIC, PTOL=10, DIRECT
24, 24
*TEMPERATURE, FILE=17, BSTEP=12(INC=2), ESTEP=12(INC=2)
*END STEP
*STEP, AMP-STEP
LIFT6, DAYS 28-29 (REL. DAY 4-5)
*STATIC, PTOL=10, DIRECT
48, 48
*TEMPERATURE, FILE=17, BSTEP=12(INC=6), ESTEP=12(INC=6)
*END STEP
*STEP, AMP-STEP
LIFT7 PLACED DAY 31 (REL. DAY 1)
*STATIC, PTOL=10, DIRECT
6, 24
*MODEL CHANGE, INCLUDE
LIFT7
*DLOAD
LIFT7B, P1, -6.2742
*TEMPERATURE, FILE=17, BSTEP=13(INC=1), ESTEP=13(INC=4)
*EL PRINT, ELSEI=LIFT7
1,1,1,1,
1,1,1,
2,2,1,2,
*PLOT, FREQ=2
LIFT7 - M17 - 2D MODEL
*DETAIL
-0.01,4295,99,0.1140,01.4704,01.0
*CONTOUR
1,13, 300, 300.
2,13, 300, 300.
3,13, 500, 100.
14,9, 100, 300.
*DISPLACED
1,250

```

```

*END STEP
*STEP,AMP-STEP
LIFT7 DAY 32 (REL DAY 2)
*STATIC,PTOL=10,DIRECT
12.24
DLOAD OP=NEW
LIFT7 BY 0.08714
*TEMPERATURE,FILE=17,BSTEP=13(INC=5),ESTEP=13(INC=8)
*END STEP
*STEP,AMP-STEP
LIFT7 DAY 33 (REL DAY 3)
*STATIC,PTOL=10,DIRECT
24.24
*TEMPERATURE,FILE=17,BSTEP=14(INC=6),ESTEP=14(INC=2)
*END STEP
*STEP,AMP-STEP
LIFT7 DAYS 34 35 (REL DAY 4-5)
*STATIC,PTOL=10,DIRECT
*TEMPERATURE,FILE=17,BSTEP=14(INC=6),ESTEP=14(INC=6)
*END STEP
*STEP,AMP-STEP
LIFT8 PLACED DAY 36 (REL DAY 1)
*STATIC,PTOL=10,DIRECT
6.24
*MODEL CHANGE,INCLUDE
LIFT8
*DLOAD
LIFT8B,P1,4,1828
*TEMPERATURE,FILE=17,BSTEP=15(INC=1),ESTEP=15(INC=4)
*EL PRINT,ELSET=LIFT8
1.1,1.1,
1.1,1.1,
2.2,1.2,
*PLOT,FREQ=2
LIFT8 M17 - 2D MODEL
*DETAIL
0 01 4295 99.0,1140 01,4752 01.0
*CONTOUR
1.11,300,300
2.13,300,300
3.13,500,100
14.9,100,300
*DISPLACED
1.250
*END STEP
*STEP,AMP-STEP
LIFT8 DAY 37 (REL DAY 2)
*STATIC,PTOL=10,DIRECT
12.24
*DLOAD,OP=NEW

```

```

LIFT8,BY,0.08714
*TEMPERATURE,FILE=17,BSTEP=15(INC=5),ESTEP=15(INC=8)
*END STEP
*STEP,AMP-STEP
LIFT8 DAY 38 (REL DAY 8)
*STATIC,PTOL=10,DIRECT
24.24
*TEMPERATURE,FILE=17,BSTEP=16(INC=2),ESTEP=16(INC=2)
*END STEP
*STEP,AMP-STEP
LIFT8,DAYS 39-40 (REL DAY 4-5)
*STATIC,PTOL=10,DIRECT
48.48
*TEMPERATURE,FILE=17,BSTEP=16(INC=6),ESTEP=16(INC=6)
*END STEP
*STEP,AMP-STEP
LIFT9 PLACED DAY 41 (REL DAY 1)
*STATIC,PTOL=10,DIRECT
6.24
*MODEL CHANGE,INCLUDE
LIFT9
*DLOAD
LIFT9B,P1,4,7056
*TEMPERATURE,FILE=17,BSTEP=17(INC=1),ESTEP=17(INC=4)
*EL PRINT,ELSET=LIFT9
1.1,1.1,
1.1,1.1,
2.2,1.2,
*PLOT,FREQ=2
LIFT9 M17 - 2D MODEL
*DETAIL
-0.01,4295.99,0,1140.01,4806.01,0
*CONTOUR
1.13,300,300
2.13,300,300
3.13,500,100
14.9,100,300
*DISPLACED
1.250
*END STEP
*STEP,AMP-STEP
LIFT9 DAY 42 (REL DAY 2)
*STATIC,PTOL=10,DIRECT
12.24
*DLOAD,OP=NEW
LIFT9,BY,0.08714
*TEMPERATURE,FILE=17,BSTEP=17(INC=5),ESTEP=17(INC=8)
*END STEP
*STEP,AMP-STEP
LIFT9 DAY 43 (REL DAY 3)

```

```

*STATIC,PTOL=10,DIRECT
24,24
*TEMPERATURE,FILE=17,BSTEP=18(INC=2),ESTEP=18(INC=2)
*END STEP
*STEP,AMP=STEP
LIFT9,DAYS 44-45 (REL. DAY 4-5)
*STATIC,PTOL=10,DIRECT
48,48
*TEMPERATURE,FILE=17,BSTEP=18(INC=6),ESTEP=18(INC=6)
*END STEP
*STEP,AMP=STEP
LIFT10 PLACED DAY 46 (REL. DAY 1)
*STATIC,PTOL=10,DIRECT
6,24
*MODEL CHANGE,INCLUDE
LIFT10
*DLOAD
LIFT108,P1,-5,2282
*TEMPERATURE,FILE=17,BSTEP=19(INC=1),ESTEP=19(INC=4)
*EL PRINT,ELSET=LIFT10
1,1,1,1,
1,1,1,1,
2,2,1,1,2,
*PLOT,FREQ=2
LIFT10 - M17 - 2D MODEL
*DETAIL
0,001,4296,0,1140,01,4866,01,0
*CONTOUR
1,13,300,300,3
2,13,300,300,3
3,13,300,300,3
14,13,300,300,3
*DISPLACED
1,250
*END STEP
*STEP,AMP=STEP
LIFT10, DAY 47 (REL. DAY 2)
*STATIC,PTOL=10,DIRECT
12,24
*DLOAD,OP=NEW
LIFT10,BY,-0,08714
*TEMPERATURE,FILE=17,BSTEP=19(INC=5),ESTEP=19(INC=8)
*END STEP
*STEP,AMP=STEP
LIFT10, DAY 48 (REL. DAY 3)
*STATIC,PTOL=10,DIRECT
24,24
*TEMPERATURE,FILE=17,BSTEP=20(INC=2),ESTEP=20(INC=2)
*END STEP
*STEP,AMP=STEP

```

```

LIFT10,DAYS 49-50 (REL. DAY 4-5)
*STATIC,PTOL=10,DIRECT
48,48
*TEMPERATURE,FILE=17,BSTEP=20(INC=6),ESTEP=20(INC=6)
*END STEP
*STEP,AMP=STEP
LIFT11 PLACED DAY 51 (REL. DAY 1)
*STATIC,PTOL=10,DIRECT
6,24
*MODEL CHANGE,INCLUDE
LIFT11
*DLOAD
LIFT118,P1,-5,2282
*TEMPERATURE,FILE=17,BSTEP=21(INC=1),ESTEP=21(INC=4)
*EL PRINT,ELSET=LIFT11
1,1,1,1,
1,1,1,1,
2,2,1,1,2,
*PLOT,FREQ=2
LIFT11 - M17 - 2D MODEL
*DETAIL
0,001,4296,0,1140,01,4926,01,0
*CONTOUR
1,13,300,300,3
2,13,300,300,3
3,13,300,300,3
14,13,300,300,3
*DISPLACED
1,250
*END STEP
*STEP,AMP=STEP
LIFT11, DAY 52 (REL. DAY 2)
*STATIC,PTOL=10,DIRECT
12,24
*DLOAD,OP=NEW
LIFT11,BY,-0,08714
*TEMPERATURE,FILE=17,BSTEP=21(INC=5),ESTEP=21(INC=8)
*END STEP
*STEP,AMP=STEP
LIFT11, DAY 53 (REL. DAY 3)
*STATIC,PTOL=10,DIRECT
24,24
*TEMPERATURE,FILE=17,BSTEP=22(INC=2),ESTEP=22(INC=2)
*END STEP
*STEP,AMP=STEP
LIFT11,DAYS 54-55 (REL. DAY 4-5)
*STATIC,PTOL=10,DIRECT
48,48
*TEMPERATURE,FILE=17,BSTEP=22(INC=6),ESTEP=22(INC=6)
*END STEP

```


<Start lift 12

```
*STEP,AMP=STEP
LIFT12 PLACED DAY 56 (REL. DAY 1)
*STATIC,PTOL=10,DIRECT
6.24
*MODEL CHANGE,INCLUDE
LIFT12
*DLOAD
LIFT12B,P1,-5.2282
*TEMPERATURE,FILE=17,BSTEP=23(INC=1),ESTEP=23(INC=4)
*EL PRINT,ELSET=LFT112
1.1.1.1,
1.1.1,
2.2.1.2,
*PLOT,FREQ=2
LIFT12 - M17 - 2D MODEL
*DETAIL
-0.001,4296.,0.,1140.01,4986.01,0.
*CONTOUR
1.13,-300.,300.,3
2.13,-300.,300.,3
3.13,-300.,300.,3
14.13,-300.,300.,3
*DISPLACED
1.250
*END STEP
*STEP,AMP=STEP
LIFT12,DAY- 57 (REL. DAY 2)
*STATIC,PTOL=10,DIRECT
12.24
*DLOAD,OP=NEW
LFT12,BY,-0.08714
*TEMPERATURE,FILE=17,BSTEP=23(INC=5),ESTEP=23(INC=8)
*END STEP
*STEP,AMP=STEP
LIFT12,DAY 58 (REL. DAY 3)
*STATIC,PTOL=10,DIRECT
24.24
*TEMPERATURE,FILE=17,BSTEP=24(INC=2),ESTEP=24(INC=2)
*END STEP
*STEP,AMP=STEP
LIFT12,DAYS 59 60 (REL. DAY 4-5)
*STATIC,PTOL=10,DIRECT
48.48
*TEMPERATURE,FILE=17,BSTEP=24(INC=6),ESTEP=24(INC=6)
*END STEP
*STEP,AMP=STEP
LIFT13 PLACED DAY 61 (REL. DAY 1)
*STATIC,PTOL=10,DIRECT
6.24
*MODEL CHANGE,INCLUDE
LIFT13
*EL PRINT,ELSET=LFT113
1.1.1.1,
1.1.1,
2.2.1.2,
*PLOT,FREQ=2
LIFT13 - M17 - 2D MODEL
*DETAIL
-0.001,4296.,0.,1140.01,5046.01,0.
*CONTOUR
1.13,-300.,300.,3
2.13,-300.,300.,3
3.13,-300.,300.,3
14.13,-300.,300.,3
*DISPLACED
1.250
*END STEP
*STEP,AMP=STEP
LIFT13,DAY 62 (REL. DAY 2)
*STATIC,PTOL=10,DIRECT
12.24
*DLOAD,OP=NEW
LFT13,BY,-0.08714
*TEMPERATURE,FILE=17,BSTEP=25(INC=5),ESTEP=25(INC=8)
*END STEP
*STEP,AMP=STEP
LIFT13,DAY 63 (REL. DAY 3)
*STATIC,PTOL=10,DIRECT
24.24
*TEMPERATURE,FILE=17,BSTEP=26(INC=2),ESTEP=26(INC=2)
*END STEP
*STEP,AMP=STEP
LIFT13,DAYS 64-65 (REL. DAY 4-5)
*STATIC,PTOL=10,DIRECT
48.48
*TEMPERATURE,FILE=17,BSTEP=26(INC=6),ESTEP=26(INC=6)
*END STEP
*STEP,AMP=STEP
LIFT14 PLACED DAY 66 (REL. DAY 1)
*STATIC,PTOL=10,DIRECT
6.24
*MODEL CHANGE,INCLUDE
LIFT14
*DLOAD
LIFT14B,P1,-5.2282
*TEMPERATURE,FILE=17,BSTEP=27(INC=1),ESTEP=27(INC=4)
*EL PRINT,ELSET=LFT114
```

Page 19 of 23

LIFT13.

```
*DLOAD
LIFT13B,P1,-5.2282
*TEMPERATURE,FILE=17,BSTEP=25(INC=1),ESTEP=25(INC=4)
*EL PRINT,ELSET=LFT113
1.1.1.1,
1.1.1,
2.2.1.2,
*PLOT,FREQ=2
LIFT13 - M17 - 2D MODEL
*DETAIL
-0.001,4296.,0.,1140.01,5046.01,0.
*CONTOUR
1.13,-300.,300.,3
2.13,-300.,300.,3
3.13,-300.,300.,3
14.13,-300.,300.,3
*DISPLACED
1.250
*END STEP
*STEP,AMP=STEP
LIFT13,DAY- 62 (REL. DAY 2)
*STATIC,PTOL=10,DIRECT
12.24
*DLOAD,OP=NEW
LFT13,BY,-0.08714
*TEMPERATURE,FILE=17,BSTEP=25(INC=5),ESTEP=25(INC=8)
*END STEP
*STEP,AMP=STEP
LIFT13,DAY 63 (REL. DAY 3)
*STATIC,PTOL=10,DIRECT
24.24
*TEMPERATURE,FILE=17,BSTEP=26(INC=2),ESTEP=26(INC=2)
*END STEP
*STEP,AMP=STEP
LIFT13,DAYS 64-65 (REL. DAY 4-5)
*STATIC,PTOL=10,DIRECT
48.48
*TEMPERATURE,FILE=17,BSTEP=26(INC=6),ESTEP=26(INC=6)
*END STEP
*STEP,AMP=STEP
LIFT14 PLACED DAY 66 (REL. DAY 1)
*STATIC,PTOL=10,DIRECT
6.24
*MODEL CHANGE,INCLUDE
LIFT14
*DLOAD
LIFT14B,P1,-5.2282
*TEMPERATURE,FILE=17,BSTEP=27(INC=1),ESTEP=27(INC=4)
*EL PRINT,ELSET=LFT114
```

Page 20 of 23

```

1.1.1.1.
1.1.1.
2.2.1.2.
*PLOT,FREQ=2
LIFT14 - M17 - 2D MODEL
*DETAIL
0.001,4296,0,1140.01,5106.01,0.
*CONTOUR
1.13,-300,300,3
2.13,-300,300,3
3.13,-300,300,3
14.13,-300,300,3
*DISPLACED
1,250
*END STEP
*STEP,AMP=STEP
LIFT14, DAY- 67 (REL. DAY 2)
*STATIC,PTOL=10,DIRECT
12,24
*DLOAD,OP=NEW
LIFT14,BY,-0.08714
*TEMPERATURE,FILE=17,BSTEP=27(INC=5),ESTEP=27(INC=8)
*END STEP
*STEP,AMP=STEP
LIFT14, DAY 68 (REL. DAY 3)
*STATIC,PTOL=10,DIRECT
24,24
*TEMPERATURE,FILE=17,BSTEP=28(INC=2),ESTEP=28(INC=2)
*END STEP
*STEP,AMP=STEP
LIFT14,DAYS 69-70 (REL. DAY 4-5)
*STATIC,PTOL=10,DIRECT
48,48
*TEMPERATURE,FILE=17,BSTEP=28(INC=6),ESTEP=28(INC=6)
*END STEP
*STEP,AMP=STEP
LIFT15 PLACED DAY 71 (REL. DAY 1)
*STATIC,PTOL=10,DIRECT
6,24
*MODEL CHANGE,INCLUDE
LIFT15,
*DLOAD
LIFT15B,P1,5 2282
LIFT15F,P1,-2 0914
*TEMPERATURE,FILE=17,BSTEP=29(INC=1),ESTEP=29(INC=4)
*EL PRINT,ELSET=LIFT15
1.1.1.1.
1.1.1.
2.2.1.2.
*PLOT,FREQ=2

```

```

LIFT15 - M17 - 2D MODEL
*DETAIL
0.001,4296,0,1140.01,5166.01,0.
*CONTOUR
1.13,-300,300,3
2.13,-300,300,3
3.13,-300,300,3
14.13,-300,300,3
*DISPLACED
1,250
*END STEP
*STEP,AMP=STEP
LIFT15, DAY- 72 (REL. DAY 2)
*STATIC,PTOL=10,DIRECT
12,24
*DLOAD,OP=NEW
LIFT15,BY,-0.08714
*TEMPERATURE,FILE=17,BSTEP=29(INC=5),ESTEP=29(INC=8)
*END STEP
*STEP,AMP=STEP
LIFT15, DAY 73 (REL. DAY 3)
*STATIC,PTOL=10,DIRECT
24,24
*TEMPERATURE,FILE=17,BSTEP=30(INC=2),ESTEP=30(INC=2)
*END STEP
*STEP,AMP=STEP
LIFT15,DAYS 74-75 (REL. DAY 4-5)
*STATIC,PTOL=10,DIRECT
48,48
*TEMPERATURE,FILE=17,BSTEP=30(INC=6),ESTEP=30(INC=6)
*END STEP
*STEP,AMP=STEP
LIFT16 PLACED DAY 76 (REL. DAY 1)
*STATIC,PTOL=10,DIRECT
6,24
*MODEL CHANGE,INCLUDE
LIFT16,
*DLOAD
LIFT16,P1,-4.1828
*TEMPERATURE,FILE=17,BSTEP=31(INC=1),ESTEP=31(INC=4)
*EL PRINT,ELSET=LIFT16
1.1.1.1.
1.1.1.
2.2.1.2.
*PLOT,FREQ=2
LIFT16 - M17 - 2D MODEL
*DETAIL
0.001,4296,0,1140.01,5214.01,0.
*CONTOUR
1.13,-300,300,3

```

```
2,13,-300,300,3
1,13,-300,300,3
14,13,-300,300,3
*DISPLACED
1,250
*END STEP
*STEP.AMP-STEP
LIFT16.DAY- 77 (REL DAY 2)
*STATIC.PTOL=10.DIRECT
12,24
*DLOAD,OP=NEW
LFT116.BY,0.08714
*TEMPERATURE,FILE=17,BSTEP=31(INC=5),ESTEP=31(INC=8)
*END STEP
*STEP.AMP-STEP
LIFT16.DAY 78 (REL DAY 3)
*STATIC.PTOL=10.DIRECT
24,24
*TEMPERATURE,FILE=17,BSTEP=32(INC=2),ESTEP=32(INC=2)
*END STEP
*STEP.AMP-STEP
LIFT16.DAYS 79-80 (REL DAY 4-5)
*STATIC.PTOL=10.DIRECT
48,48
*TEMPERATURE,FILE=17,BSTEP=32(INC=6),ESTEP=32(INC=6)
*END STEP
```

APPENDIX E: ABAQUS JOB CONTROL LANGUAGE FILES
USED WITH CYBERNET SYSTEM
FOR TEMPERATURE AND STRESS ANALYSES OF MONOLITH L-17

CYBERNET JOB CONTROL LANGUAGE FILE USED IN ABAQUS THERMAL ANALYSES (L-17)

```
/JOB
ABAQ,T20000,P2.
/USER
/CHARGE
PURGE,L7TT8/NA.
PURGE,L7TPLOT/NA.
PURGE,L7TREST/NA.
DEFINE,TAPE12-L7TREST.
DEFINE,TAPE8-L7TT8.
GET,TAPE15-L7TN.
GET,TAPE16-L7TE.
BEGIN,,ABAQUS,I-L7TD,TEXT-N,APLOT-Y,USUB-Y,INSUB-LDFLUX.
DEFINE,L7TPLOT.
REWIND,NPFILEA.
COPYBF,NPFILEA,L7TPLOT.
EXIT.
DEFINE,L7TPLOT.
REWIND,NPFILEA.
COPYBF,NPFILEA,L7TPLOT.
/EOR
/EOF
```

L7TN=node file
L7TE=element file
L7TD=command file
LDFLUX=heat subr.

CYBERNET JOB CONTROL LANGUAGE FILE USED IN ABAQUS STRESS ANALYSES (L-17)

```
/JOB
ABAQ,T30000,P2.
/USER
/CHARGE
ATTACH,TAPE17-L7TT8.
PURGE,L7SRES/NA.
PURGE,L7SPLOT/NA.
DEFINE,TAPE12-L7SRES.
GET,TAPE15-L7SN.
GET,TAPE16-L7SE.
BEGIN,,ABAQUS,I-L7SD,TEXT-N,APLOT-Y,USUB-Y,INSUB-L7SUBS.
DEFINE,L7SPLOT.
REWIND,NPFILEA.
COPYBF,NPFILEA,L7SPLOT.
REWIND,TAPE35.
COPY,TAPE35.
REPLACE,TAPE35-L7ST35.
EXIT.
DEFINE,L7SPLOT.
REWIND,NPFILEA.
COPYBF,NPFILEA,L7SPLOT.
REWIND,TAPE35.
COPY,TAPE35.
```

L7SN=node file
L7SE=element file
L7SD=command file
L7SUBS=modulus subr.

APPENDIX F: ABAQUS HEAT GENERATION SUBROUTINE DFLUX,
FILE "LDFLUX" USED IN 2-D, L-17 ANALYSIS

```

SUBROUTINE DFLUX(FLUX,TEMP,KSTEP,KINC,TIME,NOEL,NPT,COORDS,
&                JLTYP)
DIMENSION COORDS(3),Q(23),T(23)
COMMON /ELDEF/ STIME(316)
DATA ENTIME/960.1/
DATA NQ/23/
DATA T/ 6., 12., 18., 24., 30., 36., 42., 48.,
&      60., 72., 84., 96., 120., 168., 240., 288.,
&      360., 408., 480., 528., 600., 720., 960./
DATA Q/0.017385, 0.015158, 0.011682, 0.010309, 0.00800,
&      0.006862, 0.005795, 0.004910, 0.003263, 0.002897,
&      0.002211, 0.002059, 0.001357, 0.000980, 0.000628,
&      0.000507, 0.000368, 0.000305, 0.000241, 0.000214,
&      0.000201, 0.000175, 0.000118/
DATA STIME/
&      28*0.0,14*0.0,28*120.0,28*240.0,28*360.0,22*480.0,16*600.0,
&      16*720.0,16*840.0,16*960.0,16*1080.0,16*1200.0,16*1320.0,
&      16*1440.0,16*1560.0,16*1680.0,8*1800.0/
C *****
C VERSION OF USER SUBROUTINE "DFLUX" USED FOR MONOLITH L-17, 2-D MODEL
C *****
C VARIABLE DEFINITIONS-
C
C ENTIME - END OF RELATIVE HEAT GENERATION TIME + SMALL TOLERANCE (HR)
C
C NQ      - NO. OF HEAT GENERATION RATE POINTS
C
C T       - RELATIVE HEAT GENERATION TIME POINTS
C
C Q       = HEAT GENERATION POINT
C
C STIME  - VECTOR CONTAINING PLACEMENT TIME FOR EACH ELEMENT
C
C FLUX   - HEAT GENERATION RATE RETURNED TO PROGRAM
C
C
C      TREL = TIME - STIME(NOEL)
C      IF( TREL.GT.0.0.AND.TREL.LT.ENTIME ) GO TO 10
C      FLUX = 0.0
C      RETURN
C
C 10 CONTINUE
C      FLUX = 0.0
C      DO 20 I=1,NQ
C      J = I
C      IF( TREL.LE.T(I) ) GO TO 30
C 20 CONTINUE
C
C      WRITE(6,35) KSTEP,KINC,TIME,NOEL
C 35 FORMAT(/," WARNING - PASSED THROUGH DFLUX WITHOUT ASSIGNING",
&         /,"          FLUX. STEP =",I5," INC =",I5,
&         /,"          TIME =",F12.2," ELEMENT =",I5)
C      RETURN
C 30 FLUX = Q(J)
C      RETURN
C      END

```

APPENDIX G: ABAQUS USER SUBROUTINE MPC,
2-D MULTIPLE POINT CONSTRAINT
VERSION USED WITH MONOLITH L-17


```

SUBROUTINE MPC(UE,A,JDOF,N,JTYPE,X,U,NMPCE)
C
  DIMENSION A(N),JDOF(N),X(6,N),U(6,N)
  COMMON/COUNT/KINC,MINC,KITER,MITER,FATIME,ATIME,DATIME,
  1 CTIME,DCTIME,DTIME,DDTIME,HTIME,DHTIME,DDTPRE,DATPRE,HTIM1,
  2 DHTIM2,EXFAC,KSTEP,KCUTS,MCUTS,NUMBER,LSHAF1,LCUTBK,DTNEWS,
  3 KITGEN,KMDINC,TTIME,DTMIN,DTMAX,MITEIG,MITXXX,STIME,DSTIME
  4,TPREV,TNEW,TOLD,TEND
C
C *****
C SUBROUTINE MPC USED WITH L-17 2-D ANALYSIS. MPC IS MERGED WITH
C SUBROUTINE UMAT1 OR UMAT2 IN FILES "L7SUBS" AND "L7SUBN, RESPECTIVELY
C *****
C
C     FIX NODES ACROSS TOP OF VOID DURING PLACEMENT OF LIFT 8
C     STEPS 29,30,31,32,33, AND 34
C
C
C     IF(KSTEP.EQ.29.AND.JTYPE.EQ.101) GO TO 10
C     IF(KSTEP.EQ.30.AND.JTYPE.EQ.101) GO TO 10
C     IF(KSTEP.EQ.31.AND.JTYPE.EQ.101) GO TO 10
C     IF(KSTEP.EQ.32.AND.JTYPE.EQ.101) GO TO 10
C     IF(KSTEP.EQ.33.AND.JTYPE.EQ.101) GO TO 10
C     IF(KSTEP.EQ.34.AND.JTYPE.EQ.101) GO TO 10
C
C
C     NMPCE = 0
C     RETURN
10  CONTINUE
C
C     B1 = X(1,3) - X(1,2)
C     B2 = X(1,3) - X(1,1)
C     B3 = X(1,1) - X(1,2)
C
C     UE = (B2*U(2,2) - B3*U(2,3))/B1
C
C     A(1) = B1
C     A(2) = -B2
C     A(3) = -B3
C     JDOF(1) = 2
C     JDOF(2) = 2
C     JDOF(3) = 2
C
C     RETURN
C     END

```

ABAQUS USER SUBROUTINE MPC, 2-D MULTIPLE POINT CONSTRAINT USED WITH L-17

APPENDIX H: MATERIAL USER SUBROUTINE UMAT,
VERSION "UMAT1", 2-D MODULUS ROUTINE WITHOUT CREEP
USED WITH MONOLITH L-17

```

SUBROUTINE UMAT(STRESS,STATEV,DSDDDE,SSE,SPD,SGD,STRAN,DSITKAN,
1 TIME,DTIME,TEMP,DTEMP,PREDDEF,DPRED,MATERL,NDI,NSHR,NTENS,
1 NSTATV,PROPS,NPROPS,COORDS)
DIMENSION STRESS(NTENS),STATEV(NSTATV),DSDDDE(NTENS,NTENS),
1 STRAN(NTENS),DSITKAN(NTENS),PREDDEF(1),DPRED(1),
1 PROPS(NPROPS),COORDS(3)
DIMENSION EPSTH(6)
C
C ADD COMMON BLOCK COUNT TO GET STEP AND INCREMENT NUMBERS
COMMON/COUNT/KINC,XXX(17),KSTEP,XXXX(19)
C
COMMON /EVALX/ EV(16),RT(16),YEL(17),ICONT,IX
DATA RT/0.120,0.240,0.360,0.480,0.600,0.720,0.840,0.960,
6 1080,1200,1320,1440,1560,1680,1800 /
DATA YEL/4296,4332,4380,4434,4488,4560,4632,4704,4752,
6 4806,4866,4926,4986,5046,5106,5166,5214 /
DATA EV/16*0 0/
DATA IX/100/
C
C IX IS SET TO 100 SO THE E(MATERL) WILL BE PRINTED ON 1ST PASS
C
C ALWAYS PUT ALL USER MATERIALS BEFORE ANY OTHER MATERIAL
C 50 THEY WILL BE NUMBERED FIRST!!!!!!
C
C *****
C THIS SUBROUTINE UMAT IS SET UP FOR THE L-17 2-D MODEL AND IS
C MEANED WITH SUBROUTINE MFC TO COMPRISE FILE- "L7SUBS"
C *****
C SUBROUTINE FOR TIME DEPENDENT MODULUS OF ELASTICITY
C DSIG=U*(EPS-DEPSTH)
C SIG=SIG+DSIG
C WHERE D-D AT TIME I+DT/2
C PROPS(NPROPS) CONTAINS COEFFICIENT OF THERMAL EXPANSION
C NUMBER OF POINTS ON DTIME CURVE IS (NPROPS-0)/3
C STORED AS E, V, TIME
C
C IPRINT = 0
C IF(IPRINT GT 0) WRITE(6,9999) NDI,NSHR,NTENS,NPROPS
C IF(IPRINT GT 0) WRITE(6,8888) PROPS
C IF(IPRINT GT 0) WRITE(6,8888) TEMP,DTEMP,TIME,DTIME
C CALCULATE THERMAL STRAINS
C DEPSTH=PROPS(NPROPS)*DTEMP
C DO 5 K1=1,6
C EPSTH(K1)=0
C IF(K1 LE NDI) EPSTH(K1)=DEPSTH
C 5 CONTINUE
C
C CALCULATE E AND V AT TIME VTIME+DTIME

```

```

REL=0.0
DO 777 I11=1,9
I111=I11+1
IF(COORDS(2) GT YEL(I11).AND.COORDS(2).LE.YEL(I111))REL=RT(I11)
777 CONTINUE
MPOINT=(NPROPS-1)/3.
I1=3
T=TIME+DTIME*0.5-REL
DO 10 K1=1,MPOINT
IF(T LT PROPS(I1)) GO TO 12
I1=I1+3
10 CONTINUE
12 CONTINUE
IF(K1 LE 1) GO TO 20
E=PROPS(I1)
V=PROPS(2)
GO TO 40
20 CONTINUE
IF(K1 LE MPOINT) GO TO 30
I1=MPOINT+3-2
E=PROPS(I1)
V=PROPS(I1+2)
GO TO 40
30 CONTINUE
I1=K1+3
I2=I1-3
DENOM=PROPS(I1)-PROPS(I2)
F1=(PROPS(I1)-I )/DENOM
F2=1-F1
E=F1*PROPS(I2-2)+F2*PROPS(I1-2)
V=F1*PROPS(I2-1)+F2*PROPS(I1-1)
40 CONTINUE
DO 50 K1=1,NTENS
DO 49 K2=1,NTENS
DSDDE(K1,K2)=0
49 CONTINUE
50 CONTINUE
C
C FORM D BASED ON NDI AND NSHR
C
C IF(NDI.EQ.0) GO TO 150
C IF(NDI.EQ.3) GO TO 103
C IF(NDI.EQ.2) GO TO 102
C DSDDE(1,1)=E
C GO TO 150
102 CONTINUE
TERM=E/(1.-V**2)
DSDDE(1,1)=TERM
DSDDE(2,1)=V*TERM

```

```

DSDSDE(1,2)=DSDSDE(2,1)
DSDSDE(2,2)=TERM
GO TO 150
103 CONTINUE
TERM=(1.-2.*V)*(1.+V)
TERM= E/TERM
DSDSDE(1,1)=TERM*(1.-V)
DSDSDE(2,1)=TERM*V
DSDSDE(1,2)=DSDSDE(2,1)
DSDSDE(2,2)=DSDSDE(1,1)
DSDSDE(3,3)=DSDSDE(1,1)
DSDSDE(1,3)=DSDSDE(2,1)
DSDSDE(2,3)=DSDSDE(2,1)
DSDSDE(3,1)=DSDSDE(2,1)
DSDSDE(3,2)=DSDSDE(2,1)
150 CONTINUE
IF(NSHR EQ 0) GO TO 200
G=E/(2.*(1.+V))
I1=NDI+1
DO 160 K1=1,NSHR
DSDSDE(11,11)=C
I1=I1+1
200 CONTINUE
DO 300 K1=1,NTENS
DSIG=0
DO 290 K2=1,NTENS
DSIG=DSIG+DSDSDE(K1,K2)*(DSTRAN(K2)-EPSTH(K2))
290 CONTINUE
STRESS(K1)=STRESS(K1)+DSIG
SSE=SSE+(DSTRAN(K1)+EPSTH(K1))*(STRESS(K1)-DSIG+0.5)
300 CONTINUE
C IF(1PRINT GT 0) WRITE(6,8888) E,V,SSE
C IF(1PRINT GT 0) WRITE(6,8888) STRESS,STRAN,DSTRAN
C IF(1PRINT GT 0) WRITE(6,8888) DSDSDE
C99999 FORMAT(' UMAT',2016)
8888 FORMAT(2X,10E12.5)
8889 FORMAT(2X,15.2X,15.2X,15.2X,15.2X,3E12.5)
DO 778 III=1,9
IIII=IIII+1
IF(COORDS(2) GT YEL(IIII) AND COORDS(2) LE. YEL(IIII)) EV(IIII)=E
778 CONTINUE
IF(MATERL EQ IX) GO TO 400
WRITE(35,8889) KSTEP,KINC,MATERL,TIME,DTIME,EV(MAT+KL)
400 CONTINUE
IX = MATERL
RETURN
END

```

APPENDIX I: ABAQUS USER SUBROUTINE UMAT,
VERSION "UMAT2", AGING CREEP MODEL WITH SHRINKAGE
USED WITH MONOLITH L-17

```

SUBROUTINE UMAT,STRESS,STATEV,HH,SSE,SPD,SCD,TEPS,DEP,TIME,
$ DTIME,TEMP,UTEMP,PREDDEF,DPRED,MATERL,NDI,NSHR,INTENS,
$ NSTATV,PROPS,NPROPS,COOKUS)
IMPLICIT REAL (A-H,O-Z)
UMAT=1
CONCRETE MODEL WITH CREEP AND AGING
WITH IMPROVED CREEP AND AGING FACTORS
DATE: FEB 12, 1986
MODEL MODIFIED TO DISTRIBUTE INITIAL
SHRINKAGE LINEARLY BETWEEN 0 AND 1
DAYS AGE (INITIAL SHRINKAGE ACTUALLY
AN 1 DAY SHRINKAGE RATE)
MODIFIED BY: ROY L CAMPBELL, SR
DATE: FEB 24, 1986
COMMON // SINT(1)
COMMON /CELGI/ IDUM(7),IEDBR,JDUM(96)
COMMON /BLKH/ ALFAC,ALFAS,CRUSH,TREF,DJ,ECONC,ESTEEL,
$ ITER,NT,MDJUNT,M14,NCHECK,XVC,YSTEEL,
$ AN,LE,EPFSTR,EPSEFF,KRAC,SG(8),TF(4),V(8)
COMMON /BLKI/ H(4,4),STR(4),XV,YIELD,EPFRAC
DIMENSION STRESS(NTENS),AR(20,3),PH(4,4),EP(4),EPST(4),
$ DTIME(2),PROPS(NPROPS),TEPS(NTENS),DEP(NTENS),HH(NTENS,INTENS),
$ NPRINT(100),STATEV(1),IORDER(3)
LOGICAL FIRST(100),IPRINT,FIRSTE,ONEELM
DATA FIRST/100* TRUE /, NPASS/0/, MPRINT/0/, INTI/0/,
$ JELNOI/0/, NOUT/0/, FIRSTE/ TRUE /, JELNOL/0/, INTI/0/,
$ IORDER/1,3,2/, NINTI/0/, NSTEP/0/, ONEELM/ FALSE ./
DATA IAR/AR 11(S11 -), AR 21(S22 -), AR 31(S33 -),
$ AR 41(S13 -), AR 51(S31 -), AR 61(S23 -),
$ AR 71(E11 -), AR 81(E22 -), AR 91(E33 -),
$ AR101(E13 -), AR111(S11 +), AR121(S22 +),
$ AR131(TMP -), AR141(EFS -), AR151(PLA -),
$ AR161(CRK -), AR171(EPS11), AR181(EPS22),
$ AR191(EPS33), AR201(EPS13),
$ AR 12(S11 +), AR 22(S22 +), AR 32(S33 +),
$ AR 42(S13 +), AR 52(A1 -), AR 62(A2 -),
$ AR 72(ANG1 -), AR 82(ANG2 -), AR 92(ANG3 -),
$ AR102(E PHD), AR112(S YLD), AR122(EFN -),
$ AR132(TMP +), AR142(EFS +), AR152(PLA +),
$ AR162(CRK +), AR172(CK1 +), AR182(CK2 +),

```

```

$ AR192(CK3 +), AR202(UMATAGE) /
AR(,3) USED FOR INTERNAL CREEP VARIABLES
AR(17,1): EPSILON XX(RR)--STRAIN IN X (OR R) DIRECTION
AR(18,1): EPSILON ZZ(TT)-- " " " " OUT OF PLANE (OR HOOP) DIRECTION
AR(19,1): EPSILON YY(ZZ)-- " " " " Y (OR Z) DIRECTION
AR(20,1): EPSILON XY(RZ)-- SHEAR STRAIN
THESE ARE THE PHYSICAL COMPONENTS OF STRAIN.
THEY ARE EQUAL TO : (DU/DX) - (ALFA*DT) - (SHRINKAGE)
ABAQUS STRAINS ARE: (DU/DX)
SAVTIM=TIME
TIME=TIME/24.
SAVDI=DELTM
DELTM=DELTM/24.
CALL ACOFPI(SINT(IEDBR+1),JELNO,1)
IF (FIRSTE) THEN
JELNO1=JELNO
FIRSTE=.FALSE.
ENDIF
IF (NPROPS.LT.9) THEN
WRITE(NOUT,20) NPROPS
FORMAT('OTHER UMAT(AGE) SUBROUTINE MUST HAVE NPROPS .GE. ',
$ 9, NPROPS = ',15)
STOP 'TOO FEW NPROPS FOR UMAT(AGE)'
ENDIF
IF (NSTATV.LT.60) THEN
WRITE(NOUT,30) NSTATV
FORMAT('OTHER UMAT(AGE) SUBROUTINE MUST HAVE NSTATV.GE. ',
$ 60, NSTATV = ',15)
STOP 'TOO FEW NSTATV FOR UMAT(AGE)'
ENDIF
N=0
DO 40 J=1,3
DO 40 I=1,20
N=N+1
40 AR(I,J)=STATEV(N)
AR(13,1)=TEMP
AR(13,2)=TEMP+DTEMP
AR(20,2)=0.0
ECONC=PROPS(1)
XVC=PROPS(2)
CRUSH=PROPS(3)

```

```

C      ECONC=ELASTIC MODULUS AT AGE = 3 DAYS
C      CRUSH=ULTIMATE STRENGTH AT AGE = 3 DAYS
C
C      EPERAC=PROPS(4)
C      ALFAC=PROPS(5)
C      AGE=PROPS(6)
C      IF (AGE LE 0.0) THEN
C        WRITE(NOUT,50) AGE
C        STOP 'UMAT(AGE) SUBROUTINE MUST HAVE AGE GT 0'
C      ENDIF
C      STOP 'UMAT(AGE) AGE NOT POSITIVE'
C      ENDIF
C      SHRINK=PROPS(7)
C      CREEP=PROPS(8)
C      TREF=PROPS(9)
C      EPSHRK=PROPS(10)
C      IF (SHRINK LT 1.E-9) SHRINK=1.0
C      IF (CREEP LT 1.E-9) CREEP=1.0
C
C      SHRINK=SHRINKAGE MULTIPLIER - DEFAULT=1.0
C      CREEP=CREEP MULTIPLIER - DEFAULT=1.0
C
C      TIMREF=0
C      IF (NPROPS GE 11) TIMREF=PROPS(11)
C      IF (MATERL LE 100 AND FIRST(MATERL)) THEN
C        WRITE(NOUT,55) MATERL,NPROPS,ECONC,XVC,CRUSH,EPPFRAC,ALFAC,AGE,
C        SHRINK,CREEP,TREF,EPSHRK,TIMREF
C        $   FORMAT('UMAT(AGE) PROPERTIES'/' MATERL = ',15/' NPROPS = ',15/
C        $   ' ECONC = ',1PE11.3,' (PSI)/' XVC = ',0PF/3/' CRUSH = ',
C        $   1PE11.3,' (IN/IN)/' EPPFRAC = ',1PE11.3,' (IN/IN)/' ALFAC = ',
C        $   1PE11.3,' (IN/IN/DEG)/' AGE = ',1PE11.3,' (DAYS)/'
C        $   ' SHRINK = ',1PE11.3/' CREEP = ',1PE11.3/' TREF = ',1PE11.3,
C        $   ' (DEG)/' INITIAL SHRINKAGE = ',1PE11.3/' TIMREF = ',1PE11.3)
C        FIRST(MATERL)=FALSE
C      JPRINT 0
C      MPROPS=12
C      IF (NPROPS GE MPROPS) THEN
C        IPR NEAR(PROPS(MPROPS))
C        IF (IPR EQ 949) THEN
C          MPROPS=MPROPS+1
C          JPRINT-NEAR(PROPS(MPROPS))
C          IF (JPRINT LE 0 OR MPROPS LT (MPROPS+JPRINT)) THEN
C            WRITE(NOUT,60) MPROPS,JPRINT,MPROPS
C            FORMAT('BAD VALUES FOR PRINT CONTROL IN UMAT(A,E) '
C            ' MPROPS,JPRINT,MPROPS-',3I5)
C            STOP 'BAD VALUE OF PRINT CONTROL IN UMAT(A,E)'
C          ELSE
C            MPRINT=MIN(JPRINT,100)
C            DO 70 I=1,MPRINT
C
C      50      MPROPS=MPROPS+1
C      70      NPRINT(I)=NEAR(PROPS(MPROPS))
C            WRITE(NOUT,80) MPRINT,(NPRINT(I),I=1,MPRINT)
C            FORMAT('UMAT(AGE) INFORMATION PRINTED FOR THE FOLLOWING',
C            $   ' ELEMENTS. MPRINT = ',15/(5X,10I8))
C            ENDIF
C            ENDIF
C            IF (MPROPS LT MPROPS) WRITE(NOUT,90) (PROPS(I),I=1,MPROPS+1,
C            $   NPROPS)
C            $   FORMAT('UNRECOGNIZED USER PROPERTIES IN UMAT(AGE)')
C            ENDIF
C            $   (1P10E11.3))
C            ENDIF
C
C      ES=1.0
C      DTIM(1)=TIME-TIMREF
C      IF (DTIM(1).LT.0.0) THEN
C        DO 120 I=1,NTENS
C          STRESS(I)=0.0
C          DO 110 J=1,NTENS
C            HH(I,J)=0.0
C          110 HH(I,J)=0.0
C          120 HH(I,I)=ECONC
C          GO TO 900
C        ENDIF
C
C      DTIM(2)=DTIM(1)+DELTH
C      INCRMT=NEAR(AR(8,3))+1
C      NT=INCRMT
C      IF (NT.GT.2) NT=2
C
C      IF (INCRMT.EQ.1) THEN
C        DO 125 I=1,19
C          125 AR(1,2)=1.0
C        ENDIF
C
C      IF (NDI.EQ.3) THEN
C        M14=0
C        EPST(1)=TEPS(1)
C        EPST(2)=TEPS(3)
C        EPST(3)=TEPS(2)
C        EPST(4)=TEPS(4)
C        EP(1)=DEP(1)
C        EP(2)=DEP(3)
C        EP(3)=DEP(2)
C        EP(4)=DEP(4)
C        ELSE
C          M14=1
C          EPST(1)=TEPS(1)
C          EPST(3)=TEPS(2)

```

```

C      55      $   ECONC = ',1PE11.3,' (PSI)/' XVC = ',0PF/3/' CRUSH = ',
C      55      $   1PE11.3,' (IN/IN)/' EPPFRAC = ',1PE11.3,' (IN/IN)/' ALFAC = ',
C      55      $   1PE11.3,' (IN/IN/DEG)/' AGE = ',1PE11.3,' (DAYS)/'
C      55      $   ' SHRINK = ',1PE11.3/' CREEP = ',1PE11.3/' TREF = ',1PE11.3,
C      55      $   ' (DEG)/' INITIAL SHRINKAGE = ',1PE11.3/' TIMREF = ',1PE11.3)
C      FIRST(MATERL)=FALSE
C      JPRINT 0
C      MPROPS=12
C      IF (NPROPS GE MPROPS) THEN
C        IPR NEAR(PROPS(MPROPS))
C        IF (IPR EQ 949) THEN
C          MPROPS=MPROPS+1
C          JPRINT-NEAR(PROPS(MPROPS))
C          IF (JPRINT LE 0 OR MPROPS LT (MPROPS+JPRINT)) THEN
C            WRITE(NOUT,60) MPROPS,JPRINT,MPROPS
C            FORMAT('BAD VALUES FOR PRINT CONTROL IN UMAT(A,E) '
C            ' MPROPS,JPRINT,MPROPS-',3I5)
C            STOP 'BAD VALUE OF PRINT CONTROL IN UMAT(A,E)'
C          ELSE
C            MPRINT=MIN(JPRINT,100)
C            DO 70 I=1,MPRINT
C
C      60      $   MPROPS,JPRINT,MPROPS-',3I5)
C            STOP 'BAD VALUE OF PRINT CONTROL IN UMAT(A,E)'
C          ELSE
C            MPRINT=MIN(JPRINT,100)
C            DO 70 I=1,MPRINT

```

```

EPST(4)=TEPS(3)
EPST(2)=XVC*(EPST(1)+EPST(3))
EP(1)=DEP(1)
EP(3)=DEP(2)
EP(4)=DEP(3)
EP(2)=XVC*(EP(1)+EP(3))
ENDIF
C
ITER= 2
MOUNT= 1
NCHECK=1
C
IP (JELNO EQ JELNOL) THEN
INTI=INTI+1
SUM=0
DO 127 I=1,NTENS
SUM=SUM+ABS(DEP(I))
IF (SUM LT 1 E-12) THEN
NPASS=0
IF (INTI EQ 1) NSTEP=NSTEP+1
ELSE
IF (NINTI EQ 0) THEN
IF (JELNO EQ JELNOL) ONEELM=.TRUE.
NINTI=INTI-1
INTI=1
ENDIF
IF (INTI EQ 1) NPASS=NPASS+1
ENDIF
ENDIF
C
IP (JELNO EQ JELNOL) THEN
INTI=INTI+1
ELSE
INTI=1
ENDIF
IF (ONEELM) INT=INTI
C
IPRINT=.FALSE
IF (MOUNT GT 0 AND INT EQ 1) THEN
DO 130 I=1,MPRINT
IF (JELNO NE MPRINT(I)) GO TO 130
IPRINT=.TRUE
GO TO 140
130 CONTINUE
ENDIF
C
140 IF (IPRINT) WRITE(MOUT,160) JELNO,JELNOL,JELNOELM,NPASS,INCMT,
C NSTEP,INT,INTI,NINTI,NT,NDI,M14,ONEELM,SUM,AR
160 FORMAT('BEFORE STRAIN CALL JELNO,JELNOL,JELNOELM,NPASS,INCMT,
C NSTEP,INT,INTI,NINTI,NT,NDI,M14,ONEELM,SUM/AR-'/12I5,1X,111.

```

```

S IPEL1 3/(IPEIOE11.3)
C
CALL STRAIN(TEMP,DTEMP,DTIM,EP,EPST,PH,AR,AGE,SHRINK,CREEP,
.EPSHRK,SHRINK,TEMP1)
IF (NCHECK EQ 1) WRITE(6,161) DTIM(2),AR(13,1),AR(10,2),AR(9,2),
SAR(1,1),AR(3,1),AR(2,1),AR(17,1),AR(19,1),AR(18,1),AR(20,1),
SAR(16,1),AR(16,2),SHRINK,TEMP1
161 FORMAT(1X,
S F7.4,F6.1,F10.1,F5.0,F9.1,4F9.6,2F4.0,2F9.6)
C
AR(8,3)=AR(8,3)+1.0
C
DO 170 I=1,NDI
I1=IORDER(I)
STRESS(I)=AR(II,2)
HH(I,NTENS)=PH(II,4)
HH(NTENS,I)=PH(4,II)
DO 170 J=1,NDI
JJ=IORDER(J)
170 HH(I,J)=PH(II,JJ)
STRESS(NTENS)=AR(4,2)
HH(NTENS,NTENS)=PH(4,4)
C
IF (IPRINT) WRITE(MOUT,210) AR
210 FORMAT('AFTER STRAIN CALL. AR= '/(IPEIOE11.3))
C
N=0
DO 220 J=1,3
DO 220 I=1,20
M=M+1
220 STATEV(N)=AR(I,J)
C
900 JELNOL=JELNO
STATEV(40)=7HUMATAGE
IF (JELNO EQ JELNOL AND INTI.EQ.NINTI) INTI=0
C
TIME=SAVTIM
DELTA=SAVDI
RETURN
END
C
FUNCTION NEAR(X)
IMPLICIT REAL (A-H,O-Z)
NEAR=NINT(X)
RETURN
END
C
SUBROUTINE STRAIN(TEMP,DTEMP,DTIM,EP,EPST,PH,AR,AGE,SHRINK,CREEP,
EPSHRK,SHRINK,TEMP1)
IMPLICIT REAL (A-H,O-Z)

```



```

COMMON /BLKN/ ALFAC,ALFAS,CRUSH,DELT,DJ,ECONC,ESTEEL,ES,ITER,MT,
$ MOUNT,M14,NCHECK,XVC,YSTEEL,ANGLE,EFFSTR,EPSEFF,KRAC,SG(8),
$ TF(4),V(8)
COMMON /BLK1/ H(4,4),STR(4),XV,YIELD,EPFRAC
DIMENSION SIJ(4),EPP(4,4),H2(4,4),DIJ(4),TAU(4),TIJ(4),TA(4),EPS(4),
$ BF(4),B(4),FS(4),EPST(4),EP(4),PH(4,4),AR(20,3),DTIM(2)
$ S(4,3)
***** LIST OF VARIABLES PASSED TO SUBROUTINE FROM MAIN PROGRAM
C
C ALFAC = COEFFICIENT OF CONCRETE THERMAL EXPANSION
C ALFAS = COEFFICIENT OF REBAR THERMAL EXPANSION
C AR(I,J) = HISTORY VARIABLES
C CRUSH = YIELD STRESS
C DELT = REFERENCE (STRESS-FREE) TEMPERATURE
C ECONC = ELASTIC MODULUS
C EP(I,J) = 4 STRAIN INCREMENTS: RR OR XX, TT OR OUT OF PLANE,
$ ZZ OR YY, RZ OR XY
C EPST(I,J) = 4 STRAIN COMPONENTS: RR OR XX, TT OR OUT OF PLANE,
$ ZZ OR YY, RZ OR XY
C ES = THICKNESS(DEFAULT=1.0) FOR PLANE PROBLEMS
C ITER = 1. INTERMEDIATE ITERATION - NO UPDATING
$ = 2. FINAL ITERATION - ALL VARIABLES WILL BE UPDATED
$ ( NOTE: IF NEWTON ITERATION IS USED, OR IF NO
$ ITERATION, SET ITER=2 )
C MOUNT = ITERATION NUMBER IN A LOAD STEP
C M14 = 0, AXISYMMETRY
$ = 1, PLANE
C NCHECK = 0, STIFFNESS COMPUTATION
$ = 1, STRESS COMPUTATION
C NT = LOAD STEP NUMBER
C XVC = POISSON'S RATIO
***** LIST OF VARIABLES PASSED FROM SUBROUTINE TO MAIN PROGRAM
C
C ANGLE = ANGLE, IN DEGREE COUNTER CLOCKWISE, GIVING THE
$ DIRECTION OF THE MAXIMUM PRINCIPAL STRAIN OR
$ THE NORMAL TO THE CRACK SURFACE
C AR(I,J) = HISTORY VARIABLES
C EFFSTR = EFFECTIVE STRESS
C EPSEFF = EFFECTIVE STRAIN
C KRAC = CRACKING IDENTIFIER
C 1 IN FIRST DIGIT INDICATES MERIDIONAL CRACK
C 2 IN TENTH DIGIT INDICATES RADIAL CRACK
C 3 IN HUNDRETH DIGIT INDICATES ORTHOGONAL TO 1
C 0 IN ANY DIGIT INDICATES NO OR CLOSED CRACK
C PH(I,J) = 4*4 CONSTITUTIVE MATRIX
C S(4,3) = EIGHT STRESS COMPONENTS: RR,TT,ZZ,RZ,

```

```

C
C MAX PRINCIPAL STRESS, MIN. PRINCIPAL STRESS
C FIRST REBAR STRESS, SECOND REBAR STRESS
C TF(1) = INTERNAL STRESSES INCLUDING THERMAL STRESSES,
$ RR OR XX, TT, ZZ OR YY, RZ OR XY. THESE ARE
$ TO CONVERTED TO LOADS
C V(1) = EIGHT STRESS COMPONENTS: RR,TT,ZZ,RZ,
$ MAX PRINCIPAL STRAIN, MIN. PRINCIPAL STRAIN
$ FIRST REBAR STRAIN, SECOND REBAR STRAIN
C *****
C KT = 2
C INCRMT=NT
C IF (INCRMT.EQ.1) KT = 1
C AR(13,KT)=TEMP+DTEMP
C IF (KT.EQ.1) AR(13,2)=AR(13,1)
C DTEH=DTEMP
C IF(KT.EQ.1) DTEH=AR(13,2)-DELT
C MT = KT - 1
C IF(MT.EQ.0) MT = 1
C ALFAA=ALFAC
C ED=1.0
C IF(NCHECK.EQ.0.AND.M14.NE.0) ED=ES
C XV= XVC
C T= AR(13,KT)
C XK=1.0/(DTIM(INCRMT-1)+AGE)
C CALL COEF(XK,T,AGEFAC,TEMPAC)
C AGEFAC=AGEFAC*TEMPAC
C -----
C DAGE=1.0
C IF(INCRMT.EQ.1) GO TO 18
C XKM1=1.0/(DTIM(INCRMT-1)+AGE)
C TH1=AR(13,1)
C CALL COEF(XKM1,TH1,AGEM1,TEMPAC)
C AGEM1=AGEM1*TEMPAC
C DELAGE=AGEFAC-AGEM1
C DAGE=1.0*DELAGE/AGEM1
C 18 CONTINUE
C -----
C EPSEFF=AR(12,2)
C FACTR=-0.02
C IF(INCRMT.EQ.1) YIELD=CRUSH*AGEFAC
C IF(INCRMT.EQ.1) AR(11,2)=YIELD*SQRT(1.0+3.0*FACTR)
C IF(INCRMT.EQ.1) AR(10,2)=ECONC*AGEFAC
C 8/31/1985
C E1=AR(10,2)
C YIELD=AR(11,2)
C E1= AR(10,2)*DAGE
C YIELD= AR(11,2)*DAGE
C 8/31/1985
C ALFA=0.0

```

```

C 30 I 1.4
10 EPS(I) = EPST(I)
C
C CALCULATIONS OF ELEMENT STRAINS
C
DELTM = DTIM(INCRMT) * DTIM(INCRMT)
IF(INCRMT EQ 1) DELTM = DTIM(I)
SHRNK = 0
DSTRNK = 0
C
C MODIFIED BY CAMPBELL, FEB 24, 1986
IF(DTIM(INCRMT) LE 1.0) THEN
  SHRATE = EPSHRK
  DSHRNK = SHRATE * DELTM
  SHRNK = EPSHRK * DTIM(INCRMT)
GO TO 154
ENDIF
DTM = DTIM(INCRMT) 1.0
C
SHRATE = SHRNK * (204.91 * 0.15 * EXP(-0.15 * DTM)) + 145.09 * 0.0226348 *
EXP(-0.0226348 * DTM) * 1.E-6
DELTIM = DTIM(INCRMT) * DT 120.0) SHRATE = 0
DSTRNK = SHRATE * DELTM
IF(INCRMT EQ 1) DSHRNK = DSHRNK + EPSHRK
SHRNK = EPSHRK + SHRNK * (204.91 * 0.15 * EXP(-0.15 * DTM)) + 145.09 *
EXP(-0.0226348 * DTM) * 1.E-6
C
154 CONTINUE
C
C MODIFIED BY CAMPBELL, FEB 24, 1986
DTM = DTIM(INCRMT)
TEMP1 = ALFAA * DTM * DSHRNK
A = EP - EA - E * AGEEM
INCRMT = AR(8.3)
B(4) = 0.0
ESUM = ABS(EP(4))
DO 155 I = 1,3
  ESUM = ESUM + ABS(EP(I))
155 CONTINUE
DO 165 I = 1,4
  EP(I) = EP(I) - B(I)
  EP(I) = AR(I) * 16.1
  IF(ESUM GT 0) EP(I) = AR(I) * 16.1 * EP(I)
  AK(I) = 16.1 * EP(I)
  EP(I) = EP(I)
165 CONTINUE
  EP(I)
  Y = EP(I)
  XY = EP(I) * 4
  POS = SORT (XY X) / 2.0 * 2.0 * XY / 2.0 * 2.0
C

```

```

C (X+Y)/2.0
SMAX = C * RS
SHIN = C * RS
D = 10.0 * * 6
V(1) = X * D
V(2) = EPS(2) * D
V(3) = Y * D
V(4) = XY * D
V(5) = SMAX * D
V(6) = SHIN * D
EPSEFF = AR(12.2)
DO 200 J = 1,3
  DO 200 I = 1,4
    IF(INCRMT EQ 1) GO TO 203
    IN = 2
    DO 202 J = 1, IN
      CALL MEMORY(GE,DTIM,AR,INCRMT,ITER,ECONC,J,AGE,CREEP)
202 CONTINUE
C ..... 8/31/1985
C ..... CALL MATCON(T,EI,YIELD,ACEFAC,INCRMT,EPSEFF,CON,ETAN)
C ..... 8/31/1985
203 CONTINUE
  NPL = (AR(15,KT) + 0.001) / 100.0
  NPL = (AR(15,MT) + 0.001) / 100.0
C ..... 8/31/1985
C ..... IF(INCRMT GT 1) YIELD = YIELD * SQRT(1.0 + 3.0 * FACTR) * ACEFAC
C ..... IF(NPL EQ 0 AND INCRMT GT 1) YIELD = AR(11,2) * DAGE
C ..... 8/31/1985
  DELTAK = -(YIELD * AR(11,2)) / 1.732
  DELTAK = DELTAK * NPL
  EK = YIELD / 1.732
  EK2 = EK * EK
  EKK = EK2
  EI = EI * EO
  DELTAE = DELTAE * EO
  DO 310 I = 1,3
    H2(I,4) = 0.0
    H2(4,I) = 0.0
  DO 300 J = 1,3
    H2(I,J) = -1.0 / 6.0
    H2(J,I) = 2.0 / 6.0
310 CONTINUE
  H2(4,4) = 1.0
  DO 410 I = 1,4
    TA(I) = 0.0
    SG(I) = AR(1,KT)
410 CONTINUE
  DO 450 I = 1,3

```

```

TAU(I)=AR(I,1)
SIJ(I) = 0.0
DO 450 J = 1, 3
450 SIJ(I) = SIJ(I) + 2.0*HZ(I,J)*SG(J)
SIJ(4) = TAU(4)
TAU(4)=AR(4,1)
PLA = (SIJ(1)**2+SIJ(2)**2+SIJ(3)**2+2.0*SIJ(4)**2)
EFFSTR=SQRT(1.5*PLA)
SUM=SG(1) + SG(2) + SG(3)
COMP = SUM * SUM * FACTR
PLAST = (0.5 * PLA + COMP) / EK2
EPN= 0.0
IF(NPL1.GT.0.AND.PLAST.GT.0) EPN=1.0-SQRT(1.0/PLAST)
COMP1= SUM*(1.0-EPN)
CALL CONCRT(EPP,GE,DELTAE,DELTA,TAU,SIJ,EI,CON,EPN,
S ALFA,FACTR,EP,PH,AR)
DO 460 I=1,4
BF(I)= SG(I)
460 CONTINUE
IF(NCHECK.EQ.0) GO TO 2150
C
C ELEMENT COORDINATE STRESSES
C
S1= 1.5/(1.0+XV)-1.0
DO 610 I=1,4
DO 610 J=1,4
610 H(I,J)=0.0
DO 620 I=1,3
DO 615 J=1,3
615 H(I,J)=-XV/EI
H(I,1)=1.0/EI
620 CONTINUE
H(4,4)=2.0*(1.0+XV)/EI
IF(ITER.NE.2) GO TO 606
DO 605 I=1,4
AR(I+6,1)= AR(I+6,1)+EPP(I)
605 EPS(I)=AR(I+6,1)
GO TO 607
606 CONTINUE
DO 20 I=1,4
20 EPS(I)=AR(I+6,1)+EPP(I)
607 CONTINUE
IF(M14.EQ.1) V(2)=AR(8,1)*1.E6
SUM=(EPS(1)+EPS(2)+EPS(3))/3.0
DO 21 I=1,3
21 EPS(I)=EPS(I)-SUM
DO 630 I=1,4
EPP(I)=0.0
DO 630 J=1,4
630 EPP(I)=EPP(I)+H(I,J)*AR(J,KT)

```

Page 11 of 38

```

SUM= (EPP(1)+EPP(2)+EPP(3))/3.0
DO 601 I=1,3
601 EPS(I)= EPS(I)+S1*(EPP(I)-SUM)
EPS(4)=0.5*(EPS(4)+S1*EPP(4))
EPSEFF=SQRT(2./3.)*((EPS(1)**2+EPS(2)**2+EPS(3)**2+2.*EPS(4)**2))
AR(12,2)= EPSEFF
NPL1= (AR(15,KT)+0.001)/100.0
IF(ITER.EQ.2.AND.NPL1.GT.0) AR(11,2)=YIELD
IF(ITER.NE.2) GO TO 475
C.....8/31/1985
C CALL MATCON(T,EI,YIELD,AGEFAC,INCRMT,EPSEFF,CON,ETAN)
C YIELD= YIELD*SQRT(1.0+3*FACTR)
C.....8/31/1985
EK= YIELD/1.732
EK2= EK*EK
DELTA= -(YIELD-AR(11,2))/1.732
DELTAK= DELTA*NPL
SIGNT = SIJ(4) * SG(4) + 2.0 * (DELTA * EK + FACTR*COMP1 * (SG(1)
1 + SG(2) + SG(3)))
DO 470 I=1,4
SIGNT = SIGNT + SG(I) * SIJ(I)
470 CONTINUE
475 CONTINUE
DO 2136 I = 1, 4
IF (KT .EQ. 1) AR(I,2) = AR(I,KT)
SG(I) = AR(I,KT)
2136 CONTINUE
SUM = (SG(1) + SG(2) + SG(3)) / 3.0
TA(1) = SG(1) - SUM
TA(2) = SG(2) - SUM
TA(3) = SG(3) - SUM
TA(4) = SG(4)
EFFSTR = SQRT((TA(1)**2+TA(2)**2+TA(3)**2+2.0*TA(4)**2)*1.5)
SUM1=0.0
DO 571 I1=1,3
571 SUM1 = SUM1 + SG(I1)
COMP = SUM1
EFFS= EFFSTR**2+3.0*FACTR*COMP*COMP
IF(EFFS.GT.0.0) EFFSTR=SQRT(EFFS)
SUM1=SUM1/3.0
DO 572 J1=1,3
572 TA(J1) = SG(J1) - SUM1
TA(4) = SG(4)
PLA=0.5*(TA(1)**2 + TA(2)**2 + TA(3)**2 + 2.0*TA(4)**2)
PLAST = (PLA + COMP * COMP * FACTR) / EK2
IF(KT .EQ. 1) SIGNT = 0.01
PLAST-PLAST*1.001
C
C PLASTICITY CHECK
C

```

Page 12 of 38

```

C NFACT= NPL1
C IF(ITER NE 2) GO TO 577
C IF(ITER EQ 2) AR(15,MT)= NFACT*100*NPL2*10*NPL3
C MFACT= NPL
C NPL1 = 0
C IF(PLAST GT 1 0) NPL1= 1
C IF(MFACT GT 0 AND SIGMT GT 0 0) NPL1=1
C IF(NFACT GT 0 AND SIGMT GT 0 0) NPL1=1
C 577 CONTINUE
C IF(KT EQ 1) NPL1= 0
C ELEMENT PRINCIPAL STRESSES
C IF (KT .GT. 1) GO TO 380
C X = SG(1)
C Y = SG(3)
C XY = SG(4)
C RS = SQRT(((X-Y)/2.0)**2+XY**2)
C SG(5) = (X+Y)/2.0+RS
C SG(6) = (X+Y)/2.0-RS
C 348 CONTINUE
C PA=0
C IF(XY NE 0 0 OR (X-Y) NE 0 0)
C PA=0.5*ATAN2(2.0*XY,X-Y)*45.0/ATAN(1.0)
C 380 CONTINUE
C EPN = 0
C PLAST = (PLA*COMP*FA*CTR)/EKK
C IF(NFACT GT 0 AND PLAST LT 0 0) EPN = 1 0 - SORT (1 0/PLAST)
C IF(KT EQ 1) AR(14,2) = EFFSTR
C AR(14,KT) = EFFSTR
C 2150 CONTINUE
C DO 2151 I = 1,4
C DO 2151 J = 1,4
C 2151 IF(I) = IF(1) PH (I,J) * B(J)
C 2152 CONTINUE
C IF (NCHECK EQ 0) RETURN
C FINAL BOOKKEEPING
C KRAC= AR(16,KT)
C NPLAST= AR(15,KT)+0.001
C NPP= NPLAST/100
C NPL2= (NPLAST-NPP*100)/10
C NPL3= NPLAST-NPP*100-NPL2*10
C IF(ITER EQ 2) AR(15,MT)=NFACT*100*NPL2*10*NPL3
C AR(15,KT)= NPL1*100*NPL2*10*NPL3
C IF(ITER EQ 1) RETURN
C .....
C XMULT=1 0
C IF(INCRMT EQ 1) XMULT=0 0

```

```

C DO 2155 I=1,4
C 2155 TA(1)=AR(1,2)*(1 0-EPN)-AR(I,1)*XMULT
C DO 2156 I=1,4
C AR(1+8,3)=AR(1+8,3)+GE(3,1)*TA(1)*GE(4,1)
C AR(1+12,3)=AR(1+12,3)+GE(3,2)*TA(1)*GE(4,2)
C 2156 AR(1+16,3)=AR(1+16,3)+GE(3,3)*TA(1)*GE(4,3)
C USTOR=0 0
C UGEN=AR(20,2)
C DJ=1 0
C DO 635 I=1,4
C UGEN=UGEN+0.5*(AR(I,1)+AR(I,2))*EP(1)*DJ
C USTOR=USTOR+(SG(1)*EPP(1))*0.5*DJ
C 635 CONTINUE
C IF(KT EQ 1) UGEN=USTOR
C AR(20,2)=UGEN
C AR(20,1)=USTOR
C IF(KT EQ 1) RETURN
C DO 2170 I = 1, 4
C AR(1,2) = AR(I,2)*(1.0-EPN)
C AR(I,1) = AR(I,2)
C 2170 CONTINUE
C AR(10,2)= EI
C 8/31/1985
C AR(11,2)=AR(11,2)*DAGE
C 8/31/1985
C IF(NPL1 GT 0) AR(11,2)=YIELD*DAGE
C AR(13,1) = AR(13,2)
C AR(14,1) = AR(14,2)
C RETURN
C END
C SUBROUTINE CONCRT (EPS,GE,DELTA, DELTAK, TAU, TIJ, EI,
C $ CON, EPN,ALFA,FACTR,EP,PH,AR)
C IMPLICIT REAL (A-H,O-Z)
C COMMON/BLKN/ ALFAC,ALFAS,CRUSH,DELT,DJ,ECONC,ESTEEL,
C SES,ITER,NT,MCOUNT,M14,NCHECK,XVC,YSTEEL,
C $ ANGLE,EFFSTR,EPSEFF,KRAC,SG(8),TF(4),V(8)
C COMMON/BLK1/ H(4,4),STR(4),XV,YIELD,EPPFRAC
C DIMENSION ECC(4),EPS(4),BH(4,4),Q(4,4),DF(4),FS(4),SR(4),
C $ STN(4),HK(4,4),AS(6,6),AX(4),BX(4),TAU(4),TIJ(4),M2(4,4),
C $ HB(4,4),DIJ(4),GE(4,3),EP(4),PH(4,4),AR(20,3)
C DATA ZERO/0 0/
C KT = 2
C INCRMT=NT
C IF (INCRMT EQ 1) KT = 1

```

```

MT = KT - 1
IF(MT.EQ.0) MT = 1
JT = 2
CUB = FACTR
KRAC = AR(16,MT) + 0.01
KRAC = AR(16,KT) + 0.01
TH = AR(9,2)
CA = COS(TH/57.29578)
SA = SIN(TH/57.29578)
CTC = CA * CA
STC = SA * SA
STC = SA * CA
NE3 = KRAC/100
NE2 = (KRAC-NE3*100)/10
NE1 = KRAC-NE3*100-NE2*10
DEE = -DELTAEE/(EI*EI+1.0)
L1 = NE1
L2 = NE2
C1 = XV*EI/((1.0+XV)*(1.0-2.0*XV))
C2 = (1.0-XV)*EI/((1.0+XV)*(1.0-2.0*XV))
C3 = 0.5*EI/(1.0+XV)
XU = XV
DO 280 I = 1, 4
TF(I) = 0.0
DF(I) = 0.0
BF(I) = 0.0
STN(I) = 0.0
STR(I) = 0.0
DO 280 J = 1, 4
H2(I,J) = 0.0
Q(I,J) = 0.0
HK(I,J) = 0.0
280 CONTINUE
DO 285 L = 1, 3
DO 282 M = 1, 3
H2(L,M) = -XU / 3.0
282 HK(L,M) = -XV
H2(L,L) = 1.0 / 3.0
HK(L,L) = 1.0
285 CONTINUE
H2(4,4) = 2.0*(1.0+XU)/3.0
HK(4,4) = 2.0*(1.0+XV)
C
C
C
CALCULATIONS OF STRESSES FROM STRAIN HISTORIES
DO 290 I = 1, 4
SG(I) = AR(I,KT)*(1.0-EPN)
TIJ(I) = TIJ(I) * (1.0 - EPN)
ECC(I) = 1.0
DO 290 J = 1, 4

```

Page 15 of 38

```

HH(I,J) = 0.0
HB(I,J) = 0.0
290 H(I,J) = 0.0
SUM = 0.0
DO 435 I = 1, 3
K = 16+I
AR14 = AR(K,JT)
FS(I) = ARI4
IF(FS(I).LT.0.1) ECC(I) = 1.E-3
IF(FS(I).LT.0.1) FS(I) = 1.E-3
SUM = SUM + AR(I,KT)
435 CONTINUE
SUM = SUM * (1.0 - EPN)
GEN = 0.0
GEN1 = 0.0
DO 288 I = 1, 3
GENI = GENI + GE(1,I)
288 GEN = GEN + GE(1,I) - GE(2,I) * GE(3,I)
E1 = FS(1)
E2 = FS(2)
E3 = FS(3)
ALFA = 0.0
IF(ALFA.LE.0.0) GO TO 745
IF (E1 + E2 + E3 .LT. 0.1) GO TO 745
DO 738 K = 1, 4
DIJ(K) = EPS(K)
IF (MCOUNT .GT. 1) DIJ(K) = EPS(K) - EP(K)
738 CONTINUE
EPP1 = CTC * DIJ(1) + STS * DIJ(3) + STC * DIJ(4)
EPP2 = DIJ(2)
EPP3 = STS * DIJ(1) + CTC * DIJ(3) - STC * DIJ(4)
IF (NE1 .EQ. 0 .OR. EPP1 .LE. EPFRAC .OR. E1 .LT. 0.1) GO TO 742
ECC(1) = (1.0 - ALFA) * AR(17,2)
E1 = 0.0
742 IF (NE2 .EQ. 0 .OR. EPP2 .LE. EPFRAC .OR. E2 .LT. 0.1) GO TO 743
ECC(2) = (1.0 - ALFA) * AR(18,2)
E2 = 0.0
743 IF (NE3 .EQ. 0 .OR. EPP3 .LE. EPFRAC .OR. E3 .LT. 0.1) GO TO 745
ECC(3) = (1.0 - ALFA) * AR(19,2)
E3 = 0.0
745 CONTINUE
H(1,1) = C2
H(1,2) = C1
H(1,3) = C1
H(2,2) = C2
H(2,3) = C1
H(3,3) = C2
H(4,4) = C3
H(2,1) = H(1,2)
H(3,1) = H(1,3)

```

Page 16 of 38

```

H(3,2) = H(2,3)
DO 109 K=1,4
DO 109 L=1,4
PH(K,L)=H(K,L)
109 AS(K,L)=DEE*HK(K,L)+GEN*H2(K,L)
FS(4) = MIN(FS(1),FS(3))
GRATIO=EPP1/EPFRAC
IF (GRATIO.LT.1.0) GRATIO=1.0
IF(FS(4).LT.0.1) FS(4)=0.4/GRATIO
IF(ECC(4).LT.0.1) ECC(4)=0.4/GRATIO
IF (E1+E2+E3.GT.2.9) GO TO 117
DO 110 K = 1, 3
DO 110 L = 1, 3
110 HH(K,L) = HK(K,L) * FS(K) * FS(L)
HH(4,4) = 2.0 * (1.0 + XV * FS(4) )/ECC(4)
DO 115 K = 1, 3
115 HH(K,K) = 1.0/ECC(K)
DO 114 I = 1, 4
DO 114 J = 1, 4
114 HK(I,J) = HH(I,J)
CALL SYMINV(HH)
DO 116 I = 1, 4
DO 116 J = 1, 4
AS(I,J) = DEE*HK(I,J)+GEN*H2(I,J)
116 H(I,J) = HH(I,J)*EI
117 CONTINUE
Q(1,1) = CTC
Q(1,3) = STS
Q(1,4) = STC
Q(2,2) = 1.0
Q(3,1) = STS
Q(3,3) = CTC
Q(3,4) = -STC
Q(4,1) = -STC*2.0
Q(4,3) = STC*2.0
Q(4,4) = CTC*STS
DO 780 I = 1,3
780 HB(I,4) = 2.0 * Q(I,4)
HB(4,1) = 0.5 * Q(4,1)
DO 780 J = 1,3
HB(I,J) = Q(I,J)
HB(4,4) = Q(4,4)
IF (E1.GT.0.9 .AND. E3.GT.0.9) GO TO 140
DO 120 K = 1, 4
DO 120 L = 1, 4
AS(K,L) = 0.0
HK(K,L) = 0.0
DO 120 M = 1, 4
HH(K,L) = HH(K,L) + HK(K,M) * HB(M,L)

```

Page 17 of 38

```

120 AS(K,L) = AS(K,L) + H(K,M) * Q(M,L)
DO 130 K = 1, 4
DO 130 L = 1, 4
HK(K,L) = 0.0
H(K,L) = 0.0
DO 130 M = 1, 4
HK(K,L) = HK(K,L) + HB(M,K) * HH(M,L)
130 H(K,L) = H(K,L) + Q(M,K) * AS(M,L)
DO 132 K = 1, 4
DO 132 L = 1, 4
132 AS(K,L) = DEE*HK(K,L)+GEN*H2(K,L)
140 CONTINUE
DO 707 I=1,4
TF(I)=GENI*AR(I,MT)-GE(2,1)*AR(I+8,3)
-GE(2,2)*AR(I+12,3)-GE(2,3)*AR(I+16,3)
707 CONTINUE
IF(ABS(DEE).LT.1.E-9 .AND. GEN.LT.1.E-9) GO TO 740
DO 720 I = 1, 4
DO 720 J = 1, 4
HH(I,J) = 0.0
DO 720 K = 1, 4
720 HH(I,J) = HH(I,J) + H(I,K)*AS(K,J)
DO 725 I = 1,4
725 HH(I,I) = HH(I,I) + 1.0
CALL INVERT (HH,4,AX,BX)
DO 730 I = 1,4
DO 730 J = 1,4
PH(I,J) = 0.0
DO 730 K = 1,4
730 PH(I,J) = PH(I,J) + HH(I,K) * H(K,J)
DO 731 I = 1,4
DO 731 J = 1,4
731 H(I,J) = PH(I,J)
740 CONTINUE
DO 705 I = 1,4
BF(I) = 0.0
DO 705 J = 1,4
BF(I) = BF(I) - HK(I,J)*AR(J,MT)*DEE - H2(I,J) * TF(J)
705 PH(I,J) = H(I,J)
IF(M14.EQ.1) EP(2) = -(PH(2,1)*EP(1)+PH(2,3)*EP(3)+PH(2,4)*EP(4))
/PH(2,2)
EK = YIELD/1.732
EK2 = EK * EK
PP = 0.0
NPLAST = (AR(15,KT)+0.001)/100.0
NPL1 = AR(15,KT)+0.001
NPL2 = (NPL1-NPLAST*100)/10
NPL3 = NPL1-NPLAST*100-NPL2*10
IF(NCHECK.NE.1) GO TO 650
IF(M14.NE.1) GO TO 615

```

Page 18 of 38

```

DO 601 I=1,4
IF(I.EQ.2) GO TO 601
DO 600 J=1,4
IF(J.EQ.2) GO TO 600
H(I,J) = H(I,J) - H(I,2)*H(2,J)/H(2,2)
600 CONTINUE
601 CONTINUE
DO 605 I=1,4
DO 605 J=1,4
H(I,2)=0.0
H(2,2)=1.0
610 CONTINUE
DO 620 I=1,4
SR(I)=AR(I,1)
DO 620 J=1,4
SUM = (SR(I)+SR(2)+SR(3))/3.0
DO 625 I=1,3
DF(I) = SR(I) - AR(I,1)
625 SR(I) = SR(I) - SUM
DF(4) = SR(4) - AR(4,1)
EJ2 = 9.0*SUM*SUM*COD
F = 0.5*(SR(1)**2+SR(2)**2+SR(3)**2+SR(4)**2) + EJ2 - EK2
NPLAST=1
IF(F.GT.0.0) GO TO 635
NPLAST=0
GO TO 650
635 CONTINUE
SUM1 = TAU(1)+TAU(2)+TAU(3)
SUM2 = DF(1)+DF(2)+DF(3)
DO 640 I=1,3
SR(I)=DF(I)
TAU(I) = TAU(I) - SUM1/3.0
640 DF(I) = DF(I) - SUM2/3.0
SR(4)=DF(4)
T1 = 2.0*DF(4)*TAU(4)
T2 = 2.0*DF(4)*DF(4)
T3 = 2.0*TAU(4)*TAU(4)
DO 645 I=1,3
T1 = T1+DF(I)*TAU(I)
T2 = T2+DF(I)*DF(I)
T3 = T3+TAU(I)*TAU(I)
645 T2 = 0.5*T2+SUM2*SUM2*COD
T1 = T1+SUM2*SUM1*COD*2.0
T3 = 0.5*T3+SUM1*SUM1*COD
BB = T1/T2
RADCAL = (EK2-T33)/T22 + BB**2/4.0

```

```

IF(RADCAL.LE.0.0) RADCAL=BB**2/4.0
PP = -BB*0.5 + SQRT(RADCAL)
IF(PP.LT.0.0) PP=0.0
IF(PP.GT.1.0) PP=1.0
DO 646 I=1,4
646 SG(I) = AR(I,1) + PP*SR(I)
SUM = (SG(1)+SG(2)+SG(3))/3.0
DO 647 I=1,3
TIJ(4) = SG(I)-SUM
TIJ(4) = SG(4)
PLA = 0.5*(TIJ(1)**2+TIJ(2)**2+TIJ(3)**2+2.0*TIJ(4)**2)
COMP = SG(1)+SG(2)+SG(3)
PLAST = (PLA+COMP*COMP*FACTR)/EK2
IF(PLAST.LT.1.E-9) GO TO 650
EPN = 1.0-SQRT(1.0/PLAST)
DO 648 I=1,4
SG(I) = SG(I)*(1.0-EPN)
648 TIJ(I) = TIJ(I)*(1.0-EPN)
650 CONTINUE
AR(15,KT) = NPLAST*100+NPL2*10+NPL3
IF(NPLAST.EQ.0) GO TO 2100
FA = COD
CI1=2.0/3.0 * CON
SUM = SG(1)+SG(2)+SG(3)
FA = 2.0*FA*SUM
RT = 1.0-PP
DO 750 I = 1,3
750 STR(I) = TIJ(I) + FA
STR(4) = TIJ(4)
IF (FS(1) + FS(2) + FS(3) .GT. 2.9) GO TO 171
DO 151 K = 1, 4
DIJ(K) = 0.0
DO 151 L = 1, 4
151 DIJ(K) = DIJ(K) + HB(K,L)*SG(L)
DO 155 M = 1, 4
155 DIJ(M) = DIJ(M) + FS(M)
DO 156 I = 1, 4
156 DIJ(I) = DIJ(I) * (1.0 - EPN)
DO 161 K = 1, 4
STR(K) = 0.0
DO 161 L = 1, 4
161 STR(K) = STR(K) + Q(L,K) * DIJ(L)
SUM = STR(1) + STR(2) + STR(3)
DO 165 K = 1, 3
165 STR(K) = STR(K) - SUM * (1.0 / 3.0 - 2.0 * COD)
171 CONTINUE
DO 755 I = 1, 4
STM(I) = 0.0
DO 755 J = 1, 4
755 STM(I) = STM(I) + PH(I,J)*STR(J)

```

```

RS-STR(4)*STN(4) + C11*STR(4)*STR(4)
DO 760 I = 1,4
RS-RS*STR(I)*STN(I)*C11*STR(I)*STR(I)
DO 760 J = 1,4
760 HH(I,J) = STN(I)*STN(J)
DO 765 I = 1,4
DO 765 J = 1,4
765 PH(I,J) = PH(I,J) - HH(I,J)*RT/RS
DO 294 I = 1,4
294 STN(I) = -2.0 * EK * DELTAK * STN(I) * RT / RS
295 CONTINUE
300 CONTINUE
IF (E2.GT.0.9) GO TO 298
DO 675 I=1,4
IF(I.EQ.2) GO TO 675
DO 670 J=1,4
IF(J.EQ.2) GO TO 670
PH(I,J) = PH(I,J) - PH(I,2)*PH(2,J)/PH(2,2)
670 CONTINUE
675 CONTINUE
DO 680 I=1,4
DO 680 J=1,4
680 PH(I,J) = PH(J,I)
DO 297 I=1,4
PH(I,2)=0.0
297 PH(2,I) = PH(I,2)
PH(2,2)=1.0
298 CONTINUE
IF(E1.GT.0.9.AND.E3.GT.0.9) GO TO 2100
DO 785 I = 1,4
DO 785 J = 1,4
H(I,J) = 0.0
DO 785 K = 1,4
DO 790 I = 1,4
DO 790 J = 1,4
HK(I,J) = 0.0
DO 790 K=1,4
790 HK(I,J) = HK(I,J) + H(I,K) * HB(J,K)
IF(E1.GT.0.9) GO TO 685
DO 682 I=2,4
DO 681 J=2,4
681 HK(I,J) = HK(I,J) + HK(I,1)*HK(1,J)/HK(1,1)
682 CONTINUE
685 IF(E3.GT.0.9) GO TO 680
DO 687 I=1,4
IF(I.EQ.3) GO TO 687
DO 686 J=1,4
IF(J.EQ.3) GO TO 686
HK(I,J) = HK(I,1) + HK(1,J)/HK(1,1)

```

```

686 CONTINUE
687 CONTINUE
DO 688 I=1,4
DO 688 J=1,4
688 HK(I,J) = HK(J,I)
690 CONTINUE
DO 296 I = 1,4
DO 296 J = I,4
296 H(I,J) = HK(I,J) * FS(I) * FS(J)
DO 174 K = 1,4
H(K,K) = HK(K,K)*FS(K)
DO 173 L = K,4
IF (H(K,K) .LE. 0.0) H(K,L) = 0.0
173 CONTINUE
174 CONTINUE
DO 304 I = 1,4
DO 304 J = I,4
304 H(J,I) = H(I,J)
DO 2000 I = 1,4
DO 2000 J=1,4
HH(I,J) = 0.0
DO 2000 K = 1,4
2000 HH(I,J) = HH(I,J)+H(I,K)*Q(K,J)
DO 2010 I=1,4
DO 2010 J=1,4
PH(I,J) = 0.0
DO 2010 K = 1,4
2010 PH(I,J) = PH(I,J) + Q(K,I) * HH(K,J)
2100 CONTINUE
IF(M14.NE.1) GO TO 330
STN2 = STN(2)
DO 324 I = 1,4
324 STN(I) = STN(I) - STN2 * PH(I,2) / PH(2,2)
EP(2) = -(PH(2,1)*EP(1)+PH(2,3)*EP(3) + PH(2,4) * EP(4)) / PH(2,2)
PH(1,1) = PH(1,1) - PH(1,2) / PH(2,2)
PH(1,3) = PH(1,3) - PH(1,2) * PH(2,3) / PH(2,2)
PH(1,4) = PH(1,4) - PH(1,2) * PH(2,4) / PH(2,2)
PH(3,1) = PH(3,1)
PH(3,3) = PH(3,3)
PH(3,4) = PH(3,4) - PH(3,2) * PH(2,4) / PH(2,2)
PH(4,1) = PH(4,1)
PH(4,3) = PH(4,3) - PH(4,2) * PH(2,3) / PH(2,2)
PH(4,4) = PH(4,4) - PH(4,2) * PH(2,4) / PH(2,2)
DO 325 I = 1,4
PH(2,I) = 0.0
PH(I,2) = 0.0
325 CONTINUE
330 CONTINUE
DO 2050 JJ = 1,4

```



```

TF(JJ) = STN(JJ)
DO 2050 KK = 1,4
TF(JJ) = TF(JJ) + PH(JJ, KK) * BF(KK)
2050 CONTINUE
IF(INCHECK.NE.0) GO TO 375
DO 355 I=1,4
IF(FS(I) LT 1.0) FS(I)=0.0
355 TF(I) = TF(I)+AR(I,1)
TF(2) = TF(2)+FS(2)
IF(FS(1)+FS(3) GT 1.9) GO TO 375
DO 365 I=1,4
TF(I) = 0
DO 360 J=1,4
360 TFI=TFI+HB(I,J)*TF(J)
365 STN(I) = TFI+FS(I)
IF(STN(I) GT 0.0 AND NE1 EQ 1) STN(I)=0.0
IF(STN(2) GT 0.0 AND NE2 EQ 2) STN(2)=0.0
IF(STN(3) GT 0.0 AND NE3 EQ 3) STN(3)=0.0
IF((STN(1) GE 0.0 OR STN(3) GE 0.0) .AND. (NE1 EQ 1 .OR. NE3 EQ 3))
$ STN(4)=0.0
DO 370 I=1,4
TF(I) = 0
DO 370 J=1,4
370 TF(I) = TF(I)+Q(J,1)*STN(J)
375 CONTINUE
IF(ABS(AR(5,2)) LT 1 E-9 AND ABS(AR(6,2)) LT 1 E-9) GO TO 380
CALL REBAR(AR, INCHECK, ITER, DJ, ALFAS, DELT, ESTEEL, YSTEEL,
$ HK, BF, SG, V, EP)
IF(INCHECK EQ 1) GO TO 380
DO 377 I=1,4
TF(I) = TF(I)+BF(I)
DO 377 J=1,4
377 PH(I, J) = PH(I, J)+HK(I, J)
380 CONTINUE
IF (INCHECK EQ 0) RETURN
DO 2130 I=1,4
SG(I) = TF(I)
DO 2130 J=1,4
2130 SG(I) = SG(I) + PH(I, J) * EP(J)
DO 510 I = 1,4
AR(I,KT) = AR(I,MT)+SG(I)
BF(I) = AR(I,KT)
510 CONTINUE
IF(KT EQ 1) GO TO 550
E1 = AR(17, JT)
E2 = AR(18, JT)
E3 = AR(19, JT)
511 CONTINUE
AR(2,KT) = AR(2,KT) * E2
SG(2) = AR(2,KT) * AR(2,MT)

```

Page 23 of 38

```

SRI = AR(1,KT)
SR3 = AR(3,KT)
SR4 = AR(4,KT)
X = SRI
Y = SR3
XY = SR4
XX = SR2
IF (E1 + E3.GT.1.99) GO TO 515
SG1 = (CTC * SRI + STS * SR3 + 2.0 * STC * SR4) * E1
SG3 = (STS * SRI + CTC * SR3 - 2.0 * STC * SR4) * E3
SG4 = ((CTC-STC) * SR4 - STC * (SRI-SR3)) * E1 * E3
IF (SG1.GT.0.0 AND NE1.EQ.1) SG1 = 0.0
IF (SG3.GT.0.0 AND NE3.EQ.3) SG3 = 0.0
IF ((SG1.GE.0.0 OR SG3.GE.0.0) .AND. (NE1.EQ.1 .OR. NE3
1.EQ.3)) SG4 = 0.0
X = CTC * SG1 + STS * SG3 - 2.0 * STC * SG4
Y = STS * SG1 + CTC * SG3 + 2.0 * STC * SG4
XY = STC * (SG1-SG3) + (CTC-STC) * SG4
515 AR(1,KT) = X
AR(3,KT) = Y
AR(4,KT) = XY
SG(1) = AR(1,KT)-AR(1,MT)
SG(3) = AR(3,KT)-AR(3,MT)
SG(4) = AR(4,KT)-AR(4,MT)
550 CONTINUE
X = AR(1,KT) + 0.001
Y = AR(3,KT) + 0.001
XY = AR(4,KT) + 0.001
RS = SQR(((Y-X) / 2.0) ** 2 + XY ** 2)
CEN = (X+Y) / 2.0
SMAX = CEN + RS
SHIN = CEN - RS
SG(5) = SMAX
SG(6) = SHIN
PA1 = 2.0 * XY
PA2=X-Y
PA=0.0
IF(PA1.NE.0.0 OR PA2.NE.0.0)
PA=0.5*ATAN2(PA1, PA2)*45.0/ATAN(1.0)
TH=PA
560 CONTINUE
IF (ABS(AR(9, JT)) .GT. 1 E-6 .OR. NE1.NE.0 .OR. NE3.NE.0) TH=AR(9, JT)
CA = COS(TH/57.29578)
SA = SIN(TH/57.29578)
STS = SA * SA
CTC = CA * CA
STC = SA * CA
D1 = CTC * EPS(1) + STS * EPS(3) + STC * EPS(4)
D2 = EPS(2)
D3 = STS * EPS(1) + CTC * EPS(3) - STC * EPS(4)

```

Page 24 of 38

```

EPS3=P3*E3
EPS1=MAX(EPS1,ZERO)
EPS2=MAX(EPS2,ZERO)
EPS3=MAX(EPS3,ZERO)
Q1=2.0*SIGF*(1.0-0.5*S1)
Q2=2.0*SIGF*(1.0-0.5*S2)
Q3=2.0*SIGF*(1.0-0.5*S3)
SIG1=Q1*E1
SIG2=Q2*E2
SIG3=Q3*E3
IF (SG(5) .GE. 0.0 .AND. SG(6) .GE. 0.0) SIG1 = SIGF * E1
IF (SG(5) .GE. 0.0 .AND. SG(6) .GE. 0.0) SIG3 = SIGF * E3
SIG1=MAX(SIG1,ZERO)
SIG2=MAX(SIG2,ZERO)
SIG3=MAX(SIG3,ZERO)
S1 = D1
S2 = D2
S3 = D3
D1=MIN(D1,EPP1)*(1.0-E1)
D2=MIN(D2,EPP2)*(1.0-E2)
D3=MIN(D3,EPP3)*(1.0-E3)
575 CONTINUE
N = 16
DO 190 I = 1,3
K = I + N
AR(K,2) = 1.0
IF (NE1 .EQ. 0) AR(9,2) = 0.0
190 CONTINUE
C
C MATERIAL MODULI MODIFIED BY CRACKING
C
LT = 2
IF (EPFRAC .GT. 1.E3) GO TO 220
SIG1 = SIG1 - 0.1
SIG2 = SIG2 - 0.1
SIG3 = SIG3 - 0.1
D1 = D1+1.E-5
D2 = D2+1.E-5
D3 = D3+1.E-5
IF (S1 .GE. 0.0 .AND. S3 .GE. 0.0) EPS1 = P1 * E1
IF (S1 .GE. 0.0 .AND. S3 .GE. 0.0) EPS3 = P3 * E3
IF (M14 .NE. 0) GO TO 200
KRACK=2
IF (L1 .GT. 0 OR L2 .GT. 0) GO TO 192
IF (S1 .GT. S2) KRACK=1
192 CONTINUE
GO TO (200,195),KRACK
195 IF (S2 .LT. EPS2 .AND. AR(2,KT) .LT. SIG2) GO TO 200
IF (D2 .LT. 0.0) GO TO 200
AR(N+2,2) = 0.0
C
C
C

```

```

EPP1 = CTC*EP(1)+STS*EP(3)+STC*EP(4)
EPP2 = EP(2)
EPP3 = STS*EP(1)+CTC*EP(3)-STC*EP(4)
X = AR(1,KT)
Y = AR(3,KT)
XY = AR(4,KT)
SG(5)=CTC * X + STS * Y + 2.0 * STC * XY
SG(6)=STS * X + CTC * Y - 2.0 * STC * XY
V(5) = D1 * 1.E6
V(6) = D3 * 1.E6
EPS(1)= EP(1)
EPS(2)= EP(2)*FS(2)
EPS(3)= EP(3)
EPS(4)= EP(4)
IF(NE1+NE3 EQ 0) GO TO 570
EPS(4)= ((CTC-STS)*EP(4)+2.0*STC*(EP(3)-EP(1)))*FS(4)
EPS(1)= EPP1*FS(1)
EPS(2)= EPP2*FS(2)
EPS(3)= EPP3*FS(3)
DO 566 I=1,4
FS(I) = 0
DO 566 J=1,4
566 FS(I,J)= FS(I)+HB(J,I)*EPS(J)
DO 567 I=1,4
567 EPS(I)= FS(I)
570 CONTINUE
ANGLE=TH
ME3=KRACK/100
ME2=(KRACK-ME3*100)/10
ME1=KRACK-ME3*100-ME2*10
IF(NE3 EQ 0) ME3=ME3
IF(NE2 EQ 0) ME2=ME2
IF(NE1 EQ 0) ME1=ME1
E1 = 1-NE1
E2 = 1-NE2/2
E3 = 1-NE3/3
SIGF= EPFRAC*EI
CF=0.1
EX1=2.0*SIGF
S1=D1/EPFRAC
S2=D2/EPFRAC
S3=D3/EPFRAC
C
C CRACKING CRITERION
C
P1=2.0*PFRAC*(1.0-SG(5)/EX1)
P2=2.0*EPFRAC*(1.0-AR(2,KT)/EX1)
P3=2.0*EPFRAC*(1.0-SG(6)/EX1)
EPS2=P2*E2
EPS1=P1*E1
C
C

```

```

C IF (L2.EQ.0 AND L1.EQ.0) GO TO 220
200 CONTINUE
IF (S1.LT.EPS1 AND SC(5).LT.SIG1) GO TO 210
IF (D1.LT.0.0) GO TO 210
AR(N+1,2) = 0.0
AR(9,2) = TH
C IF (L1.EQ.0) GO TO 220
210 CONTINUE
IF (S3.LT.EPS3 AND SC(6).LT.SIG3) GO TO 220
IF (D3.LT.0.0) GO TO 220
C IF (L1.EQ.0 OR L2.EQ.0) GO TO 220
AR(N+3,2) = 0.0
220 CONTINUE
ME1 = 1.001 - AR(N+1,2)
ME2 = (1.001 - AR(N+2,2)) * 2.0
ME3 = (1.001 - AR(N+3,2)) * 3.0
AR(16,2) = 100*ME3 + 10*ME2 + ME1
C IF (ME1.NE.0) RETURN
C IF (ME2.NE.0) ME2=ME2
C IF (ME3.NE.0) ME3=ME3
AR(16,2) = 100 * ME3 + 10 * ME2 + ME1
KKAAC= AR(16,2)
ANGLE= AR(9,2)
RETURN
END
SUBROUTINE INVERT(A,NN,M,C)
C*****
C GENERAL MATRIX INVERSION SUBROUTINE
C*****
C IMPLICIT REAL (A-H,O-Z)
C DIMENSION A(1),M(1),C(1)
C DO 90 I=1,NN
90 M(I)=-1
DO 140 I=1,NN
C LOCATE LARGEST ELEMENT
D=0
DO 112 L=1,NN
IF (M(L)) 100,100,112
100 J=L
DO 110 K=1,NN
IF (M(K)) 103,103,108
103 IF (ABS(D) - ABS(A(J))) 105,105,108
105 ID=L
KD=K
D=A(J)
108 J=J+NN

```

Page 27 of 38

```

110 CONTINUE
112 CONTINUE
C INTERCHANGE ROWS
TEMP=-M(LD)
M(LD)=M(KD)
M(KD)=TEMP
L=LD
K=KD
DO 114 J=1,NN
C(J)=A(L)
A(L)=A(K)
A(K)=C(J)
L=L+NN
114 K=K+NN
C DIVIDE COLUMN BY LARGEST ELEMENT
NR=(KD-1)*NN+1
NH=NR+NN-1
DO 115 K=NR,NH
115 A(K)=A(K)/D
C REDUCE REMAINING ROWS AND COLUMNS
L=1
DO 135 J=1,NN
IF (J-KD) 130,125,130
125 L=L+NN
GO TO 135
130 DO 134 K=NR,NH
A(L)=A(L)-C(J)*A(K)
134 L=L+1
135 CONTINUE
C REDUCE ROW
C(KD)=-1.0
J=KD
DO 140 K=1,NN
A(J)=-C(K)/D
140 J=J+NN
C INTERCHANGE COLUMNS
DO 200 I=1,NN
L=0
150 L=L+1
IF (M(L)-I) 150,160,150
160 K=(L-1)*NN+1
J=(I-1)*NN+1
M(L)=M(I)
M(I)=I
DO 200 L=1,NN
TEMP=A(K)
A(K)=A(J)
A(J)=TEMP
J=J+1
200 K=K+1

```

Page 28 of 38

```

RETURN
END
SUBROUTINE MATCON(T,EI,YIELD,AGEFAC,INCRMT,EPSEFF,CON,ETAN)
IMPLICIT REAL (A-H,O-Z)
E0 = 2.076E6*AGEFAC
EE = 3.350E6*AGEFAC
EPO = 2240 E-6
SSO = 4650 *AGEFAC
FACTR = -0.02
EPLYO = SSO*0.5/EE
EPRAC = 465.0/EE
EPHIN = 1.E-9
IF(1/INCRMT.GT.1) GO TO 100
EI = EE
YIELD = SSO/2
RETURN
100 EPEFF = MAX(EPSEFF,EPHMIN)
EPNORM = EPEFF/EPO
SPLUS = EE / ( 1.+(EE/E0-2.)*EPNORM+EPNORM**2 )
EPS = (SPLUS)**2
SPLUS = SPLUS*EPEFF
EPM = (SPLUS/EPO)**2
ETAN = (EPS-EPN)/EE
YIELD = SPLUS
IF (EPEFF.LE.EPO) YIELD = SSO*0.5
CON = ETAN*EE/(EE-ETAN)
IF (ABS(CON).LT.0.001*EE) CON = SIGN(CON,CON)*0.001*EE
IF (CON.LT.0.001*EE) CON = 0.001*EE
EI = EE
IF (EPEFF.LE.EPO) RETURN
EI = EE*(SPLUS/SSO)**2
RETURN
END
SUBROUTINE SYMINV(H)
IMPLICIT REAL (A-H,O-Z)
DIMENSION H(4,4)
DET = H(1,1)*H(2,2)*H(3,3)-H(2,3)*H(2,3)*H(1,2)*H(2,3)*
H(1,3)-H(1,2)*H(3,3)+H(1,3)*H(1,2)*H(2,3)-H(2,2)*H(1,3)
H(2,1) = (H(1,2)*H(3,3)-H(2,3)*H(1,3))/DET
H(3,1) = (H(1,2)*H(2,3)-H(2,2)*H(1,3))/DET
H(3,2) = (H(1,1)*H(2,3)-H(1,2)*H(1,3))/DET
H11 = (H(2,2)*H(3,3)-H(2,3)*H(2,3))/DET
H22 = (H(1,1)*H(3,3)-H(1,3)*H(1,3))/DET

```

Page 29 of 38

```

H33 = (H(1,1)*H(2,2)-H(1,2)*H(1,2))/DET
H(1,1) = H11
H(2,2) = H22
H(3,3) = H33
H(4,4) = 1.0/H(4,4)
H(1,2) = H(2,1)
H(1,3) = H(3,1)
H(2,3) = H(3,2)
RETURN
END
SUBROUTINE TRANSF (A,Q,B)
IMPLICIT REAL (A-H,O-Z)
THIS ROUTINE CREATES Q AND B (BOTH 4X4) OUT OF THE TRANSFORMATOR
MATRIX A. Q AND B MAY THEN BE USED TO TRANSFORM A 4X4 TENSOR.
DIMENSION A(3,3),Q(4,4),B(4,4),VCTR(3)
DATA VCTR/ 1.0, 0.0, 1.0 /
C = A(1,1)
S = A(3,1)
DO 200 I=1,3
DO 100 K=1,3
B(I,K) = A(I,K)*A(I,K)
100 Q(I,K) = B(I,K)
B(4,1) = -VCTR(1)*C*S
B(1,4) = -2.0*B(4,1)
Q(4,1) = -B(1,4)
Q(1,4) = -B(4,1)
200 CONTINUE
B(4,4) = C*C-S*S
Q(4,4) = B(4,4)
RETURN
END
SUBROUTINE REBAR(AR,NCHECK,ITER,DJ,ALFAS,DELT,ESTEEL,YSTEEL,
HS,TS,SG,V,EP)
IMPLICIT REAL (A-H,O-Z)
DIMENSION AR(20,2),A(3,3),B(4,4),Q(4,4),PH(4,4),HS(4,4)
1 ,EP(4),TS(4),TF(4),SG(8),V(8)
C*****
C THIS SUBROUTINE APPLIED FOR 2D CASE
C*****
DO 10 I=1,4
TS(I) = 0.0
DO 10 J=1,6
10 HS(I,J) = 0.0

```

Page 30 of 38

```

NP1= 0
NP2= 0
IF (ABS (AR (5,2)) .GT. 0.0) NP1=1
IF (ABS (AR (6,2)) .GT. 0.0) NP2=2
NPLAST= AR (15,2)
NPL1= NPLAST/100
NPL2= (NPLAST-NPL1*100)/10
NPL3= NPLAST-NPL1*100-NPL2*10
IF (NP1.EQ.0) GO TO 100
CALL ROTAT (AR (7,2),A)
CALL TRANSF (A,Q,B)
CALL HHH (AR,ALFAS,DELT,NP1,AR (5,1),AR (11,1),NPL2,ESTEEL,
1 YSTEEL,NCHECK,EP,Q,B,PH,SG,V,TF)
IF (NCHECK.EQ.1) GO TO 25
AREA= AR (5,2)/DJ
DO 20 I=1,4
TS (I)= TF (I)*AREA
DO 20 J=1,4
20 HS (I,J)= PH (I,J)*AREA
GO TO 100
25 AR (11,1)= SG (7)
IF (ITER.EQ.2) AR (5,1)=AR (11,1)
100 CONTINUE
IF (NP2.EQ.0) GO TO 200
IF (AR (6,2) LT 0.0) GO TO 105
CALL ROTAT (AR (8,2),A)
CALL TRANSF (A,Q,B)
105 CONTINUE
CALL HHH (AR,ALFAS,DELT,NP2,AR (6,1),AR (12,1),NPL3,ESTEEL,
1 YSTEEL,NCHECK,EP,Q,B,PH,SG,V,TF)
IF (NCHECK.EQ.1) GO TO 125
AREA= ABS (AR (6,2))/DJ
DO 120 I=1,4
TS (I)= TS (I)+TF (I)*AREA
DO 120 J=1,4
120 HS (I,J)= HS (I,J)+PH (I,J)*AREA
GO TO 200
125 AR (12,1)= SG (8)
IF (ITER.EQ.2) AR (6,1)=AR (12,1)
200 CONTINUE
AR (15,2)= NPL1*100+NPL2*10+NPL3
RETURN
END
SUBROUTINE ROTAT (TH,A)
IMPLICIT REAL (A-H,O-Z)
DIMENSION A (3,3)

```

Page 31 of 38

```

IF (ABS (TH) .LT. 1.E-6) GO TO 10
C= 0.0
S= 1.0
IF (ABS (TH) .GT. 89.999) GO TO 10
AA= TH/57.29578
C= COS (AA)
S= SIN (AA)
10 CONTINUE
DO 20 I=1,3
DO 20 J=1,3
20 A (I,J)= 0.0
A (1,1)= C
A (1,3)= -S
A (3,1)= S
A (3,3)= C
A (2,2)= 1.0
RETURN
END
SUBROUTINE HHH (AR,ALFAS,DELT,M,SIG1,SIG,NP,ES,
1 Y,NCHECK,EP,Q,B,PH,SG,V,TF)
C****
C SUBROUTINE TO CALCULATE STEEL ELEMENT STRESSES
C****
IMPLICIT REAL (A-H,O-Z)
DIMENSION EP (4),Q (4,4),B (4,4),PH (4,4),SG (8),V (8),TF (4),
1 EPS (3),SIJ (3),H (4),AR (20,2)
DO 20 I=1,4
TF (I)= 0.0
DO 10 J=1,4
10 PH (I,J)= 0.0
20 PH (I,1)= ES
SG (6+M)= 0.0
PH1= ES
EK2= Y*Y/3.0
IF (NP.EQ.0) GO TO 780
COM=0.001
SIJ (1)= 2.0*SIG/3.0
SIJ (2)= -SIG/3.0
SIJ (3)= -SIG/3.0
PLA=0.5*(SIJ (1)**2+SIJ (2)**2+SIJ (3)**2)/EK2
CON=COM/(1.0-CON)*2.0/3.0
CI=ES*CON
EPN=1.0-SQRT (1.0/PLA)
DO 460 I=1,3
460 SIJ (I)=SIJ (I)*(1.0-EPN)
DO 750 K=1,3
EPS (K)=0.0
DO 750 L=1,3

```

Page 32 of 38

```

750 EPS(K)=EPS(K)+PH(K,L)*SIJ(L)
RS=0 0
DO 760 K=1,3
760 RS=RS+SIJ(K)*(CI*SIJ(K)+EPS(K))
RT=1 0/RS
DO 770 I=1,3
DO 770 J=1,3
770 PH(I,J)=PH(I,J)-EPS(I)*EPS(J)*RT
PH(1,1)=PH(1,1)-PH(1,3)*PH(3,1)/PH(3,3)
PH(1,2)=PH(1,2)-PH(1,3)*PH(3,2)/PH(3,3)
PH(2,2)=PH(2,2)-PH(2,3)*PH(3,2)/PH(3,3)
PH(2,1)=PH(2,1)
PH(1,1)=PH(1,1)-PH(1,2)*PH(1,2)/PH(2,2)
780 CONTINUE
DO 30 I=1,4
DO 30 J=1,4
30 PH(I,J)=0 0
IF(N.EQ.1 OR AR(6,2).GE.0.0) GO TO 90
PH(2,2)=PH11
PH(2,1)=PH11
IF(NC.CHECK.EQ.1) GO TO 35
BF=SIG1-PH11*ALFAS*DELT
TF(2)=BF
RETURN
35 CONTINUE
V(6*N)=V(2)
SG(6*N)=SIG1+PH11*EP(2)
GO TO 50
90 CONTINUE
PH(1,1)=PH11
IF(NC.CHECK.EQ.1) GO TO 120
BF=SIG1-PH11*ALFAS*DELT
DO 100 I=1,4
100 H(I)=PH11*Q(I,I)
DO 110 I=1,4
TF(I)=Q(I,I)*BF
DO 110 J=1,4
110 PH(I,J)=Q(I,I)*H(J)
RETURN
120 CONTINUE
DEPS=0 0
VV=0 0
DO 40 I=1,4
VV=VV+Q(I,I)*V(I)
40 DEPS=DEPS+Q(I,I)*EP(I)
V(6*N)=VV
SG(6*N)=SIG1+PH11*DEPS
50 CONTINUE
S11(1)=2.0*SG(6*N)/3 0
S11(2)=-SG(6*N)/3 0
S11(3)=SG(6*N)/3 0

```

Page 33 of 38

```

CRIT=SQRT(1.5*(SIJ(1)**2+SIJ(2)**2+SIJ(3)**2))
NFACT=NP
DS1=SG(6*N)-SIG1
SIGNT=DS1*SIJ(1)
NP=0 0
PLA=CRIT*CRIT/(3.0*EK2)
IF(PLA*.02.GT.1.0) NP=1
IF(SIGNT.GE.0.0.AND.NFACT.EQ.1) NP=1
IF(SIGNT.LT.0.0.AND.NFACT.EQ.1) NP=0
RETURN
END
SUBROUTINE MEMORY(CE,DTIM,AR,INCRMT,ITER,E10,IN,AGE,CREEP)
IMPLICIT REAL (A-H,O-Z)
DIMENSION DTIM(2),CE(4,3),TSE(6,2),AR(20,3)
DIMENSION CE(3),SE(6),FEE(3,2),FI(3,2),PI(2)
TIMEFAC=1.0
TSE(1,1)=AR(IN,3)
TSE(1,2)=AR(4,3)
IF(IN.NE.1) TSE(1,2)=0.0
SE(1)=AR(4+IN,3)
I=2
J=2*I-2
J1=J+1
T1=AR(13,1)
T3=0.5*(AR(13,1)+AR(13,2))
T2=(T1+T3)/2.0
DTM=DTIM(INCRMT-1)*TIMEFAC+AGE
IF(INCRMT.EQ.1) DTM=AGE
DTP=DTM(INCRMT)*TIMEFAC+AGE
DELTM=DTP-DTM
DT=(DTP-DTM)/12.0
XX=DTM
DO 190 JJ=1,2
DO 50 M=1,3
GO TO (10, 20, 30), M
10 T=T1
20 T=T2
XX=XX+DELTM*0.25
GO TO 40
30 T=T3
XX=XX+DELTM*0.25
40 CONTINUE
XKN=1.0/XX
CALL COEF(XKN,T,AFAC,TEMFAC)
CON=CREEP/AFAC

```

Page 34 of 38

```

CALL SHIFT1(T,R,A,D,CON,XX,IN)
RO-R
FI(M,1)=R/R0
FI(M,2) = D
FEE(M, JJ)=A*R
50 CONTINUE
TIM-MIN(DELTM,1 0/R)
DT1-TIM/12 0
TS2 =DT*(FI(1,2) + 4 0 * FI(2,2) + FI(3,2))
TS1 =DT*(FI(1,1)+4 0*FI(2,1)+FI(3,1))
IF(JJ EQ 1) TSE(J,1)=TSE(J-1,1)+TS1
IF(JJ EQ 2) TSE(J,1)=TSE(J,1)+TS1
IF(IN NE. 1) GO TO 51
IF(JJ EQ 1) TSE(J,2)=TSE(J-1,2)+TS2
IF(JJ EQ 2) TSE(J,2)=TSE(J,2)+TS2
51 CONTINUE
T1=T3
T3=AR(13,2)
T2=0 5*(T1+T3)
190 CONTINUE
TSE1=TSE(3,1)-TSE(1,1)
TSE3=TSE(3,1)-TSE(2,1)
TSE2=(TSE1+TSE3)/2 0
TM=DT1
DO 150 JJ=1,2
DO 100 M=1,3
GO TO (60,70,80),M
60 TS-TSE1
GO TO 90
70 TS-TSE2
GO TO 90
80 TS-TSE3
90 CONTINUE
CONST=-RO*TS
CE(M) = FEE(M, JJ) * EXP(CONST)
100 CONTINUE
SUM-TM*(CE(1)+4 0*CE(2)+CE(3))
PJ(JJ)=SUM
TSE1=TSE3
TSE3=TSE(3,1)-TSE(3,1)
TSE2=0 5*(TSE1+TSE3)
150 CONTINUE
CONST=RO*(TSE(3,1)-TSE(1,1))
ERX1=EXP(-CONST)
ERX2=1 0/ERX1
SE(2)=SE(1)*ERX1+PJ(1)
SE(3)=SE(2)+PJ(2)
EJ1=SE(3)+TSE(3,2)
EJ2=SE(1)+TSE(1,2)
GE(1, IN)=3 0*(EJ1-EJ2)

```

```

GE(2, IN)=ERX1-1 0
SE(1)=SE(1)*ERX1
SUM1=(SE(1)+4 0*SE(2)+SE(3))/6 0
GE(3, IN)=3 0*SUM1*ERX2
GE(4, IN)=ERX1
IF(ITER NE. 2) RETURN
AR(4+IN, 3)=SE(3)
AR(IN, 3)=TSE(3,1)
IF(IN EQ 1)AR(4, 3)=TSE(3,2)
RETURN
END
SUBROUTINE SHIFT1(TEMP,R,A,D,CON,XX,IN)
IMPLICIT REAL (A-H,O-Z)
INDEX=1
T=TEMP
IF(TEMP.LT.60.0) TEMP=60.0
IF(INDEX.GT.0) GO TO 50
APO = 0.10425
AP1 = -0.02775
AP2 = 0.0062667
CON=1.0
FF =(APO+AP1*LOG10(XX))*0.625
F = FF*EXP(AP2*T)
F=F*CON*1.E-6
R = 0.07
DT=T-200.0
IF(DT.LT.0.0) DT=0.0
D1=0.00075*DT+1.0E-5
D2=0.0015
D=MIN(D1,D2) * F
GO TO (5,10,20) ,IN
5 A=0.5*F
R=0.6
D=0.0
GO TO 30
10 A=1.5*F
R=0.07
D=0.0
GO TO 30
20 A=(0.056*DT-DT*DT*1.511E-4)*F
R=0.0046
30 CONTINUE
RETURN
50 CONTINUE
IF(INDEX.GT.1) GO TO 500
D= CON*0.0002

```

```

TK=(T-32.0)*5.0/9.0+273.0
R1=(70.0-32.0)*5.0/9.0+273.0
E=RT-EXP(4345.0/(1.98*TK))/EXP(4345.0/(1.98*RT))
CONN=EQT*1.E-6
D=3.779E-4*CON*CONN
GO TO (100,200,300),IN
100 CONTINUE
A=CON*0.64014
A*CONN*CON*0.0579386
X=6.938
RETURN
200 CONTINUE
A=CON*1.233
R=0.2303
A*CONN*CON*0.132428
R=0.2
D=0.0
RETURN
300 CONTINUE
A=CON*1.6
R=0.007
D=0.0
RETURN
400 CONTINUE
***** NEW MATERIAL DATA FOR HANFORD CONCRETE - OCTOBER, 1979
TK=(T-32.0)*5.0/9.0+273.0
E=RT-EXP(4345.0/(1.98*TK))
A=1.11E-4*E*RT
D=3.8265E-7*E*RT
R=0.23
ET=A*515
EM=D*516
RETURN
END
SUBROUTINE CEFUN(XN,TEMP,AGEFAC,TEMPAC)
*****
C CALCULATION OF AGE AND TEMPERATURE DEPENDENT COEFFICIENTS OF THE
C CREEP FORMULA
*****
TEMP=ICIT REAL (A,H,O,Z)
COMMUNICATE A0,A1,A2,A3,A4,A5,AP0,AP1,AP2,AP3,AP4,AP5
*****
2500
NWS=1
TEMP=TEMP
IF TEMP LT 60.0) TEMP=60.0
T=TEMP-32.0)*5.0/9.0

```

```

XK=1.0/28.0
FF1=0.0
DO 10 I=1,2
FF1=FF1
A0=201881+T*(-1.98117E-4+T*(5.31521E-5-T*4.23376E-7))
A1=-5.41464+T*(-.40337+T*(-5.36256E-3+T*2.33622E-5))
A2=69.245+T*(-3.38663+T*(-6.42465E-3+T*3.4411E-4+T))
A3=-583.108+T*(19.8205+T*(-.683703-.67766E-2+T))
A4=3356.7+T*(-83.0216+T*(-5.91922+5.39942E-2+T))
A5=7664.4+T*(1324.39E3+T*(17.0764-.150322+T))
FF1=A0+XK*(A1+XK*(A2+XK*(A3+XK*(A4+XK*(A5))))
T=(70.0-32.0)*5.0/9.0
10 CONTINUE
FF1=FF1*.E-6
FF1=FF1*.E-6
ET28=1.0/FF1
ERT28=1.0/FF1
TSHAPE=ET28/ERT28
TH=1.0/XN-1.0
ETATAU=1.E6*(0.606117*(1.0-EXP(-0.2*TH))+0.978921*
(1.0-EXP(-0.789875*TH))+8.06452E-3*TH+4.1)*TSHAPE
TH=3.0-1.0
ETA3=1.E6*(0.606117*(1.0-EXP(-0.2*TH))+0.978921*
(1.0-EXP(-0.789875*TH))+8.06452E-3*TH+4.1)*TSHAPE
AGEFAC=ETATAU/ETA3
TEMPAC=TSHAPE
IF(NWS.EQ.1) RETURN
ALFA=0.926+4.444*XN
ESTAR=ET28/ALFA
AGEFAC=ESTAR/ERT28
FF1=FF1*ALFA
T=(TEMP-32.0)*5.0/9.0
BETA=0.56+12.245*XN
XK=1.0/28.0
TIME=1.0/XK
15 CONTINUE
AP0=-0.76945+T*(7.70542E-3+T*(-8.38733E-5+T*3.82484E-7))
AP1=14.0236+T*(-7.13801+T*(1.12008E-2+5.71309E-5+T))
AP2=422.681+T*(21.8111+T*(-3.47742+1.78503E-3+T))
AP3=6016.54+T*(304.577+T*(4.84830+2.48844E-2+T))
AP4=39844.4+T*(1986.93+T*(-31.4952+1.61156+T))
AP5=98581.7+T*(4865.40+T*(76.8028-.391529+T))
F2=1.E6*(AP0+XK*(AP1+XK*(AP2+XK*(AP3+XK*(AP4+XK*(AP5))))))
IF(F2 GT 0) GO TO 20
TIME=TIME+.5
XK=1.0/TIME
GO TO 15
20 CONTINUE
F2=F2*BETA
RETURN
END

```


END

9-87

DTIC